University of Southampton

The Role of the Embryonic Transcription Factor, Pax-3

by

Andrew John Bingham

A thesis presented for the degree of

DOCTOR OF PHILOSOPHY

Department of Biochemistry

Faculty of Science

September 2002

UNIVERSITY OF SOUTHAMPTON

ABSTRACT

FACULTY OF SCIENCE

BIOCHEMISTRY

Doctor of Philosophy

THE ROLE OF THE EMBRYONIC TRANSCRIPTION FACTOR, PAX-3

By ANDREW JOHN BINGHAM

Pax-3 is a member of the Pax gene family of embryonic transcription factors that possess a conserved paired box motif coding for a 128 amino acid DNA binding domain called the paired domain. Pax proteins play important roles in vertebrate development. *Pax-3* is expressed from embryonic day 8.5 in the developing central and peripheral nervous systems, as well as in developing limb muscle. Mutations in the *Pax-3* gene give rise to developmental defects, characterised by the splotch phenotype in mice and Waardenburg Syndrome in humans. Abnormalities include spina bifida and exencephaly, limb deformities, pigmentation defects and loss of hearing. To further define the role that Pax-3 plays during embryogenesis, the regulation of Pax-3 activity was studied in the sensory neuron-derived cell line ND7. Attempts were also made to uncover novel molecular targets for Pax-3 in neuronal cells.

Expression of *Pax-3* is restricted to undifferentiated ND7 cells, and is dependent on serum factors. Removal of serum leads to a rapid fall in *Pax-3* mRNA expression, followed by cell cycle arrest and morphological differentiation. In the presence of 0.5% and 1% serum Pax-3 promoter activity was shown to decrease by the same amount as it did in the complete absence of serum, despite the fact that only 0% and 0.5% serum resulted in a decreased rate of ND7 cell proliferation. Therefore in neuronal cells the extent of cell proliferation may not be directly dependent on the level of *Pax-3* transcription. In addition to peptide growth factors, serum lipids were shown to be necessary for the induction of Pax-3 promoter activity. The promoter may also undergo auto-regulation, as suggested by the fact that low levels of Pax-3 stimulated promoter activity whereas higher levels of Pax-3 repressed it. Pax-3 promoter activity was also modulated by Brn-3 proteins, which play important roles in neuronal cell differentiation.

Pax-3 may also be regulated at the post-translational level by phosphorylation. PKA and PKC have been implicated in the control of cell proliferation and differentiation, and potential sites for both these kinases are located within the DNA binding domains of Pax-3. *In vitro* kinase assays using bacterially expressed Pax-3 proteins showed that Pax-3 could be phosphorylated within its DNA binding domains by PKA and PKC. In addition, PKA mediated phosphorylation increased the DNA binding affinity of Pax-3 *in vitro*, whereas PKC mediated phosphorylation had no effect on the affinity of Pax-3 for the binding-sites tested. Bacterially expressed Pax-3 was also phosphorylated by nuclear extracts made from neuronal cells. Moreover, Pax-3 was differentially phosphorylated by nuclear extracts made from ND7 cells at different phases of the cell cycle, with G_1 phase extracts resulting in the greatest amount of phosphorylation. Since *Pax-3* mRNA expression also increases during G_1 phase, reaching a peak in late G_1, phosphorylation may help control Pax-3 activity in mitotically active cells during embryogenesis.

The ligand-binding domain of the oestrogen receptor (ER™) has been used as a molecular switch to control the activity of a range of transcription factors. Therefore in an attempt to identify novel molecular targets for Pax-3 in neuronal cells, a Pax3-ER™ fusion protein was cloned and expressed in ND7 cells. Although it had no effect on the growth rate of dividing ND7s, Pax3-ER™ increased the rate of cell death in serum starved ND7 cells. As the transactivation function of the Pax3-ER™ protein was not proven, an antisense *Pax-3* approach was used to identify potential Pax-3 target genes in the neuroblastoma cell line Kelly. In Kelly cells the levels of N-Myc protein were shown to increase when Pax-3 was downregulated. However, it is not known whether N-*Myc* expression is directly regulated by Pax-3.

CONTENTS

List of Figures

List of Tables

Acknowledgements

I would firstly like to thank Dr Karen Lillycrop for her supervision during my time in the lab and for all her useful advice with regards to the preparation of this thesis. Secondly I wish to acknowledge my friends and colleagues, as well as my family. I am especially grateful to my parents for all their help and encouragement along the way.

Abbreviations

aa	Amino acid
ARMS	Alveolar rhabdomyosarcoma
as	Antisense
ATP	Adenosine trisphosphate
BCA	Bicinchoninic acid
bHLH	Basic helix-loop-helix
bp	Base pair
C	Celsius
C-	Carboxyl
cAMP	Cyclic adenosine monophosphate
CAT	Chloramphenicol acetyl transferase
cDNA	Complementary deoxynucleic acid
CKII	Casein kinase II
CMV	Cytomegalovirus
CREB	Cyclic AMP response element binding protein
Cys	Cysteine
Da	Daltons
DEPC	Diethyl pyrocarbonate
DMEM	Dulbecco's modified eagle medium
DMSO	Diethyl-methyl sulphonate
DNA	Deoxynucleic acid
dNTP	Deoxynucleic trisphosphate
DRG	Dorsal root ganglia
DTT	Dithiothreitol
E	Embryonic day
ECL	Enhanced chemiluminescence
EDTA	Ethylene-diamine-tris-acetate
EGF	Epidermal growth factor
EMSA	Electrophoretic mobility shift assay
ER	Oestrogen receptor
eRMS	Embryonal rhabdomyosarcoma

eSC	Embryonic schwann cell
FCS	Fetal calf serum
(a,b) FGF	(acidic, basic) Fibroblast growth factor
Gly	Glycine
Gsb-d	Gooseberry distal
Gsb-p	Gooseberry proximal
HD	Homeodomain
IPTG	Isopropyl β-D-thiogalactoside
kbp	Kilo base pair
kDa	Kilo Dalton
LB	Millers Luria broth
M	Molar
mA	Milliamps
MAP kinase	Mitogen activated protein kinase
MBP	Myelin basic protein
mRNA	Messenger ribonucleic acid
N-	Amino
NCAM	Neural cell adhesion molecule
NLS	Nuclear localisation signal
NT	Neural tube
nt	Nucleotide
Oct	Octamer binding protein
OD	Optical density
OP	Octapeptide
Pax	Paired box
PBS	Phosphate buffered saline
PCR	Polymerase chain reaction
PD	Paired domain
PEG	Polyethylene glycol
PKA	cAMP dependent protein kinase A
PKC	Protein kinase C
PMSF	Phosphomethylsulphonylfluoride
prd	Paired

Pro	Proline
PRS	Paired domain recognition sequence
RB	Retinoblastoma
RNA	Ribonucleic acid
RNase A	Ribonuclease A
rpm	Revolutions per minute
RT PCR	Reverse transcriptase polymerase chain reaction
SDS	Sodium dodecyl sulphate
SDS-PAGE	Sodium dodecyl sulphate polyacrylamide gel electrophoresis
Ser	Serine
Sey	Small eye
Sp	Splotch
Sp^d	Splotch delayed
Sp^r	Splotch retarded
SRE	Serum response element
SRF	Serum response factor
STE	Sodium-tris-EDTA
TAE	Tris-acetate-EDTA
TBE	Tris-borate-EDTA
TEMED	N, N, N', N', -tetramethylenediamine
Thr	Threonine
TLC	Thin layer chromatography
TRP-1	Tyrosinase-Related Protein-1
Un	Undulated
V	Volts
WS (1, 2)	Waardenburg Syndrome (Type 1, 2)

Chapter 1

Introduction

1 Introduction

1.1 Embryogenesis

All somatic cells of an embryo are derived from the same fertilised egg by successive rounds of mitotic cell division. As a result these cells all contain the same genetic information. The formation of different cell types in the developing embryo therefore relies upon the controlled expression of different sets of genes in different cells. These genes code for proteins that determine cell behaviour, which in turn influences how the embryo develops. This is exemplified by a number of model systems of embryonic development such as that of the mouse, which is outlined below.

The mouse has a life cycle of 9 weeks from fertilisation to mature adult, which is a relatively short developmental time span for a mammal. In addition it is relatively easy to study mutations in genes that cause developmental defects in mice. Consequently the mouse is the mammalian model system most commonly used to study human development. The period of mouse embryogenesis lasts 18 days, from fertilisation to birth. Following fertilisation, a process called cleavage occurs whereby cells divide by mitosis in the absence of cell growth. Implantation of the embryo occurs at embryonic day 4.5 (E4.5). Gastrulation begins at E7, resulting in the formation of the 3 germ layers (mesoderm, endoderm and ectoderm) of the embryo. The notocord, a rod-like structure formed from the mesoderm, runs from head to tail and lies underneath the future nervous system. The notocord subsequently induces the neural plate in the ectoderm above it. The neural plate folds to form the neural tube, which gives rise to the spinal cord and brain. Upon neural tube closure neural crest cells migrate from the dorsal aspect of the neural tube and give rise to a wide variety of cell types. Pigment cells (melanocytes), Schwann cells, cartilage in the head and cells of the adrenal cortex are all derived from

neural crest cells. In addition neural crest cells give rise to sensory neurons in the dorsal root ganglia of the peripheral nervous system, as well as sympathetic neurons of the autonomic nervous system (Wolpert, 1998). The pathways by which neural crest cells migrate from the neural tube are illustrated in figure 1.1.

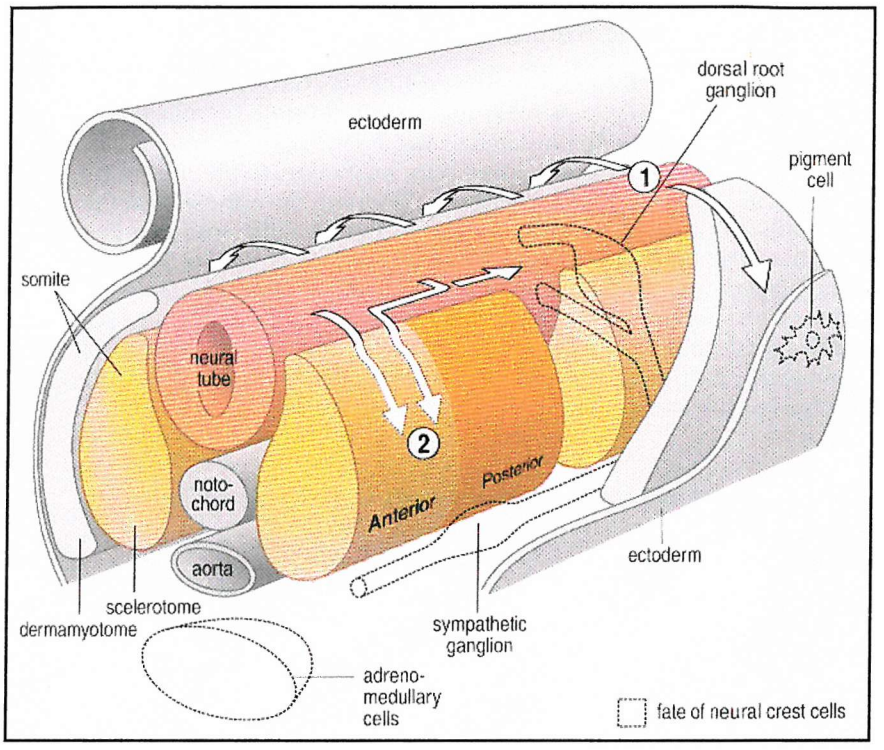

Fig. 1.1 Emigration of neural crest cells from the dorsal aspect of the neural tube
Source: Wolpert (1998)
(1) Neural crest cells that give rise to melanocytes (pigment cells) migrate dorso-laterally over the top of the somites. **(2)** Neural crest cells migrate ventrally into the somites to form dorsal root ganglia, and migrate through the anterior half of the somites to form sympathetic ganglia. Neural crest cells that give rise to cells of the adrenal cortex also migrate by this pathway.

The paraxial mesoderm on either side of the notocord differentiates to form somites. Part of each somite forms sclerotome, which develops into parts of the vertebral column. The remainder of each somite consists of dermamyotome that differentiates into dermatome

(which forms the dermis) and myotome (which forms body wall and limb muscles). The lateral mesoderm flanks the somites, and develops into parts of the kidney, lung, liver and gut. The embryonic endoderm meanwhile forms parts of the gut, liver and lungs (Lobe, 1992).

1.2 Control of gene expression during development

Many developmental control genes code for transcription factors that can activate or repress transcription of other genes during development. Transcription factors have a domain structure. DNA binding domains allow transcription factors to bind to specific DNA sequences in the upstream regulatory regions of their target genes. In addition domains for transcriptional activation and repression allow transcription factors to promote or inhibit transcription from the promoters of their target genes.

1.2.1 DNA binding domains of transcription factors

1.2.1.1 *The helix-turn-helix motif*

Homeotic genes are a group of developmental control genes that have been characterised in invertebrates such as the fruitfly *Drosophila melanogaster*. The homeotic genes are found in gene clusters, with each gene containing a 183 base pair sequence called the homeobox. This conserved motif codes for the homeodomain, which is the DNA binding domain of these transcription factors (Graba *et al.*, 1997, Reichert and Simeone, 1999). The homeodomain contains a helix-turn-helix motif, in which a α-helix is followed by a β-turn and then another α-helix (figure 1.2). The first α-helix lies across the DNA major groove while the second α-helix, termed the recognition helix, fits into the major groove and makes sequence specific DNA contacts (Latchman, 1990).

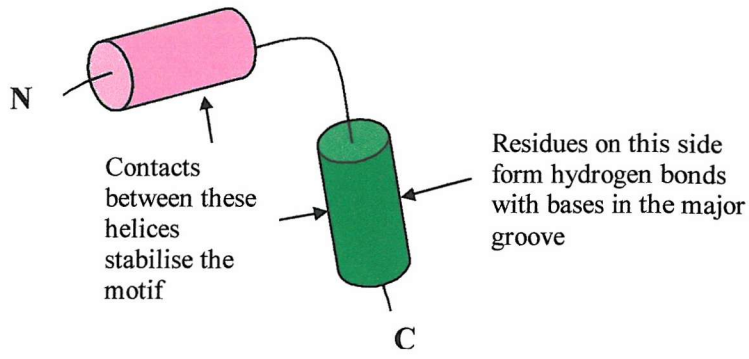

Fig. 1.2 Schematic diagram of a helix-turn-helix motif

Source: Stryer (1995)

A green cylinder is used to represent the recognition helix while the other α-helix that stabilises the interaction of the recognition helix with DNA, is represented by a pink cylinder.

Homeobox-containing genes were subsequently discovered in vertebrates such as *Xenopus*, mouse and human. In the mouse these genes, termed Hox genes, exist in clusters on chromosomes 2,6,11 and 15, with each gene cluster containing between 7 and 11 genes (Favier and Dolle, 1997). Hox genes are first expressed at E8 in the developing ectoderm and mesoderm, and the level of expression peaks at E12. Within each gene cluster Hox genes are expressed sequentially. For example, with regards development of the nervous system, Hox genes located at the 3' end of a cluster are expressed first, in the most anterior parts of the developing brain. Then, proceeding upstream in the gene cluster, Hox genes are expressed in more posterior parts of the brain and spinal cord (Carpenter, 2002). This corresponds to the sequence in which the embryo develops, from anterior to posterior. Inappropriate expression of the homeotic genes in *Drosophila* results in altered segmental identities such as legs growing out of the head instead of antennae. This process is termed homeosis. Ectopic expression of Hox genes results in

equivalent developmental defects in vertebrates, such as malformations of the vertebral column that cause structures to form in anterior regions of the spine that normally form in more posterior regions. In addition Hox gene mutants show severe developmental defects, indicating that these genes are important regulators of vertebrate embryogenesis (Lobe, 1992, Wolpert, 1998).

The *Drosophila* developmental control genes *paired (prd),* gooseberry-proximal (*gsb-p*) and *gooseberry-distal* (*gsb-d*) contain a second conserved sequence called the paired box that codes for a 128 amino DNA binding domain called the paired domain. The *Pax* (for paired box) gene family of murine genes was subsequently identified on the basis of their homology to the *Drosophila* paired box sequence. As described in section 1.4, some *Pax* genes also contain a paired-type homeobox that codes for a paired-type homeodomain. Unlike other classes of homeodomain proteins, paired-type homeodomain proteins bind to DNA as co-operative dimers, recognising two TAAT half-sites. Both homo-dimers and hetero-dimers can form on these DNA binding sites (Wilson *et al.*, 1993). Other members of the paired class of homeodomain proteins, such as the aristaless protein of *Drosophila*, contain a homeodomain but no paired domain. The murine equivalent of the *aristaless* gene is *Alx-4* (aristalesshomeobox-4), which belongs to a family of paired-type homeodomain containing genes that includes *Alx-3* and *Cart-1* (Qu *et al.*, 1997). Genes that code for proteins with paired-type homeodomains are required for patterning during development. For example, *Alx-4* is expressed in mesenchymal cells up to day 11.5 of embryogenesis. It is detected in the craniofacial regions, the 1st branchial arch and the limb buds. *Alx-4* is expressed in the anterior mesenchyme of the developing limb bud. It has been shown that mesenchymal cells on the posterior side of the limb bud (the zone of polarising activity) are required for producing anterior-posterior polarity in this region.

Alx-4 expression in the anterior mesenchymal cells of the limb bud suggests that it (and probably other genes as well) is involved in specifying the anterior side of the limb bud.

The homeodomain is also found in POU domain proteins that are coded for by another set of developmental control genes. The POU domain is a 150-160 amino acid region consisting of a 75-82 amino acid POU specific (POU_S) domain, a short variable linker region, and a 60 amino acid POU homeodomain (POU_H). Although originally found in the mammalian transcription factors Pit-1, Oct-1 and Oct-2, and the nematode transcription factor Unc-86, the POU domain has now been identified in a large number of genes. Both the POU_S and POU_H domains contain helix-turn-helix motifs that make sequence specific contacts with DNA. However, the POU_S domain differs from the POU_H domain in that it is more similar to prokaryotic repressor proteins that bind to DNA via helix-turn-helix motifs. In the POU_S domain as well as in prokaryotic repressor proteins, α helices either side of the helix-turn-helix motif stabilise its interaction with DNA whereas in the POU_H domain, a single α helix stabilises the helix-turn-helix motif (Herr and Cleary, 1995). *POU* genes play important roles during cell specification. For example, in *C.elegans*, *Unc-86* is required during neurogenesis for the development of a range of neuronal cell types, especially sensory neurones. Pit-1 plays an important role in the development of the pituitary gland, where it activates expression of the growth hormone and prolactin genes. Mutations in *Pit-1* result in dwarfism in mice and humans. Oct-2 binds to regulatory sequences in the promoters of immunoglobulin genes, and controls the expression of these genes during B cell development (Ruvkun and Finney, 1991, Latchman, 1999).

1.2.1.2 The Zinc Finger motif

GATA proteins are transcription factors expressed during development that are involved in cell lineage specification. Thus GATA proteins activate genes that promote differentiation of precursor cells into specific cell types. The DNA binding domain of a GATA protein consists of two zinc finger motifs, each of which contains four cysteine residues coordinated tetrahedrally to a zinc atom (Figure 1.3). A finger-like projection is formed by an anti-parallel β-hairpin followed by a turn and then an alpha helix. Two Cys residues from the β-hairpin and two Cys residues from the alpha helix bind to the zinc atom in the centre, which stabilises the structure. The two zinc fingers enter DNA from opposite sides of the helix, and both make DNA contacts in the major groove. The alpha helix of each zinc finger is the principal recognition element. Residues from the N-terminal part of this helix form hydrogen bonds with exposed bases in the DNA major groove. Multiple residues also form non-specific contacts with the sugar-phosphate backbone.

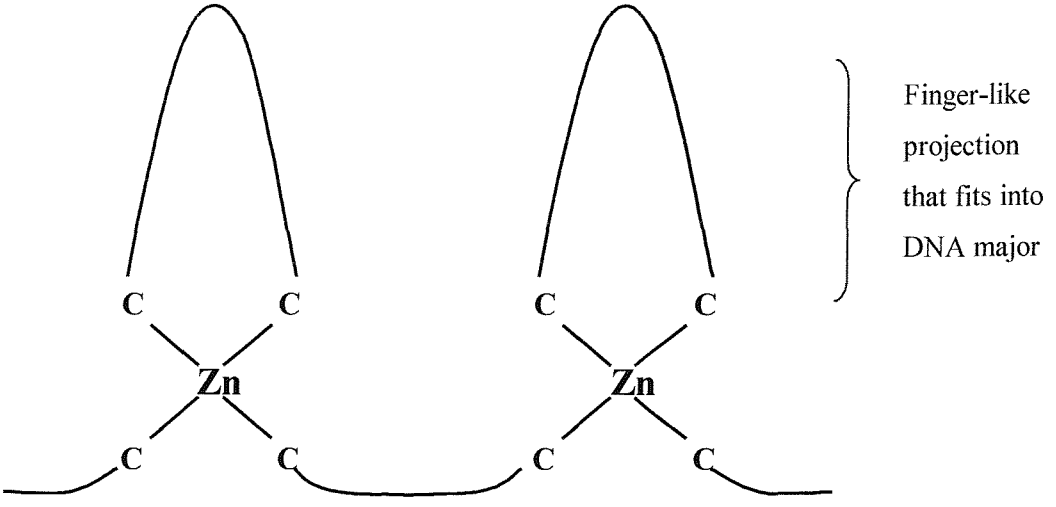

Fig. 1.3 Schematic diagram of a pair of cysteine zinc finger motifs

The two finger-like projections fit into the DNA major groove by entering the DNA from opposite sides of the helix (Latchman, 1990).

Six GATA genes have been identified in vertebrates. These genes have been split into two subfamilies based on differences in expression patterns and the amino acid sequences of the proteins that they code for. GATAs 1-3 are expressed in the developing haematopoietic system. Each factor has a specific role in development and activates a distinct set of target genes. GATAs 4-6 are required for the development of the vertebrate heart. Recognition sites for these proteins are found in the promoters of cardiac specific genes. As with GATAs 1-3, GATAs 4-6 have distinct spatial and temporal expression patterns during vertebrate development. Therefore each factor appears to have a distinct role in embryonic and postnatal development (Morrisey *et al.*, 1997).

DNA binding domains consisting of two zinc finger motifs are also found in members of the steroid/thyroid hormone receptor family of transcription factors. Upon binding their respective hormones, these transcription factors activate or repress gene transcription via distinct but related palindromic DNA sequences. Amino acids in the N-terminal zinc finger determine the binding site specificity of the protein, whereas amino acids in the C-terminal zinc finger determine the spacing between the two DNA half-sites to which the protein binds (Schwabe *et al.*, 1993).

1.2.1.3 Basic helix-loop-helix and basic leucine zipper motifs

A superfamily of proteins that regulate cell-type specific transcription as well as cell proliferation and differentiation, is defined by the basic-helix-loop-helix (bHLH) motif. For example, the Myc family of proteins that regulate cell proliferation and differentiation and have been implicated in tumourigenesis, contain the bHLH motif (Luscher and Larsson, 1999), as do the MyoD family of myogenic transcription factors

(Molkentin and Olson, 1996). The bHLH proteins bind to DNA as dimers. MyoD proteins, for example, dimerise with the ubiquitously expressed E proteins. These dimers bind to the CANNTG (E-box) recognition site in the promoters of muscle specific genes. The HLH structure that consists of two amphipathic α helices separated by an intervening non-helical loop facilitates dimerisation of bHLH proteins. As shown in figure 1.4, dimerisation brings together the basic DNA binding domains of two bHLH proteins, allowing them to bind to the two halves of the E-box recognition site. Only the myogenic bHLH proteins can activate the myogenic program by virtue of two conserved amino acids in the basic region of these proteins that are missing in all other bHLH proteins. These two amino acids facilitate the specific interaction of myogenic bHLH proteins with a coactivator that promotes transcription of muscle specific genes (Edmondson and Oldson, 1993).

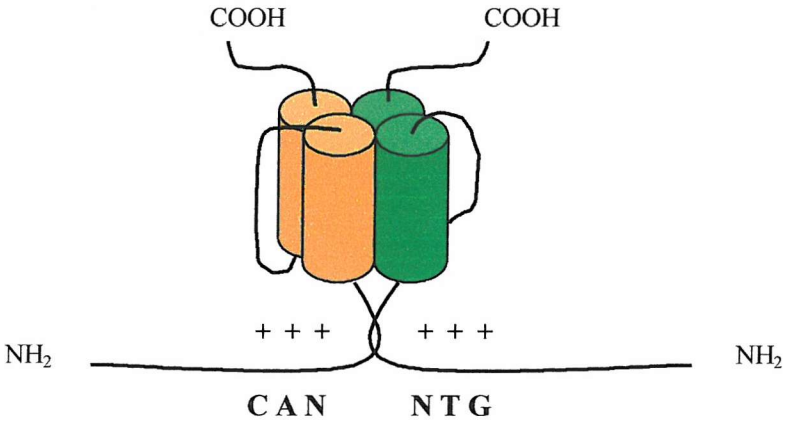

Fig. 1.4 Schematic representation of a dimer formed by two bHLH proteins
Orange cylinders represent the HLH of one protein, while green cylinders represent the HLH of the other protein. Dimerisation via the HLH motifs aligns the basic DNA binding domains of the two proteins correctly over the DNA recognition site, CANNTG (Edmondson and Olson, 1993).

Similar to the bHLH motif, the basic-leucine zipper motif is another DNA binding domain that is found in a range of transcription factors such as Fos and Jun (Chinenov and Kerppola, 2001). Instead of interactions between HLH structures, α helices that each contain 4-5 leucine residues every seven amino acids, facilitate dimerisation. As the leucine residues occur every 2 turns of the α helix such that their hydrophobic side chains are exposed on the same side of each helix, leucines on separate α helices can interdigitate, as shown in figure 1.5. As in the bHLH motif, dimerisation brings the basic DNA binding domains of two leucine zipper proteins together so that they can bind to the DNA recognition sequence.

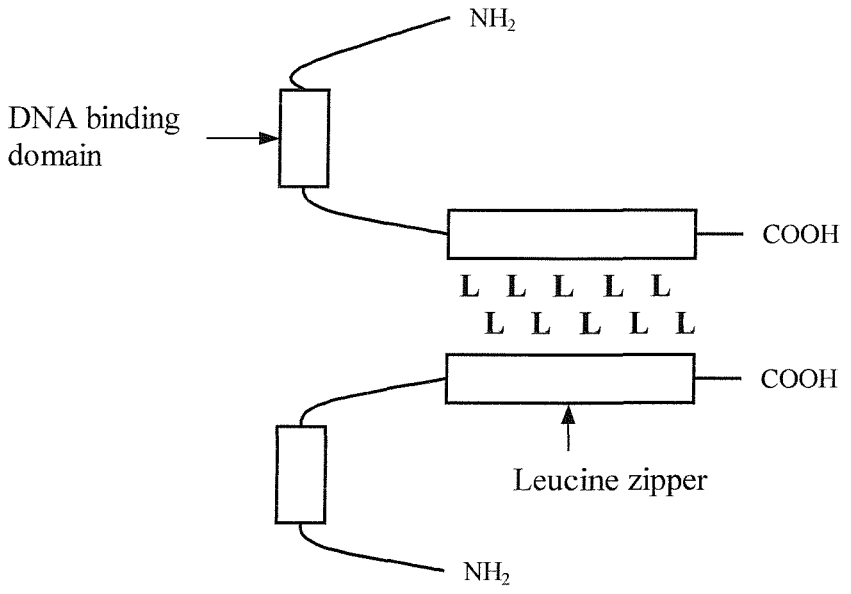

Fig. 1.5 Schematic representation of a dimer formed by two basic-leucine zipper proteins

Dimerisation via the leucine zipper motif aligns the basic DNA binding domains of the two proteins correctly over the DNA recognition site (Latchman, 1990).

1.2.2 Activation of Transcription

DNA binding of a transcription factor alone is not sufficient to induce the transcription of target genes. In addition the transcription factor must interact with the general transcription machinery either directly or indirectly via a coactivator (Sauer and Tjian, 1997). Specific regions within transcription factors have been identified that can activate transcription following DNA binding. The activation domains of a number of transcription factors including the steroid/thyroid hormone receptors contain a high proportion of acidic amino acids that are arranged in an amphipathic α helix in which all the negative charges are aligned on one surface of the helix. Other activation domains are rich in amino acids such as glutamine or proline (Latchman, 1990). In each case the activation domain interacts with components of the pre-initiation-complex of general transcription factors that recruits RNA polymerase to the transcription start site in the gene promoter. By helping to form and stabilise the pre-initiation-complex, transcription factor activation domains stimulate transcription initiation (Stargell and Struhl, 1996).

As well as interacting with the general transcription machinery, transcriptional activators also promote transcription by inducing the formation of a more open chromatin structure in the gene promoter. This is necessary because DNA in eukaryotic cells is tightly packaged as a result of being wrapped around histone core particles to form nucleosomes, which are themselves then further condensed. This makes the DNA inaccessible to DNA binding proteins, and so in order for transcription to take place the chromatin structure of a gene has to be decondensed. However, even in a decondensed chromatin state, DNA is still wrapped around histone core particles making it difficult for transcription factors and RNA polymerase to gain access to their binding sites. In addition tight packaging of DNA in nucleosomes hinders the progression of RNA

polymerase along the DNA during transcription. This block to transcription is removed partly by the action of protein complexes called nucleosome-remodelling factors that catalyse the sliding of histone octamers along DNA, resulting in the exposure of transcription factor binding sites in non-nucleosomal DNA. Nucleosome remodelling factors are directed to promoters by direct association with the transcription factors themselves. In addition acetylation of histones makes nucleosomal DNA more accessible to transcription factors and RNA polymerase. The N-terminal tails of histones contain a high proportion of positively charged lysine residues. Acetylation of the lysine residues reduces the overall positive charge on the histones, which weakens the interaction between the histones and DNA, making the nucleosomal DNA more accessible to transcription factors. As for the recruitment of nucleosome remodelling factors by transcription factors, transcriptional activators are associated with histone acetyltransferases that catalyse the acetylation of histones. Many cofactors as well as the general transcription factor TAFII250 have been shown to contain acetyltransferase activity (Cooper, 2000).

1.2.3 Repression of Transcription

Repressor proteins can inhibit transcription indirectly by suppressing transcriptional activator proteins, either by preventing them from binding to DNA or by interfering with their activation domains once they are bound to DNA (Levine and Manley, 1989). Transcription factors may also inhibit transcription directly via a transcription inhibition domain that acts to destabilise the pre-initiation-complex and therefore inhibits the rate of transcription (Manley *et al.*, 1996, Rojo, 2001) For example, the *Krüppel* gene product, which is involved in embryonic development in *Drosophila*, actively represses

transcription via an N-terminal repression domain that contains an α-helix with a glutamine-rich surface (Licht *et al.*, 1994).

In the same way that transcriptional activators are associated with acetyltransferases, repressor proteins can inhibit transcription by recruiting histone deacetylases to their target promoters. Thus removal of acetyl groups from the N-terminal tails of histones strengthens the interaction between histones and DNA, resulting in a more closed chromatin structure. This in turn inhibits the assembly of the general transcription machinery as well as the progression of RNA polymerase along the DNA during transcription (Cooper, 2000).

1.3 Control of transcription factor activity

1.3.1 Regulation of protein synthesis

Some transcription factors are expressed only in a particular cell type to ensure that the genes they control are expressed in a tissue specific manner. For example, the B cell specific coactivator OCA-B, which is essential for the activation of immunoglobulin genes, interacts with the DNA bound transcription factors Oct-1 and Oct-2 to stimulate transcription (Gstaiger *et al.*, 1996).

Regulation of transcription factor synthesis is also controlled at the post-transcriptional level. One way in which this can be achieved is by altering the half-life of the mRNA that codes for a transcription factor. Increasing the stability of the mRNA template used in translation leads to an increase in the amount of protein synthesised. For example the mRNAs transcribed from genes involved in cell growth such as *c-fos* and *c-myc*, have very short half-lives. However, upon stimulation of cell growth by growth factors, mRNAs are produced that have much longer half-lives. This allows more of the

transcription factor to be synthesised, resulting in an increased rate of cell proliferation Sachs, 1993).

1.3.2 Regulation of protein activity

1.3.2.1 Inhibitory protein-protein interactions

The activities of many transcription factors are controlled post-translationally. Such proteins may be expressed in a large number of different cell types but are only activated in response to a specific signal or in a specific cell type. Certain transcription factors are maintained in an inhibitory protein complex until signals to activate the transcription factor are received that result in its release from this complex. For example, in the absence of hormone, the steroid hormone receptors are complexed with heat shock protein 90 (hsp90). However, upon binding their respective hormones, this complex dissociates allowing the receptor protein to bind to DNA and activate transcription (Chambraud *et al.*, 1990, Pratt *et al.*, 1997). Secondly, as already described, MyoD family proteins dimerise with E proteins on E box recognition elements in the promoters of muscle specific genes. Like the MyoD and E proteins, the Id (inhibitor of differentiation) protein also has a HLH motif but lacks a basic domain and so is unable to bind to DNA. However, Id does bind to E proteins and in so doing, removes the dimerisation partners for MyoD. This prevents activation of the myogenic program until signals are received that result in the induction of muscle cell differentiation, partly by reducing the level of Id expression (Edmondson and Olson, 1993).

1.3.2.2 Post-translational modification of transcription factors

As well as being controlled by interactions with other proteins, transcription factor activity is regulated by direct modification of the protein itself. Phosphorylation, for

example, has been shown to control the activity of many different transcription factors. Phosphorylation can affect transcription factor function on three main levels (Hunter & Karin 1992). Firstly the nuclear localisation of transcription factors can be controlled by phosphorylation. Thus proteins can be sequestered in the cytoplasm where they are prevented from accessing their target sequences. For example NF-κB is held in the cytoplasm in its inactive form bound to the inhibitory protein IκB. Phosphorylation of IκB, followed by the degradation of this inhibitory protein, unmasks the nuclear localisation signal of NF-κB. This in turn allows NF-κB to translocate into the nucleus where it activates transcription of its target genes (Ghosh & Baltimore, 1990, Rothwarf and Karin, 1999).

Phosphorylation can also affect the interaction of transcription factor transactivation domains with the transcriptional machinery. For example the cyclic AMP response element binding protein (CREB) mediates transcriptional activation of cyclic AMP responsive genes when it is phosphorylated by PKA (Mayr and Montminy, 2001). Phosphorylation does not affect dimerisation of CREB or its ability to bind to DNA, but has a positive affect on transactivation. The phosphorylation site is located outside the DNA binding and dimerisation domains of CREB and lies close to the transactivation domain (Gonzalez *et al.*, 1989).

There are many examples in which phosphorylation affects the DNA binding activity of a transcription factor. The DNA binding activity can be affected both positively and negatively by phosphorylation. The c-Jun protein is phosphorylated on two serine residues and one threonine residue, all of which are located immediately to the N-terminal side of the DNA binding domain of the protein (Boyle *et al.*, 1991). These

residues are phosphorylated *in vitro* by glycogen synthase kinase 3 (GSK-3), which has been shown to inhibit DNA binding of bacterially expressed c-Jun protein. Since the phosphorylated amino acids are located just outside the DNA binding domain of c-Jun, phosphorylation is thought to inhibit DNA binding by causing electrostatic repulsion between phosphate groups on the protein and phosphates on the DNA. Activation of PKC causes dephosphorylation of c-Jun, resulting in an increase in DNA binding affinity and increased transcriptional activation of reporter genes *in vitro*. TPA (a phorbol ester tumour promoter) can directly activate PKC. This leads to the activation of genes containing the cis-acting TPA response element (TRE). The AP-1 complex, formed by either c-Jun homodimers or heterodimers of Jun and Fos, recognises the TRE. It has been proposed that PKC causes dephosphorylation of c-Jun by activating a protein phosphatase. Thus, in non-stimulated cells the DNA binding domain of c-Jun is phosphorylated. Cell stimulation by TPA and growth factors causes dephosphorylation of c-Jun, which activates the protein by increasing its DNA binding activity.

An example of a transcription factor the DNA binding activity of which is increased by phosphorylation is the serum response factor (SRF). This protein binds the serum response element (SRE) in the *c-fos* promoter and thus activates transcription of the *c-fos* gene (Ramirez *et al.*, 1997). SRF is phosphorylated *in vitro* by casein kinase II (CKII) on four serine residues, all of which are located upstream of the DNA binding domain (Manak *et al.*, 1991). Phosphorylated SRF binds to DNA *in vitro* with higher affinity than unphosphorylated SRF. The SRF protein binds to DNA as a homodimer. Phosphorylation was shown not to affect the dimerisation potential of SRF. Also the possibility of an N-terminal inhibitory domain (towards DNA binding) inactivated by phosphorylation has been ruled out. Instead it seems that phosphorylation of SRF

produces a conformational change in its DNA binding domain, which enables the protein to bind more readily to DNA.

The crystal structure of the Oct-1 POU domain protein bound to DNA (Klemm *et al.*, 1994) shows that the POU_S and POU_H domains, held together by the variable linker, bind on opposite sides of the major groove. The linker is not a rigid structure and thus provides flexibility in the way the POU domain binds to DNA. Oct-1 and Oct-2 have very similar POU domains and both recognise the same octamer DNA sequence found in a range of promoters including the histone H2B promoter. Pit-1 binds to the octamer sequence but this is not its preferred binding site. POU proteins are able to bind to a range of recognition sites. This allows them to interact with different regulatory proteins and so activate transcription of different genes. For example Oct-1 and Oct-2, in addition to the octamer site, also recognise low affinity sites such as the TATGARAT sequence. Pit-1 binds to a series of sites in the prolactin and growth hormone promoters. Post-translational modification can modify the DNA binding properties of POU proteins. For example phosphorylation of Pit-1 by PKA has been shown to alter the DNA binding site specificity of the protein (Kapiloff *et al.*, 1991). PKA phosphorylates Pit-1 both *in vitro* and *in vivo*. A threonine in the homeodomain of Pit-1 is phosphorylated within the PKA site: RRTT/S*I (the asterisk indicates the phosphorylated amino acid). This sequence is conserved throughout the POU domain family. Consequently it has been proposed that other POU proteins may be phosphorylated by PKA *in vivo*. PKA mediated phosphorylation of Pit-1 has different effects on binding to different binding sites. Binding to some sites is decreased when Pit-1 is phosphorylated, whereas phosphorylation has either no effect or a positive effect on binding to other sites. Methylation interference studies showed that for a site towards which phosphorylation of

Pit-1 has no effect on protein-DNA binding, the conformation of Pit-1 on the DNA altered when the protein was phosphorylated. Such a conformational change could allow proteins to present their transactivation domains in different ways to the transcriptional apparatus assembled on a promoter. This in turn could lead to differential regulation of gene expression.

Some transcription factors are differentially phosphorylated through the cell cycle. Oct-1 is a widely expressed protein implicated in the regulation of housekeeping genes that contain octamer-binding sites, such as the histone H2B gene. PKA phosphorylates Oct-1 *in vitro* at a site in its homeodomain. This site is also phosphorylated *in vivo*, but only during M phase of the cell cycle (Segil *et al.*, 1991). Both *in vitro* and *in vivo* phosphorylation of Oct-1 causes a decrease in the DNA binding activity of the protein. Thus Oct-1 may be inactivated during mitosis as a result of phosphorylation, perhaps mediated by PKA. Phosphorylation of DNA binding proteins may be a way of dissociating them from DNA at the start of mitosis to allow DNA condensation to occur. During S phase Oct-1 is in its least phosphorylated state, and so is able to activate transcription of the H2B gene in order to produce histones needed in DNA synthesis. Other POU proteins are also regulated by M-phase specific phosphorylation. For example, GHF-1 (Pit-1) is phosphorylated during M phase by a cell cycle-regulated protein kinase (Caelles *et al.*, 1995). This kinase, distinct from PKA, decreases the DNA binding activity of GHF-1 and the transactivation of reporter genes.

Although normally confined to cell surface proteins and proteins that are present within the lumens of intracellular organelles, glycosylation has been shown to modulate the activity of transcription factors. For example, the Sp1 family of transcription factors that

bind to GC-rich decanucleotide sequences (the GC-box) are modified by O-linked glycosylation, phosphorylation and acetylation (Bouwman and Philipsen, 2002). Glycosylation decreases the transcriptional activity of Sp1 by inhibiting its interactions with components of the pre-initiation complex (Yang *et al.*, 2001). In addition Pax-6 has been shown to undergo O-linked glycosylation in quail cells (Lefebvre *et al.*, 2002).

1.4 The *Pax* gene family

There are nine *Pax* genes in mice, which all code for transcription factors that are expressed during embryogenesis. These genes belong to a family of paired box-containing genes that have been isolated in mice and humans based on sequence similarity to developmental control genes found in *Drosophila*. The paired box motif was originally found in a subset of *Drosophila* homeobox genes that includes *paired* (*prd*), *gooseberry-proximal* (*gsb-p*), and *gooseberry-distal* (*gsb-d*). The *Drosophila* genes *Pox-meso* and *Pox-neuro* were also found to contain a paired box but lack the homeobox motif. The paired box-containing genes in mice have been termed *Pax-1* to *Pax-9* while those in humans are called PAX1 to PAX9. Paired box genes have been found in a range of other organisms including zebrafish and chicken. The paired box motif codes for a 128 amino acid DNA binding domain called the paired domain, which is located close to the N-terminus of Pax proteins. As shown in figure 1.6, the *Pax-3*, *Pax-4*, *Pax-6* and *Pax-7* genes also contain a region that codes for a second DNA binding domain of 61 amino acids called a paired type homeodomain. The coding region for the homeodomain is located at the 3' end of the paired box. In these Pax proteins both the paired domain and the homeodomain contain helix-turn-helix motifs that are used for sequence specific binding to DNA. The *Pax-2*, *Pax-5* and *Pax-8* genes code for proteins with partially formed homeodomains that are lacking the helix-turn-helix motif.

In addition all *Pax* genes except *Pax-4* and *Pax-6* contain a region in between the paired domain and homeodomain coding regions that codes for a conserved octapeptide sequence. However, the function of this octapeptide is unknown. The nine *Pax* genes have been subdivided into subgroups according to similarities in protein structure and patterns of expression during embryogenisis (Chalepakis *et al.*, 1992, Wehr and Gruss, 1996, Dahl *et al.*, 1997).

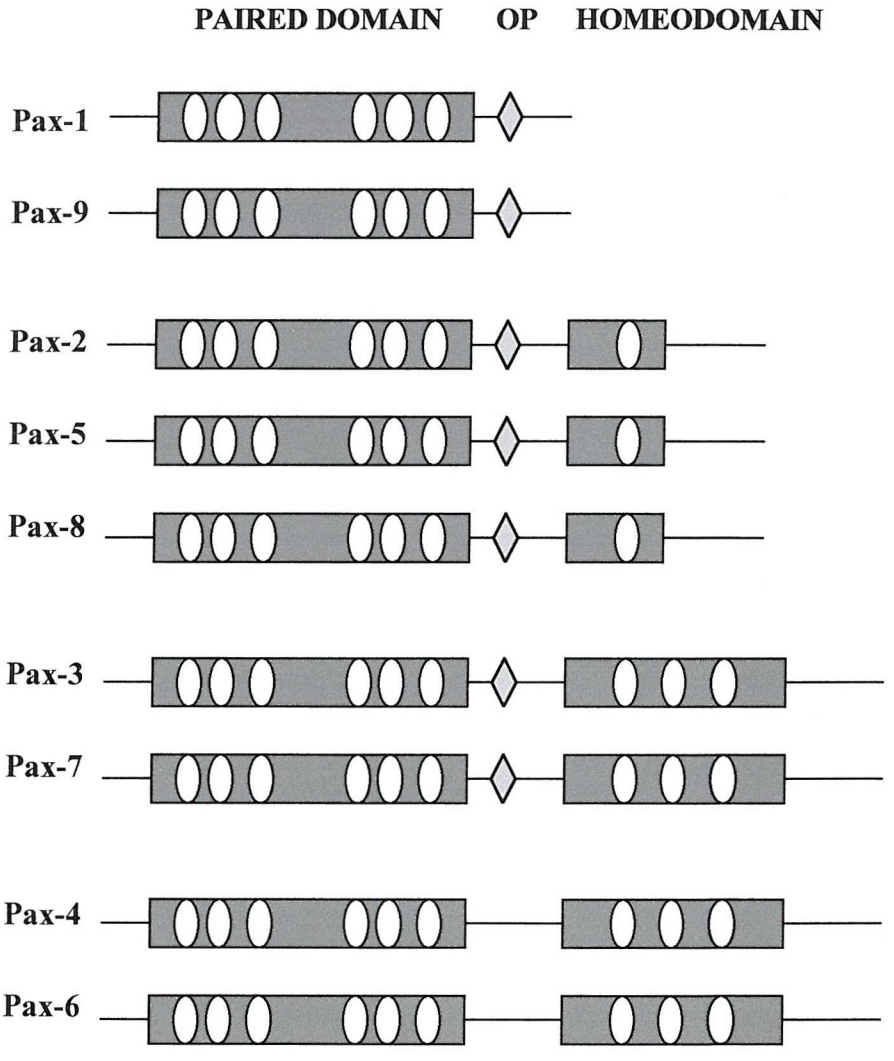

Fig. 1.6 Protein structure of Pax genes

The paired domain and homeodomain are shown as grey boxes containing α helices, which are represented by white ovals. The octapeptide (OP) is shown as a grey diamond (Mansouri *et al.*, 1994).

1.5 Expression of *Pax* Genes and *Pax* mutants

All *Pax* genes except *Pax-1* and *Pax-9* are expressed in the developing brain and spinal cord. *Pax* genes that code for both a paired domain and a homeodomain are expressed first, from embryonic day 8.5 (days after conception), before the onset of cellular differentiation. Thus *Pax-3*, *Pax-6* and *Pax-7* are the first *Pax* genes to be expressed, and expression of these genes is restricted to dividing cells. *Pax* genes that do not code for a homeodomain (Pax-2, Pax-5 and Pax-8) are first expressed at embryonic day 9.5-10.5. These genes are only expressed in post-mitotic cells (Wehr and Gruss, 1996).

Pax-1 and Pax-9

Pax-1 is expressed from embryonic day 9 (E9) in the vertebral column, and is later expressed in the sternum and thymus. Undulated (un) mice carry a mutated form of the *Pax-1* gene that causes malformation of the vertebral column. A point mutation in *Pax-1* causes a Gly to Ser substitution at position 15 of the Pax-1 paired domain. This decreases the DNA binding affinity and binding site specificity of the Pax-1 protein. In addition it is thought that mutations in the PAX1 gene could contribute to the pathogenesis of spina bifida in humans (Chalepakis *et al.*, 1991). *Pax-9* is also expressed in the vertebral column during embryogenesis, as well as in the tail, head and limbs. The Pax-9 protein is highly homologous to Pax-1 (Neubuser *et al.*, 1995).

Pax-2, Pax-5 and Pax-8

During embryogenesis *Pax-2* is expressed in the developing brain and spinal cord, as well as in the eye, ear and kidney. The mouse strain *Krd* (kidney and retinal defects) has a large chromosomal deletion that includes the *Pax-2* locus. In the heterozygous state affected mice develop with kidney defects, while homozygotes are more severely

affected and die prior to embryo implantation. Another mutant *Pax-2* allele (*Pax-2* ^{1NEU}) has a one base pair insert in the *Pax-2* gene that causes a frameshift, resulting in premature termination of translation and the formation of a Pax-2 protein that lacks most of the paired domain and all of the homeodomain. Mutant embryos show defects in brain, eye, ear and kidney. The molecular defect is equivalent to a mutation in the human PAX2 gene that results in renal-coloboma syndrome (Favor *et al.*, 1996).

Pax-5 is initially expressed only in the developing brain and spinal cord during embryogenesis. Expression is later detected in the developing liver, where Pax-5 is believed to be involved in the early stages of B-lymphocyte differentiation. *Pax-5* is also expressed in adult testis (Adams *et al.*, 1992).

Pax-8 shows a similar expression pattern to *Pax-2*, being expressed from E10.5 in the developing kidney. *Pax-8* is also expressed at this time in the thyroid gland (Zannini *et al.*, 1992), and between E11.5 and E12.5 *Pax-8* is expressed in the developing brain and spinal cord (Plachov *et al.*, 1990).

Pax-3 and Pax-7

The *Pax-3* and *Pax-7* genes show overlapping expression patterns during embryogenesis. The expression of *Pax-3* is described in detail below. Mutations in *Pax-3* cause the splotch phenotype in mice and mutations in PAX3 lead to Waardenburg syndrome in humans. *Pax-7* is expressed from E8 to E17 in the developing brain and spinal cord. It is also expressed during myogenesis in migratory limb muscle precursor cells (Jostes *et al.*, 1990, Schafer *et al.*, 1994).

Pax-4 and Pax-6

Both *Pax-4* and *Pax-6* are expressed in the developing pancreas, where they are required for the development of endocrine cells. The Pax-4 and Pax-6 proteins, which contain both a paired domain and a homeodomain, recognise common DNA sequences in target genes. Pax-4 can function as a transcriptional repressor, and is believed to inhibit Pax-6 mediated stimulation of gene expression during early pancreatic development (Smith *et al.*, 1999).

From E8.5 *Pax-6* is expressed in mitotically active cells of the developing brain and spinal cord. *Pax-6* is also expressed in the developing eye, pituitary and nasal epithelia. Small eye (Sey) in mice is a condition caused by mutations in the *Pax-6* gene. Homozygotes develop without eyes and with a shortened snout, whereas heterozygotes have smaller eyes than normal. This is equivalent to the human syndrome aniridia, which is caused by a mutated PAX6 gene, and affects the development of the iris, cornea, lens, retina and optic nerve (Hill *et al.*, 1991, Epstein *et al.*, 1994).

Vertebrate *Pax* genes are of interest because mutations in four of these genes have been shown to result in developmental defects in mice and humans. The phenotypes that result from all of these mutations correlate well with the expression patterns of the *Pax* genes involved. This implies that *Pax* genes play important roles in the development of certain structures during embryogenesis.

1.6 Expression of *Pax-3*

1.6.1 Expression in developing spinal cord and brain

Northern hybridisation of mRNA from mouse embryos showed that *Pax-3* is expressed between E8.5 and E17, with the highest level of *Pax-3* expression detected between E9 and E12. *Pax-3* expression decreased steadily from day 13, with no *Pax-3* expression detected in adult tissues including the brain and spinal cord (Goulding *et al.*, 1991).

Pax-3 is first expressed in the dorsal part of the recently closed neural tube (developing brain and spinal cord) at E8.5. By E10 *Pax-3* is detected in the dorsal neural tube along the entire anterior-posterior axis of the embryo. The developing neural tube has a dorsal-ventral polarity, generated by signals from the floorplate and underlying notochord. As shown in figure 1.7, *Pax-3* is expressed in the dorsal aspect of the neural tube, in the alar and roof plates, but is absent from the basal and floor plates in the ventral half of the neural tube. *Pax-3* expression is restricted to the dorsal neural tube prior to the formation of the alar and basal plates. Therefore Pax-3 could be involved in the process that generates each of these compartments, which give rise to different sorts of neuronal precursors. Thus Pax-3 may help to separate the neural tube into different regions during embryogenesis.

1.6.2 Expression in neural crest cells

As already described, during embryogenesis, *Pax-3* is expressed in the dorsal region of the neural tube from which neural crest cells migrate. In day 10-12 embryos *Pax-3* transcripts are detected in spinal ganglia that are derived from neural crest. In day 10-13 embryos *Pax-3* is also detected in structures of the skull and face derived from neural

crest (Goulding *et al.*, 1991). This indicates that *Pax-3* is expressed in neural crest cells during embryogenesis.

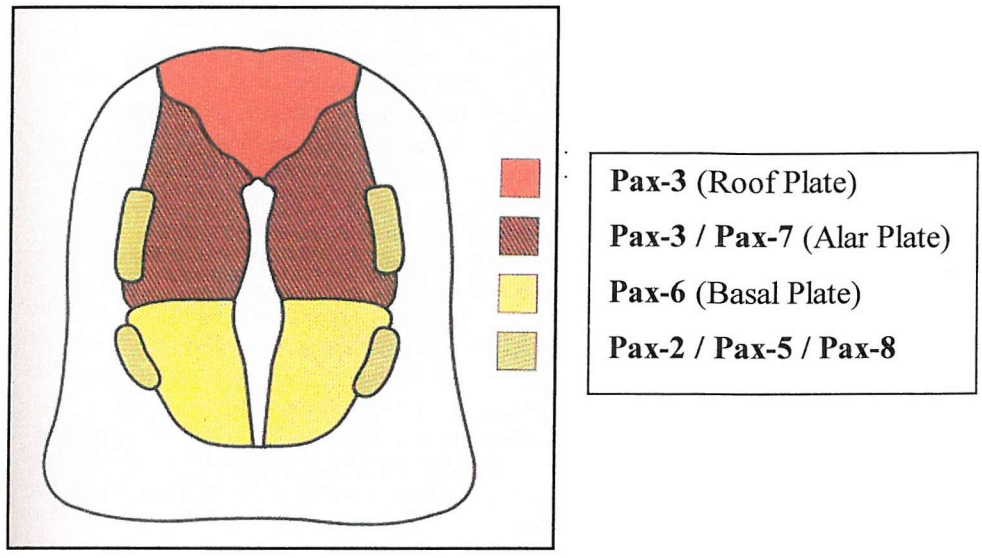

Fig. 1.7 Expression of *Pax-3* and other *Pax* genes in the neural tube

Source: Gruss & Walther (1992)

The figure shows the transverse plane of a mouse spinal chord at day 11 of embryogenesis. *Pax-3* and *Pax-7* are expressed in the alar plate while *Pax-3* alone is seen in the roof plate. *Pax-6* is expressed throughout the basal plate but is not expressed in the floor plate, which is located below the basal plate. *Pax-2*, *Pax-5* and *Pax-8* are expressed in specific regions of the alar and basal plates.

1.6.3 Expression in mesoderm and limb buds

The somites, which are derived from the paraxial mesoderm, are formed during the early stages of embryogenesis on both sides of the neural tube (figure 1.1). Muscle cells and certain structures of the skeleton, are subsequently formed from cells in the somites (Daston *et al.*, 1996, Tremblay *et al.*, 1998). This is illustrated in figure 1.8.

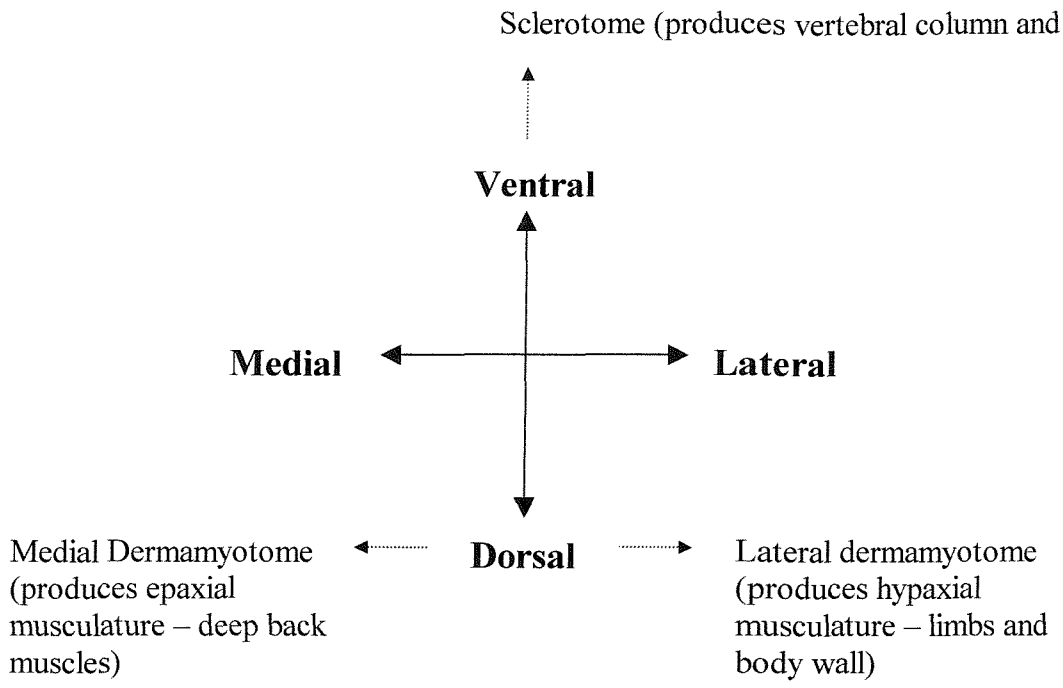

Fig. 1.8 Development of somites in different regions of the neural tube
The fate of cells derived form different regions of the somites surrounding the neural tube are indicated by dashed arrows.

At E9.5, *Pax-3* is expressed in both the dorsal and ventral regions of the developing somites. Between E10 and E11, however, *Pax-3* expression becomes restricted to the dermamyotome, and is upregulated in the lateral dermamyotome. At this time limb muscle precursor cells, which originate from the lateral dermamyotome, migrate to the limb buds where they develop into limb muscle. *Pax-3* is expressed in these migratory cells, and between E9.5 and E11 it is also expressed in the limb buds. Expression of *Pax-3* in the limbs declines after E11 (Bober *et al.*, 1994, Tremblay *et al.*, 1998).

1.7 *Pax-3* mutations and splotch

The mouse splotch mutant is associated with neural tube defects and malformation of structures derived from neural crest cells (Epstein *et al.*, 1991). Homozygous splotch mice die *in utero*, and develop spina bifida and exencephaly. Both these developmental

defects are caused by the neural tube failing to close properly. Neural crest derivatives are also affected such that spinal ganglia, schwann cells and structures of the skull and face all fail to form properly. Heterozygous splotch mice are less severely affected and survive beyond birth. They mainly show pigmentation defects, caused by deficiencies in melanocytes derived from the neural crest.

Mutations in the *Pax-3* gene are responsible for the splotch phenotype seen in mice. *Pax-3* has been mapped to the same region of mouse chromosome 1 as the splotch locus (Epstein *et al.*, 1991). In addition, *Pax-3* is expressed in the same structures that are affected in splotch mice. Several splotch alleles exist. Sp and Sp-delayed (Sp^{d}) are spontaneous mutations, while Sp-retarded (Sp^{r}), Sp^{1H} and Sp^{2H} mutations have been induced by X-irradiation. Sp, Sp^{1H} and Sp^{2H} homozygotes survive until E16 and have spina bifida, exencephaly and fail to form neural crest cell derivatives. Sp^{d} homozygotes suffer only from spina bifida. However, Sp^{r} homozygotes are the most severely affected and are thought to die prior to implantation of the embryo.

The Sp^{r} allele has a deletion in chromosome 1 which includes the *Pax-3* locus. Therefore no Pax-3 protein is produced in homozygous Sp^{r} mice. The Sp^{2H} mutant produces a truncated Pax-3 protein that lacks the entire paired type homeodomain and C-terminal part of the protein. Consequently one of the DNA binding domains and the transcription activation domain are missing from this protein (Epstein *et al.*, 1991).

The Sp allele has a mutation in the 3' splice site of intron 3 of the *Pax-3* gene. This results in 4 differently spliced *Pax-3* mRNAs that have been detected in homozygous splotch mice. In two of these transcripts alternative splice sites have been used in exon 4.

This results in a frameshift and premature termination of translation due to the use of in frame termination codons. In a third transcript intron 3 is retained, which again results in a frame shift that causes premature termination of translation after exon 3. The Pax-3 paired domain and octapeptide are coded for by exons 2-4 of the *Pax-3* gene. The homeodomain and C-terminus of Pax-3 are coded for by exon 5 (Goulding *et al.*, 1991). Consequently Pax-3 proteins coded for by the three transcripts described above will contain only a partial paired domain and will lack everything C-terminal of this. Therefore such proteins will be non-functional. A fourth transcript is produced using the 3' splice site at the end of intron 4 instead of the one at the end of intron 3. This removes exon 4 although no premature termination of translation occurs. However, the Pax-3 protein coded for by this transcript will lack the end of the paired domain and the octapeptide. This is also thought to be a non-functional protein since the splotch phenotype still occurs in mice carrying the Sp allele (Epstein *et al.*, 1993).

The splotch-delayed allele (Sp^d) is the only splotch allele that codes for a full length Pax-3 protein. However this protein contains a single glycine-to-arginine substitution within the paired domain. This inhibits the DNA binding affinity of the Pax-3 paired domain *in vitro*. It also reduces the binding affinity of the homeodomain. These affects on DNA binding are thought to account for the phenotype of homozygous Sp^d embryos (Underhill *et al.*, 1995).

In addition to defects in the developing nervous system and structures derived from neural crest, homozygous splotch mice also fail to develop limb muscles. Between E9.5 and E11 limb muscle precursor cells migrate from the lateral dermamyotome to the limb buds (Daston *et al.*, 1996). *Pax-3* expressing cells show the same distribution pattern as

this in wild type embryos. However, in homozygous splotch embryos *Pax-3* is neither expressed in the lateral dermamyotome or in the limb buds. Consequently limb muscle precursors fail to migrate to the limb buds. As a result these embryos lack forelimb, hindlimb and shoulder muscles, which is evident by E12.5 (Daston *et al.*, 1996, Tremblay *et al.*, 1998).

1.8 Mutations in the human PAX3 gene - Waardenburg syndrome

The human disorder Waardenburg syndrome type I (WS I) has been mapped to a region on the long arm of human chromosome 2. This part of chromosome 2 is homologous to the Sp/*Pax-3* locus on mouse chromosome 1 (Tassabehji *et al.*, 1992). In addition WS causes similar developmental defects to those found in splotch mice. Taken together these findings suggested that WS was the human equivalent of splotch. This was confirmed when it was found that WS patients have mutations in the human PAX3 gene. This gene codes for a protein that shows extremely high amino acid sequence similarity within the paired domain to the mouse Pax-3 protein (Chalepakis *et al.*, 1994). The WS.05 family has a deletion in the PAX3 paired domain, while the WS.15 and WS.Brazil families both have point mutations in the paired domain. All of these mutations decrease the DNA binding activity of the PAX3 protein *in vitro*.

All WS patients are heterozygous for the condition. It is assumed that homozygous WS, if it occurs, causes death *in utero*. Type I WS patients have a facial defect called dystopia canthorum, which is caused by the outward displacement of the inner canthi of the eyes. This defect is absent in type II WS. Other cranio-facial defects are also apparent, which are caused by deficiencies in cranial neural crest cells. In addition WS patients show pigmentation defects, such as a white forelock, and occasionally suffer from

sensorineural deafness (Epstein *et al.*, 1991, Tassabehji *et al.*, 1992). These two symptoms are caused by deficiencies in melanocytes derived from the neural crest. These cells are responsible for pigmentation and they also develop into cells of the ear that are involved in hearing. Some WS patients also show signs of mental retardation. The molecular basis of splotch and WS, as well as the phenotypes associated with these disorders, are summarised in table 1.1.

Table 1.1 Developmental defects of splotch & Waardenburg syndrome

Disorder	*Molecular Defect*	*Homozygous Phenotype*	*Heterozygous Phenotype*
Splotch	Mutation in mouse *Pax-3* gene or deletion at *Pax-3* locus	• Death *in utero* • Spina bifida and Exencephaly • Dysgenesis of structures derived from the neural crest • Lack of limb musculature	• Survive beyond birth • Pigmentation defects • Cranio-facial defects • Curly tail
Waardenburg Syndrome	Mutation in human PAX3 gene		• Facial defect dystopia canthorum (Type I only) • Pigmentation defects • Sensorineural deafness • Mental retardation

1.9 Roles of Pax-3

1.9.1 Cell Proliferation and Differentiation

Pax-3 is a developmental control gene that is expressed in a spatially and temporally restricted fashion during embryogenesis. It is only expressed in dividing cells, being down regulated when these cells start to differentiate (Goulding *et al.*, 1991). This pattern of expression has led to the suggestion that Pax-3 is required to maintain the cells in which it is expressed in a dividing state and prevent the onset of differentiation. The *Pax-2* and *Pax-8* genes, as well as being expressed during embryogenesis, are expressed at high levels in Wilms tumours. This suggests that developmental control genes may also be involved in signalling pathways that lead to cancer. Overexpression of *Pax-3* in fibroblast cells in tissue culture was shown to cause cell transformation (Maulbecker and Gruss, 1993). Fibroblasts that had been stably transfected with a Pax-3 expression vector containing the cytomegalovirus (CMV) promoter were able to grow in soft agar. These cells also displayed anchorage-independent growth and, when injected subcutaneously into mice, induced the growth of well-vascularised tumours.

Rhabdomyosarcomas (RMSs) are pediatric soft tissue tumours of skeletal muscle origin. In the more prevalent form, embryonal RMS, either PAX3 or PAX7 is expressed at elevated levels compared with normal human myoblasts. In the more aggressive form, alveolar RMS, a chromosomal translocation leads to the formation of a fusion protein in which the PAX3 DNA binding domains are linked to the transcriptional activation domain of the forkhead protein FKHR. This fusion protein is a more potent transcriptional activator than PAX3 itself (Bennicelli *et al.*, 1996). In addition both PAX3 and PAX3-FKHR can prevent the differentiation of cultured myoblast cells (Epstein *et al.*, 1995), an effect that is abolished by mutations in the paired domain or

homeodomain of PAX3. This suggests that the role of Pax-3/PAX3 in myogenesis is to stimulate myoblast proliferation and prevent the onset of differentiation until these cells reach the limb buds, where they receive signals to differentiate into functional skeletal muscle cells. Thus enhancement of PAX3 transactivation function in human myoblasts, caused either by elevated PAX3 protein levels or by the formation of a PAX3-FKHR fusion protein, is thought to contribute to the development of RMSs by inducing excessive cell proliferation.

During myogenesis Pax-3 has been implicated in the control of *myoD* and *myf5* expression. Both the MyoD and Myf5 proteins are required during the early stages of myogenesis, to commit multipotential somite cells to the myogenic lineage and subsequently to promote the proliferation and migration of myoblasts. *Myf5* is first expressed in the somites at E8, while *Pax-3* is first expressed in the somites at E8.5 and *myoD* is first expressed here at E10 (Borycki and Emerson, 1997). In cultured cells from the somites of chick embryos, Pax-3 was shown to upregulate *myoD* expression whilst maintaining *myf5* expression (Maroto *et al.*, 1997). Further evidence that Pax-3 is an upstream regulator of *myoD*, was provided by Tajbakhsh *et al.* (1997) using splotch / *myf5* double mutant mouse embryos. In *myf5* single gene knockout embryos, redundancy between the MyoD and Myf5 proteins allows MyoD to compensate for the lack of Myf5. Consequently, the myogenic lineage can still be established in these embryos and so myogenesis still occurs. However in the splotch / *myf5* double mutant mouse embryos, *myoD* was not expressed, and as a result no body muscles were formed. This showed that Pax-3 is required during mouse embryogenesis for *myoD* to be expressed. However, it is not known whether Pax-3 directly activates *myoD* expression or whether it exerts its effects by some indirect mechanism.

Embryonic schwann cells are derived from the neural crest. These immature proliferating cells express Pax-3, but do not express genes that are associated with mature schwann cells such as Myelin Basic Protein (MBP). However, when embryonic schwann cells differentiate to form myelinating schwann cells, expression of *Pax-3* decreases while expression of MBP increases. In cotransfection experiments Pax-3 was shown to repress MBP promoter activity. Pax-3 could also bind *in vitro* to the region of the MBP promoter that mediated this effect (Kioussi *et al.* 1995). Thus Pax-3 may serve to maintain the phenotype of embryonic schwann cells by repressing myelin-specific genes such as MBP.

1.9.2 Cell Migration

During embryogenesis neural crest cells migrate from the dorsal aspect of the neural tube to different regions of the embryo, where they differentiate into both neuronal and non-neuronal cell types. Since neural crest derivatives fail to form properly in splotch mutant embryos, Pax-3 may be required to facilitate the migration of the neural crest cells from which these structures are derived. Indeed, Serbedzija and McMahon (1997) showed that in splotch mouse embryos, neural crest cells fail to emigrate from the neural tube resulting in the loss of neural crest derivatives. Therefore Pax-3 may regulate genes that code for proteins involved in cell adhesion and cell migration. Expression of the N-CAM (neural cell adhesion molecule) gene is strictly regulated during embryogenesis at the time of neural tube closure and neural crest migration. N-CAM is expressed in the developing neural tube as well as in some neural crest derivatives, although it is not expressed in migrating neural crest cells. N-CAM is expressed at lower levels in the neural tubes of splotch mouse embryos than in the neural tubes of wild type embryos (Epstein *et al.*, 1991). In addition to the two isoforms of N-CAM detected in the

developing neural tubes of wild type mouse embryos, a third higher molecular weight isoform is produced in the neural tubes of splotch embryos (Moase and Trasler, 1991). This suggests that Pax-3 is involved in the post-translational modification of the N-CAM protein, which in turn may affect the function of N-CAM in the developing neural tube. It is not clear whether Pax-3 directly affects expression of the N-CAM gene. In cotransfection experiments using fibroblast cells, Pax-3 was shown to repress transcription from the N-CAM promoter. However, Pax-3 failed to bind to this promoter *in vitro*, suggesting that the repression of transcription may have been mediated by squelching (Chalepakis *et al.*, 1994). In contrast, both *Pax-3* and N-CAM are expressed in embryonic schwann cells. However, upon differentiation of embryonic schwann cells into mature myelinating schwann cells, both *Pax-3* and N-CAM are downregulated. Microinjection of *Pax-3* DNA into cultured schwann cells resulted in the induction of N-CAM expression in these cells (Kioussi *et al.*, 1995). This suggested that Pax-3 activates the expression of N-CAM in schwann cells, although a direct stimulatory effect of Pax-3 on the N-CAM promoter has not been demonstrated.

Pax-3 is also required during myogenesis for the migration of limb muscle precursors from the lateral dermamyotome to the limb buds. The *c-met* gene, which codes for a tyrosine kinase receptor protein, has been identified as a molecular target for Pax-3. Like *Pax-3*, *c-met* is expressed in cells of the lateral dermamyotome that generate limb muscle precursors. It is also expressed in the migratory myoblasts that colonise the limb buds, where the receptor for the *c-met* gene product (Scatter Factor/Hepatocyte Growth Factor) is expressed. *C-met* expression is required for limb muscle development as shown by the fact that homozygous *c-met* knockout mice fail to develop limb muscles. As in splotch mouse embryos, the limb muscle precursors of *c-met* knockouts fail to migrate to the

limb buds (Bladt *et al.*, 1995). Down-regulation of *Pax-3* in the lateral dermamyotome of splotch embryos coincides with a lack of *c-met* expression. In cultured myoblast cells over-expression of *Pax-3* led to increased expression of endogenous *c-met* (Epstein *et al.*, 1996). In addition a Pax-3 paired domain binding site in the promoter of the human c-MET gene was sufficient for Pax-3 to activate transcription from this promoter in cell culture. Therefore, during the development of limb muscle, Pax-3 appears to induce the expression of *c-met*, which is essential for the migration of limb muscle precursor cells to the limb buds.

In an experiment by Daston *et al.* (1996) cells taken from the lateral dermamyotomes of wild type and splotch mouse embryos were cultured alone for 2 days and then tested for the expression of myogenin. This gene, expressed during early myoblast differentiation, was not expressed in cells from either wild type or splotch embryos. However, when lateral dermamyotome cells from these embryos were grafted onto the forelimbs of chick embryos, myogenin was expressed in the transplanted cells after two days. Significantly cells taken from splotch embryos (which do not produce a functional Pax-3 protein) as well as from wild type embryos expressed myogenin. This indicates that Pax-3, although required for migration of myoblasts to the limb buds, is not involved in their differentiation into limb muscle.

1.9.3 Cell Survival

Bernasconi *et al.* (1996) showed that down-regulation of the PAX3-FKHR fusion protein in alveolar RMS cells results in increased cell death by apoptosis. Similarly, in embryonal RMS cells that express abnormally high levels of PAX3, down-regulation of PAX3 leads to an increased rate of apoptotic cell death. Therefore PAX3 appears to

promote the survival of cancer cells by inhibiting apoptosis. The anti-apoptotic effects of PAX3 in RMS cells lines are mediated, at least in part, by the upregulation of the anti-apoptotic protein BCL-XL. In cotransfection experiments both PAX3 and PAX3-FKHR activated transcription from a region of the BCL-XL promoter that contains a homeodomain-binding site (Margue *et al.*, 2000).

Pax-3 also seems to promote cell survival during normal embryonic development. An increased rate of apoptotic cell death is associated with the dorsal aspect of the neural tube in homozygous splotch embryos when compared to wild type mouse embryos, which could account for the neural tube defects that are produced in splotch. This suggests that Pax-3, which is expressed in the dorsal neural tube, inhibits apoptosis during embryogenesis. It is thought that the increased level of apoptotic cell death that is observed in homozygous splotch embryos compared with wild type embryos may be mediated by the product of the tumour suppressor gene, p53 (Pani *et al.*, 2002). The p53 protein, which induces apoptosis in response to DNA damage and thus inhibits growth of transformed cells *in vivo*, has also been implicated in the control of apoptosis during embryogenesis. Homozygous splotch embryos that were wild type for p53 were shown to develop neural tube defects, and displayed increased levels of apoptosis in the dorsal aspects of their neural tubes when compared to p53 knockout splotch embryos, which developed without neural tube defects. Moreover, the level of p53 protein was 2-fold higher in homozygous splotch embryos than in wild type embryos. There was no effect on the level of p53 mRNA expression however, implying that the lack of Pax-3 protein in splotch embryos results in the stabilisation of the p53 protein. Therefore during embryogenesis Pax-3 may promote cell survival in the developing neural tube by preventing the accumulation of p53 protein and thus inhibiting p53 dependent apoptosis.

1.10 The Pax-3 protein and DNA binding

The Pax-3 protein is 479 amino acids long. It contains two DNA binding domains, the paired domain and the paired type homeodomain, that are separated by an octapeptide of unknown function. The protein also has domains for the activation and inhibition of transcription. The domain structure of the Pax-3 protein is illustrated in figure 1.9.

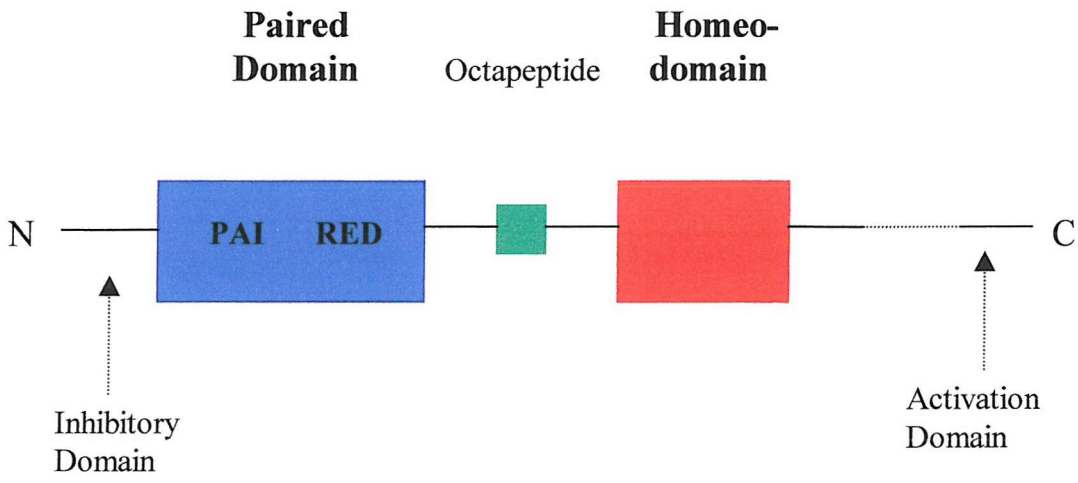

Fig. 1.9 Domain structure of the Pax-3 protein

The paired domain, subdivided into the PAI and RED subdomains, is shown as a blue rectangle. The octapeptide is shown as a green square, while the homeodomain is represented by a red rectangle.

1.10.1 The Paired Domain

The 128 amino acid paired domain is located at the N-terminus of the Pax-3 protein. The first 74 amino acids of the paired domain are basic and highly conserved amongst the paired gene family. The carboxyl 54 amino acids are more divergent. *Pax-3* belongs to a subclass of paired box-containing genes that includes *Pax-7*, the human equivalents of *Pax-3* and *Pax-7*, and the *Drosophila* genes *prd*, *gsb-d* and *gsb-p*. The paired domains

of the proteins coded for by all of these genes have very similar amino acid sequences (Goulding *et al.*, 1991).

The paired domains of Pax proteins consist of two subdomains, each of which contains three α helices. The 2nd and 3rd helices and the 5th and 6th helices form helix-turn-helix motifs in the N-terminal subdomain (PAI domain) and the C-terminal subdomain (RED domain) respectively. Consensus recognition sequences for sequence specific DNA-binding proteins *in vitro* are commonly derived using a PCR based method to select specific binding sites from a random pool of oligonucleotides (Pollock and Treisman, 1990). This method has been used to select a 14 base pair optimal binding sequence for the paired domain of the *Drosophila* prd protein, and a 15 base pair binding site for the paired domain of Pax-3 (Vogan & Gros 1997). The crystal structure of the prd paired domain bound to its consensus binding site showed that the N-terminal subdomain makes sequence specific contacts in the DNA major groove. The third α helix in the N-terminal subdomain (amino acids 47-60) is the recognition helix that makes sequence specific DNA contacts. However, as shown in figure 1.10, the C-terminal subdomain of the prd paired domain does not make contact with the DNA (Xu *et al.*, 1995).

The amino acids in the paired domain from the prd protein that make DNA contacts are all conserved in the Pax-3 paired domain. Moreover the *in vitro* derived Pax-3 paired domain binding site was of similar length to the prd paired domain site, suggesting that the Pax-3 paired domain also binds to DNA using only its N-terminal subdomain. However, this may not always be the case *in vivo* since there are two naturally occurring isoforms of Pax-3 that are generated by alternative splicing, one of which (Pax-3 Q^-) lacks a glutamine residue in the linker region between the two subdomains of the paired

domain (Vogan *et al.*, 1997). In the developing mouse embryo the Q^+ isoform was shown to be twice as abundant as the Q^- isoform. This ratio remained the same from embryonic days 9.5 to 14.5, and in all regions of the embryo where Pax-3 was expressed. However, the paired domain of Pax-3 Q^- could bind twice as strongly as the paired domain of Pax-3 Q^+ *in vitro* to a consensus Pax-6 paired domain site. This Pax-6 binding site is longer (26 base pairs) than the 14 base pair sequence recognised by the paired domain of the prd protein. A crystal structure of the human PAX6 paired domain - DNA complex showed that this paired domain could bind DNA using both its N-terminal and C-terminal subdomains (Xu *et al.*, 1999). In the paired domain of Pax-3 Q^-, the linker region between the two subdomains is equal in length to that of PAX6. Taken together these findings suggest that the paired domain of the Q^- isoform of Pax-3 may bind to DNA using both its N-terminal and C-terminal subdomains.

The crystal structure of the human PAX6 paired domain bound to its consensus-binding site is represented in figure 1.11. The protein-DNA contacts made by the N-terminal subdomain of the PAX6 paired domain are identical to those made by the N-terminal subdomain of the paired domain from the prd protein. However in contrast to prd, the linker region of the PAX6 paired domain makes extensive minor grove contacts, and the C-terminal subdomain makes contacts in the DNA major groove.

Major groove contacts *Minor groove contacts*

Residues: 46, 47, 48, 49, 51, 52 Residues: 14, 15, 69, 70, 71

Contacts with sugar–phosphate backbone

Residues: 6, 7, 12, 14, 15, 16, 17, 18, 23, 36, 37, 41, 45, 46, 49, 51, 52, 56, 65, 66, 69, 70, 71

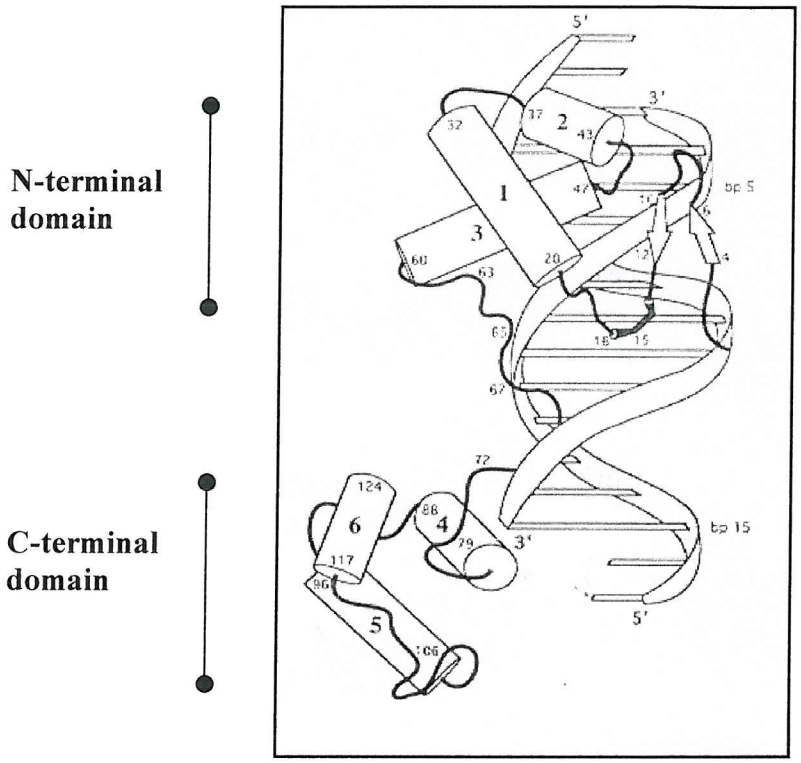

Fig. 1.10 Paired domain – DNA contacts of the *Drosophila* prd protein

The residues in the paired domain of the prd protein that contact DNA are given at the top of the figure. A sketch of the paired domain bound to DNA is shown below, with α helices represented by cylinders and a β sheet represented by arrows (Xu *et al.*, 1995).

N-terminal domain DNA contacts

Direct contacts in minor groove
14, 15

Water-mediated contacts in minor groove
15, 15, 16

Direct contacts in major groove
46, 47, 48, 49

Water-mediated contacts in major groove
48, 52

Contacts with DNA backbone
1, 6, 7, 12, 16, 18, 25, 35, 37, 46, 47, 49, 52, 56

Linker – DNA contacts

Direct contacts in minor groove
69, 69, 70, 71, 74

Contacts with DNA backbone
65, 66, 67, 73, 74, 75, 76

C-terminal domain DNA contacts

Direct contacts in major groove
122, 125

Water-mediated contacts in major groove
118, 121

Contacts with DNA backbone
116, 119, 122 (strand 1)
95, 96, 97, 121, 125 (strand 2)

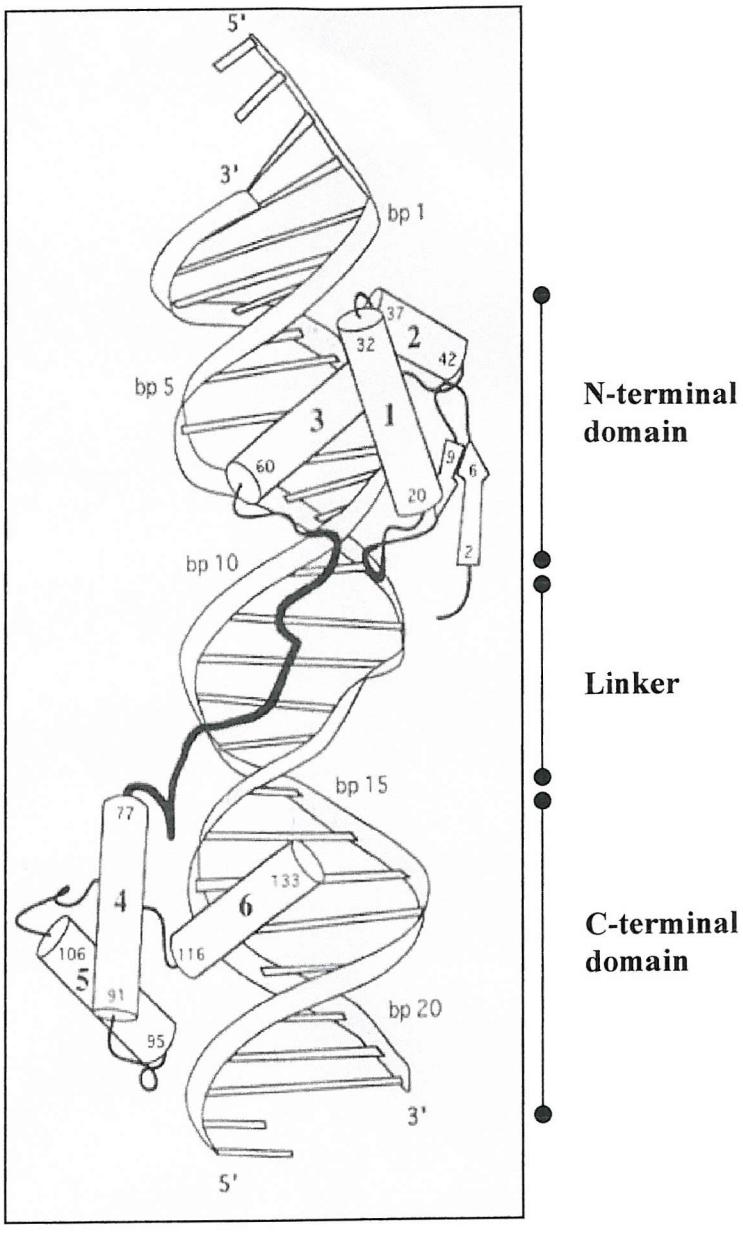

Fig. 1.11 Paired domain – DNA contacts of the human PAX6 protein

The residues in the paired domain of the PAX6 protein that contact DNA are given on the left of the figure. A sketch of the paired domain bound to DNA is shown on the right, with α helices represented by cylinders and the β sheet represented by arrows (Xu *et al.*, 1999).

1.10.2 The Paired Type Homeodomain

The second DNA binding domain in Pax-3 is a paired type homeodomain. This domain is also found in Pax-7, and in the prd, gsb-d and gsb-p proteins. The homeodomains of all these proteins have very similar amino acid sequences (Goulding *et al.*, 1991). As in the individual subdomains of the paired domain, the homeodomain contains three α helices. The 2nd and 3rd helices form a helix-turn-helix motif, with the 3rd helix being the recognition helix that binds to DNA in the major groove. However in contrast to the paired domain, an N-terminal arm precedes the three α helices in the homeodomain. This part of the homeodomain, which has no defined secondary structure, binds to DNA in the minor groove.

Paired type homeodomains bind to palindromic DNA sites that consist of two inverted TAAT half sites. The homeodomains bind to these sites as cooperative dimers. Paired type homeodomains can form both hetero- and homo-dimers on palindromic binding sites. This has been demonstrated *in vitro* for the *Drosophila* prd and gdb-d proteins. Also the Pax-3 protein can form heterodimers with Pax-7 on a palindromic homeodomain site *in vitro* (Schafer *et al.*, 1994). Since *Pax* genes have overlapping patterns of expression during embryogenesis, the formation of heterodimeric complexes between paired type homeodomains may have functional significance for Pax proteins *in vivo*.

In homeodomains the 9th residue of the recognition helix interacts with the base pairs immediately 3' of the TAAT core sequence. These base pairs are situated between the two half sites of the palindromic sequences bound by paired type homeodomains. It was shown that the 9th residue of the recognition helix of the paired type homeodomain

determines the spacing between the two half sites, as well as the nature of the bases present between the half sites and the extent of the cooperative interactions between the two homeodomains. For example when the 9th residue is serine, as in the prd and Pax-3 proteins, the homeodomain binds preferentially as a cooperative dimer to palindromic TAAT sites separated by 2 bases, referred to as a P2 site. However, a glutamine at position 9 facilitates binding to a P3 site in which the two half sites are separated by 3 bases. A high-resolution crystal structure of the homeodomain from the prd protein bound to DNA as a cooperative dimer has been determined (Wilson *et al.*, 1995 and figure 1.12). The two homeodomains interact when bound to the DNA. The N-terminal arm of one homeodomain interacts with helix two of the 2nd homeodomain. The recognition helices of each homeodomain insert into consecutive major grooves of the DNA. Two residues in the recognition helix make direct contacts with DNA bases. Other residues of the recognition helix, including the 9th residue, interact with DNA in the major groove via water molecules. In addition to the recognition helix, the N-terminal arm may also be required for paired type homeodomains to bind to DNA as cooperative dimers. Two residues from the N-terminal arm insert into the minor groove. Here they form both direct and water mediated contacts with the TAAT motif.

The binding of paired type homeodomains to DNA as cooperative dimers increases the binding site specificity of this domain. Palindromic homeodomain binding sites are longer and therefore occur more rarely in the genome than sequences recognised by other classes of homeodomain. In order to attain high binding site specificity other types of homeodomain, which bind to DNA as monomers, have to make use of additional DNA binding domains and cofactors (Wilson *et al.*, 1993).

Direct contacts with bases in the major groove

Val-47 and Asn- 51

Water mediated contacts with bases in the major groove

Ser-50

Direct and water mediated contacts in the minor groove

Arg-2 and Arg-5

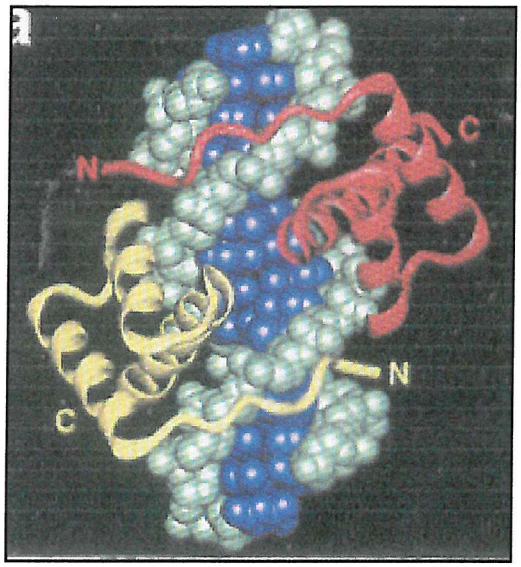

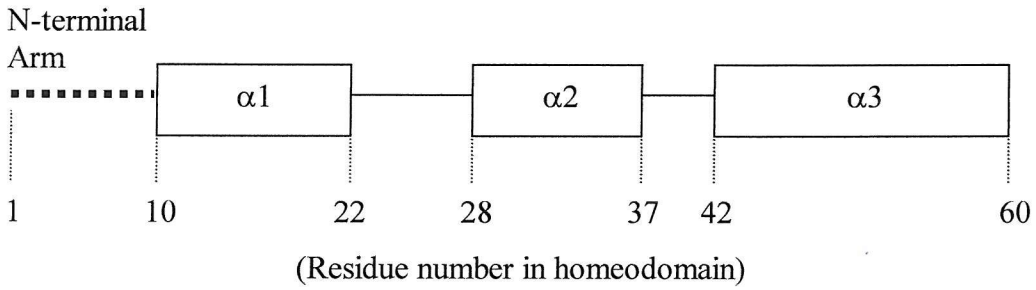

Fig. 1.12 Homeodomain – DNA contacts

The residues in the homeodomain of the prd protein that contact DNA are given at the top of the figure. The picture underneath shows two prd homeodomains (shown as red and yellow ribbons) bound to DNA as a cooperative dimer. The DNA backbone is shown in green, and the bases in blue. The domain structure of the homeodomain is illustrated at the bottom of the figure, showing the position of each α helix in the homeodomain (Wilson *et al.*, 1995).

1.10.3 Domains for transcriptional activation and inhibition

When Pax-3 DNA binding sites are placed in front of a minimal promoter, Pax-3 can use these sequences to modulate the transcription rate of a linked reporter gene (Chalepakis *et al.*, 1994). In cell culture experiments low concentrations of Pax-3 activate transcription whilst higher concentrations inhibit transcription. This suggests that Pax-3 contains domains for both transcriptional activation and inhibition. Thus Pax-3 may be able to activate and repress the transcription of target genes *in vivo*.

To map the transcriptional activation and inhibition domains in Pax-3, fusion proteins were made between the DNA binding domains of the yeast transcription factor GAL4 and various fragments of the Pax-3 protein (Chalepakis *et al.*, 1994). Co-transfecting these fusion proteins with a reporter construct that contained two GAL4 DNA binding sites upstream of TK-CAT (a minimal promoter linked to the CAT reporter gene), showed the effect of different regions of Pax-3 on transcription. It was found that the first 90 amino acids at the N-terminus of Pax-3 (including the first 57 amino acids of the paired domain) strongly inhibited transcription. The 78 C-terminal amino acids of Pax-3 activated transcription. Therefore the N-terminus of Pax-3 contains a transcription inhibition domain while the C-terminus contains a transcription activation domain. The carboxyl portion of the Pax-3 protein is very Pro-Ser-Thr rich. It does not contain any α helical regions. This region of Pax-3 is similar to one found in the Oct-2 protein that is necessary for transcriptional activation by Oct-2 (Tamaka & Herr 1990).

1.10.4 Cooperative interactions between the paired domain and homeodomain

Several Pax proteins including Pax-3 bind *in vitro* to the *e5* sequence. This binding site is derived from the promoter of the *Drosophila even-skipped* gene. It contains an ATTA motif that the homeodomain binds to and a GTTCC motif that the paired domain (PAI subdomain only) binds to. Efficient binding of Pax-3 to the *e5* site requires the presence of both these motifs. This suggests that the paired domain and homeodomain of Pax-3 interact in order to give high affinity DNA binding (Chalepakis *et al.*, 1994).

As already described, as well as binding to *e5*, full-length Pax-3 forms cooperative dimers on a P2 homeodomain site. Pax-3 also binds to a P1 site that contains a single homeodomain motif. However, binding to P1 is a considerably weaker than binding to either P2 or *e5*. The Sp^d mutant Pax-3 protein has an arginine instead of a glycine at position 9 of the paired domain. In wild type Pax-3, this residue is present in a β-turn that joins two antiparallel β-sheets to form a β-hairpin motif. This structure precedes the first α-helical region of the paired domain (Underhill and Gros, 1997. See also figure 1.10 above). When the paired domain binds to DNA, the β-hairpin contacts the sugar-phosphate backbone. It also stabilises the helix-turn-helix motif of the PAI subdomain that binds in the major groove, as well as a second β-turn that contacts the DNA minor groove. The point mutation in the Sp^d Pax-3 protein disrupts the β-turn and consequently destabilises the paired domain–DNA interaction. *In vitro* the Sp^d mutation inhibits binding of Pax-3 to *e5*. Significantly binding of the mutant protein to the P2 site is also inhibited (Underhill *et al.*, 1995). Therefore, in the context of the full-length Pax-3 protein, the paired domain affects the DNA binding properties of the homeodomain. Similarly the homeodomain can influence the binding properties of the paired domain. Full-length Pax-3 binds optimally to a different paired domain recognition sequence

(PRS) than the Pax-1 protein, that contains a paired domain but no homeodomain. However when the homeodomain of Pax-3 is deleted, the PRS bound by this protein is very similar to the one bound by Pax-1 (Chalepakis *et al.*, 1994).

Disruption of the β-hairpin motif, as in the Sp^d mutant Pax-3 protein, inhibits homeodomain – DNA binding itself rather than affecting dimerisation of Pax-3 on P2 sites. This is shown by the fact that the Sp^d mutant protein also fails to bind *in vitro* to the P1 (single homeodomain) site. Within the full-length Pax-3 protein the paired domain also affects the sequence specificity of the homeodomain. Wild type Pax-3 protein binds to P2 sites as cooperative dimers but it binds only weakly to P3 sites as a monomer. However a Pax-3 protein with a large deletion in the paired domain is able to bind to P3 as a dimer. This supports previous findings that isolated homeodomains of the paired class can dimerise on both P2 and P3 sites (Underhill and Gros, 1997).

As well as the β-hairpin motif helix 2 of the Pax-3 paired domain is also a key regulator of homeodomain – DNA binding activity. This is the 1^{st} helix of the helix-turn-helix motif in the PAI subdomain. Removal of this helix has the same affect on homeodomain – DNA binding as disruption of the β-hairpin motif. In addition the linker region between the paired domain and the homeodomain appears to be involved in the interaction between these domains (Fortin *et al.*, 1998).

The paired domain and homeodomain can bind to DNA *in vitro* when expressed on their own in separate polypeptides. However interactions between these two domains occur that affect their DNA binding properties. These interactions may affect the selection of target sites by Pax proteins *in vivo*.

1.10.5 Different modes of DNA binding displayed by Pax proteins

Pax proteins may recognise different target sites *in vivo* by using different combinations of their DNA binding domains. For example the paired domain consists of two subdomains, each of which has the potential to bind DNA via a helix-turn-helix motif. The paired domain of the prd protein binds DNA using only its PAI subdomain. However, Pax-5 and Pax-6 can use both the PAI and RED subdomains to bind DNA. In addition a Pax-6 isoform with an insertion in the PAI subdomain can bind using only the RED subdomain (Jun and Desplan, 1996).

Pax proteins that contain a homeodomain as well as a paired domain may bind to target sites *in vivo* using a combination of these two domains. The prd protein binds most strongly *in vitro* to composite paired domain and homeodomain sites. It binds less well to individual paired domain or homeodomain sites. Moreover in order for prd to function *in vivo* it appears to require both its DNA binding domains (Bertuccioli *et al.*, 1996). As already mentioned Pax-3 can also bind to composite paired domain and homeodomain sites as well as individual binding sites.

Intermolecular interactions between Pax proteins that contain homeodomains could allow these proteins to recognise another set of DNA target sites *in vivo*. For example Pax-3 can bind cooperatively to a palindromic homeodomain site either as a homo-dimer or as a hetero-dimer with Pax-7 (Schafer *et al.*, 1994).

Thus by using different modes of DNA binding Pax / homeodomain proteins can potentially regulate a wide range of target genes. Binding to DNA in different conformations could result in distinct interactions between the C-terminal transactivation

domain of the Pax protein and the basal transcriptional machinery. The Pax protein could also interact with different cofactors, depending on how it was bound to the DNA. This in turn could lead to the activation or repression of different target genes. This is summarised in figure 1.13, where each function represents the targeting of a different set of genes.

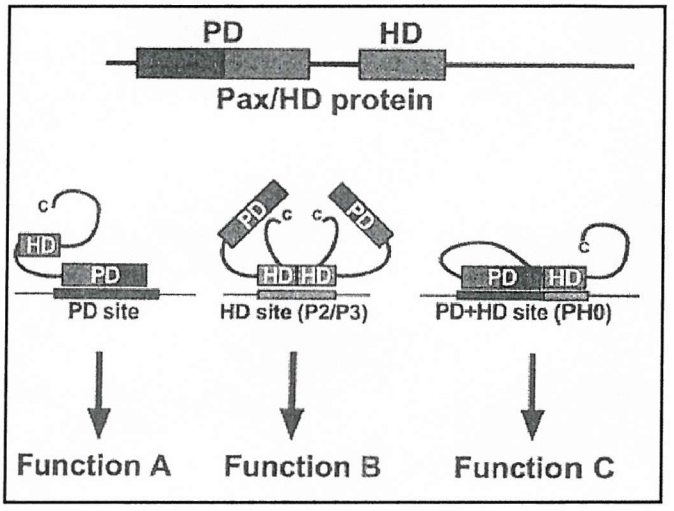

Fig. 1.13 Different DNA-binding conformations of Pax / homeodomain proteins
Pax proteins that contain both a paired domain and a homeodomain could bind to DNA in different conformations *in vivo*. The paired domain alone could bind (PD site). Alternatively the protein could dimerise on a palindromic homeodomain site (P2/P3 site) or the protein could bind to a composite paired domain and homeodomain site (PHO) using both its DNA binding domains (Sheng *et al.*, 1997).

1.11 Aims

Pax-3 plays an important role in both early embryogenesis and in the development of cancer. However, little is known of the factors that control its expression or activity. Therefore the aims of this project were three-fold. Firstly, the potential for Pax-3 activity to be regulated by phosphorylation was to be studied, with particular emphasis being placed on the effect of phosphorylation on Pax-3 DNA binding activity. Secondly, factors that control *Pax-3* expression in neuronal cells were to be investigated. Thirdly, since very few direct Pax-3 target genes have been identified to date, attempts would be made to identify novel molecular targets for Pax-3 in neuronal cells.

Chapter 2

Materials and Methods

2 Materials and Methods

2.1 General Laboratory Chemicals and buffers

General chemicals were purchased mainly from Sigma UK Ltd. or Fisher Scientific Ltd. Enzymes were purchased either from Promega UK Ltd. or Helena Biosciences. Tissue culture products were from Gibco BRL. Protogel was purchased from National Diagnostics and radiochemicals were from Amersham International. Where necessary solutions were sterilised by autoclaving at 115 pounds per square inch for 20 minutes. Antibiotics and other heat sensitive or low volume solutions were sterilised by filtration through a 0.22 μm filter (Millipore UK Ltd.).

2.2 Equipment

Beckman – 21 RPM x 1000 centrifuge for 50-400 ml volumes and 2-30 ml high-speed volumes (>5000 rpm). Sigma 3K10 Howe centrifuge for lower speed (<5000 rpm) volumes less than 50 ml. MSE Microcentaur centrifuge for volumes less than 1 ml. Teche Progene polymerase chain reaction machine. UVP transilluminator and UV camera. R100 Luckham Rotatest orbital shaker. Sartorius balance. Hook and Tucker Rotamixer. Biorad mini-gel apparatus and Semi-dry western transfer cell. Biorad Powerpac 200 and 300. Grant 1000C water bath. Molecular Dynamics STORM phosphorimager. Beckman LS 6500 Scintillation Counter. Biohit Biological Safety Class II Cabinet and Biohit CO_2 incubator.

2.3 Buffers and their contents

Table 2.1

Buffer	Contents
Phosphate buffered saline (PBS)	140 mM NaCl, 2.7 mM KCl, 9.2 mM Na_2HPO_4, 1.84 mM KH_2PO_4 (pH 7.2).
Sodium-tris-EDTA (STE)	0.1 M NaCl, 10 mM Tris-HCl (pH 8.0), 1 mM EDTA
Tris-borate-EDTA 10X conc. (TBE)	450 mM Tris, 400 mM boric acid, 10 mM EDTA (pH 8.0)
Tris-acetate-EDTA 50X conc. (TAE)	2 M Tris-HCl, 57.1 % (w/v) glacial acetic acid, 50 mM EDTA (pH 8.0)
Tris-glycine buffer	25 mM Tris-HCl (pH 8.0), 250 mM glycine, 0.1 % (w/v) SDS
Laemmli buffer	50 mM Tris-HCl (pH 6.8), 100 mM DTT, 2 % (w/v) SDS, 0.1 % (w/v) bromophenol blue, 10 % (w/v) glycerol
Agarose gel loading buffer	15 % Ficoll in sterile water with a small spatula measure of Orange G dye
Western Blot transfer buffer	39 mM glycine, 48 mM Tris-HCl (pH 8.0), 0.037 % (w/v) SDS, 20 % (w/v) methanol
Coomassie blue stain	50 % (w/v) Tri-chloroacetic acid, 0.25 % (w/v) Coomassie blue
Destain	5 % (v/v) acetic acid, 45 % methanol

2.4 Bacterial Growth Media and Solutions

2.4.1 Millers Luria Broth (LB) Medium

LB medium (Gibco BRL) was made up by dissolving 20g of the powdered mix in 1L of distilled water. This was immediately autoclaved.

2.4.2 LB agar

To make plates on which to grow *Escherichia coli*, 1.5 % agar was added to LB before autoclaving. Once the LB-agar had cooled to 50 ^{0}C it was poured onto sterile plastic petri dishes (20 ml/90 cm plates). These plates were allowed to cool to room temperature, air dried at 37 ^{0}C, then stored at 4 ^{0}C.

2.4.3 LB broth and LB agar supplemented with Ampicillin

Bacteria containing plasmids that express the Amp^{r} (ampicillin resistance) gene were grown in LB or on LB-agar plates containing ampicillin. Powdered ampicillin (Sodium salt, Sigma) was dissolved in filter sterilised Anal R water to a final concentration of 100 mg/ml. It was then sterilised by filtration through a 0.2 μm filter, aliquoted (1ml) into eppendorf tubes, and stored at –20 ^{0}C. Ampicillin was added to LB or LB-agar to give a final concentration of 100 μg/ml.

2.4.4 LB agar with X-Gal

When using the blue/white selection plasmids pBluescript and pGEM T-Easy, agar plates that had been supplemented with ampicillin were coated with X-Gal (40 μl of a 20 mg/ml solution in DMSO) 30 minutes before adding the bacterial culture.

2.4.5 2X YT-G Medium

This media was used in the expression of GST-Pax3 fusion proteins. It was made up in distilled water using Tryptone (16g/l), Yeast Extract (10g/l) and NaCl (5g/l). The pH of the media was adjusted to 7.0 with NaOH, and then autoclaved. Once the media had cooled, a sterile 20% (w/v) glucose solution was added to give a final concentration of 2 % glucose. Ampicillin was also added to a final concentration of 100 μg/ml.

2.5 Bacteria and Plasmids

2.5.1 Bacterial strains

DH5α (Gibco BRL) genotype: supE45 Dlac endU169 (ϕ80 lacZ ΔM15) hsdR17 recA1 endA1 gyrA96 thi-1-relA.

2.5.2 Bacterial storage

Long-term storage of bacteria was as a 50 % bacterial culture in LB with 50 % glycerol, placed at –80 ^{0}C. For short-term storage LB agar plates were used. Using a flame-sterilised platinum wire, a bacterial culture was transferred to the plate. The plate was then incubated over night at 37 ^{0}C to allow the bacteria to grow. Following bacterial cell growth the plate was sealed with Parafilm and stored at 4 ^{0}C.

2.5.3 Bacterial cell growth

Routinely, bacteria were grown from a single colony on an LB agar plate. Using a flame-sterilised platinum wire a single colony of bacteria was picked from the plate and transferred to a 10 ml culture of LB medium. Bacteria were grown at 37 ^{0}C overnight on a rotary shaker.

2.5.4 Preparation of Competent *E. coli*

DH5α cells were grown up over night at 37 ^{0}C in LB. 100 µl of the over night culture was diluted into 10 ml of LB. This was grown at 37 ^{0}C to an $O.D_{600}$ of approximately 0.5. The Culture was centrifuged for 10 minutes at 3000 rpm. The pellet was then resuspended in 5 ml of ice cold $CaCl_2$ (100mM - filter sterilised). This was centrifuged for 10 minutes at 3000 rpm, 4 ^{0}C. The pellet was resuspended in 0.5 ml ice cold $CaCl_2$.

2.5.5 Transformation of competent cells

1µl of an ice-cold DNA/ligation mixture was added to 100µl of competent cells. The sample was left on ice for 30 minutes. It was then heat shocked at 42 ^{0}C for 2 minutes to promote the uptake of DNA into the competent cells. After leaving the sample on ice for 30 minutes to recover, 200µl of LB was added to promote growth of the transformed cells. The cells were then spread on LB-ampicillin plates and left to grow at 37 ^{0}C.

2.6 Plasmids and their features

Table 2.2

Plasmid	Relevent Features	Reference
pGEX2T	GST gene fusion vector with an inducible tac promoter. Ampicillin resistance.	Pharmacia
pGEM T-Easy	TA cloning vector. Ampicillin resistance.	Promega
pBluescript	Cloning vector. Ampicillin resistance.	Stratagene
pBabe Puro	Retroviral expression vector containing the SV40 early promoter. Resistance to Ampicillin and Puromycin.	Morganstern & Land (1990)
pcDNA3.1+	Mammalian expression vector containing the CMV promoter. Resistance to Ampicillin and Neomycin	Invitrogen

2.7 Preparation of DNA

2.7.1 Phenol/chloroform extraction

An equal volume of phenol/chloroform (1:1 v/v) was first added to the DNA. The sample was then mixed well in order to denature any protein present, causing it to aggregate and precipitate. Subsequently centrifuging for 3 minutes at 12000 rpm causes the phenol/chloroform to separate from the aqueous layers and the aggregated protein collects at the interface. The top aqueous layer is then removed and the DNA precipitated using ethanol.

2.7.2 Ethanol precipitation

Two volumes of ethanol and 0.1 volumes 3M sodium acetate were added to aqueous DNA. To precipitate the DNA, the sample was left at –20 ^{0}C for 10 minutes and then centrifuged for 10 minutes at 12000 rpm. The resulting DNA pellet was air dried for 2-3 minutes and then re-suspended in the required amount of distilled water.

2.7.3 Small-scale preparation of DNA (Miniprep)

DNA minipreps were used to isolate plasmid DNA from bacteria. The following protocol is a modified version of the one described in Sambrook *et al.* (1989). An over night culture of bacteria containing plasmid DNA was centrifuged for 10 minutes at 2500 rpm. The cell pellet was then suspended in 100µl solution 1 (autoclaved) and left for 5 minutes at room temperature. Solution 1 contains; 50 mM Glucose, 25 mM Tris Cl (pH 8.0), 10 mM EDTA (pH 8.0). 200µl solution 2 (filter sterilised) was then added to the sample. The tube was inverted twice and left on ice for 5 minutes. Samples were inverted carefully to prevent shearing of the genomic DNA. Solution 2 contains; 0.2 M sodium hydroxide, 1 % SDS. 150µl solution 3 (autoclaved) was then added. The tube

was shaken until the sample turned white, then left on ice for 15 minutes. Solution 3 precipitates protein and cell fragments. It contains: 5 M potassium acetate (60 ml), glacial acetic acid (11.5 ml), distilled water (28.5 ml). The sample was then centrifuged at 12000 rpm for 10 minutes. The resulting supernatant contains the plasmid DNA. The pellet contains the genomic DNA, protein and cell fragments. The supernatant was put into a clean tube. Any remaining protein was then removed by phenol/chloroform extraction. The top layer was put into a clean tube, and the plasmid DNA precipitated with 3 volumes of 100% ethanol. The sample was left at -20 ^{0}C for 10-30 minutes and then centrifuged at 12000 rpm for 15 minutes to sediment the DNA. The pellet was washed with 500µl of 70% ethanol to remove excess salts, and then re-suspended in the required amount of AnalR water.

2.7.4 Large-scale preparation (Maxiprep)

450ml of LB broth was inoculated with a static culture of bacteria (5ml) or with a bacterial colony picked from a plate. This culture was grown overnight at 37 ^{0}C on an orbital shaker. The bacteria were harvested by centrifugation at 4000 rpm for 25 minutes at 4 ^{0}C in the Sigma centrifuge. The bacterial pellet was then suspended in 4ml of Sucrose-Tris buffer [25 % (w/v) Sucrose, 50 mM Tris (pH 8.0)] and 1 mg/ml lysozyme. This was left on ice for 15 minutes, and then EDTA was added to a final concentration of 10 mM. The suspension was again left on ice for 15 minutes, before adding a ½ volume of 3x Triton buffer [3 % (w/v) Triton X-100, 150 mM Tris (pH 8.0), 187.5 mM EDTA (pH 8.0)]. The suspension was mixed gently to prevent shearing the genomic DNA and left on ice for 30 minutes. It was then centrifuged in a Beckman centrifuge at 18000 rpm for 1 hour at 4 ^{0}C. The supernatant was transferred to a 50 ml Falcon tube. 4M NaCl was added to give a final concentration of 0.5M. The supernatant was then subjected to a

phenol/chloroform wash to remove any remaining protein followed by a chloroform wash. A 10 % solution of PEG 6000 was added to precipitate the DNA. The PEG was dissolved at 37 ^{0}C and the DNA was allowed to precipitate by leaving the solution at 4 ^{0}C for 1 hour. It was then centrifuged in a Beckman centrifuge at 12000 rpm for 20 minutes at 4 ^{0}C. The supernatant was discarded and the pellet dissolved in 500 µl of 0.1 M Tris (pH 8.0). 10 µl of a 10 mg/ml solution of RNase A was then added to the solution, which was left at 37 ^{0}C for 30 minutes. Following this an equal volume of PEG buffer [10 mM Tris (pH 8.0), 1 mM EDTA (pH 8.0), 1 M NaCl, 20 % (w/v) PEG 6000] was added and the solution left on ice for 1 hour. This was centrifuged at 12000 rpm for 15 minutes. The supernatant was discarded and the pellet dissolved in 400 µl of 10 mM Tris (pH 8.0) and 0.5 M NaCl. A phenol/chloroform extraction and chloroform wash was then carried out. The DNA was precipitated with 3 volumes of 100 % ethanol and 0.1 volumes of 250 mM NaCl. This was left at –20 ^{0}C for 10 minutes and then centrifuged at 12000 rpm for 10 minutes. The DNA pellet was washed with 70 % ethanol. After removing this ethanol the pellet was allowed to air dry and was then re-suspended in 100 µl AnalR water. Finally the DNA was treated with 3 µl of a 10mg/ml solution of RNase A for 1 hour at 37 ^{0}C.

2.8 Analysis and Manipulation of DNA

2.8.1 Restriction digests

Restriction enzymes and 10x restriction enzyme buffers were stored at –20 ^{0}C. Restriction enzymes are stored in glycerol. They were added to reactions such that the final glycerol concentration did not exceed 10 %. This was to prevent loss of enzyme activity. Enzymes were added at an activity of approximately 5-10 units/µg DNA.

2.8.2 Ligation of DNA

Double stranded DNA was ligated using T4 DNA Ligase and 10x ligase buffer. Typically 1:1, 1:3 and 1:6 molar ratios of vector to insert DNA were used to clone DNA fragments into plasmid vectors. 100 ng of vector DNA was used in all ligations. In addition the ligation mixtures contained the required volume of insert DNA, 1µl of 10x ligase buffer [700 mM Tris-HCl (pH 7.5), 70 mM $MgCl_2$, 10 mM DTT, 1 mM ATP] and 3 units of T4 DNA ligase. The reactions were made up to 10µl using nuclease-free water. Tubes containing the reactions were centrifuged to mix the contents and then incubated at 4 ^{0}C over night.

2.8.2.1 Filling in recessed 3' ends of plasmid DNA

Before ligating DNA that has been digested using two different restriction enzymes, blunt ends must be produced from the sticky, non-complementary ends. Therefore DNA of this kind was first heated to 65 ^{0}C for 15 minutes to denature the restriction enzymes. The DNA was then blunt ended using 5 units of DNA Polymerase I large (Klenow) fragment in the presence of 40 µM dNTPs. The reaction mixture was left at room temperature for 30 minutes. The dNTPs fill in the recessed 3' ends of the double stranded DNA. This reaction is catalysed by the Klenow fragment of DNA Pol.I which has 5'-3' DNA Polymerase activity, 3'-5' exonuclease activity, but no 5'-3' exonuclease activity.

2.8.2.2 Phosphatase treating plasmid DNA

When the vector and insert DNA had been cut with the same restriction enzyme, the vector DNA was treated with Calf Intestinal Alkaline Phosphatase prior to ligating with

chances of vector DNA reannealing as opposed to ligating with insert DNA. Cut vector DNA was first phenol chloroform treated and ethanol precipitated to remove the restriction enzyme. The DNA pellet was resuspended in 20 µl of distilled water. 1 unit of calf intestinal alkaline phosphatase (CIP) was then added along with 2.5 µl of 10x alkaline phosphatase buffer. The sample was left at 37 ^{0}C for 30 minutes. In order to stop the reaction 50 µl water, 8.5 µl 10x STE and 3 µl 10 % SDS were added, and the sample was heated to 65 ^{0}C for 15 minutes. The DNA was then phenol/chloroform treated and ethanol precipitated to clean it up prior to ligation with the insert DNA.

2.8.3 Agarose Gel Electrophoresis

DNA samples were separated and characterised by agarose gel electrophoresis. This method was also used to purify specific DNA fragments from agarose gels using a gel extraction kit (Qiagen). 0.6-1.5 % (w/v) agarose gels were used, with higher percentage gels allowing greater separation of low molecular weight DNA fragments, and lower percentage gels giving greater separation of larger fragments. To prepare an agarose gel, a microwave was used to melt the agarose in 1x TAE buffer. Once the gel had cooled to 50 ^{0}C, ethidium bromide was added to a final concentration of 10 µg/ml. The gel was then poured into an electrophoresis tray with plastic combs inserted to form loading wells. Once the gel had set the combs were removed. The gel was then placed into an electrophoresis tank containing platinum wire electrodes that run across the whole width of the tank at both ends. 1x TAE buffer was poured into the tank to cover the gel. DNA samples were then loaded with 0.2 volumes of agarose gel loading dye. A small aliquot of a 1 kbp DNA ladder was added to an adjoining well as a size marker. A voltage of 100V was then applied across the gel. The DNA fragments migrated at different rates according to size such that the smallest fragments migrated the furthest through the gel.

In order to visualise the DNA, the gel was placed under a UV Transilluminator. Ethidium bromide intercalates with the DNA, causing it to fluoresce under UV light.

2.8.4 Quantitation of DNA

The concentration of a DNA sample was estimated by measuring its O.D at 260 nm. 5 µl of the DNA sample was made up to 500 µl with sterile water. This was then placed in a quartz cuvette, and the absorbance measured using the Gene Quant (Pharmacia) spectrophotometer. After multiplying the absorbance reading by the dilution factor, the answer was multiplied by 50 to calculate the DNA concentration in µg/ml, since an O.D of 1 at 260 nm is equivalent to a concentration of 50 µg/ml.

2.9 Polymerase Chain Reaction

2.9.1 Primers

Bluescript – GAAATTAACCCTCACTAAAGGG

Pax-3 Homeodomain – TGACGGAATTCATCAGTTGATTGGC

2.9.2 Primer Design

Oligonucleotides used as PCR primers were bought from Gibco BRL. The following criteria were applied to primer design:

- Primers should be 18-30 nucleotides long
- The T_m (melting temperature) should be approximately the same for both primers
- The G + C content of primers should be approximately 50 % to avoid very high annealing temperatures
- Primers should not contain palindromic sequences that may cause them to fold back on themselves.

2.9.3 PCR Conditions

Each PCR cycle consists of a template denaturation step, followed by a primer annealing step, and then a chain elongation step. Between 30 and 40 PCR cycles were carried out per reaction. DNA templates were denatured at 94 ^{0}C for 40 seconds. The annealing temperature to be used in each reaction was determined by the T_m of the two primers. A temperature of (T_m –2) ^{0}C was used for 40 seconds. The elongation temperature using Taq DNA Polymerase was 72 ^{0}C. The time of this last step is dependent upon the length of the DNA template to be amplified. PCRs were carried out in a total volume of 50 µl. A typical reaction contains: 0.5-1.0 µg template DNA, 300 ng of each primer, 12.5 mM dNTPs, 5 µl 10x reaction buffer [100 mM Tris-HCl (pH 8.3), 500 mM KCl] and 2 units Taq DNA Polymerase.

2.9.4 Isolation of RNA for use in reverse transcriptase (RT) PCR

Cell pellets were resuspended in 1ml TRIZOL® reagent (Invitrogen) and incubated at room temperature for 5 minutes. Next 200µl chloroform was added, the sample shaken for 15 seconds and then incubated for a further 2 minutes at room temperature. The sample was centrifuged for 15 minutes at 12000x g. The top layer was transferred to a new tube, and 500µl isopropanol was added to it. After leaving the sample for 10 minutes at room temperature it was centrifuged for 10 minutes at 12000x g. The supernatant was removed and the pellet allowed to air dry for 2-3 minutes. The RNA pellet was then resuspended in 10µl DEPC-treated water.

2.9.5 cDNA synthesis for use in RT-PCR

cDNA synthesis was carried out in a total volume of 20µl. 1µg RNA was first heated at 65 ^{0}C for two minutes, before being chilled on ice. The RNA was then combined with

4µl of a 1mM dNTP mix, 2µl (20 pmol.) random hexamers, 5mM $MgCl_2$, 2µl 10x reaction buffer [100 mM Tris-HCl (pH 8.3), 500 mM KCl] and 5 units of Avian Myeloblastosis Virus Reverse Transcriptase (Promega). The RT-PCR was carried out at 37 ^{0}C for 1 hour.

2.10 Cell Culture

2.10.1 ND7 cell culture

ND7 cells were grown in tissue culture flasks in DMEM containing 10 % (v/v) foetal calf serum (FCS), 0.4 mM Glutamine and 0.2 % Penicillin/Streptomycin (10000 units/ml penicillin and 10000 µl/ml streptomycin). To transfer ND7 cells to tissue culture plates, a confluent flask of ND7 cells was hit with a hand to disconnect the cells from the flask surface. A sample of cells was then removed for counting on a Neubauer haemocytometer. The cells were plated out to give 5 x 10^5 cells per plate. The volume of each plate was then adjusted to 5 ml with DMEM. All cells were maintained using a Class II biological safety cabinet and a 5% CO_2 incubator at 37 ^{0}C.

2.10.2 Serum starvation of ND7 cells

ND7 cells were grown up on tissue culture plates over night in medium containing 10% FCS. The following morning this medium was removed and the plates washed with DMEM. 5 ml of serum free medium was then added to each plate. The cells were incubated in serum free medium for 24 hours in order to synchronize them so that the vast majority of cells would be in phase G_0 of the cell cycle.

2.10.3 Kelly cell culture

Kelly cells were grown in RPMI medium containing 10 % (v/v) FCS, 0.4 mM Glutamine and 0.2 % Penicillin/Streptomycin (10000 units/ml penicillin and 10000 µl/ml streptomycin). Trypsin-EDTA was used to transfer Kelly cells from flasks to tissue culture plates.

2.10.4 Transfections

Plasmid DNA used to transfect cells was obtained from DNA Maxipreps. DNA was transfected into cells using the calcium phosphate method as described by Gorman (1985). 5µg of DNA and 31µl of 2mM $CaCl_2$ were added to tube A. This tube was made up to a final volume of 250µl. Tube B contained 250µl of 2 x HBS. This was made up as a 10 x stock containing: 8.18 % (w/v) NaCl, 5.94 %(w/v) Hepes, 0.2 % (w/v) Na_2HPO_4. 2 x HBS was used at pH 7.12. The contents of tube A were added dropwise to tube B. This forms a translucent precipitate. The precipitate was pipetted onto the cells, which were then incubated at 37 ^{0}C for 6 hours. Fresh media was then applied to the cells.

2.10.5 Harvesting cells

Media was removed from the plates, which were then washed with 1 x PBS. The cells were then harvested in 1 ml of PBS using a cell scraper. The cells were pipetted into tubes and pelletted by microcentrifuging at 5000 rpm for 3 minutes.

2.10.6 Whole cell extracts

Whole cell extracts were carried out on cell pellets. The extraction buffer used for this contains: 20 mM Hepes pH 7.8, 450 mM NaCl, 0.4 mM EDTA, 0.5 mM DTT, 25 % Glycerol, 0.5 mM PMSF (added just before buffer was used). Each cell pellet was

dissolved in 100 µl extraction buffer. The samples were then freeze/thawed five times (frozen on dry ice and then left at 37 ^{0}C for 3 minutes). The samples were spun for 10 minutes at 12000 rpm and 4 ^{0}C. The supernatants (cell extracts) were kept.

2.10.7 Nuclear/cytoplasmic extracts

Nuclear/cytoplasmic extracts were carried out on cell pellets. These pellets were resuspended in 400 µl of Buffer A [10 mM Hepes (pH 7.9), 10 mM KCl, 0.1 mM EDTA, 0.1 mM EGTA, 1 mM DTT, 0.5 mM PMSF]. Buffer A was stored at -20 ^{0}C and kept on ice during use. PMSF was added to buffer A just before use. After 10 minutes 25 µl NP-40 (10 %) was added, and samples were then vortexed for 10 seconds. Following this, the samples were left on ice for 5 minutes. They were then centrifuged at 13000 rpm for 30 seconds. The supernatant (cytoplasmic fraction) was collected. The pellets were resuspended in 50 µl Buffer C [20 mM Hepes, 0.4 M NaCl, 1 mM EDTA, 1 mM EGTA, 1 mM DTT, 1 mM PMSF] and left on ice for 15 to 30 minutes with mixing. The samples were then spun at 13000 rpm for 5 minutes, and the supernatant (nuclear fraction) was kept.

2.10.8 Protein Assays

BCA protein assay reagents (PIERCE) were used to standardise protein levels in whole cell and nuclear extracts. The BCA protein assay is based upon the biuret reaction in which protein reduces Cu $^{2+}$ to Cu $^{1+}$ under alkaline conditions. Two stable reagents (protein assay reagents A and B respectively) were mixed together in a 50:1 ratio to give one working reagent that contains bicinchoninic acid (BCA). One Cu $^{1+}$ ion binds to two molecules of BCA, resulting in a colour change of the working reagent from green to purple. This purple product has a strong absorbance at 562nm, which is linear with

increasing protein concentrations. Therefore the absorbance recorded for a sample is determined by the amount of protein present in that sample. To compare the amounts of protein present in a range of cell extracts, 5µl of each extract was added to 750µl of BCA working reagent. Two tubes containing working reagent alone were used as controls. All tubes were incubated at 37 ^{0}C for 30 minutes. After this time the O.D of each sample was measured at 560nm, using the control tubes as blanks.

2.10.9 Chloramphenicol Acetyl Transferase (CAT) assay

Cells that had been transiently transfected with DNA by the calcium phosphate method were harvested 50-60 hours post transfection into PBS. The cells were pelleted by microcentrifugation (3000rpm, 3 minutes) and then resuspended in 100µl of 0.25mM Tris-HCL (pH 7.8). The cells were lysed by freeze/thawing (dry ice for 5 minutes, then 37 ^{0}C for 2 minutes) 5 times. The cell fragments were removed by microcentrifugation (13000rpm, 5 minutes) and the supernatant then transferred to a clean tube. The protein content of each sample in an experiment was analysed by BCA protein assay. Then an equal amount of each sample was added to 35µl of 0.5M Tris-HCL (pH 7.8), 20µl of 4mM acetyl CoA and [^{14}C]-chloramphenicol (1µCi). This reaction was made up to 146µl with sterile water and then incubated at 37 ^{0}C for 6 hours. For each sample the chloramphenicol and derivatives were extracted by adding 1ml of ethyl acetate, vortexing for 30 seconds, and then centrifuging at 5000rpm for 3 minutes. The top layer was transferred to a clean tube and dried down using an evacuated rotary evaporator. The chloramphenicol and derivatives were then resuspended in 15µl of ethyl acetate and spotted onto a TLC plate. These samples were then separated by chromatography using chloroform/methanol (95:5). The chloramphenicol and derivatives were visualised using autoradiography and a STORM phosphorimager.

2.11 Purification and Detection of GST-Pax3 Fusion Proteins

2.11.1 Expression of GST-Pax3 Fusion Proteins

Colonies of DH5αs transformed with pGEX vectors were picked from LB-ampicillin plates and grown over-night in 10ml of 2X YT-G media supplemented with (100 μg/ml) ampicillin. The next day 100μl of these over-night cultures were added to 10ml of fresh media, and these cultures were then grown for 3-4 hours at 37 ^{0}C. Then, during the log phase of growth, these cultures were induced with 100mM IPTG at 37 ^{0}C. After 3 hours the cultures were centrifuged for 10 minutes at 12000 rpm. Cell pellets were resuspended in 0.5ml of ice-cold PBS and transferred to clean tubes. Cells were then lysed by sonication. Samples were sonicated on ice in short bursts until they had partially cleared. The tubes were then centrifuged at 12000 rpm for 5 minutes to remove insoluble material. The supernatants were transferred to clean tubes. 20μl of a 50% slurry of Glutathione-Sepharose 4B (Amersham Pharmacia) were added to each supernatant. The tubes were then mixed gently on a roller over-night at 4 ^{0}C. The next day the tubes were centrifuged at 12000 rpm for 1 minute to sediment the beads. Supernatants were discarded, and the beads washed 3 times with 500μl of PBS to remove non-specifically bound proteins. The beads were then resuspended in 10μl of distilled water and 10μl of 2X SDS loading buffer. Samples were then analysed by SDS-PAGE and Western blotting.

2.11.2 SDS-Polyacrylamide Gel Electrophoresis (SDS-PAGE)

SDS-PAGE is used to separate proteins according to size. SDS, an anionic detergent, denatures proteins and gives them an overall negative charge. DTT is also added to reduce disulphide bridges. The charge to mass ratio of all proteins under these conditions is approximately equal. Thus electrophoresis separates these proteins according to size

alone. The polyacrylamide gel acts as a molecular sieve, allowing small proteins to travel further during electrophoresis than large proteins.

To prepare a 10 % SDS gel a resolving gel was first made using the following: 4 ml water, 3.3 ml of 30% Protogel (to give 10% acrylamide final concentration), 2.5 ml of 1.5M Tris (pH 8.8), 0.1 ml of 10% SDS, 0.1 ml of 10% ammonium persulphate, 4µl TEMED. Immediately after adding TEMED, the resolving gel was poured between two glass plates so that they were ¾ filled. A layer of butanol was then added to the top of the gel to level it out. Once the gel had set the butanol was poured off. A 5% stacking gel was then added on top of the resolving gel. This was made using the following: 2.7 ml water, 0.67 ml of 30% Protogel, 0.5 ml of 1M Tris (pH 6.8), 40µl of 10% SDS, 40µl of 10% ammonium persulphate, 4µl TEMED. A gel comb was inserted into the stacking gel, and the gel was left to set. Once the gel had set the comb was removed and the gel apparatus was lowered into an electrophoresis tank, which was then filled with 1 x Tris-Glycine running buffer. Using a needle and syringe the wells were washed with running buffer. An equal volume (typically 10 µl) of 2 x SDS loading buffer was added to each protein sample. The samples were then boiled for 5 minutes to denature them. A Gilson pipette was used to load the protein samples and an aliquot of molecular weight marker into the wells. The protein gel was run at 200V for approximately 40 minutes. It was then either stained for 10 minutes with Coomassie blue and destained in 45 % methanol / 5 % acetic acid, or transferred onto a Hybond-C transfer filter for Western blotting.

2.11.3 Western blotting

Proteins were transferred from the SDS-Polyacrylamide gel to a Hybond-C nitrocellulose membrane (Amersham International) by electrophoresis, using a Semi-Dry Transfer

Apparatus (Biorad). Six pieces of 3MM chromatography paper (Whatman International) and one nitrocellulose membrane were cut to the exact size of the protein gel. The membrane was first soaked in methanol for 1-2 minutes. The membrane and six filter papers were then soaked in a small amount of transfer buffer (20% methanol, 1x Tris-Glycine buffer) for 5 minutes. Following this, all sheets were assembled on the Semi-Dry Transfer Apparatus. Three sheets of filter paper were placed on top of the anode. Air bubbles were removed using a roller, and the membrane was then aligned on top of these filter papers. The gel was placed exactly on top of the membrane. The other three filter papers were then placed on top of the gel. Air bubbles were removed as before. The cathode was placed on top of this stack. A current of 100 mA was applied for 1 hour to transfer the proteins. The gel was then stained in Coomassie Blue to check that transfer of proteins to the membrane had occurred.

The membrane was then placed in a small amount (30-40 ml) of 10% (w/v) non-fat dried milk (Marvel) dissolved in PBS-0.1% Tween. The membrane was blocked for 30-60 minutes at room temperature, or at 4^0C over-night. This reduces the amount of antibody bound non-specifically to the membrane. Excess Marvel was then removed from the membrane by rinsing it twice in PBS-0.1% Tween, followed by two five-minute washes in PBS-0.1% Tween.

A primary antibody that recognises the target protein was then applied to the membrane. Primary antibodies were dissolved in 5% (w/v) Marvel-PBS-0.1% Tween, at concentrations ranging from 1:500 to 1:2000. The antibody was added to the membrane in a 50 ml Falcon tube. This was left on a roller for 1 hour at room temperature, or at 4

^{0}C over night. The membrane was then subjected to three five-minute washes in PBS-0.1% Tween to remove non-specifically bound antibody.

In order to detect bound primary antibody, the membrane was incubated with a secondary antibody, dissolved in 5% (w/v) Marvel-PBS-0.1% Tween. This was left for 45 minutes at room temperature with shaking. Secondary antibodies were conjugated to HRP (Horse Raddish Peroxidase). The reaction catalysed by this enzyme emits light, which can be detected by exposure to X-ray film.

Membranes were then washed three times in PBS-0.1% Tween. This was followed by three one-minute washes in distilled water. Membranes were then developed using the Enhanced Chemiluminescence (ECL) kit from Amersham International.

2.12 *In Vitro* phosphorylation of GST-Pax3 fusion proteins

Equal amounts of GST and GST-Pax3 proteins were used in 20 µl kinase assays with the purified catalytic subunits of Protein Kinase C (PKC) and Protein Kinase A (PKA). PKC reactions contained 10mM $MgCl_2$, 10mM $CaCl_2$, 30 µCi [γ-^{32}P] ATP and 10ng of PKC catalytic subunit. PKA reactions contained 10mM $MgCl_2$, 10mM $CaCl_2$, 30 µCi [γ-^{32}P] ATP and 25 units of PKA catalytic subunit. Kinase reactions were carried out at 37 ^{0}C for 30 minutes. The glutathione beads were then washed three times with 200 µl PBS to remove unincorporated [γ-^{32}P] ATP. The beads were then resuspended in 10µl distilled water and 10µl 2x SDS-loading buffer. The samples were boiled for 5 minutes before being run out on a 10% SDS-Polyacrylamide gel. This gel was stained with Coomassie Blue, destained and then dried down on a gel drier. It was then placed in a cassette and exposed to X-Ray film at –80 ^{0}C. The film was developed and then aligned with the

protein gel in order to determine whether any of the proteins of interest had been phosphorylated.

2.13 Analysis of Pax-3 DNA binding activity

2.13.1 The Electrophoretic mobility Shift Assay (EMSA)

The electrophoretic mobility shift assay is used to study the binding of a protein to a specific DNA sequence. The DNA binding activity of many transcription factors has been analysed in this way. The protein is mixed with a radiolabelled oligonucleotide probe containing a binding site for that protein. The mixture is then electrophoresed on a non-denaturing polyacrylamide gel. Free unbound DNA runs to the bottom of the gel, whereas DNA which has protein bound to it moves more slowly through the gel. This results in a 'band shift' (an name more commonly used for EMSAs), which can be detected by autoradiography.

2.13.2 Thrombin Digestion of GST-Pax3

In order to study the DNA binding properties of the bacterially expressed Pax-3 protein, it was first cleaved from its GST protein tag using thrombin protease (Pharmacia). To do this GST-Pax3 protein was bound to 40µl of glutathione-sepharose 4B (50% slurry) over-night at 4 ^{0}C. The beads were then washed 3 times with PBS and resuspended in 40µl of distilled water. 1µl of thrombin solution (1 cleavage unit / µl in PBS) was then added. The reaction was mixed gently at 28 ^{0}C for 3 hours. The glutathione-sepharose 4B was then sedimented by centrifugation at 12000 rpm for 4 minutes. The supernatant, containing the Pax-3 protein, was transferred to a clean tube.

2.13.3 Probe Labelling

The oligonucleotides used in band shifts with Pax-3 are listed below. All oligonucleotides were purchased from either Oswel or Gibco BRL.

e5 5' CTCAGCACCGCACG**ATTA**GCACC**GTTCC**GCTTC 3'

met 5' AGACTCG**GTCCC**GCTTATCTC 3'

P1 5' GATCCTGAGTC**TAAT**TGAGCGTCTGTAC 3'

P2 5' GATCCTGAGTC**TAATTGATTA**CTGTACAGG 3'

SRE 5' GGGAGGCTCACATAGGGAGCTCAG 3'

DNA probes were annealed by mixing equimolar amounts of complementary oligonucleotides at 80 ^{0}C for 5 minutes, before allowing them to cool slowly to room temperature. 25ng of the annealed oligonucleotide was then labelled in a 50µl reaction containing 5 units of T4 polynucleotide kinase, 20µCi [γ-^{32}P] ATP, in the presence of 50mM Tris-HCl (pH 7.6), 10mM $MgCl_2$, 5mM DTT and 0.1mM EDTA. Labelling was carried out at 37 ^{0}C for 30 minutes. The reaction was then made up to 100µl with distilled water, and the labelled oligonucleotide separated from unincorporated label by centrifugation (1000 rpm for 5 minutes) through a 1ml G-25 sephadex column.

2.13.4 EMSA DNA Binding Conditions

Band shift reactions contained 7µl of supernatant from the thrombin digest (containing Pax-3 protein), 10µl 2x Parker Buffer [40mM Hepes (pH 7.4), 100mM KCl, 2mM 2-mercaptoethanol, 20 % glycerol], 1µg poly dIdC, and were made up to 20µl with distilled water. In competition reactions 50-500 fold molar excesses of specific or non-specific oligonucleotides were also added. The reactions were left on ice for 10 minutes.

Radiolabelled oligonucleotide was then added at 200 counts per second. Following this the reactions were left at room temperature for 10 minutes, and then loaded onto a 4% acrylamide, 0.25% TBE gel which had been pre-run for 30 minutes at 150V. Samples were then electrophoresed for 2.5 hours at 150V. Subsequently the gel was dried down and the results analysed by autoradiography or phosphorimage analysis.

2.13.5 The Effect of Phosphorylation on the DNA Binding Activity of Pax-3

The effect of kinase phosphorylation on the DNA binding activity of Pax-3 was tested by first treating the protein with a protein kinase in the presence or absence of ATP *in vitro*. Pax-3 protein was added to a 26µl reaction containing 13µl of 2x Parker buffer, 1µg of poly dIdC, 1mM $MgCl_2$, 1mM $CaCl_2$ and 30µM ATP (or 1µl of water in the negative control). Reactions were left on ice for 10 minutes. The protein kinase was then added and the reactions left at 37 ^{0}C for 30 minutes. Subsequently the radiolabelled oligonucleotide probe was added at 200 counts per second and the reactions left at room temperature for 10 minutes, before being resolved on a 4% non-denaturing gel as described. The gel was then dried down and the results analysed by autoradiography.

Chapter 3

Phosphorylation of Pax-3

3 Phosphorylation of Pax-3

3.1 Introduction

Post-translational modification plays an important role in the control of transcription factor activity. In particular there are many examples of transcription factors being regulated by phosphorylation. The nuclear localisation of transcription factors can be controlled by phosphorylation, as in the case of NF-κB. In its inactive state, this transcription factor is sequestered in the cytoplasm bound to the inhibitory protein IκB. Upon phosphorylation of IκB, the protein complex dissociates allowing NF-κB to translocate to the nucleus and activate transcription of its target genes. Phosphorylation can also alter the transactivation properties of transcription factors by affecting the way their transactivation domains interact with the transcriptional machinery on a promoter. For example CREB is phosphorylated in a region close to its transactivation domain by PKA. This results in greater transcriptional activation of cyclic AMP responsive genes. In addition the phosphorylation of a transcription factor often affects its DNA binding activity. Phosphorylation can have a negative effect on DNA binding by causing electrostatic repulsion between phosphate groups on the protein and the negatively charged DNA. This is the case for the c-Jun protein, which binds to TPA response elements (TREs) in the promoters of its target genes, either as a homodimer or by forming heterodimers with Fos. Activation of PKC is thought to lead to the activation of a protein phosphatase, which then dephosphorylates c-Jun leading to an increase in binding affinity for TRE. Phosphorylation can also increase the DNA binding affinity of a transcription factor, possibly by inducing a conformational change in the protein. For example the serum response factor (SRF) binds to the serum response element (SRE) in the promoter of the c-fos gene, resulting in the transcriptional activation of this gene. Phosphorylation of SRF in a region N-terminal to its DNA binding domain is thought to

induce a conformational change in the protein that increases its affinity for the SRE. In addition some transcription factors display altered binding site specificity in response to phosphorylation. For example the POU protein Pit-1 is phosphorylated by PKA at a site in its homeodomain that is conserved throughout the POU domain family of proteins. Binding to some POU domain sites is decreased when Pit-1 is phosphorylated by PKA, whereas binding to other sites is either unaffected or is increased (Kapiloff *et al.*, 1991). At DNA sites where Pit-1 binding is unaffected, the conformation of the protein on the DNA was shown to change in response to phosphorylation. This in turn could change the way the activation domain of Pit-1 interacts with the transcriptional machinery *in vivo*. Therefore even when the DNA binding activity of the protein is unchanged, the ability of Pit-1 to activate transcription of its target genes may be affected by phosphorylation.

Little is known about the effect phosphorylation has on the activity of the Pax family of proteins. Poleev *et al.* (1997) showed that the ability of Pax-8 to activate the Pax8-TK-CAT reporter construct in which a Pax-8 binding site was placed upstream of the thymidine kinase (TK) minimal promoter was enhanced in response to PKA. However, *in vitro* kinase assays failed to reveal PKA phosphorylation of a recombinant GST-Pax8 protein, even though a potential PKA motif occurred at two positions in the Pax-8 sequence. Furthermore, immunoprecipitation of Pax-8 from cells grown in the presence of [^{32}P] orthophosphate showed that although Pax-8 was phosphorylated in growing cells its phosphorylation state was not influenced by activation of the cyclic AMP signalling pathway. This implied that PKA activates Pax-8 by a mechanism other than direct phosphorylation of the protein. A cell line deficient in both PKA and Pax-8 was cotransfected with a Pax-8 expression vector and the Pax8-TK-CAT reporter. A modest induction of the CAT reporter was observed when compared to cells transfected with

Pax8-TK-CAT alone. However, the level of activation of Pax8-TK-CAT was significantly increased when the cells were also transfected with a PKA expression vector. In further studies, different regions of the Pax-8 protein were fused to the DNA binding domain of GAL4. These Pax-8 deletion mutants were cotransfected into the PKA/Pax-8 deficient cell line with a GAL4-TK-CAT reporter construct. As seen with the Pax8-TK-CAT transfections, strong induction of GAL4-TK-CAT was observed in response to PKA. This effect was dependent upon the transactivation domain of Pax-8. Thus it was proposed that the activation of Pax-8 by PKA was mediated through its activation domain with no direct phosphorylation of Pax-8 by PKA. It may be that PKA alters the phosphorylation state of a coactivator, which in turn allows the Pax-8 transactivation domain to interact more efficiently with the transcriptional machinery.

Prosite (an online database) was used to scan the entire Pax-3 amino acid sequence for potential protein kinase phosphorylation sites. The results of this scan with regards to potential PKA and PKC sites are shown in figure 3.1. According to the Prosite database, Pax-3 does not contain any PKA sites but it does contain six potential PKC sites. It is possible for protein kinases to phosphorylate substrates at sites that do not conform to the full consensus sequence for that enzyme. Therefore Pax-3 may be phosphorylated by PKA even though it contains no consensus PKA sites. Thus it was important to determine whether Pax3 could be phosphorylated *in vitro* by PKA and PKC, since phosphorylation may affect the activity of Pax-3 *in vivo*.

1 MetThrThrLeuAlaGlyAlaValProArgMetMetArgProGlyProGlyGlnAsnTyrProArgSer 23

24 GlyPheProLeuGluValSerThrProLeu**GlyGlnGlyArgValAsnGlnLeuGlyGlyValPheIle** 46

47 **AsnGlyArgProLeuProAsnHisIleArgHisLysIleValGluMetAlaHisHisGlyIleArgPro** 69

70 **CysValIleSerArgGlnLeuArgValSerHisGlyCysValSerLysIleLeuCysArgTyrGlnGlu** 92

93 **ThrGlySerIleArgProGlyAlaIleGlyGlySerLysProLysGlnValThrThrProAspValGlu** 115

116 **LysLysIleGluGluTyrLysArgGluAsnProGlyMetPheSerTrpGluIleArgAspLysLeu** 137

138 **LeuLysAspAlaValCysAspArgAsnThrValProSerValSerSerIleSerArgIleLeuArgSer** 160

161 **LysPheGlyLys**GlyGluGluGluGluAlaAspLeuGluArgLysGluAlaGluGlu**SerGluLys**Lys 183

184 AlaLys**HisSerIleAspGlyIleLeu**SerGluArg**AlaSer**AlaProGlySerAspGluGlySerAspIle 207

208 AspSerGluProAspLeuProLeuLysArgLys**GlnArgArgSerArgThrThrPheThrAlaGlu** 229

230 **GlnLeuGluGluLeuGluArgAlaPheGluArgThrHisTyrProAspIleTyrThrArgGluGlu** 251

252 **LeuAlaGlnArgAlaLysLeuThrGluAlaArgValGlnValTrpPhe**SerAsnArg**ArgAlaArg** 273

274 **TrpArgLysGlnAlaGly**AlaAsnGlnLeuMetAlaPheAsnHisLeuIleProGlyGlyPheProPro 296

297 ThrAlaMetProThrLeuProThrTyrGlnLeuSerGluHisSerTyrGlnProThrSerIleProGlnAla 320

321 ValSerAspProSerSerThrValHisArgProGlnProLeuProProSerThrValHisGlnSerThrIlePro 345

346 SerAsnAlaAspSerSerSerAlaTyrCysLeuPro**SerThrArg**HisGlyPheSerSerTyrThrAspSer 369

370 PheValProProSerGlyProSerAsnProMetAsnProThrIleGlyAsnGlyLeuSerProGlnValMet 393

394 GlyLeuLeuThrAsnHisGlyGlyValProHisGlnProGlnThrAspTyrAlaLeuSerProLeuThrGly 417

418 GlyLeuGluProThrThrThrValSerAlaSerCys**SerGlnArg**LeuGluHisMetLysAsnValAsp 440

441 SerLeuProThrSerGlnProTyrCysProProThrTyrSerThrAlaGlyTyrSerMetAspProValThr 464

465 GlyTyrGlnTyrGlyGlnTyrGlyGlnSerLysProTrpThrPhe

Fig. 3.1 (A) The Pax-3 amino acid sequence, showing the locations of potential PKC phosphorylation sites, as determined using the Prosite online database

The paired domain (aa 34-164), octapeptide (aa 186-193) and homeodomain (aa 219-279) are shown in bold. Potential PKC sites are shown in red.

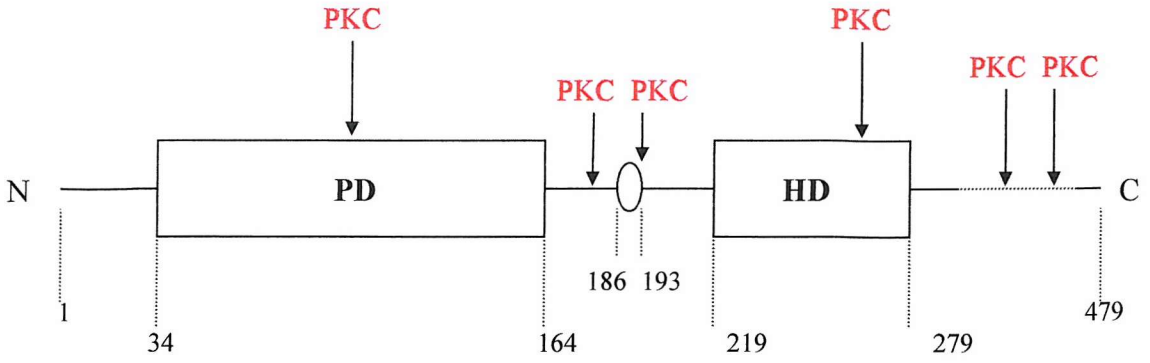

Fig. 3.1 (B) Domain Structure of the Pax-3 protein, showing the locations of potential PKC phosphorylation sites, as determined using Prosite

PD, paired domain; HD, homeodomain; ◯ = octapeptide. The numbers refer to amino acids residues in the Pax-3 protein.

3.2 Cloning and Expression of a GST-Pax 3 Fusion Protein

In order to determine whether Pax-3 could be phosphorylated by PKA and PKC, purified Pax-3 protein was prepared. To achieve this a mouse full length *Pax-3* cDNA was subcloned from the Bluescript II SK plasmid into the pGEX2T vector. The entire coding region plus 560 nucleotides of 3' untranslated sequence (UTR) of *Pax-3* had previously been cloned into the pBluescript II SK vector. This 2000 base pair cDNA sequence was engineered to contain a BamHI cleavage site just upstream from the ATG translation start codon. It also has an EcoRI cleavage site at its 3' end.

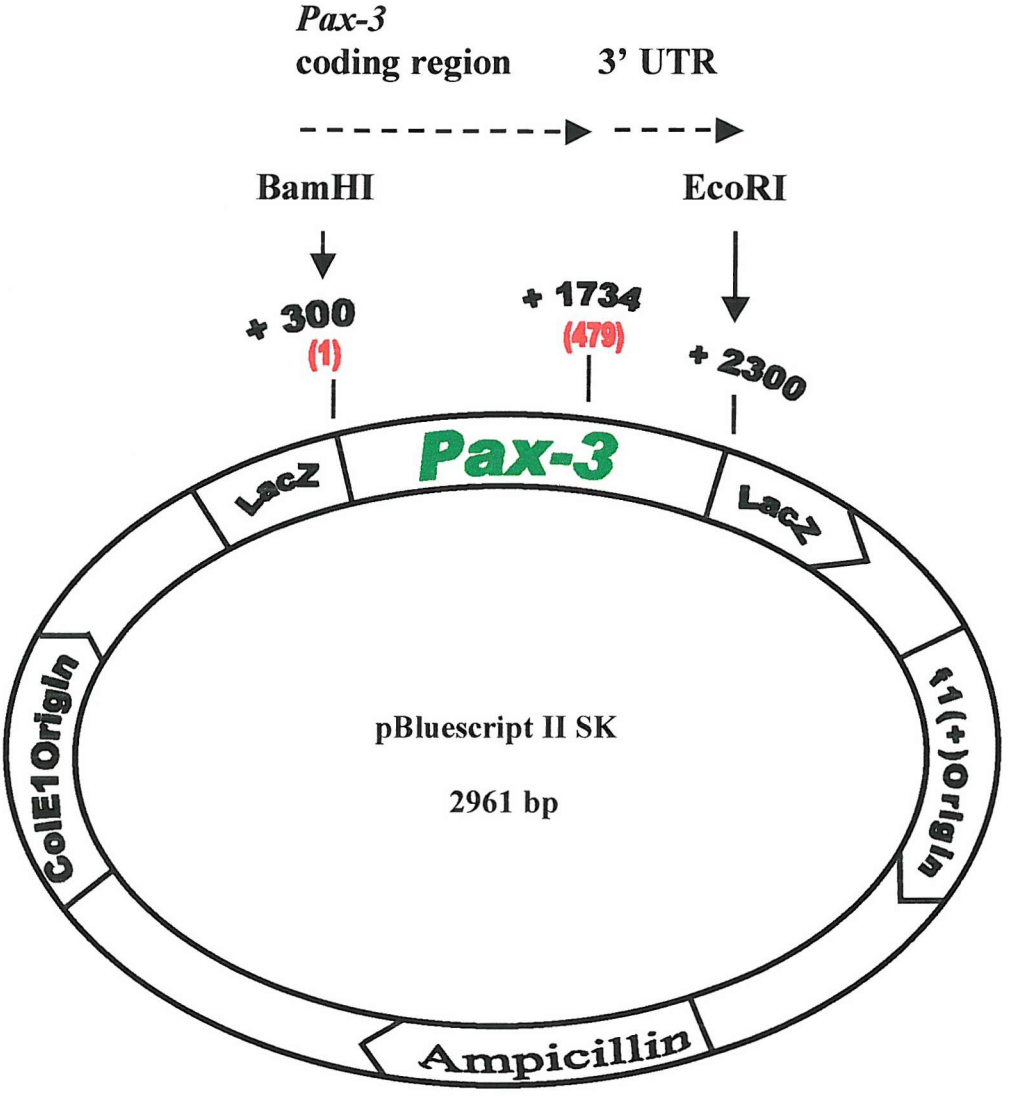

Fig. 3.2 Schematic diagram to show *Pax-3* cDNA cloned into pBluescript II SK
Numbers that are preceded by + signs refer to the *Pax-3* cDNA. The numbers in red are the corresponding amino acids in the Pax-3 protein.

To clone *Pax-3* into the pGEX2T vector, the *Pax-3* cDNA sequence was excised from the pBS-*Pax3* construct using BamHI and EcoRI and subcloned into the BamHI and EcoRI sites of pGEX2T. Attempts were then made to express a GST-full length Pax-3 fusion protein in DH5α cells. However no soluble Pax-3 protein was obtained.

3.2.1 Purification of the DNA binding domains of Pax-3

Since a full length Pax-3 protein could not be expressed, a GST fusion protein containing only the DNA binding domains (DBDs) of Pax-3 was cloned and expressed. Kinase assays were then carried out to determine whether this region of the Pax-3 protein, which contains multiple phosphorylation sites, could be phosphorylated *in vitro* by PKA and PKC. As shown in figure 3.3, a PCR assay was used to clone the DNA binding domains of Pax-3.

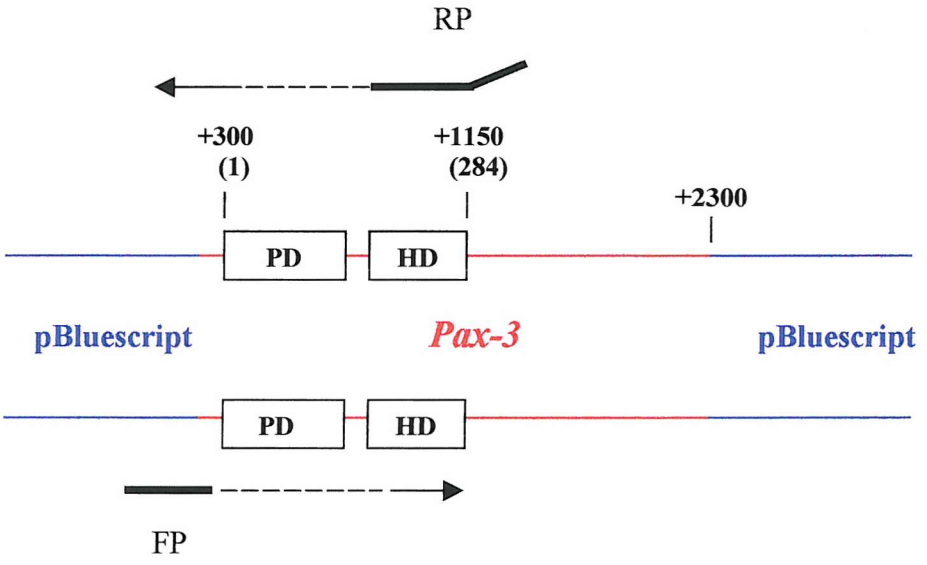

Fig. 3.3 Amplification of the Pax-3 DNA binding domains by PCR

An 850 base pair region of *Pax-3* cDNA that contains the coding regions for both DNA binding domains of Pax-3 was amplified by PCR. The forward primer anneals to pBluescript II SK immediately 5' to the BamHI site at the start of *Pax-3*. The reverse primer, which contains an EcoRI site, anneals to *Pax-3* at the end of the homeodomain-coding region. The numbers with + signs before them refer to the *Pax-3* cDNA. The numbers in brackets are the corresponding amino acids in the Pax-3 protein. PD, paired domain; HD, homeodomain.

The PCR product was first ligated into the pGEM-T Easy vector. It was then subcloned from pGEM-T Easy into pGEX2T using BamHI and EcoRI.

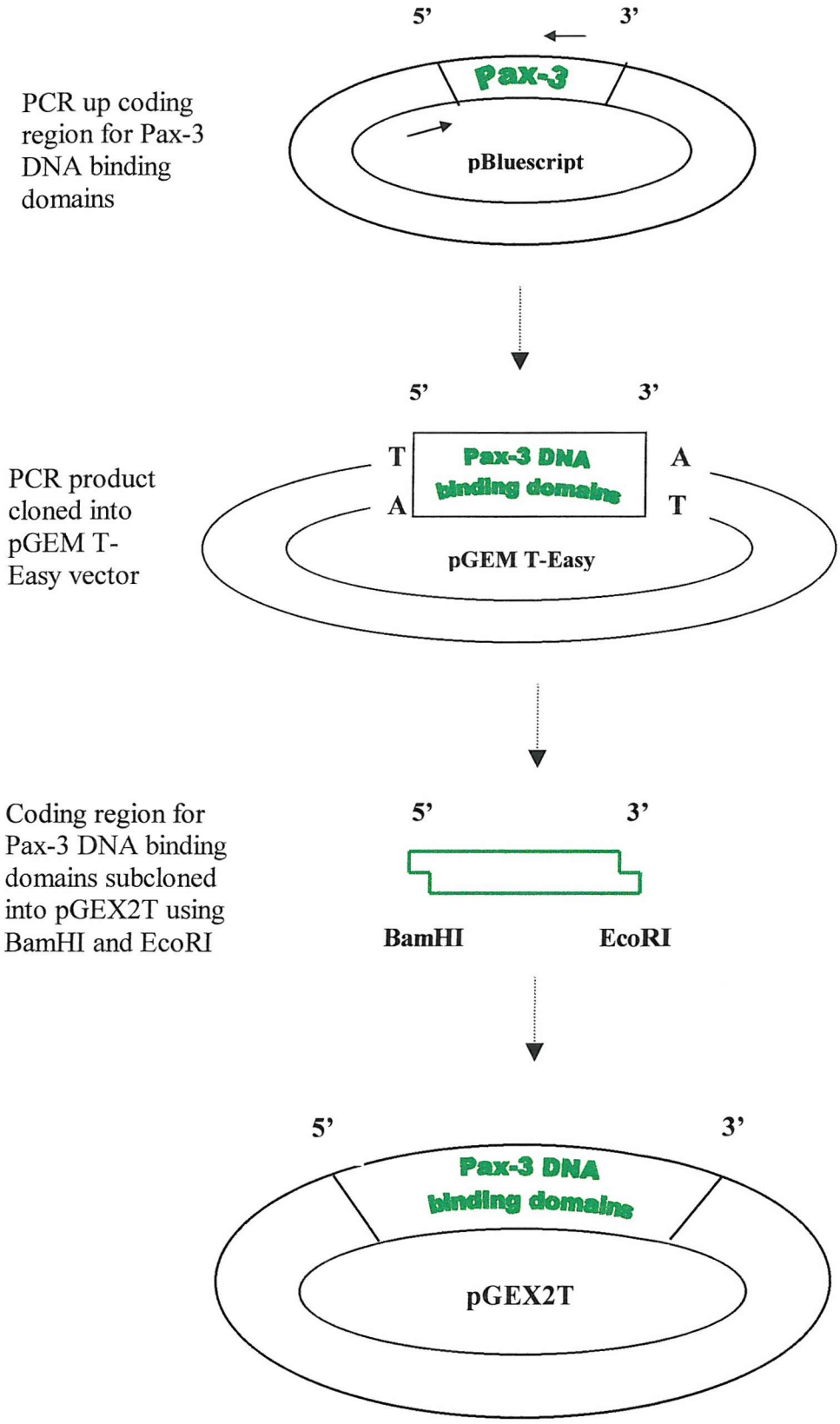

Fig. 3.4 Summary of the cloning steps used to isolate the GST-*Pax3* construct

The sequence of the *Pax-3* cDNA in the pGEX2T vector was confirmed by DNA sequencing. Hereafter this construct is referred to as GST / Pax3-DBD:

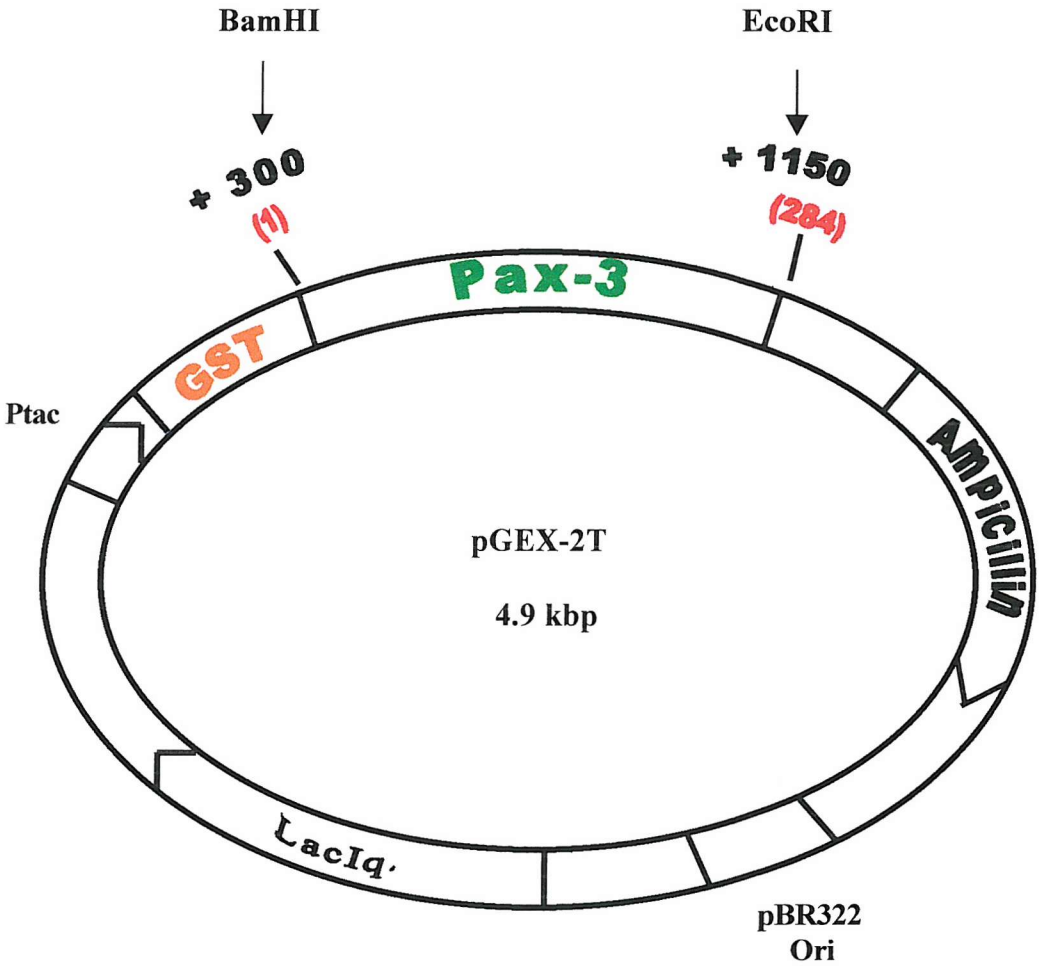

Fig. 3.5 Schematic diagram to show the coding region for the Pax-3 DNA binding domains cloned into the pGEX2T vector

The coding regions for the paired domain, octapeptide and homeodomain of Pax-3 were cloned into the BamHI and EcoRI sites of pGEX2T. The numbers with + signs before them refer to the *Pax-3* cDNA. The numbers in red are the corresponding amino acids in the Pax-3 protein.

3.2.2 Expression of the GST / Pax3-DBD fusion protein

Having cloned the coding region for the DNA binding domains of Pax-3 into the pGEX2T vector, the GST / Pax3-DBD fusion protein was expressed and purified. As shown in figure 3.6, GST / Pax3-DBD was expressed in bacteria and purified by affinity chromatography using Glutathione Sepharose 4B.

An empty pGEX2T vector was also used to express GST protein alone. Protein expression from the pGEX-2T plasmid is under the control of the *tac* promoter, which is induced using the lactose analog isopropyl β-D-thiogalactoside (IPTG). Figure 3.7 shows samples of purified GST and GST / Pax3-DBD proteins which have been resolved by 10% SDS-PAGE. The protein gel shows that the GST / Pax3-DBD protein (58 kDa) was expressed in bacteria and could be purified on glutathione beads. The molecular weight of GST / Pax3-DBD was predicted using Compute pI/MW. This is an online database that calculates the molecular weight (MW) of a protein from its amino acid sequence. The size of GST / Pax3-DBD estimated from the band on the protein gel is equal to the predicted molecular weight of this protein.

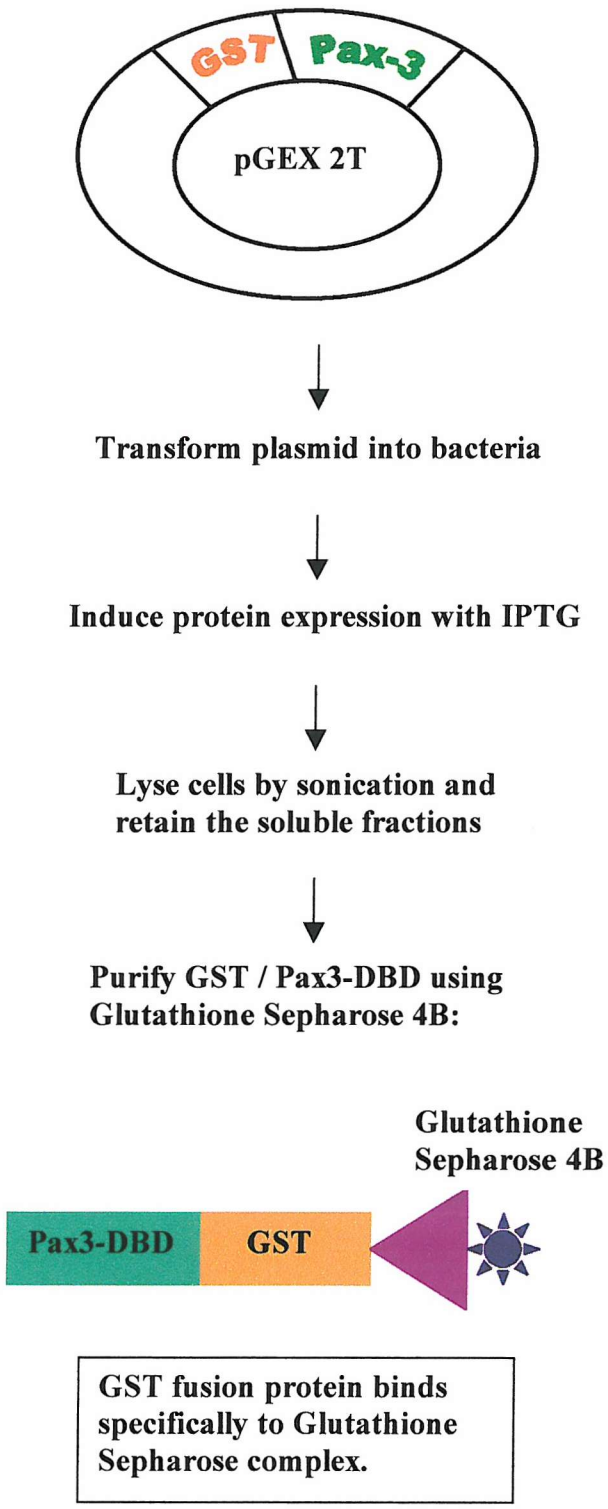

Fig. 3.6 The procedure used to express the GST / Pax3-DBD fusion protein and purify it on Glutathione-Sepharose beads

Details of the experimental procedures described in this figure can be found in Materials and Methods.

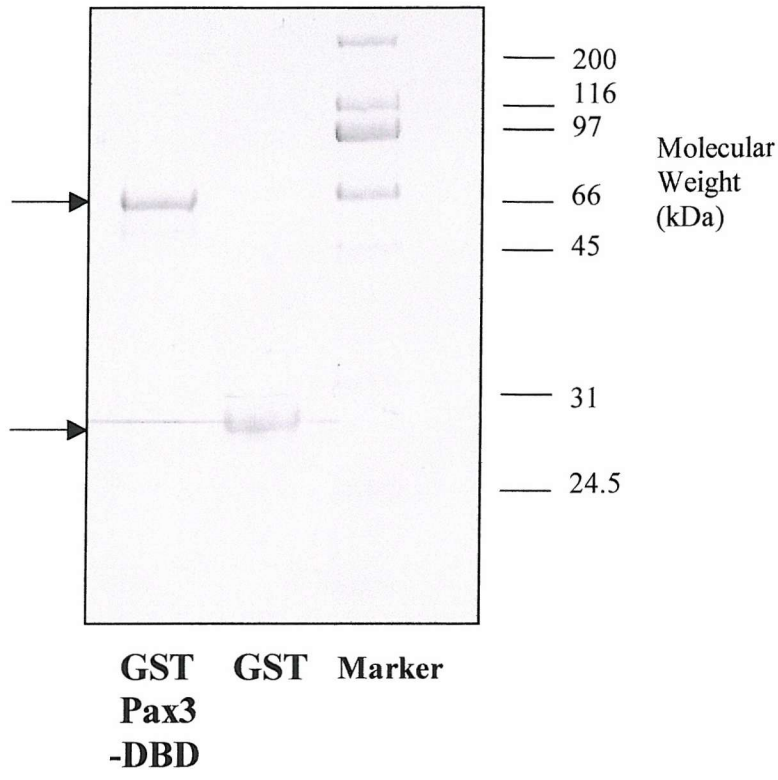

Fig. 3.7 Expression of GST and GST / Pax3-DBD Proteins

Protein expression was induced in log phase cultures using 2 mM IPTG for 3 hours at 37 ^{0}C. Following purification on Glutathione-Sepharose 4B, the protein samples were resolved by 10% SDS-PAGE. Protein was detected by staining the gel with Coomassie blue. The locations of the GST and GST / Pax3-DBD protein bands on the de-stained gel are marked with arrows.

3.3 Phosphorylation of Pax-3 *in vitro* by PKA and PKC

Having expressed and purified the DNA binding domains of Pax-3 as a GST-Pax3 fusion protein, we determined whether this protein could be phosphorylated *in vitro* by PKA and PKC. Phosphorylation mediated by both these protein kinases has been implicated in the control of transcription factor activity.

Cyclic AMP-dependent protein kinase (protein kinase A)

The cAMP-dependent protein kinase (protein kinase A) is involved in a range of cellular processes including cell cycle progression, differentiation and apoptosis (Matten *et al.*, 1994, Cho-Chung, 1990, Chen, 1998, Gjersten *et al.*, 1995). The protein kinase A (PKA) holoenzyme consists of two catalytic subunits bound to a dimer of regulatory subunits, of which there are two types. The second messenger cyclic AMP binds to the regulatory subunits resulting in their dissociation. This releases, and thus activates, the catalytic subunits of PKA. Type I regulatory subunits hold the PKA holoenzyme in the cytoplasm until it is activated by cyclic AMP, at which point the catalytic subunits translocate to the nucleus. Type II regulatory subunits can bind to a range of proteins called AKAPs (A kinase anchoring proteins), which serve as targeting subunits. This has the affect of localising the PKA holoenzyme to specific areas of the cell where it is needed to phosphorylate target proteins. For example PKA holoenzyme associates with microtubules by binding to microtubule associated protein 2 (MAP-2). This protein is itself an *in vitro* target for phosphorylation by PKA (Hubbard *et al.*, 1993).

Protein kinase C

At least 10 isoforms of PKC exist, all of which are serine/threonine protein kinases activated by Ca^{2+} and/or phospholipid. The conventional isoforms of PKC (α, βI, βII and γ) require phosphatidylserine, diacylglycerol and Ca^{2+} for their activation. The unconventional or novel PKCs (δ, ε, η and θ) are not Ca^{2+}-dependent, whereas the atypical PKCs (ξ and λ) require only phosphatidylserine for activation (Ohno and Suzuki, 1995). PKCs are synthesised as single polypeptide chains with a C-terminal catalytic domain. Binding sites for phosphatidylserine, diacylglycerol and Ca^{2+} are located within an N-terminal regulatory domain. On binding these ligands, a

pseudosubstrate domain dissociates from the catalytic domain of the enzyme resulting in activation of PKC. It is the binding of ligands such as phorbol esters to plasma membrane receptors coupled to phospholipase C (PLC) via G proteins that leads to PKC activation. Activated PLC cleaves phosphoinositol-4,5-bisphosphate (PIP_2) into 1,2-diacylglycerol (DAG) and inositol-1,4,5-trisphosphate (IP_3). The insoluble DAG remains in the membrane whereas IP_3 diffuses through the cytoplasm and activates Ca^{2+} channels in the endoplasmic reticulum membrane. The subsequent release of Ca^{2+} into the cytoplasm activates PKC and causes it to translocate to the plasma membrane where it binds DAG and phosphatidylserine. As well as being active in the cytoplasm, almost all PKC isoforms have been identified in the nucleus (Martelli *et al.*, 1999).

PKC is believed to be involved in both cell proliferation and cell differentiation. In T lymphocytes, for example, PKC activation results in cell proliferation. However PKC activation results in the differentiation of HL-60 leukemia cells into macrophages. PKC has been linked to the MAP kinase cell-signalling pathway in which it is thought to activate Ras. The different effects of PKC on cell proliferation versus differentiation could be due to differential activation of PKC isoforms in different cell types. In one type of cell a certain PKC isoform could phosphorylate substrates in the mitogenic pathway of that cell. In another cell type different PKC isoforms might be activated that stimulate differentiation by phosphorylating different substrates (Clemens *et al.*, 1992). Indeed substrate specificity requirements may vary between the different PKC isoforms as suggested by Marais *et al.* (1990). In a study of the conventional PKC isoforms, it was shown that optimal substrates for PKC-γ differed slightly from those determined for PKC-α and PKC-β_1. In addition to their effects on cell proliferation and differentiation, some PKC isoforms are involved in apoptosis. Various changes are seen in the cell

nucleus during apoptosis including the proteolytic degradation of nuclear proteins. It is believed that phosphorylation of such proteins by PKCs can induce conformational changes that render them susceptible to proteolytic cleavage (Martelli *et al.*, 1999).

3.3.1 *In vitro* phosphorylation of GST / Pax3-DBD by PKA and PKC

In order to determine whether Pax-3 could be phosphorylated within its DNA binding domains, the GST and GST / Pax3-DBD proteins were used in *in vitro* kinase assays with the catalytic subunits of PKA and PKC. Equal amounts of protein were used in each kinase assay, and the reactions were then analysed by SDS-PAGE. Following electrophoresis, protein gels were stained with Coomassie blue, destained and then dried down and autoradiographed. Figure 3.8 shows the results of typical PKA and PKC assays in which GST alone and GST / Pax3-DBD proteins were incubated with [γ-^{32}P] ATP in the presence and absence of the protein kinase.

The results show that [γ-^{32}P] ATP was not incorporated into either GST or GST / Pax3-DBD in the absence of PKA. However, phosphate incorporation was observed in the GST / Pax3-DBD protein when PKA was added, although the GST protein alone was not phosphorylated by PKA. In the presence of PKA, in addition to the GST / Pax3-DBD band that runs at 58 kDa, there are also several lower running bands on the autoradiograph. These bands are believed to represent breakdown products of GST / Pax3-DBD that are phosphoryated by PKA. Alternatively they could be bacterial proteins that were copurified with the GST / Pax3-DBD protein, and like GST / Pax3-DBD are substrates for PKA *in vitro*.

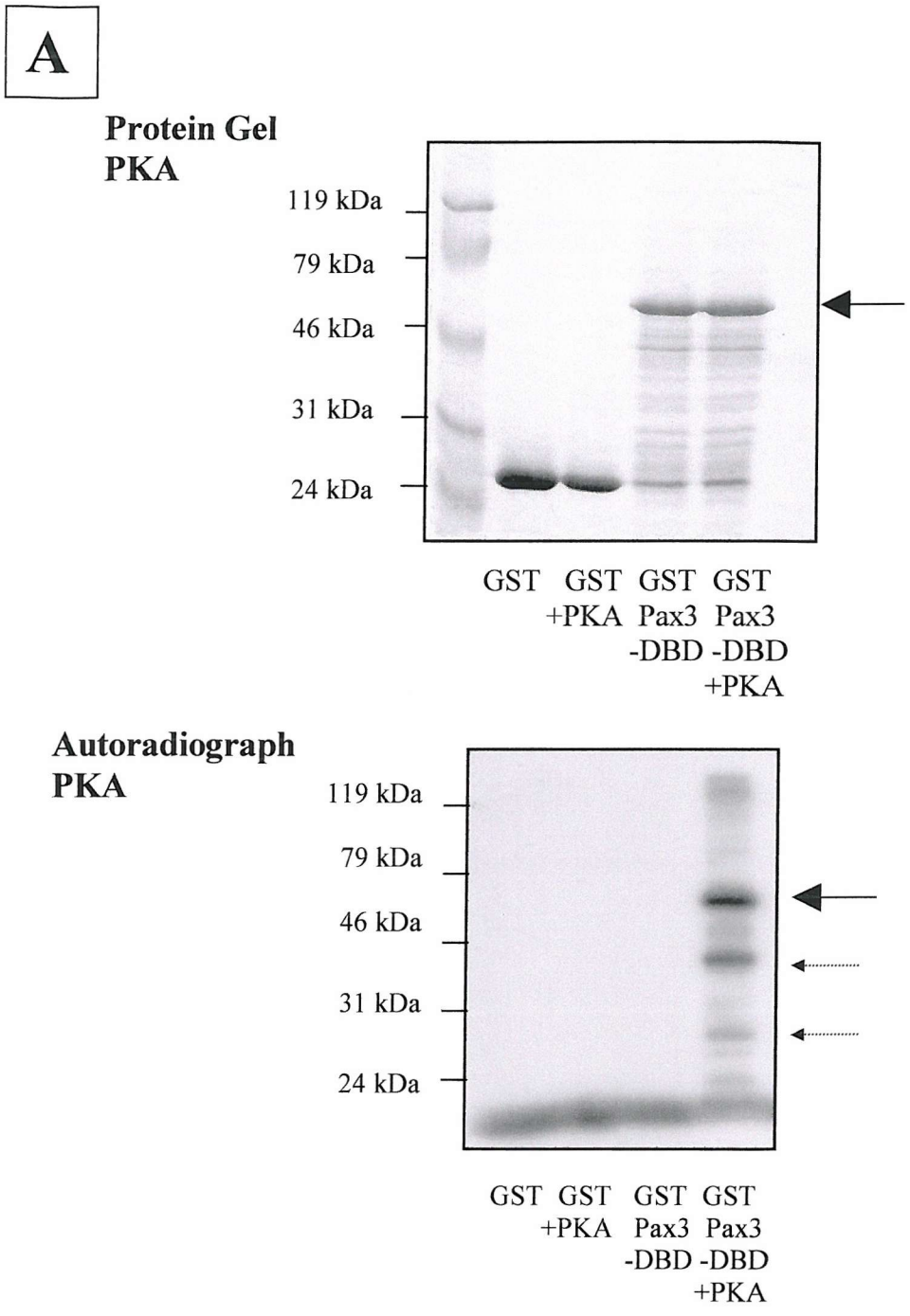

Fig. 3.8 (A) *In Vitro* Phosphorylation of GST / Pax3-DBD by PKA

Approximately 1μg of GST / Pax3-DBD and 1μg of GST alone were incubated with PKA *in vitro*. Kinase assays were then analysed by SDS-PAGE, followed by autoradiography. The location of the GST / Pax3-DBD protein on the protein gel (stained with Coomassie blue) and autoradiograph is marked with an arrow. Dashed arrows indicate breakdown products of the fusion protein that are also substrates for PKA.

B

Protein Gel
PKC

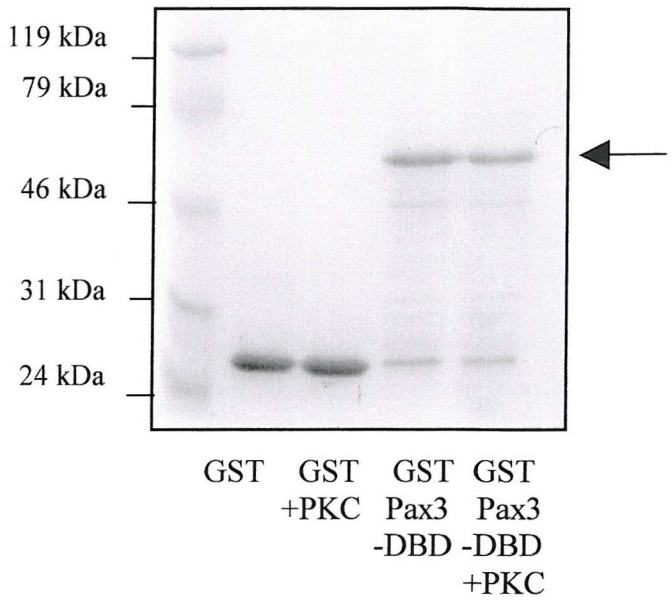

Autoradiograph
PKC

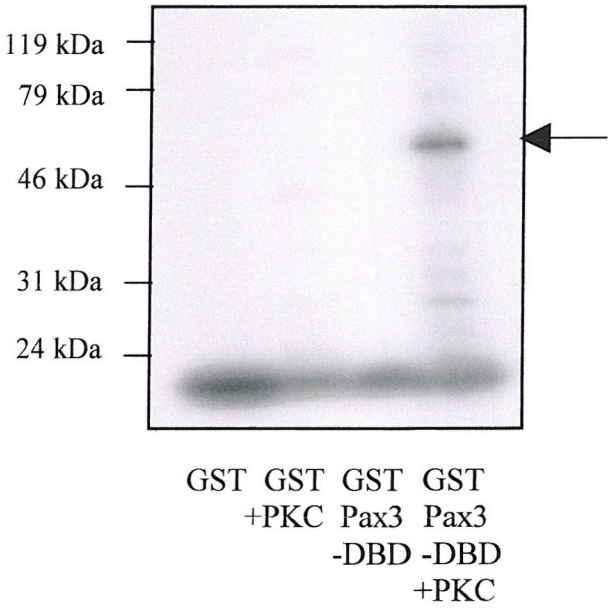

Fig. 3.8 (B) *In Vitro* Phosphorylation of GST / Pax3-DBD by PKC

Approximately 1μg of GST / Pax3-DBD and 1μg of GST alone were incubated with PKC *in vitro*. Kinase assays were then analysed by SDS-PAGE, followed by autoradiography. The location of the GST / Pax3-DBD protein on the protein gel (stained with Coomassie blue) and autoradiograph is marked with an arrow.

Similarly in the absence of PKC, [γ-^{32}P] ATP was not incorporated into either the GST or GST / Pax3-DBD proteins. However, the GST / Pax3-DBD protein was phosphorylated when PKC was present in addition to [γ-^{32}P] ATP.

In both the PKA and PKC assays phosphate was not incorporated into the GST protein alone even in the presence of protein kinase. This implies that the Pax-3 part of the GST / Pax3-DBD fusion protein was phosphorylated in the kinase assays that were carried out. Therefore it can be concluded that a Pax-3 protein containing both the paired domain and the homeodomain but no transactivation domain can be phosphorylated *in vitro* by PKA and PKC.

The results showed that Pax-3 could be phosphorylated *in vitro* by PKA even though the Prosite database failed to pick out any potential PKA phosphorylation sites in the Pax-3 sequence. This prompted a search of the Pax-3 amino acid sequence to look for sites that might be phosphorylated by PKA *in vitro*. Kemp *et al.* (1977) showed that the serine residue in the peptide Leu-Arg-Arg-Ala-Ser-Leu-Gly could be phosphorylated *in vitro* by PKA. This peptide was derived from a sequence in pyruvate kinase, a protein that is phosphorylated by PKA *in vivo*. At least one of the arginine residues on the N-terminal side of the phosphoacceptor serine were required for PKA to phopsphorylate this peptide *in vitro*. Peptides were phosphorylated much less efficiently when either of these arginine residues was replaced with an alanine. The reaction efficiency was also reduced, although not as significantly, when either of the arginines was replaced by lysine. In both cases the V_{max} of the phosphorylation reaction remained approximately the same but the K_m was increased, indicating that the affinity of PKA for the peptide had been reduced. Phosphorylation also occurred less efficiently when the phosphoacceptor serine was

replaced by threonine. Feramisco *et al.* (1980) extended these *in vitro* phosphorylation studies with PKA to show that the spacing between the phosphoacceptor residue and the N-terminal basic amino acids was also important. The phosphorylation reaction was impaired when the two arginine residues N-terminal to the phosphoacceptor serine were placed either right next to or more than one amino acid away from the serine. The same effects were reported for peptides that contained Lys-Arg on the N-terminal side of the phosphoacceptor serine rather than Arg-Arg. However, naturally occurring PKA substrates that have Lys-Arg before the phosphoacceptor residue (for example phosphorylase kinase and glycogen synthase) contain the sequence Lys-Arg-X-X-Ser. It is possible that within the context of a full protein as opposed to short peptides, a spacing of two amino acids between Lys-Arg and the phosphoacceptor serine provides the optimum site for phosphorylation by PKA. Finally it was also shown that peptides representing optimum PKA sites contained a hydrophobic amino acid in the position immediately C-terminal to the phosphoacceptor residue. The presence of basic amino acids on the C-terminal side of the phosphoacceptor residue had a negative influence on phosphorylation by PKA.

The results of such *in vitro* PKA phosphorylation studies led to the determination of a consensus PKA site as being **RR**X**S/T***Y (Kennelly and Krebs 1991, Tasken *et al.*, 1995) where X represents any amino acid and Y is usually a hydrophobic residue. The asterisk marks the position of the phosphoacceptor residue. This consensus PKA site corresponds to the sequence that the Prosite database searches for in target proteins.

In vitro peptide studies had shown that changing the number or spacing of basic amino acids on the N-terminal side of the phosphoacceptor serine drastically reduces the

binding affinity and rate of catalysis with respect to PKA. However, some native substrates of PKA contain the sequence **RXS*Y** and some contain the sequence **KR**XX**S***Y (Kemp and Pearson 1990, Walsh and Van Patten 1994, Tasken *et al.*, 1995). Therefore within the context of a whole protein, sequences that do not conform to the full consensus PKA site as determined from *in vitro* studies on peptides can still be phosphorylated by PKA. Even so, it seems likely that these sites represent weak PKA sites *in vivo*, which may bind to PKA with lower affinity than substrates containing the sequence **RR**XS/T*Y. A search of the Pax-3 protein for sequences corresponding to **RXS***Y and **KR**XX**S***Y revealed three weak PKA sites. The locations of these sites in the Pax-3 sequence are shown in figure 3.9.

Prosite highlighted six potential PKC sites in Pax-3. All these sites correspond to the PKC consensus sequence **S/T***X**R/K** as determined by Woodgett *et al.* (1986). However, the discovery that Pax-3 contains weak PKA sites that were not detected by Prosite, suggested that additional PKC sites could also be present in the Pax-3 sequence. As in the case of PKA, *in vitro* phosphorylation studies using peptides were used to determine optimum PKC phosphorylation sites. Woodgett *et al.* (1986) proposed that a single basic amino acid on the C-terminal side of the phosphoacceptor residue was required in order to attain efficient phosphorylation of peptide substrates *in vitro* by PKC. As a result a consensus sequence of **S/T***X**R/K** was suggested, in which X is usually an uncharged amino acid. Further *in vitro* studies by House *et al.* (1987) used peptides based on the site phosphorylated by PKC in the glycogen synthase protein. The PKC site in glycogen synthase contains a single arginine residue on the N-terminal side of the phosphoacceptor serine. When the number of arginine residues N-terminal to the serine was increased, the peptide became a better substrate for PKC. Similarly the

phosphorylation reaction became more efficient when basic residues were placed on the C-terminal side of the serine as well as on the N-terminal side of it. As in the case of PKA, replacing the arginines with lysines had a slight inhibitory effect on phosphorylation by PKC. In addition serine was phosphorylated more efficiently by PKC than threonine. As well as glycogen synthase, peptides corresponding to the PKC sites in Ribosomal protein S6 and the EGF receptor were also phosphorylated *in vitro* by PKC. Both the ribosomal protein S6 and EGF receptor peptides contained basic amino acids on both sides of the phosphoacceptor serine. As a result these peptides were better substrates for PKC *in vitro* than the glycogen synthase peptide.

In support of these findings, Kennelly and Krebs (1991) reported that in a survey of 68 PKC sites on 29 proteins approximately half contained basic amino acids on both sides of the phosphoacceptor residue. About a quarter of the sites had basic amino acids on the N-terminal side only, and a quarter had basic amino acids on the C-terminal side only. In most cases these basic residues were located in the –2 and –3 positions (the phosphoacceptor residue was designated position 0) and/or in the +2 and +3 positions. A basic residue was located in the –1 position in only 9 cases and in the +1 position in only 5 cases. Taken together this work showed that optimum PKC substrates possessed basic amino acids on both sides of the phosphoacceptor residue. Substrates containing basic amino acids on one side of the phosphoacceptor residue only were phosphorylated less efficiently by PKC. The spacing between the basic amino acids and the phosphoacceptor residue was shown to vary between substrates. Thus it was proposed that the full consensus sequence for phosphorylation by PKC is $\mathbf{K/R}_{1\text{-}3}X_{0\text{-}2}\mathbf{S/T}^{*}X_{0\text{-}2}\mathbf{R/K}_{1\text{-}3}$. Weaker PKC phosphorylation sites are represented by the sequences $\mathbf{S/T}^{*}X_{0\text{-}2}\mathbf{R/K}_{1\text{-}3}$ and $\mathbf{R/K}_{1\text{-}3}X_{0\text{-}2}\mathbf{S/T}^{*}$. A search of the Pax-3 protein for these PKC sites picked up all six of the PKC

sites that were detected by Prosite. Additional PKC sites were also discovered in the paired domain, linker region and homeodomain of the protein. The locations of the PKC sites in Pax-3 are shown in figure 3.9. All except one of these sites corresponds to either the weak PKC site **S/T*** X_{0-2}**R/K**$_{1-3}$ or **R/K**$_{1-3}X_{0-2}$**S/T***. Ser 222 of Pax-3 occurs within the sequence Arg-Arg-Ser-Arg. This corresponds to the full consensus site for PKC, **K/R**$_{1-3}X_{0-2}$**S/T*** X_{0-2}**R/K**$_{1-3}$. However, as described by Kennelly and Krebs (1991), in physiological PKC substrates, the basic residues that are required for substrate specificity are present in the –1 and +1 positions in only a few cases. This suggests that the best PKC substrates require these basic amino acids to be more than one residue away from the phosphoacceptor serine.

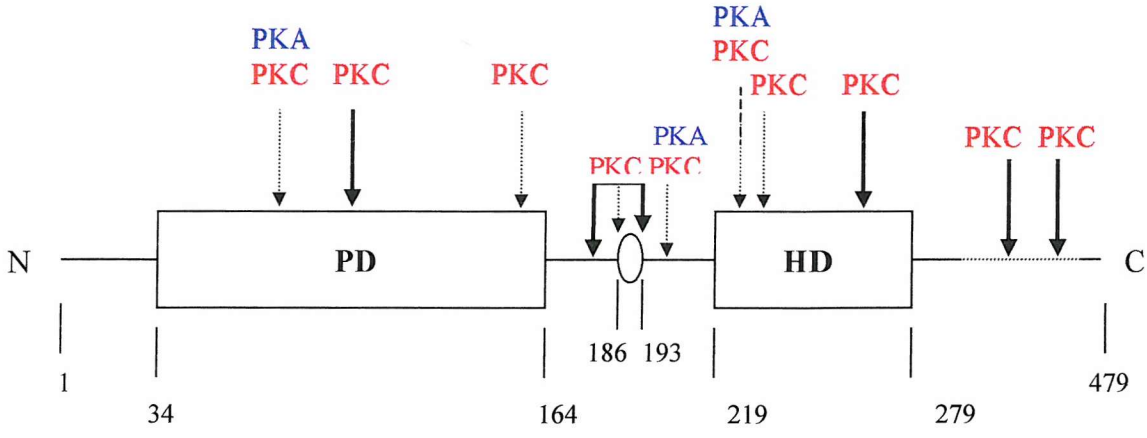

Fig. 3.9 (A) Domain Structure of the Pax-3 protein, showing the locations of potential PKA and PKC phosphorylation sites

PD, paired domain; HD, homeodomain; ⬯ = octapeptide. Sites marked by dashed arrows are those that were not identified using the Prosite database. The numbers refer to amino acids residues in the Pax-3 protein.

1 MetThrThrLeuAlaGlyAlaValProArgMetMetArgProGlyProGlyGlnAsnTyrProArgSer 23

24 GlyPheProLeuGluValSerThrProLeu**GlyGlnGlyArgValAsnGlnLeuGlyGlyValPheIle** 46

47 **AsnGlyArgProLeuProAsnHisIleArgHisLysIleValGluMetAlaHisHisGlyIleArgPro** 69

70 **CysValIleSerArgGlnLeu**ArgValSer**HisGlyCysValSerLysIleLeuCysArgTyrGlnGlu** 92

93 **ThrGly**SerIleArg**ProGlyAlaIleGlyGlySerLysProLysGlnValThrThrProAspValGlu** 115

116 **LysLysIleGluGluTyrLysArgGluAsnProGlyMetPheSerTrpGluIleArgAspLysLeu** 137

138 **LeuLysAspAlaValCysAspArgAsnThrValProSerValSer**SerIleSerArg**IleLeuArgSer** 160

161 **LysPheGlyLys**GlyGluGluGluGluAlaAspLeuGluArgLysGluAlaGluGluSerGluLysLys 183

184 AlaLysHisSer**IleAspGlyIleLeu**SerGluArgAlaSerAlaProGlySerAspGluGlySerAspIle 207

208 AspSerGluProAspLeuProLeuLysArgLys**GlnArgArgSer**ArgThrThr**PheThrAlaGlu** 229

230 **GlnLeuGluGluLeuGluArgAlaPheGluArgThrHisTyrProAspIleTyrThrArgGluGlu** 251

252 **LeuAlaGlnArgAlaLysLeuThrGluAlaArgValGlnValTrpPhe**SerAsnArgArg**AlaArg** 273

274 **TrpArgLysGlnAlaGly**AlaAsnGlnLeuMetAlaPheAsnHisLeuIleProGlyGlyPheProPro 296

297 ThrAlaMetProThrLeuProThrTyrGlnLeuSerGluHisSerTyrGlnProThrSerIleProGlnAla 320

321 ValSerAspProSerSerThrValHisArgProGlnProLeuProProSerThrValHisGlnSerThrIlePro 345

346 SerAsnAlaAspSerSerSerAlaTyrCysLeuProSerThrArgHisGlyPheSerSerTyrThrAspSer 369

370 PheValProProSerGlyProSerAsnProMetAsnProThrIleGlyAsnGlyLeuSerProGlnValMet 393

394 GlyLeuLeuThrAsnHisGlyGlyValProHisGlnProGlnThrAspTyrAlaLeuSerProLeuThrGly 417

418 GlyLeuGluProThrThrThrValSerAlaSerCysSerGlnArgLeuGluHisMetLysAsnValAsp 440

441 SerLeuProThrSerGlnProTyrCysProProThrTyrSerThrAlaGlyTyrSerMetAspProValThr 464

465 GlyTyrGlnTyrGlyGlnTyrGlyGlnSerLysProTrpThrPhe

Fig. 3.9 (B) The Pax-3 amino acid sequence, showing the locations of potential PKA and PKC phosphorylation sites

The paired domain (aa 34-164), octapeptide (aa 186-193) and homeodomain (aa 219-279) are shown in bold. Potential PKC sites are shown in red, and PKA sites in blue. All potential PKA sites are also potential PKC sites. Sites that are underlined refer to those that were identified using the Prosite database.

3.3.2 GST-paired domain and GST-homeodomain proteins

The results have shown that both PKA and PKC phosphorylate Pax-3 *in vitro* within the region of the protein that contains the DNA binding domains. This part of the Pax-3 protein consists of 33 amino acids at the N-terminus, followed by the 128 amino acid paired domain, a 54 amino acid linker region that separates the two DNA binding domains, and then the 61 amino acid homeodomain. To further define the site(s) of phosphorylation within the DNA binding domains of Pax-3, two more GST-*Pax3* constructs were isolated, and then expressed in bacteria. The first of the resulting fusion proteins (GST-PD) incorporates amino acids 1-188 of Pax-3, up to and including the third residue of the octapeptide. The second protein (GST-HD) incorporates amino acids 189-284 of Pax-3, up to the C-terminal end of the homeodomain. The domain structures of the GST-PD and GST-HD proteins are shown in figure 3.10. Having been expressed in bacteria and purified as described for the GST-Pax3 protein, both GST-PD and GST-HD were subjected to *in vitro* kinase assays with PKA and PKC.

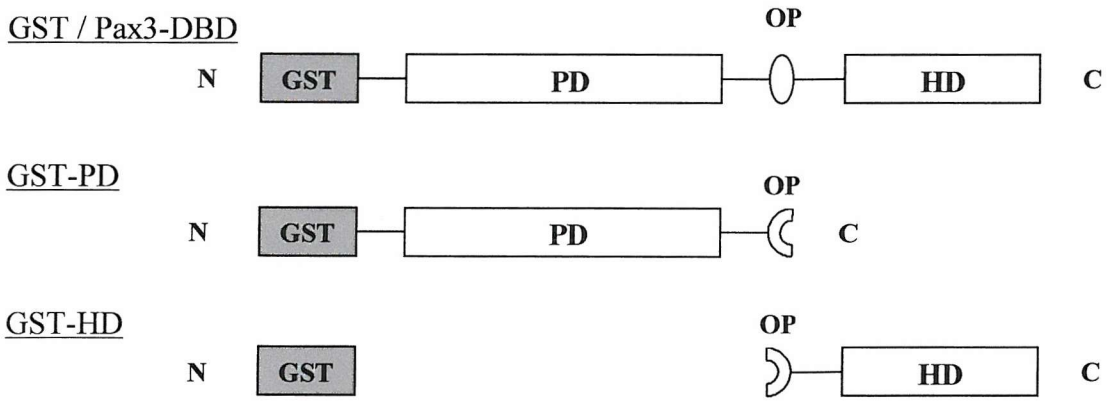

Fig. 3.10 Domain structures of the three GST-Pax3 fusion proteins

PD, paired domain; OP, octapeptide; HD, homeodomain.

3.3.3 Preparation of the GST-paired domain protein

A GST-paired domain construct (GST-*PD*) was derived from the GST / *Pax3-DBD* construct in the following way. GST / *Pax3-DBD* DNA was first digested with EcoRI, which cuts immediately 3' of the coding region for the homeodomain. It was then digested with ClaI, which cuts Pax-3 in the linker region, 71 nucleotides downstream of the paired domain-coding region and 92 nucleotides upstream of the homeodomain coding region. The vector DNA was purified by gel extraction, blunt ended and then religated. Recombinant clones were then selected for by restriction mapping. This is summarised in figure 3.11.

To confirm that the DNA isolated was GST-*PD*, plasmids were first digested with HindIII as there is a single HindIII site at position 1066 in the *Pax-3* cDNA, which lies within the coding region for the homeodomain. The plasmid DNA was also digested with BamHI and PstI. This double digest distinguishes GST-*PD* DNA from vector DNA alone. As shown in figure 3.12, digesting GST-*PD* DNA as well as the pGEX2T plasmid alone with BamHI and PstI produced a 4 kbp vector band on an agarose gel. The GST-*PD* construct also dropped out a 1.5 kbp insert band, in contrast to the vector DNA that produced only a 1.0 kbp band. The difference in size can be accounted for by the 560 base pairs of *Pax-3* cDNA that had been cloned into the pGEX2T vector. This construct will be referred to as GST–*PD* from now on. It codes for the first 189 amino acids of Pax-3, which includes the entire paired domain.

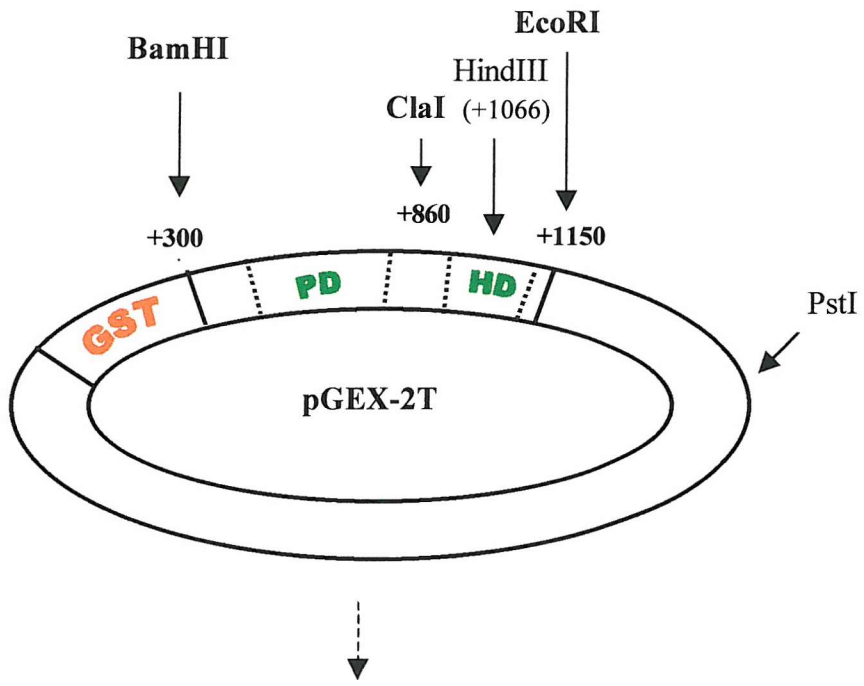

- Cut with ClaI and EcoRI
- Blunt-ended vector and religated
- Transformed into DH5αs

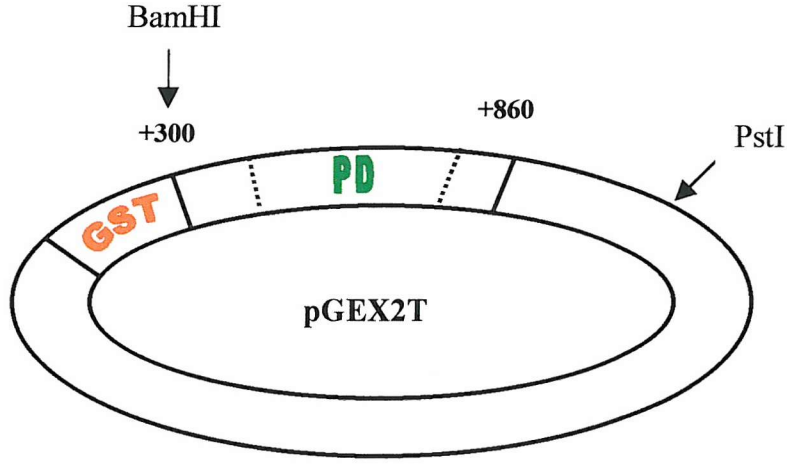

Restriction digest to confirm size of Pax-3 insert:

Cut with BamHI
PstI
[1.5 kbp insert]

Restriction digest to show Pax-3 homeodomain is missing:

Cut with HindIII
[GST-PD remains uncut]

Fig. 3.11 Cloning and restriction mapping of the GST-*PD* construct

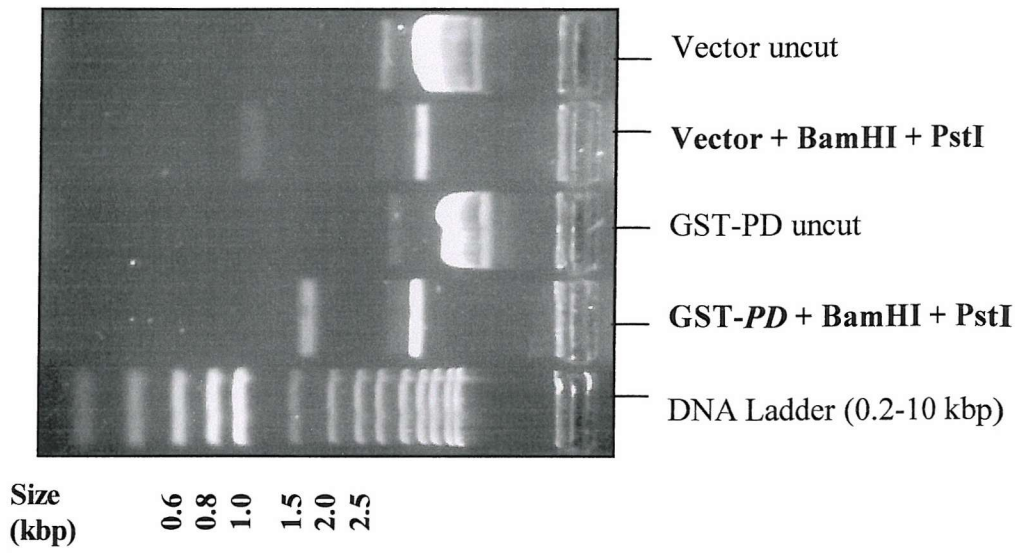

Fig. 3.12 Picture of an agarose gel showing pGEX2T and pGEX2T–*PD* DNA cut with BamHI and PstI

Having cloned the coding region for the first 189 amino acids of Pax-3 into the pGEX2T plasmid, the GST-PD protein was expressed in bacteria and purified in the same way as the GST / Pax3-DBD protein. Figure 3.13 shows a picture of a protein gel on which samples of GST alone, GST / Pax3-DBD and GST-PD proteins were run out. The figure shows that the GST-PD protein (predicted molecular weight 48kDa) could be expressed in bacteria and purified on glutathione beads. The band that can be seen in the GST-PD lane of the protein gel runs just above the 45kDa marker band, confirming that this is the GST-PD protein.

The amino acid sequence of the Pax-3 moiety in the GST-PD protein is shown in figure 3.14. Highlighted are the locations of potential PKA and PKC sites. In the first 189 amino acids of Pax-3 there are five potential PKC sites and one potential PKA site. To determine whether the paired domain protein could be phosphorylated at any of these sites, it was subjected to *in vitro* kinase assays with the purified catalytic subunits of

PKA and PKC. The GST and GST / Pax3-DBD proteins were also used in these assays for comparison. The results are shown in Figure 3.15. Both GST / Pax3-DBD and GST-PD proteins were phosphorylated by PKA as shown by the incorporation of [γ-^{32}P] ATP in the presence of the kinase. However the GST protein was not phosphorylated by PKA. This implies that it was the Pax-3 moieties in the GST-Pax3 fusion proteins that were phosphorylated by PKA. Similarly the GST protein was not phosphorylated by PKC, whereas both the GST / Pax3-DBD and GST-PD proteins were phosphorylated. Thus both the DNA binding domains of Pax-3, as well as the isolated paired domain of Pax-3 can be phosphorylated *in vitro* by the catalytic subunits of both PKC and PKA.

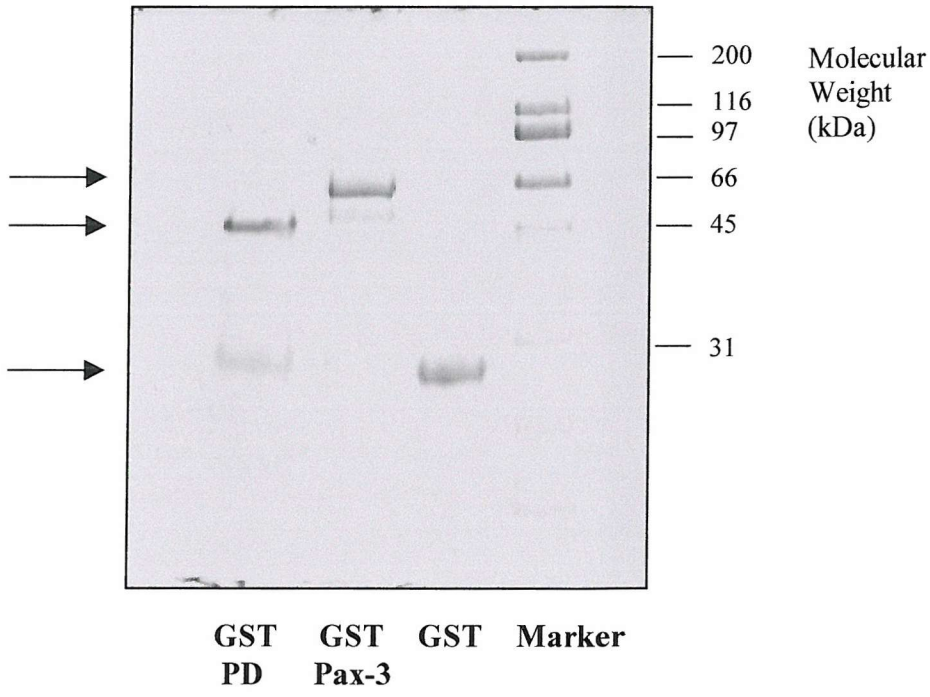

Fig. 3.13 Expression of GST-PD protein

Protein expression was induced in log phase cultures using 2 mM IPTG for 3 hours at 37 ^{0}C. Following purification on Glutathione-Sepharose 4B, the protein samples were resolved by 10% SDS-PAGE. Protein was detected by staining the gel with Coomassie blue. The locations of the GST, GST / Pax3-DBD and GST-PD protein bands on the de-stained gel are marked with arrows.

A

1	MetThrThrLeuAlaGlyAlaValProArgMetMetArgProGlyProGlyGlnAsnTyrProArgSer	23
24	GlyPheProLeuGluValSerThrProLeu**GlyGlnGlyArgValAsnGlnLeuGlyGlyValPheIle**	46
47	**AsnGlyArgProLeuProAsnHisIleArgHisLysIleValGluMetAlaHisHisGlyIleArgPro**	69
70	**CysValIleSerArgGlnLeu**ArgValSer**HisGlyCysValSerLysIleLeuCysArgTyrGlnGlu**	92
93	**ThrGly**SerIleArg**ProGlyAlaIleGlyGlySerLysProLysGlnValThrThrProAspValGlu**	115
116	**LysLysIleGluGluTyrLysArgGluAsnProGlyMetPheSerTrpGluIleArgAspLysLeu**	137
138	**LeuLysAspAlaValCysAspArgAsnThrValProSerValSer**SerIleSerArg**IleLeuArgSer**	160
161	**LysPheGlyLys**GlyGluGluGluGluAlaAspLeuGluArgLysGluAlaGluGluSerGluLysLys	183
184	AlaLysHisSer**Ile**	

B

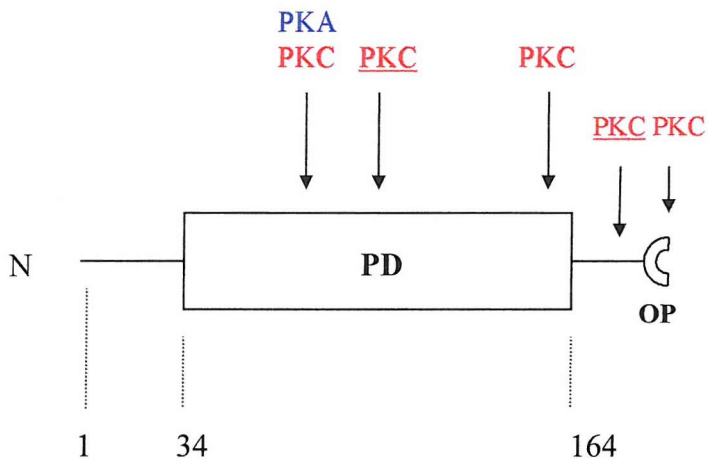

Fig. 3.14 (A) The amino acid sequence of the Pax-3 paired domain protein showing the locations of potential PKA and PKC sites

The 33 amino acids N-terminal to the Pax-3 paired domain, the paired domain itself (shown in bold) and the first 25 amino acids of the linker region make up the Pax-3 part of the GST-PD protein. Sequences in red represent potential PKC sites. A potential PKA site, which is also a potential PKC site, is shown in blue.

(B) Domain structure of the Pax-3 paired domain protein showing the locations of potential PKA and PKC sites

PD, paired domain; OP, octapeptide. Numbers refer to amino acids residues in the Pax-3 protein. Sites that are underlined refer to those that were identified using Prosite.

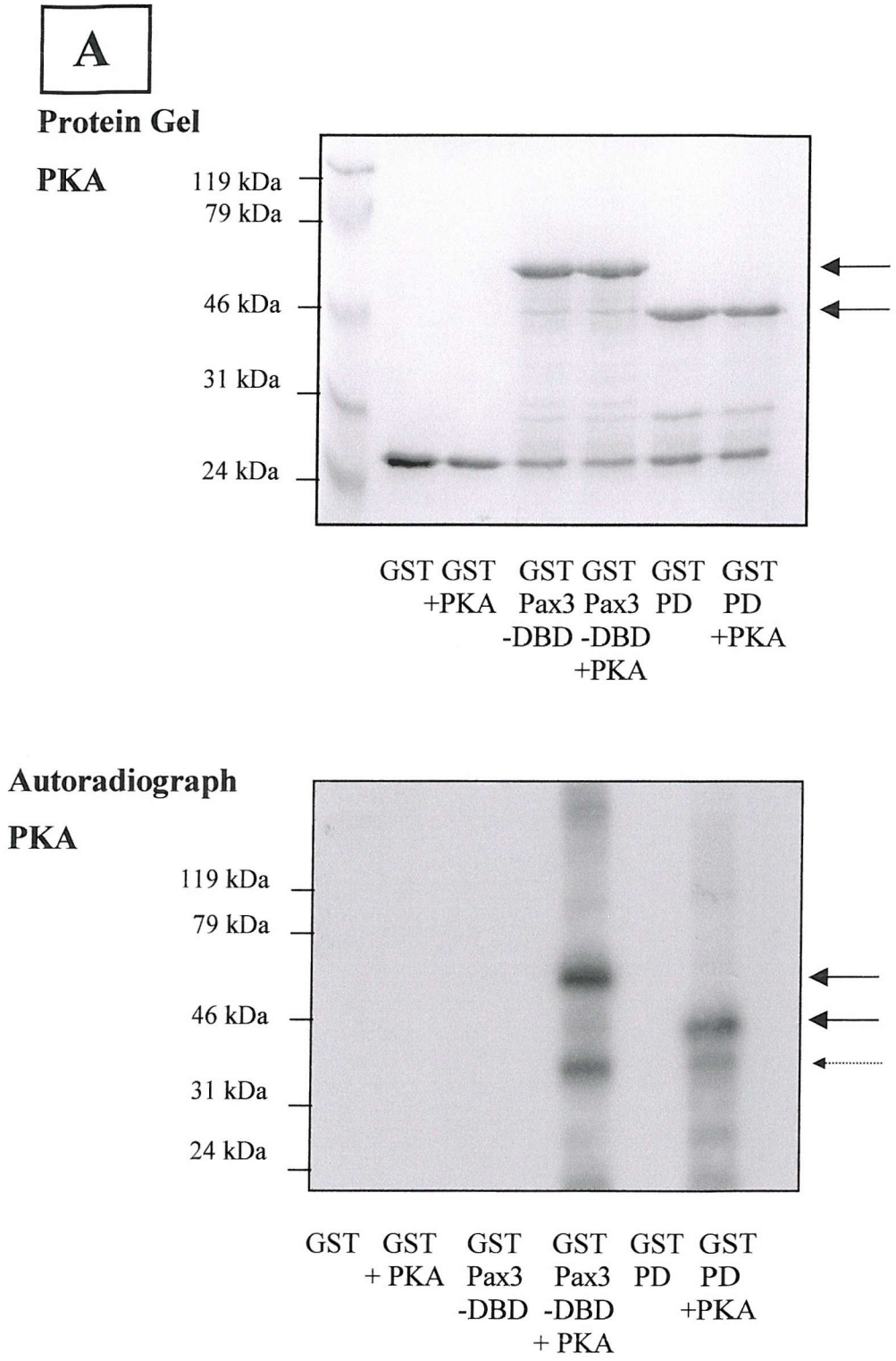

Fig. 3.15 (A) *In Vitro* Phosphorylation of GST / Pax3-DBD and GST-PD by PKA

Approximately 1μg of GST, GST / Pax3-DBD and GST-PD proteins were incubated with PKA *in vitro*. The kinase assays were then analysed by 10% SDS-PAGE, followed by autoradiography. The locations of the GST, GST / Pax3-DBD and GST-PD proteins are marked with arrows. The dashed arrow shows the location of other PKA substrates, presumed to be breakdown products of GST / Pax3-DBD and GST-PD respectively.

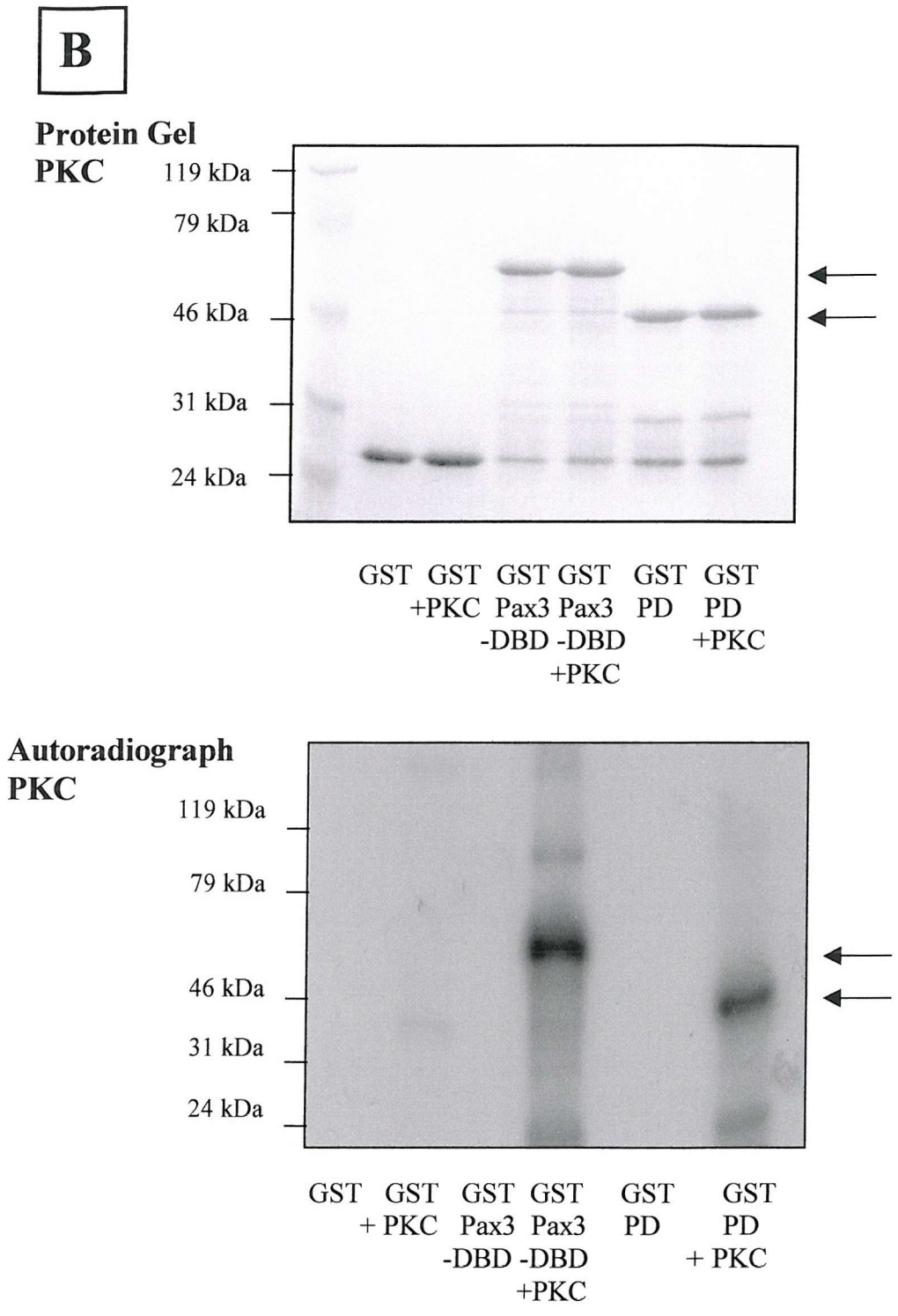

Fig. 3.15 (B) *In Vitro* Phosphorylation of GST / Pax3-DBD and GST-PD by PKC

Approximately 1μg of GST, GST / Pax3-DBD and GST-PD proteins were incubated with PKC *in vitro*. The kinase assays were then analysed by 10% SDS-PAGE, followed by autoradiography. The locations of the GST, GST / Pax3-DBD and GST-PD proteins are marked with arrows.

In figure 3.15, more intense bands were observed for the GST / Pax3-DBD protein than the GST-PD protein on both the PKA and PKC autoradiographs, even though equal amounts of each protein were loaded on the gel. Therefore phosphorylation may have occurred at multiple sites, with the GST / Pax3-DBD protein being phosphorylated at more sites within the Pax-3 sequence than the GST-PD protein. In support of this hypothesis, three potential PKA sites have been identified in the GST / Pax3-DBD sequence but only one of these sites is present in the GST-PD sequence. Similarly GST / Pax3-DBD contains ten potential PKC sites whereas GST-PD has only five potential PKC sites.

3.3.4 Preparation of the GST-homeodomain protein

It had been demonstrated that Pax-3 could be phosphorylated *in vitro* by PKA and PKC either within the paired domain itself or in the N-terminal half of the linker region that separates the paired domain from the homeodomain. To determine whether the region of Pax-3 that contains the C-terminal half of the linker and the homeodomain could also be phosphorylated *in vitro* by PKA and PKC, a GST fusion protein containing the Pax-3 homeoodomain (HD) was produced. The GST-*HD* construct was derived from the GST / *Pax3-DBD* construct using restriction digests as illustrated in figure 3.16. The GST / *Pax3-DBD* DNA was cut with BamHI and ClaI to remove the coding region for the first 189 amino acids of the Pax-3 protein, which includes the entire paired domain. The vector DNA was then gel purified, blunt ended and reannealed. The BamHI site was reformed when the vector, having been cut with BamHI and ClaI and then blunt-ended, was reannealed. Consequently GST-*HD* DNA can be linnearised with BamHI, producing an insert band of 5.3 kbp. However the ClaI site was destroyed when the vector was

blunt ended and religated. Consequently ClaI will not cut GST-*HD*. HindIII has a single recognition site in the Pax-3 homeodomain and no sites in the vector. SmaI has two recognition sites in the Pax-3 paired domain but no sites in the vector. Therefore HindIII will cut GST-*HD* DNA to give a single band at 5.3 kbp, but SmaI will not digest GST-*HD* DNA.

Four separate clones were digested with BamHI, ClaI, HindIII and SmaI. Fractions of these digests were then analysed by electrophoresis on an agarose gel. As shown in figure 3.17, all four clones were linnearised by BamHI and HindIII, but were not cut by ClaI or SmaI. The cut DNA produced a band on the gel of just over 5 kbp. The GST-*HD* construct is approximately 5.3 kbp. In contrast, vector DNA alone was linnearised by BamHI, but was not cut by SmaI, ClaI or HindIII. This implies that the four clones shown in figure 3.16 are all GST-*HD* recombinants. The GST-*HD* construct codes for the C-terminal half of the linker region between the paired domain and the homeodomain as well as the homeodomain itself.

Having cloned the coding region for amino acids 190-284 of Pax-3 into the pGEX2T plasmid, the GST-HD protein was expressed in bacteria and purified in the same way as the GST / Pax3-DBD and GST-PD proteins. Figure 3.17 shows a picture of a protein gel on which samples of GST alone and GST-HD proteins were run out. In the GST-HD lane of the gel a dark band runs halfway between the 31 kDa and 46 kDa marker bands. Since the predicted molecular weight of GST-HD is 37 kDa, this confirmed that the GST-HD had been expressed in bacteria.

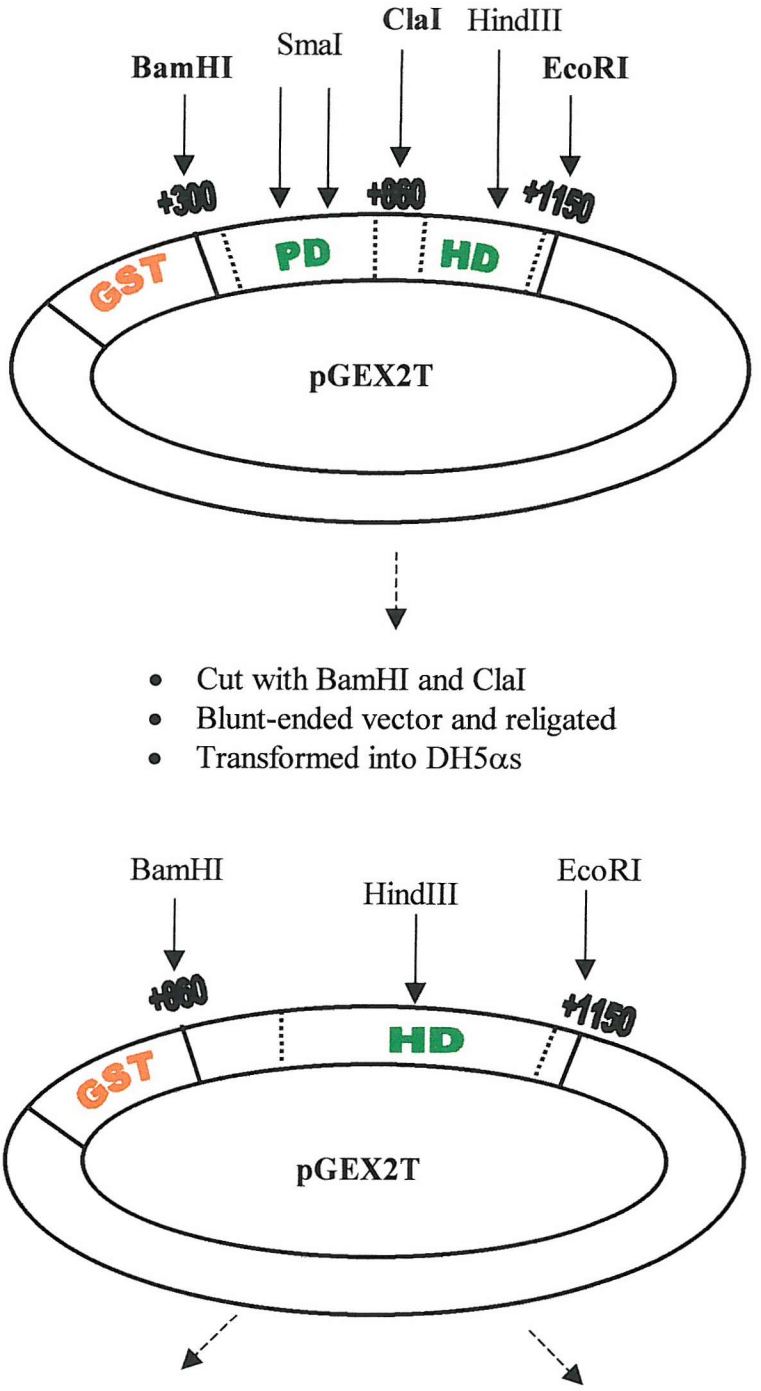

Fig. 3.16 Cloning and restriction mapping of the GST-*HD* construct

PD, paired domain; HD, homeodomain. Numbers refer to nucleotides in the *Pax-3* cDNA sequence.

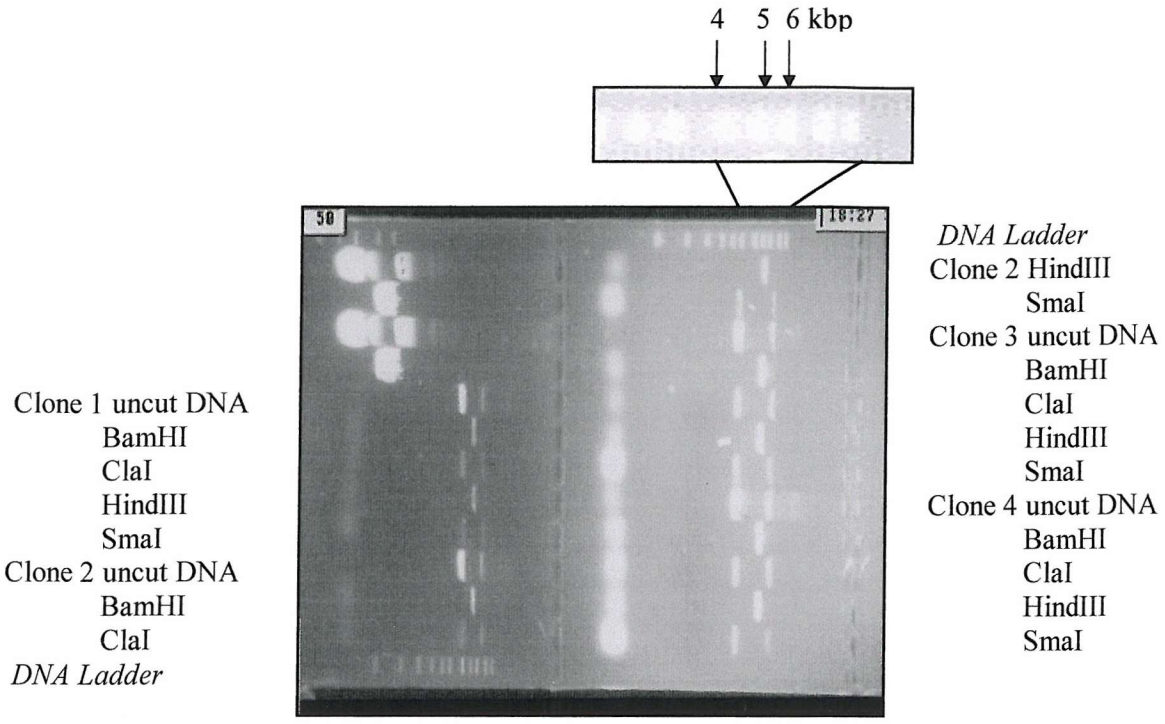

Fig. 3.17 Picture of an agarose gel showing GST-*HD* clones digested with BamHI, ClaI, HindIII and SmaI

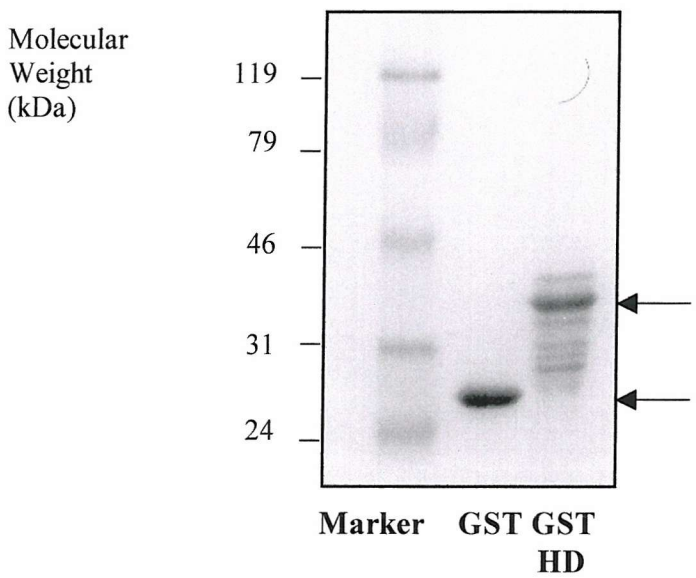

Fig. 3.18 Expression of GST-HD protein

Protein expression was induced in log phase cultures using 2mM IPTG for 3 hours at 37 ^{0}C. Following purification on Glutathione-Sepharose 4B, protein samples were resolved by 10% SDS-PAGE. Protein was detected by staining the gel with Coomassie blue. The locations of the GST and GST-HD protein bands on the gel are marked with arrows.

The amino acid sequence and domain structure of the Pax-3 moiety in the GST-HD protein are shown in figure 3.19. The locations of potential PKA and PKC sites are highlighted as for the GST / Pax3-DBD and GST-PD proteins. The GST-HD protein contains two potential PKA sites and five potential PKC sites. Therefore to determine whether this Pax-3 homeodomain protein could be phosphorylated, it was subjected to *in vitro* phosphorylation using PKA and PKC. As shown in figure 3.20 (A) the GST-HD protein was phosphorylated by PKA, but the GST protein alone was not phosphorylated. The red dot on the autoradiograph shows where the film lines up with the GST-HD band on the protein gel. The corresponding band on the autoradiograph is smeary, indicating that proteins that ran both higher and lower than GST-HD on the protein gel were also phosphorylated by PKA. Proteins that run lower than GST-HD could be breakdown products of this fusion protein. Higher bands might be due to GST-HD protein that has been phosphorylated at multiple sites by PKA. Alternatively, higher running proteins could be contaminants from the bacterial extracts that were co-purified with the GST-HD protein. Similarly, although a band was seen on the autoradiograph in the GST + PKA lane, this represents a protein which is larger than the 26 kDa GST protein. Therefore this is thought to be a contaminant, perhaps a bacterial protein, which is also a substrate for *in vitro* phosphorylation by PKA.

The GST-HD protein was also subjected to *in vitro* phosphorylation using PKC. GST and GST-PD proteins were included in the same experiment for comparison. The results are shown in figure 3.20 (B). The GST-HD protein was not a substrate for *in vitro* phosphorylation by PKC. As previously shown PKC did phosphorylate the GST-PD protein, although GST alone was not phosphorylated. Two faint bands are also present on the autoradiograph in the GST +PKC and GST-PD +PKC lanes. These bands

correspond to proteins that run higher on the SDS gel than the GST-PD protein. Therefore it is assumed once again that such proteins are contaminants of the bacterial extracts that have been co-purified with the GST fusion proteins.

A

	AspGlyIleLeuSerGluArgAlaSerAlaProGlySerAspGluGlySerAspIle	207
208	AspSerGluProAspLeuProLeuLysArgLys**GlnArgArgSerArgThrThrPheThrAlaGlu**	229
230	**GlnLeuGluGluLeuGluArgAlaPheGluArgThrHisTyrProAspIleTyrThrArgGluGlu**	251
252	**LeuAlaGlnArgAlaLysLeuThrGluAlaArgValGlnValTrpPheSerAsnArgArgAlaArg**	273
274	**TrpArgLysGlnAlaGly**AlaAsnGlnLeuMet	

B

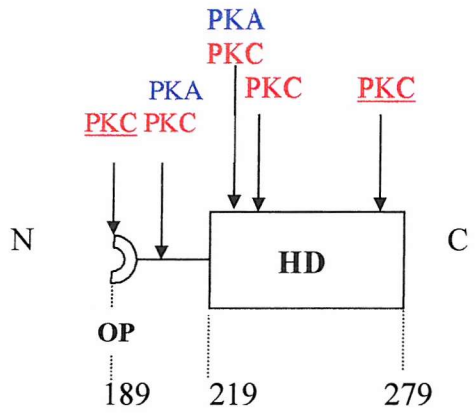

Fig. 3.19 (A) The amino acid sequence of the Pax-3 homeodomain protein showing the locations of potential PKA and PKC sites

The last 30 amino acids of the linker region plus the homeodomain itself (shown in bold) make up the Pax-3 part of the GST-HD protein. Potential PKC sites are shown in red. Potential PKA sites (also PKC sites) are shown in blue.

(B) Domain structure of the Pax-3 homeodomain protein showing the locations of potential PKA and PKC sites

OP, octapeptide; HD, homeodomain. The numbers refer to amino acids in the Pax-3 protein. Sites that are underlined refer to those that were identified using Prosite.

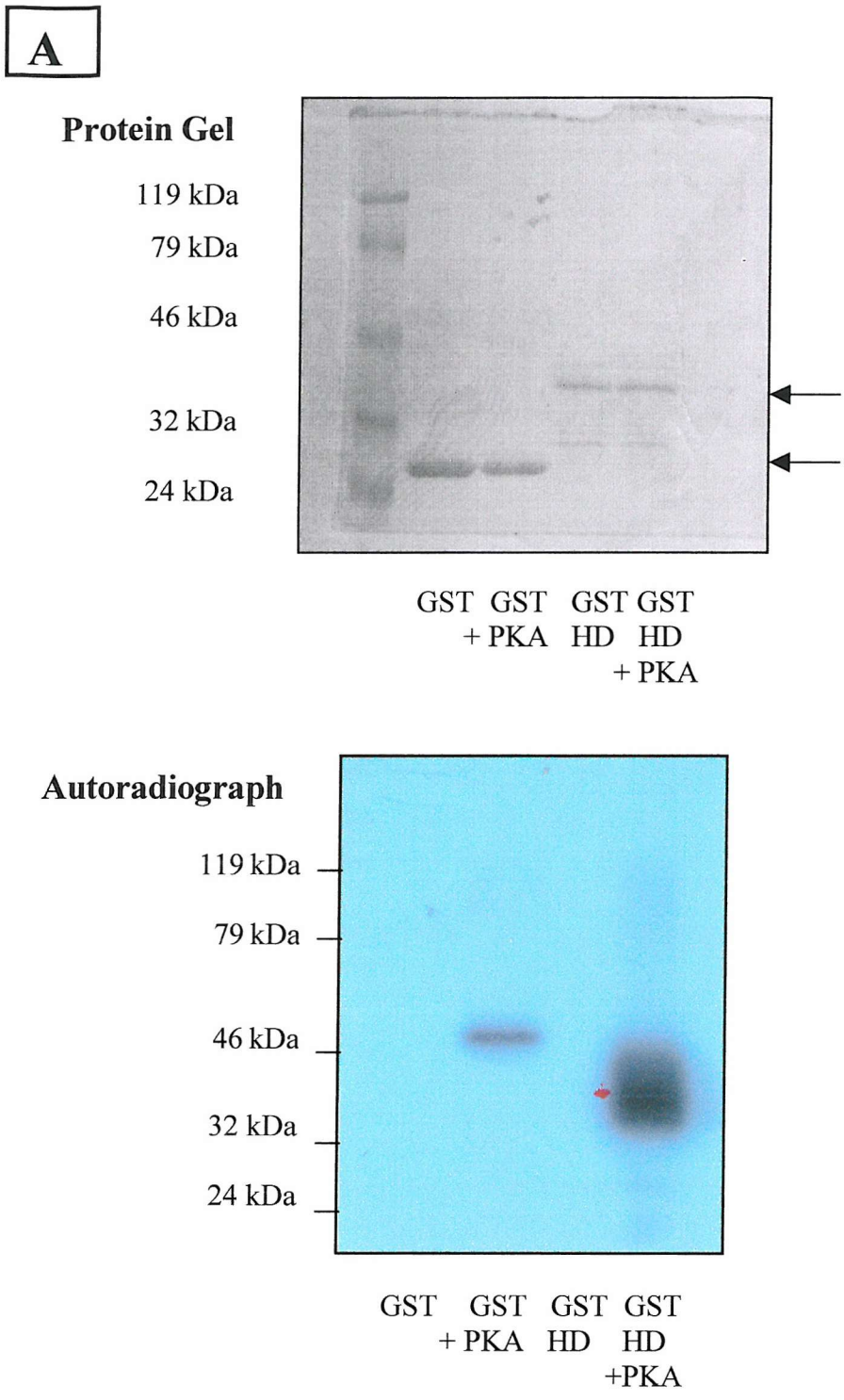

Fig. 3.20 (A) *In vitro* Phosphorylation of GST-HD by PKA

Approximately 1μg of GST-HD and 1μg GST alone were incubated with PKA *in vitro*. Reactions were analysed by 10% SDS-PAGE, followed by autoradiography. The locations of GST and GST-HD are marked with arrows on the protein gel picture. A dot on the autoradiograph corresponds to the GST-HD band on the protein gel.

B

Protein gel

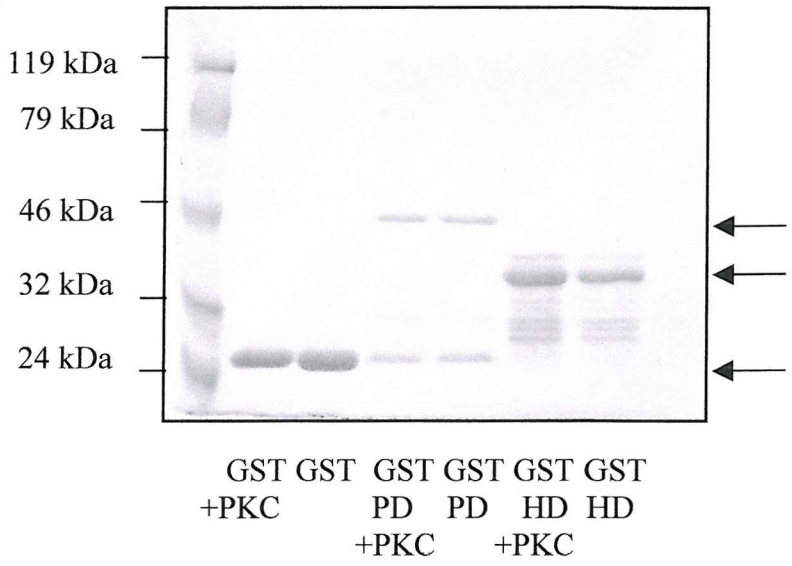

Autoradiograph

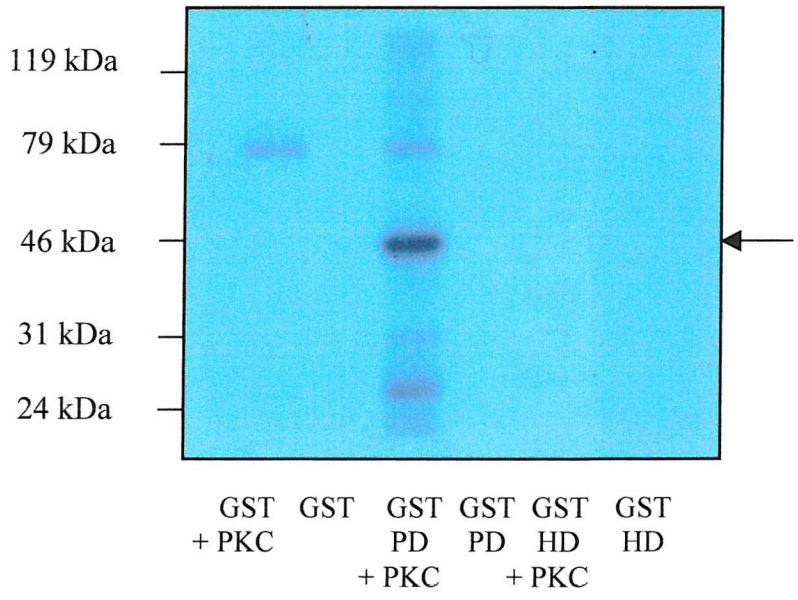

Fig. 3.20 (B) *In vitro* Phosphorylation of GST-HD and GST-PD by PKC

Approximately 1μg of GST-HD, 1μg of GST-PD and 1μg of GST alone were incubated with PKC *in vitro*. Reactions were analysed by 10% SDS-PAGE, followed by autoradiography. The locations of all three proteins are marked with arrows on the picture of the protein gel. The GST-PD protein is also marked with an arrow on the autoradiograph.

The results show that the Pax-3 moiety of the GST-HD protein can be phosphorylated *in vitro* by PKA. There are two potential PKA sites within the GST-HD protein. Both these sites are weak sites since they do not conform to the complete consensus sequence for PKA. Therefore, as in the case of the GST-PD protein, it appears that the Pax-3 homeodomain protein is also phosphorylated by PKA at weak PKA sites.

There are also five potential PKC sites in the GST-HD protein. The PKC site closest to the N-terminus of the homeodomain bears the closest resemblance to the consensus sequence for PKC. The other four sites are weak PKC sites. Despite the presence of these potential phosphorylation sites, the GST-HD protein could not be phosphorylated *in vitro* by PKC.

3.4 Phosphorylation of Pax-3 by Nuclear Extracts

The results presented so far showed that Pax-3 could be phosphorylated *in vitro* by purified serine/threonine protein kinases. However it was not known whether Pax-3 could be phosphorylated *in vivo*. Therefore the capacity for Pax-3 to be phosphorylated by kinases present in the nuclei of different cell types was examined. To achieve this nuclear extracts were made from ND7 cells, Cos-1 cells and IMR-32 cells. ND7 is a neuronal cell line, made by fusing a mouse neuroblastoma cell with a rat dorsal root ganglion cell (Wood *et al.*, 1990). IMR-32 is a human neuroblastoma cell line. Both of these cell lines express endogenous Pax-3. In contrast, the Cos-1 cell line is derived from monkey kidney cells, which do not express endogenous Pax-3.

In the case of the ND7s, extracts were first made from cells that had been grown continuously in medium containing 10% serum. These cells would have been undergoing

mitotic cell division. In addition extracts were also made from ND7 cells grown in the absence of serum for 24 hours before being harvested. This treatment leads to cell cycle arrest and morphological differentiation in ND7 cells. In the case of the IMR-32 and Cos-1 cells, extracts were only made from cells that had been grown continuously in media containing 10% serum.

The GST / Pax3-DBD, GST-PD and GST-HD proteins, as well as GST alone, were incubated with the nuclear extracts in the presence of [γ-^{32}P] ATP *in vitro*. As shown in figure 3.21, none of these nuclear extracts phosphorylated the GST protein alone. However, the GST / Pax3-DBD protein was phosphorylated by the ND7 nuclear extracts. The same level of phosphorylation was induced by extracts made from dividing and serum starved ND7 cells. In addition GST / Pax3-DBD was phosphorylated by the IMR-32 extract. The level of phosphorylation was the same as that induced by the ND7 nuclear extracts. In contrast the GST / Pax3-DBD protein was not phoshorylated by kinases present in the Cos-1 nuclear extract.

Similarly the GST-HD protein was phosphorylated by both ND7 extracts and by the IMR-32 extract. As for GST / Pax3-DBD, each extract induced approximately the same amount of phosphorylation. No phosphorylation of GST-HD was seen in the presence of the Cos-1 nuclear extract.

In contrast to the GST / Pax3-DBD and GST-HD proteins, only very weak phosphorylation of the GST-PD protein by the ND7 nuclear extracts was detected. This protein was not phosphorylated at all by either the IMR-32 or Cos-1 nuclear extracts.

A

Protein Gel

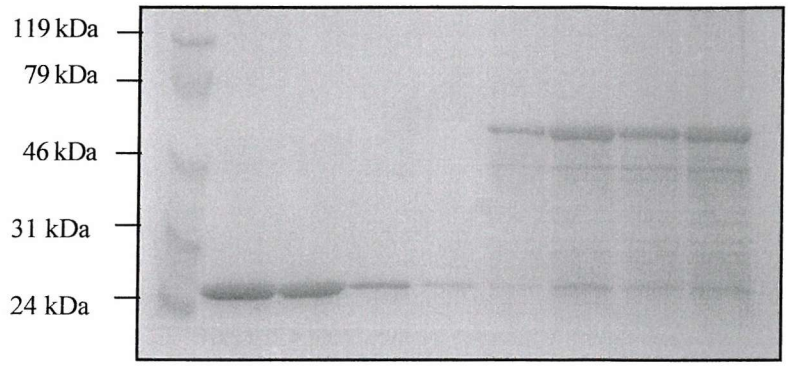

Autoradiograph

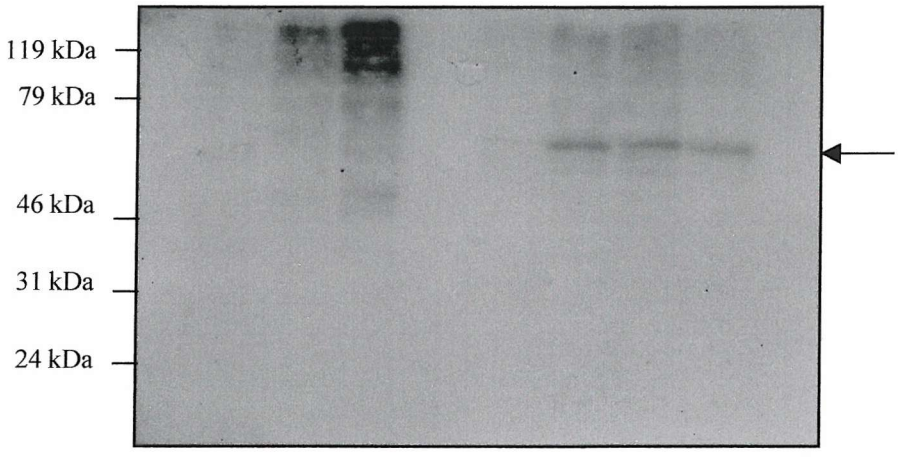

Fig. 3.21 Phosphorylation of GST–Pax3 fusion proteins using nuclear extracts

(A) Approximately 1μg of the GST and GST / Pax3-DBD proteins were subjected to *in vitro* phosphorylation with nuclear extracts (5μg total protein), and then analysed by 10% SDS-PAGE and autoradiography. The location of the GST / Pax3-DBD protein on the autoradiograph is marked with an arrow. SS, serum strarved cells; 10%, cells grown continuously in medium containing 10% serum.

B

Protein Gel

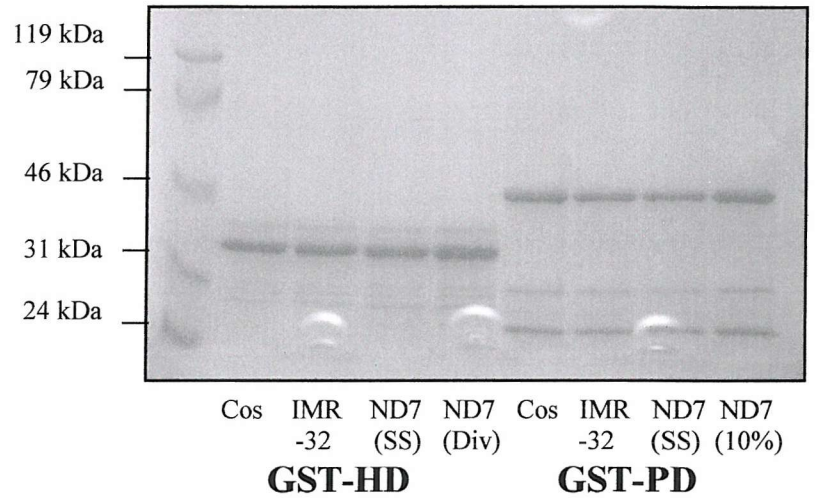

Autoradiograph

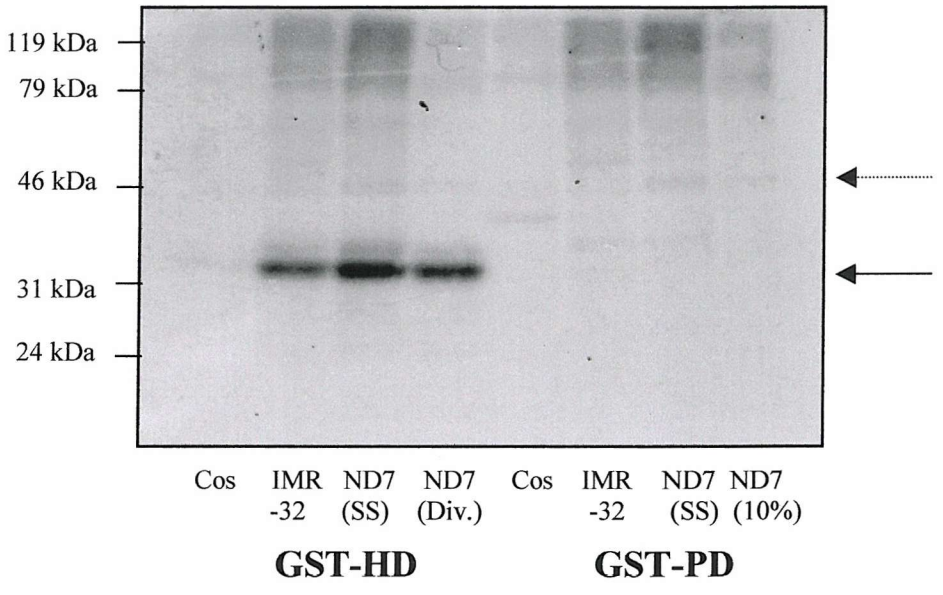

Fig. 3.21 Continued

(B) Approximately 1μg of GST-HD and GST-PD proteins were subjected to *in vitro* phosphorylation with nuclear extracts (5μg total protein), and then analysed by 10% SDS-PAGE and autoradiography. The positions of the GST-HD and GST-PD proteins on the autoradiograph are marked with an arrow and a dashed arrow respectively.

C

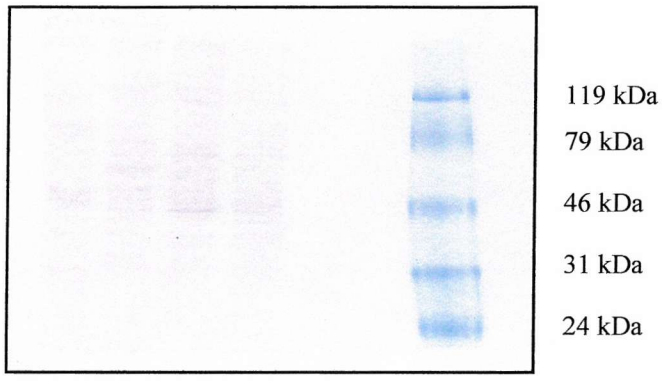

Fig. 3.21 Continued

(C) Aliquots of each nuclear extract (5μg of total protein) were analysed by 10% SDS-PAGE to ensure that the total protein levels in each of the extracts used for the kinase assays were approximately the same. The protein gel was stained with Coomassie blue and then de-stained as described in Materials and Methods.

3.5 Phosphorylation of Pax-3 through the cell cycle

The results have shown that Pax-3 can be phosphorylated *in vitro* by nuclear extracts made from both dividing and quiescent ND7 cells. It has previously been shown using an antisense *Pax-3* approach that preventing endogenous Pax-3 expression in ND7 cells leads to the morphological differentiation of these cells into a mature sensory neurone like phenotype, and a cessation in cell proliferation (Reeves *et al.*, 1999). This suggests that Pax-3 may help to keep ND7 cells in a dividing state, and prevent them from differentiating. Thus Pax-3 could be involved in ND7 cell cycle regulation. Such a role for Pax-3 *in vivo* is supported by evidence that the Pax-3 protein interacts with RB proteins, a family of negative cell cycle regulators (Wiggan *et al.* 1998). This interaction prevents Pax-3 from activating the transcription of reporter genes that have been cloned downstream of a Pax-3 binding site and minimal promoter.

The potential for Pax-3 to be differentially phosphorylated through the cell cycle was investigated. The aim was to determine whether nuclear extracts made from ND7 cells at different points in the cell cycle could phosphorylate Pax-3, and if so to what extent. To achieve this ND7 cells were first growth arrested by growing them in the absence of serum for 24 hours. Medium containing 10% serum was added back to the cells so that they would re-enter the cell cycle, and cells were then harvested at different time points in order to make nuclear extracts. Time points were chosen in order to coincide with different points in the cell cycle. FACS (fluorescence activated cell sorter) analysis was used to determine the length of each phase of the ND7 cell cycle. Table 3.1 shows the percentage of ND7 cells in each phase of the cell cycle at each time point. Figure 3.22 illustrates the duration of each phase of the ND7 cell cycle as determined by FACS analysis.

Table 3.1 – FACS analysis of ND7 cells

The table shows the percentage of cells in each phase of the cell cycle when growth arrested (0 hours), and at various time points following release from growth arrest by the addition of 10% serum to the growth medium.

Hours	0	1	3	6	12	18	24
% G_0/G_1 – phase cells	89	84	82	83	48	36	42
% S – phase cells	8	10	14	15	43	42	18
% G_2/M – phase cells	3	6	4	2	9	22	40

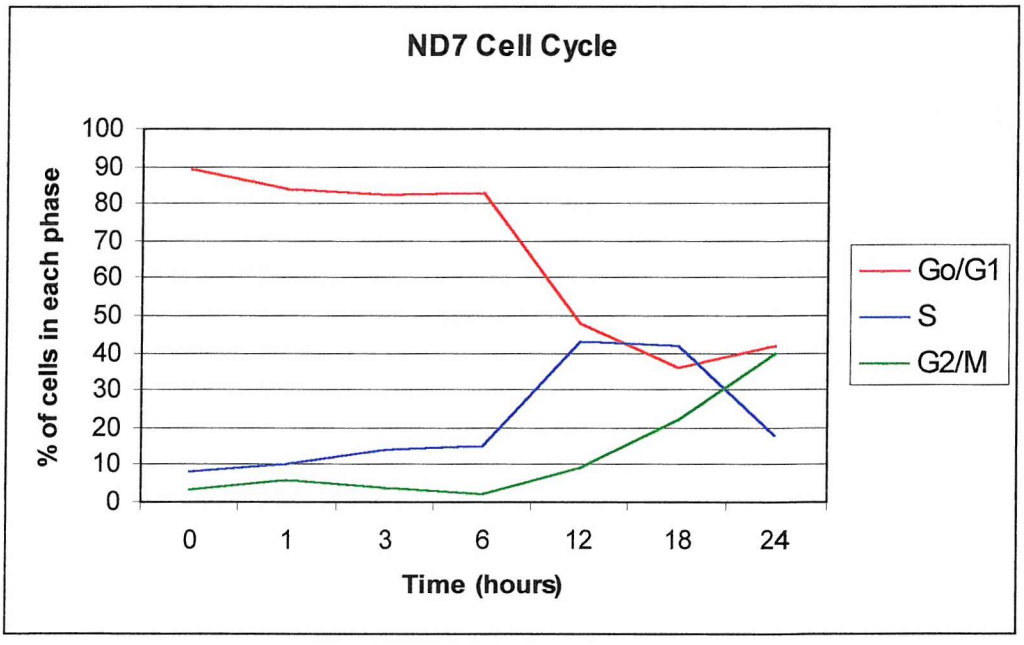

Fig. 3.22 A graph to show the duration of each phase of the ND7 cell cycle

Data obtained from FACS analysis of ND7 cells (table 3.1) is plotted on a graph to illustrate when each phase of the cell cycle finishes and the next one begins.

During the first 6 hours of the cell cycle the vast majority of the cells are in G_1 phase. The G_1/S phase transition occurs between 6 and 12 hours, as the percentage of cells in G_1 phase decreases and the percentage of cells in S phase increases during this time. The peak in the number of cells in S phase occurs between 12 and 18 hours, indicating that S phase of the cell cycle occurs between these times. The ND7s start to pass into the G2 and M phases after 18 hours. At 24 hours the number of cells in G_0/G_1 has started to increase again, indicating that the ND7 cells have passed through one complete cell cycle by this time.

Nuclear extracts were made from cells 0, 3, 6, 10 and 18 hours after growth in 10% serum. At 0 hours the cells will be growth arrested, while after 3 hours the cells should have entered G_1 phase. The majority of cells harvested after 6 hours will still be in G_1 phase, although some may be starting to pass into S phase. After 10 hours some cells will still be in G_1 phase, although most will have progressed into S phase. The vast majority of cells harvested after 18 hours will be in the G_2/M phases of the cell cycle. Nuclear extracts made from ND7 cells harvested at each of these time points were used to phosphorylate recombinant GST / Pax3-DBD protein using [γ-^{32}P] ATP. As shown in figure 3.23, phosphorylated proteins were resolved on an SDS-Polyacrylamide gel, which was then stained with Coomassie blue, dried down and autoradiographed. Equal amounts of GST / Pax3-DBD protein were used in each reaction. However, the autoradiograph of the protein gel shows that the amount of GST / Pax3-DBD phosphorylation was not the same in each case. As previously shown, a nuclear extract made from serum starved (growth arrested) ND7 cells could phosphorylate GST / Pax3-DBD. An extract made 3 hours after serum starvation, when the cells were in G_1 phase, phosphorylated GST / Pax3-DBD to a similar extent. The amount of phosphorylated

protein peaked 6 hours after serum starvation, since the extract made at this stage resulted in the most intense band on the autoradiograph. After 10 hours, when the cells would have been progressing into S phase, the level of phosphorylation had decreased again. Very little phosphate was incorporated when extracts made from cells harvested 18 hours after serum starvation were used. This time point marks the end of the ND7 cell cycle, when the majority of cells are in the G_2/M phases.

Therefore nuclear extracts made from ND7 cells in G_1 phase of the cell cycle were responsible for the highest level of GST / Pax3-DBD phosphorylation. RT-PCR analysis of *Pax-3* expression has shown that *Pax-3* mRNA levels are significantly increased during G_1, reaching a peak 6 hours into the cell cycle. Therefore upregulation of *Pax-3* expression towards the end of G_1 phase may be accompanied by an increase in Pax-3 phosphorylation. If this is the case then phosphorylation may be involved in controlling Pax-3 activity *in vivo*.

Protein Gel

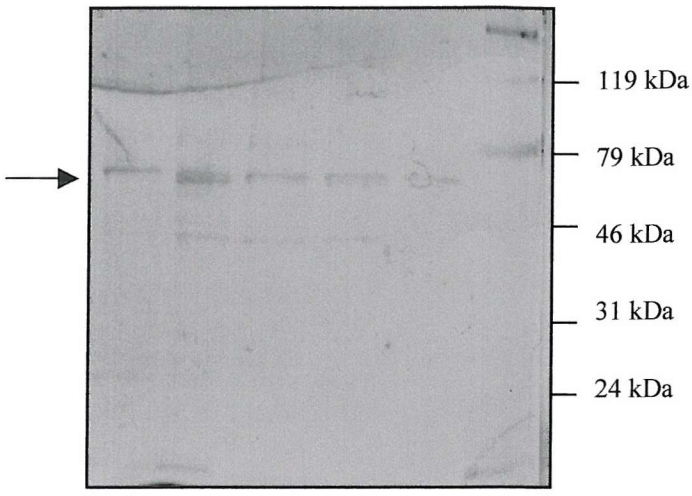

+18 +10 +6 +3 SS

[Hours after serum starvation]

Autoradiograph

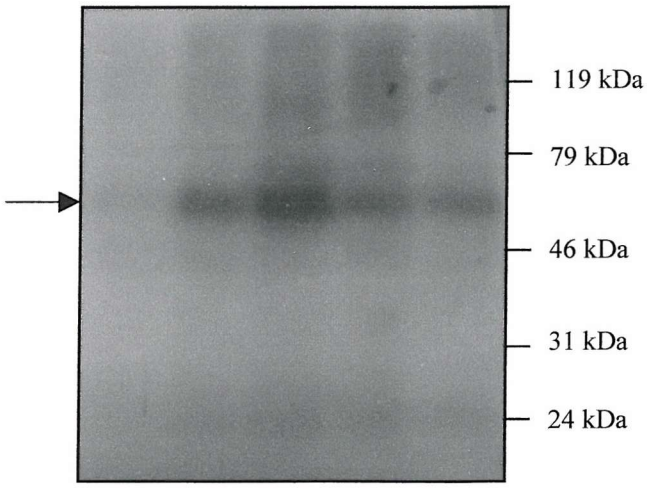

+18 +10 +6 +3 SS

[Hours after serum starvation]

Fig. 3.23 Phosphorylation of GST / Pax3-DBD *in vitro* by ND7 nuclear extracts

10% serum was added back to serum starved **(SS)** ND7 cells, which were then cultured for the times shown before being harvested. Aliquots of nuclear extracts (5μg total protein) made from the cells at each time point were used to phosphorylate 1μg of GST / Pax3-DBD. The reactions were then analysed by 10% SDS-PAGE and autoradiography. The locations of the GST / Pax3-DBD protein on the protein gel and on the autoradiograph are marked with arrows.

3.6 Discussion

There are many examples in which direct phosporylation of a transcription factor can alter its activity either by affecting the way it binds to DNA or by having some effect on either the nuclear localisation or the transactivation function of the protein. Little is known about the effect phosphorylation might have on the activity of Pax proteins. The Pax-8 protein contains two potential sites for phosphorylation by PKA, and the transactivation of reporter genes by Pax-8 is enhanced by PKA. At present it is not known whether Pax-3 activity is also influenced by phosphorylation. As shown in figure 3.27, all the Pax proteins contain potential sites for one or more of the serine/threonine protein kinases PKA, PKB and PKC. The Pax-3 protein has three potential PKA sites and 12 potential PKC sites. Both these protein kinases have been implicated in the regulation of transcription factor activity. Therefore the ability of PKA and PKC to phosphorylate Pax-3 *in vitro* was determined. It was shown that a GST-Pax3 fusion protein containing both the DNA binding domains of Pax-3 could be phosphorylated *in vitro* by the catalytic subunit of PKA. GST protein expressed alone was not phosphorylated. This implied that Pax-3 was phosphorylated by PKA *in vitro* within its DNA binding domains. Pax-3 was also phosphorylated *in vitro* within its DNA binding domains by the catalytic subunit of PKC. Another GST fusion protein containing the Pax-3 paired domain plus the N-terminal half of the linker region that joins the paired domain to the homeodomain was expressed and purified. This protein was also phosphorylated *in vitro* by the catalytic subunits of PKA and PKC. A GST fusion protein containing the C-terminal half of the linker region in addition to the homeodomain itself was also expressed and purified. This protein was phosphorylated *in vitro* by the PKA catalytic subunit, although phosphorylation by PKC was not detected.

These data indicate that *in vitro* PKA phosphorylates both the paired domain and the homeodomain of Pax-3. PKA may also phosphorylate Pax-3 in the linker region that separates the DNA binding domains. The positions of the three potential PKA sites identified in the Pax-3 sequence are illustrated in figure 3.24.

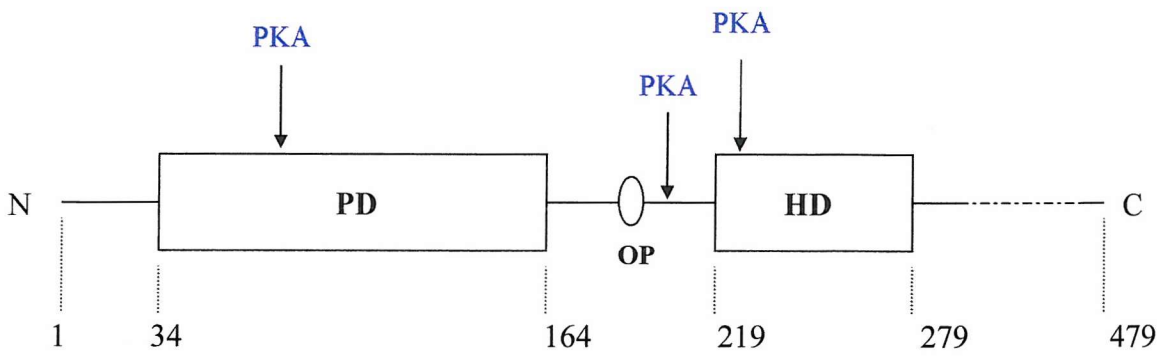

Fig. 3.24 Domain structure of Pax-3, showing the locations of potential PKA phosphorylation sites

PD, paired domain. OP, octapeptide. HD, homeodomain. The numbers refer to amino acids in the Pax-3 sequence.

None of the potential PKA sites in Pax-3 conform to the full consensus sequence for PKA, and are therefore considered to be weak sites. However, since the GST / Pax3-DBD, GST-PD and GST-HD proteins were all phosphorylated by PKA *in vitro*, Pax-3 must have been phosphorylated at weak PKA sites. Since the GST-PD protein contains only one potential PKA site, it is assumed that the Pax-3 paired domain was phosphorylated by PKA at this site *in vitro*. The GST-HD protein contains two potential PKA sites, one in the linker region and another in the Pax-3 homeodomain. Either or both of these sites may have been phosphorylated by PKA. Of the three potential PKA sites present in Pax-3, the site in the linker region is most likely to be a substrate for

PKA *in vitro*. This PKA site has an uncharged alanine residue on the C-terminal side of the phosphoacceptor serine; optimum substrates for PKA usually have an uncharged amino acid in this position. The PKA site in the paired domain has a histidine residue after the serine, which can be either positively charged or neutral at physiological pH. The homeodomain site is the least likely substrate for PKA since it has an arginine residue after the serine. This amino acid is positively charged and hydrophilic. Moreover, basic residues on the C-terminal side of the phosphoacceptor residue are known to have a negative influence on phosphorylation by PKA.

It is not known whether any of the PKA sites identified in the Pax-3 sequence are phosphorylated by PKA *in vivo*. The PKA site that occurs at position 46 of the paired domain is conserved in Pax-7, the other member of the subclass of Pax proteins to which Pax-3 belongs. This site is also conserved in Pax-1 and Pax-9, as well as in Pax-2, Pax-5 and Pax-8. The fact that such a range of Pax proteins possess a PKA site at this position in their paired domain suggests that phosphorylation at this site by PKA may be important for the function of these proteins *in vivo*. The PKA site at the start of the Pax-3 homeodomain is also conserved in Pax-7, although the PKA site in the linker region of Pax-3 is not conserved. Therefore phosphorylation of the Pax-3 homeodomain by PKA may also be implicated in Pax-3 function *in vivo*.

As shown in figure 3.25, potential PKC sites occur in the paired domain, in both halves of the linker region and in the homeodomain of Pax-3. *In vitro* kinase assays showed that Pax-3 was phosphorylated *in vitro* by PKC within the paired domain itself and/or in the N-terminal half of the linker region. However, it appears that neither the C-terminal half of this linker region or the homeodomain are phosphorylated *in vitro* by PKC. All except

one of the potential PKC sites in Pax-3 has the sequence **S/T*** X_{0-2}**R/K**$_{1-3}$ or **R/K**$_{1-3}X_{0-2}$**S/T***. Both these sites represent weak PKC sites since they have basic amino acids on one side of the phosphoacceptor residue only. The full consensus PKC site, **K/R**$_{1-3}X_{0-2}$**S/T*** X_{0-2}**R/K**$_{1-3}$, has basic amino acids on both sides of the phosphoacceptor residue. The potential PKC site at the start of the Pax-3 homeodomain (Ser 222) could be considered to be a consensus PKC site since it has arginine residues on both sides of the phosphoacceptor serine. However, the vast majority of physiological substrates for PKC that contain consensus PKC sites have a spacing of at least one amino acid between the phosphoacceptor Ser/Thr and the basic residues on either side. Therefore phosphorylation at Ser 222 by PKC *in vitro* may be no more likely to occur than phosphorylation at any of the other putative PKC sites in Pax-3.

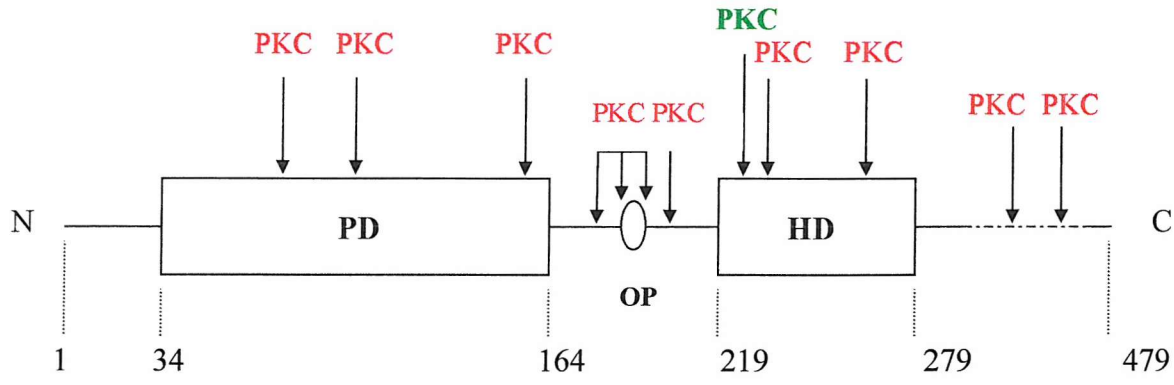

Fig. 3.25 Domain structure of Pax-3, showing the locations of potential PKC phosphorylation sites

PD, paired domain. OP, octapeptide. HD, homeodomain. The numbers refer to amino acids in the Pax-3 sequence. Weak PKC sites are shown in red. The site that most closely matches the consensus PKC sequence is shown in green.

The exact locations of the sites phosphorylated by PKC *in vitro* have yet to be determined. Furthermore, as in the case of PKA mediated phosphorylation, it is not known whether Pax-3 is phosphorylated by PKC *in vivo*. However, some of the PKC sites in Pax-3 are conserved in other Pax proteins as shown in figure 3.26. The PKC site at position 46 of the paired domain is conserved in Pax-7, Pax-1 and Pax-9, and in Pax-2, Pax-5 and Pax-8. The site at position 62 of the paired domain is conserved in Pax-7 and Pax-8. A third PKC in the Pax-3 paired domain (position 120) is conserved in Pax-1 and Pax-9. In addition a PKC site in the N-terminal half of the linker region, two sites at the start of the homeodomain (positions 4 and 7) and a site towards the end (position 50) of the homedomain are all conserved in Pax-7. The conservation of these sites within the Pax protein family, suggests that phosphorylation of the Pax-3 protein within the paired domain and homeodomain may be important in terms of its function *in vivo*.

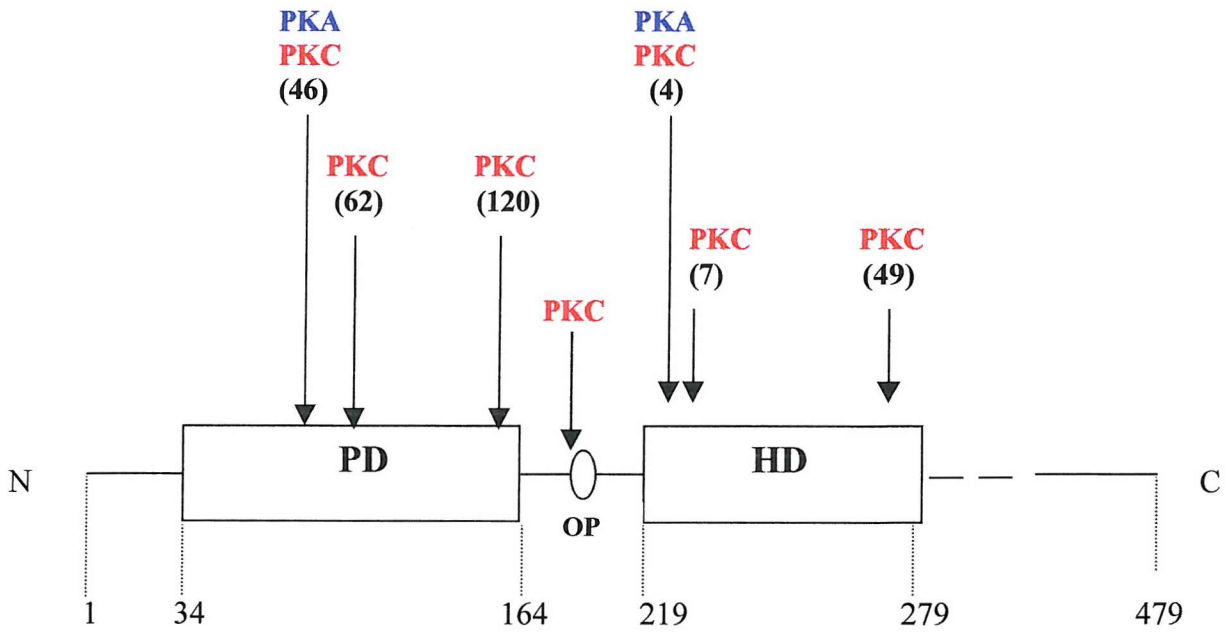

Fig. 3.26 Conservation of PKA and PKC sites amongst Pax proteins

PD, paired domain; OP, octapeptide; HD, homeodomain. Numbers in brackets refer to positions in the PD and HD. Numbers without brackets are amino acids in Pax-3.

Future work on Pax-3 phosphorylation could be carried out in order to determine which sites in the Pax-3 sequence are phosphorylated by PKA and PKC. Proteins such as c-Jun (Boyle *et al.*, 1991) and the insulin receptor protein (Asamoah *et al.*, 1995) have been analysed in this way. Pax-3 protein that had been phosphorylated *in vitro* or *in vivo* (obtained by immunoprecipitating Pax-3 from cells treated with [^{32}-P] orthophosphate) would first be resolved by SDS-PAGE. The Pax-3 protein band would then be cut from the gel and extracted. The protein would be digested fully with trypsin to give a series of peptides. These peptides could then be analysed by a technique called two-dimensional phosphopeptide mapping. Here the peptides are applied to a thin layer chromatography plate, before being resolved in the horizontal direction by electrophoresis and in the vertical direction by ascending chromatography. Phospho-peptides in the sample are then visualised by autoradiography. To determine whether PKA or PKC could phosphorylate Pax-3 at a particular site, that site could be mutated, by replacing the serine/threonine residue with a non-phosphorylatable residue like alanine. Two-dimensional phosphopeptide mapping of the wild type and mutant proteins would then be carried out. If a phospho-peptide were missing from the mutant protein sample when compared to the wild type, it would suggest that the site in question was phosphorylated in the wild type Pax-3 protein.

Pax-3 is thought to be involved in cell growth. It is expressed only in dividing cells, and following the down-regulation of Pax-3 these cells start to differentiate. Both PKA and PKC have roles in cell proliferation and differentiation as well. Therefore phosphorylation of the Pax-3 protein by PKA and PKC *in vivo* may be significant in terms of Pax-3 function. As already described there are two types of PKA regulatory subunit, which associate with the catalytic subunits of PKA to give two distinct forms of

the holoenzyme, termed type I and type II PKA. Type I PKA is thought to be a positive regulator of cell growth since high levels of this enzyme are associated with actively dividing cells. However, in differentiated cells the balance is shifted such that type II PKA is more abundant then type I PKA (Cho-Chung, 1990). In many cancer cells the ratio of regulatory subunit type I to type II is higher than in normally dividing cells. This is thought to contribute to cell transformation during the development of cancer. Cyclic AMP analogues that are selective for the type II regulatory subunit can restore the normal balance between type I PKA and type II PKA isoforms. In the human glioma cell line A-172, this has been shown to decrease cell proliferation as well as increase cell differentiation and subsequent apoptosis (Chen *et al.*, 1998). Thus phosphorylation of Pax-3 by PKA may contribute to its apparent roles in cell proliferation and differentiation. Phosphorylation by PKA type I might activate Pax-3 enabling it to transcribe genes that promote cell proliferation, and switch off genes that promote differentiation.

Similarly PKC has been implicated in the control of cell proliferation and differentiation. PKC appears to be a negative regulator of the eukaryotic cell cycle, where it acts at the transition points between the G_1 and S phases and between the G_2 and M phases (Livneh and Fishman, 1997). Growth inhibitory effects and the stimulation of cell differentiation by PKC isoforms have been demonstrated in a range of cell types, whereas PKC activates cell proliferation in other cells (Clemens *et al.*, 1992). Thus if Pax-3 was phosphorylated by PKC *in vivo*, its ability to activate genes involved in cell proliferation could be enhanced. Alternatively a decrease in DNA binding activity or transactivation potential of Pax-3 in response to phosphorylation by PKC might occur. This could

prevent Pax-3 from activating genes that promote cell differentiation. Hence these cells would remain in a proliferating state.

As well as being substrates for *in vitro* phosphorylation by PKA and PKC, the GST-Pax3 proteins were also phosporylated *in vitro* by nuclear extracts. Nuclear extracts made from dividing and quiescent ND7 cells phosphorylated the GST / Pax3-DBD and GST-HD proteins, while low levels of phosphorylation were seen for the GST-PD protein. In addition IMR-32 extracts phosphorylated the GST / Pax3-DBD and GST-HD proteins but not the GST-PD protein. None of the proteins were phosphorylated by Cos-1 nuclear extracts. Therefore kinases present in the nuclei of ND7 and IMR-32 cells can phosphorylate Pax-3 *in vitro* either within the homeodomain itself or the C-terminal half of the linker region between the paired domain and homeodomain. In addition to phosphorylating these regions of Pax-3, ND7 kinases also cause some phosphorylation within the paired domain and/or the N-terminal half of the linker region joining the two DNA binding domains. Thus extracts made from neuronal cell lines that express endogenous Pax-3 (ND7 and IMR-32) were able to phosphorylate Pax-3 *in vitro.* However, extracts made from Cos-1 cells that do not express endogenous Pax-3 could not phosphorylate Pax-3 *in vitro.* This suggests that Pax-3 may be phosphorylated *in vivo* by kinases that are specific to neuronal cell types or that Pax-3 phosphorylation is dependent upon neuronal specific cofactors.

The purified protein kinases and nuclear extracts that phosphorylate Pax-3 *in vitro* are summarised in table 3.2. The number of ticks assigned to each protein shows the relative amount of phosphorylation that was observed.

Table 3.2 Phosphorylation of GST-Pax3 fusion proteins by purified protein kinases and nuclear extracts

Protein	Phosphorylated By PKA?	Phosphorylated By PKC?	Phosphorylated By Nuclear Extracts?			
			ND7 (div.)	ND7 (ss)	IMR-32	Cos-1
GST / Pax3-DBD	✓✓	✓✓	✓✓	✓✓	✓✓	×
GST-PD	✓	✓	✓	✓	×	×
GST-HD	✓	×	✓✓	✓✓	✓✓	×

For the kinase assays carried out with purified PKA and PKC, comparing bands on the autoradiographs indicated that more phosphate was incorporated into GST / Pax3-DBD than GST-PD. In order to prove this, known amounts of GST / Pax3-DBD and GST-PD proteins could be subjected to *in vitro* phosphorylation by PKA and PKC. The phosphorylated proteins would then be analysed by SDS-PAGE. After drying down the protein gels, the GST / Pax3-DBD and GST-PD protein bands would be excised and the radioactivity contained in each one calculated by liquid scintillation counting. From the results phosphate incorporation into each protein by PKA and PKC could be calculated, and expressed as the number of moles of phosphate per mole of protein.

Assuming that the level of phosphate incorporation was higher for GST / Pax3-DBD than GST-PD, this would imply that a greater proportion of the GST / Pax3-DBD protein was phosphorylated by PKA and PKC *in vitro*. The GST / Pax3-DBD protein could make a better substrate for phosphorylation by PKA and PKC than GST-PD. The tertiary structure of the Pax-3 moiety in the GST / Pax3-DBD protein may differ from its structure in the GST-PD protein since the former protein contains both DNA binding domains whereas GST-PD contains only the Pax-3 paired domain.

	NUMBER OF PKA SITES		NUMBER OF PKB SITES		NUMBER OF PKC SITES	
	CONSENSUS	'WEAK'	CONSENSUS	'WEAK'	CONSENSUS	'WEAK'
Pax-1	-	4	-	2	1	7
Pax-2	-	2	-	-	1	10
Pax-3	-	3	-	-	1	11
Pax-4	-	-	-	1	-	6
Pax-5	-	1	-	-	1	5
Pax-6	-	2	1	1	-	9
Pax-7	-	3	-	-	1	8
Pax-8	-	3	-	1	1	11
Pax-9	-	1	-	1	-	7

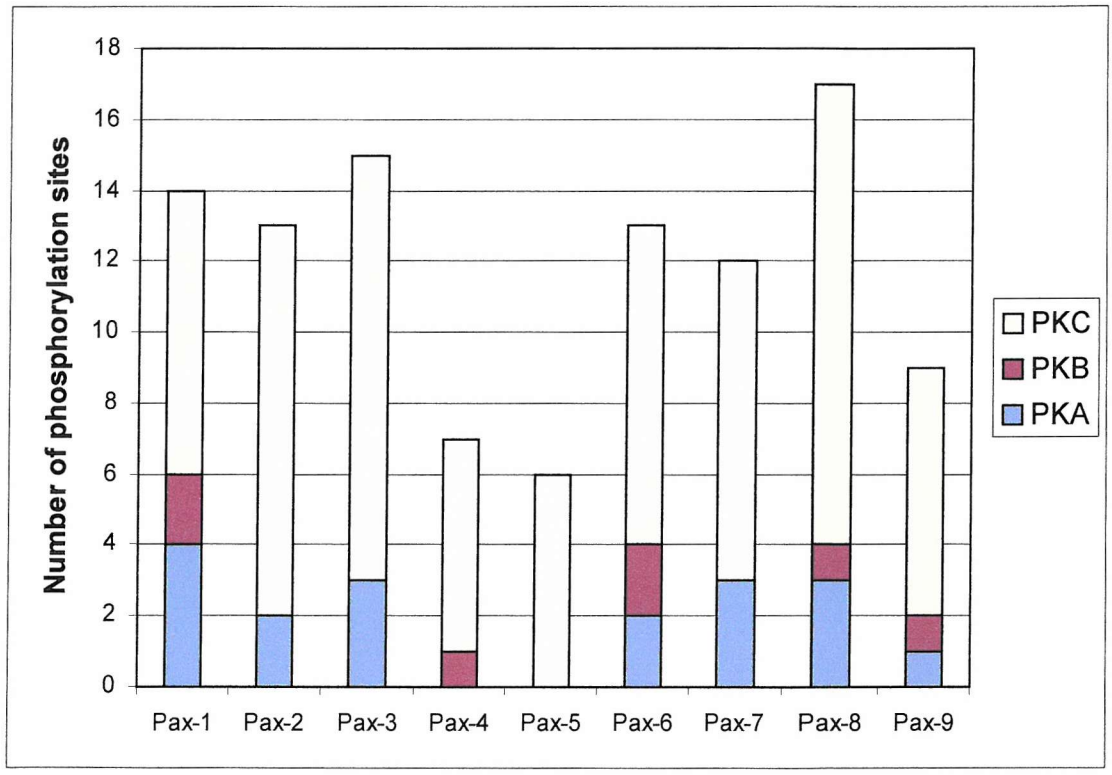

Fig. 3.27 Potential PKA, PKB and PKC sites in Pax proteins

PKB sites correspond to those described by Brazil and Hemmings (2001). References for the PKA and PKC sites are given in the text.

Alternatively the proteins may have been phosphorylated at multiple sites, with GST / Pax3-DBD being phosphorylated at more sites than GST-PD. This possibility is supported by the fact that potential sites for phosphorylation by PKA and PKC are spread throughout the paired domain, linker region and homeodomain of Pax-3. It was subsequently shown that the GST-HD protein, which contains the C-terminal half of the linker region as well as the homeodomain itself, was also phosphorylated *in vitro* by PKA. However, GST-HD was not phosphorylated by PKC, despite there being five potential PKC sites in the GST-HD sequence. The conformation of the Pax-3 moiety in the GST-HD protein may be such that it prevents the potential PKC sites in the homeodomain from being phosphorylated by PKC *in vitro*.

As already described, the GST-Pax3 proteins were also phosphorylated *in vitro* by nuclear extracts. Since PKA and PKC can both localise to the cell nucleus, it is possible that these kinases were responsible for the phoshorylation of Pax-3 mediated by nuclear extracts. However, as shown in figure 3.28, Pax proteins also contain potential phosphorylation sites for protein kinases other than PKA and PKC. Pax-3 has six potential CKII sites and four potential MAP kinase sites. Therefore either or both of these protein kinases may have caused the phosphorylation of Pax-3 mediated by nuclear extracts.

Mitogen activated protein kinase (MAP kinase) translocates from the cytoplasm to the nucleus of cells following stimulation by mitogens. It is a proline directed serine/threonine protein kinase that is thought to be involved in the phosphorylation of a range of transcription factors in the nucleus. For example c-Myc and NF-IL6, a leucine zipper transcription factor, are both phosphorylated by MAP kinase within their

transactivation domain, leading to the increased transactivation of target genes (Davis, 1993). MAP kinase has also been implicated in the control of the cell cycle in eukaryotic cells (Wilkinson and Millar, 2000). Progression through the eukaryotic cell cycle is governed by the expression of cyclin dependent kinases (CDKs) and their regulatory subunits called cyclins. On their own CDKs are inactive catalytic subunits. They are activated when they bind to their cyclin partners. In the G_1 phase of the cell cycle D type cyclins are expressed, which form complexes with CDK4 and CDK6. Towards the end of G_1 phase cyclins E and A are expressed, which go on to form complexes with CDK2 during S phase. MAP kinase helps to control the levels of cyclins and cyclin/CDK complexes that are required for cells to progress from G_1 to S phase of the cell cycle. Of the four potential MAP kinase sites in the Pax-3 sequence, two are located in the C-terminus, which is not present in any of the GST-Pax3 fusion proteins that were expressed. However, there is one site immediately N-terminal to the paired domain and another site in the paired domain itself. All the potential MAP kinase sites located in the Pax-3 sequence are weak sites. However, since Pax-3 appears to be phosphorylated at weak PKA and PKC sites *in vitro*, it might also be phosphorylated at weak MAP kinase sites. Consequently MAP kinase may have been responsible for the phosphorylation of the GST / Pax3-DBD and GST-PD proteins observed in the presence of nuclear extracts, although phophorylation of GST-HD *in vitro* was probably not due to MAP kinase. In addition this kinase is unlikely to have been responsible for the phosphorylation of GST-Pax3 proteins mediated by nuclear extracts that were made from serum starved ND7 cells. This is because MAP kinase is activated in response to mitogens, which would not be available when these cells were grown in the absence of serum.

	Number of CKII sites	Number of MAP Kinase sites	
		Consensus	Weak
Pax-1	2	4	4
Pax-2	5	-	5
Pax-3	6	-	4
Pax-4	2	1	6
Pax-5	5	-	9
Pax-6	2	2	4
Pax-7	3	-	1
Pax-8	6	2	9
Pax-9	2	1	8

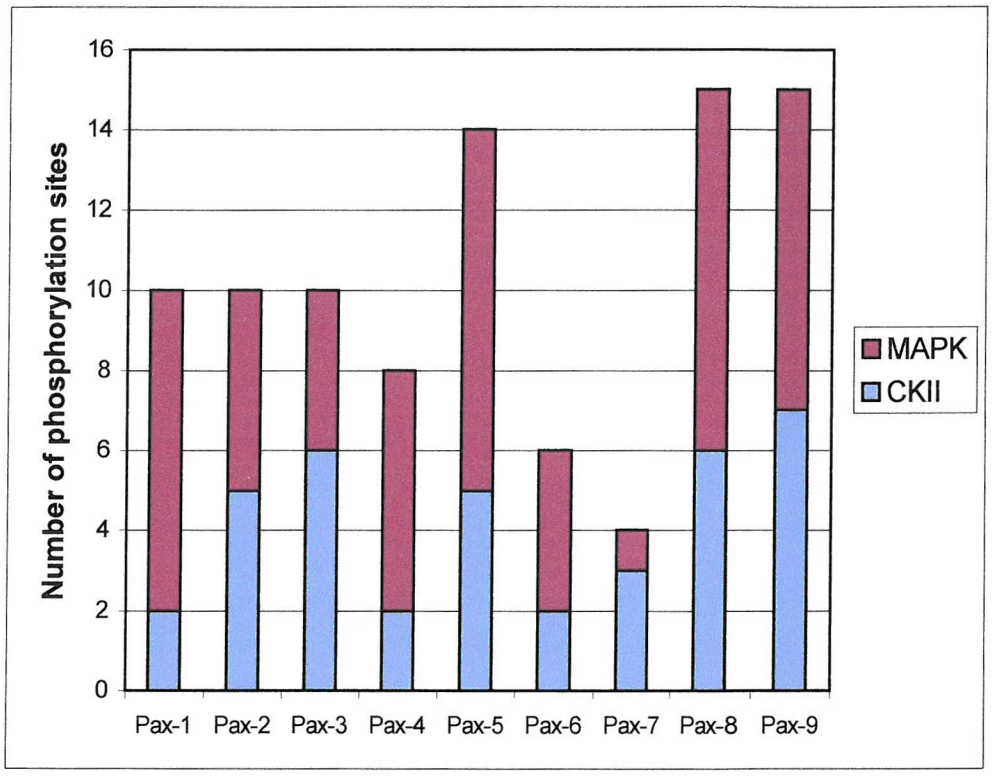

Fig. 3.28 Potential CKII and MAP Kinase sites in Pax proteins

CKII sites correspond to those described by Guerra *et al.* (1999). MAP Kinase sites are those described by Davis (1993).

Casein kinase II (CKII) is another serine/threonine protein kinase. The physiological roles of CKII are not well characterised but it is thought to be involved in cell proliferation and tumourigenesis (Guerra *et al.*, 1999). CKII has been shown to phosphorylate some transcription factors, with the DNA binding properties of those proteins being altered as a result. For example CKII can phosphorylate the Myc and Max proteins. Both these proteins have basic helix-loop-helix structures, and bind to DNA either as Max homodimers or Myc-Max heterodimers. CKII mediated phosphorylation inhibits binding of Max homodimers to DNA although Myc-Max DNA binding is not affected (Berberich and Cole, 1992). Similarly the c-Jun protein is phosphorylated by CKII at two sites near the DNA binding domain. This inhibits binding of c-Jun to DNA (Lin *et al.*, 1992). In contrast to these effects, CKII mediated phosphorylation can increase the DNA binding activity of the SRF (serum response factor) protein. This protein binds to the SRE (serum response element) in the c-fos promoter. Phosphorylation of SRF by CKII alters the conformation of the DNA binding domain, thus allowing it to bind more strongly to DNA. The site of phosphorylation is N-terminal to the DNA binding domain of SRF (Manak and Prywes, 1991). Of the six potential CKII sites in the Pax-3 sequence, two are located in the C-terminus. However, three sites are present in the GST-HD protein. Two of these sites are in the C-terminal half of the linker while the other one is in the homeodomain itself. There is also a potential CKII site in paired domain of Pax-3. Therefore it is possible that CKII was involved in the phosphorylation of the GST / Pax3-DBD, GST-PD and GST-HD proteins mediated by nuclear extracts.

Having shown that the GST-Pax3 proteins could be phosphorylated by nuclear extracts from different cell types, it was also demonstrated that GST / Pax3-DBD could be

differentially phosphorylated by extracts made from ND7 cells at different stages of the cell cycle. Extracts made from cells that were in late G_1 phase resulted in the most phosphorylation of GST / Pax3-DBD. Interestingly, at this stage of the cell cycle *Pax-3* expression also increases, as determined by RT-PCR. Therefore it is possible that as Pax-3 protein levels increase the amount of Pax-3 phosporylation also increases. Thus, *in vivo* Pax-3 might be phosphorylated by protein kinases that are upregulated during G_1 phase of the cell cycle. As already mentioned cyclin dependent kinases (CDKs), in conjunction with their regulatory subunits cyclins, are vitally important for controlling progression through the cell cycle. D type cyclins complexed with CDK 4 and 6 are active during G_1 phase. Cyclin E complexed with CDK 2 acts at the G_1 / S transition, while cyclin A / CDK 2 is active during S phase. Little is known about proteins that are phosphorylated by these CDKs during the cell cycle. However, one important target for CDKs that act during G_1 phase and at the G_1 / S phase transition is the Retinoblastoma (pRB) protein (Ekholm and Reed, 2000). pRB was originally identified as the product of the retinoblastoma gene, RB1. pRB is a nuclear phosphoprotein, the activity of which is controlled through the cell cycle by phosphorylation. In G_0 and G_1 under-phosphorylated pRB is synthesised. However, at the G_1/S phase boundary multiply phosphorylated pRB is produced. The underphosphorylated form of pRB becomes prominent again during the G_2 and M phases (Mihira *et al.*, 1989). It was proposed that pRB is involved in the control of cell proliferation because it becomes phosphorylated just before the start of DNA synthesis. In fact pRB forms complexes with the E2F family of transcription factors, which control genes involved in DNA synthesis (Chellappan *et al.*, 1991). The interaction of pRB with E2F represses E2F-dependent transcription. Only the underphosphorylated form of pRB can interact with E2F proteins. However, during G_1 phase and at the G_1 / S phase transition pRB is phosphorylated by CDK 4/6 and CDK 2

respectively. This prevents pRB from interacting with E2F. Subsequently E2F is able activate its target genes.

In addition to the phosphorylation of RB proteins, direct phosphorylation of a transcription factor by a CDK has also been demonstrated. Cyclin A / CDK 2 complexes were shown to phosphorylate the SP1 transcription factor. This resulted in an increase in the DNA binding activity of the SP1 protein (De Boja *et al.*, 2001). Therefore it is possible that the activity of Pax-3 is also affected by phosphorylation mediated by CDKs. However Endicott *et al.* (1999) described the consensus sequence for phosporylation by CDKs 1, 2, 4 and 6 as being: S/T*- P – X – K/R (the asterisk shows the serine/threonine residue on which phosphorylation occurs, and X represents any amino acid). This site does not occur anywhere in the Pax-3 amino acid sequence. Therefore it seems unlikely that Pax-3 could be phosphorylated *in vivo* by CDKs that are expressed during G_1 and S phase of the cell cycle.

If Pax-3 is not phosphorylated by CDKs then other protein kinases, active during G_1 phase, must be responsible for the peak in Pax-3 phosphorylation that appears to occur at this point in the cell cycle. As already mentioned Pax-3 contains potential phosphorylation sites for MAP kinase. Upon stimulation of cells with mitogens, this enzyme normally translocates to the nucleus. Brunet *et al.* (1999) prevented this nuclear translocation by expressing an inactive form of a cytoplasmic phosphatase that normally serves to inactivate MAP kinase. Under these conditions cytoplasmic proteins were still phosphorylated by MAP kinase, but the enzyme was prevented from gaining access to its nuclear targets. As a result cells were unable to progress from G_1 to S phase, as shown by the absence of DNA synthesis. Work by other groups demonstrated that MAP kinase

helps to control the progression of cells through G_1 phase and into S phase. As already mentioned cyclin D1 forms complexes with CDKs 4 and 6, which are required for progression through G_1. MAP kinase stimulates expression of the cyclin D1 gene. This induction is dependent upon sites in the cyclin D1 promoter for AP-1 and Ets proteins. It is thought that MAP kinase phosphorylates the AP-1 and Ets proteins, which then bind to the cyclin D1 promoter and activate expression of the cyclin D1 gene (Albanese *et al.*, 1995). As well as increasing the expression of cyclin D1, MAP kinase also helps stabilise the cyclin D protein. Glycogen synthase kinase-3 (GSK-3) phosphorylates cyclin D at a specific threonine residue, thus triggering the proteosomal degradation of cyclin D protein. However, the MAP kinase pathway activates PI3-kinase, which in turn stimulates PKB. As a result GSK-3 is phosphorylated and its catalytic activity inhibited by PKB. Therefore less cyclin D protein is phosphorylated by GSK-3 and so cyclin D becomes less susceptible to degradation (Diehl *et al.*, 1998). MAP kinase also stimulates the expression of p21 during early G_1 phase of the cell cycle (Bottazzi *et al.*, 1999). The p21 protein is an inhibitor of CDKs and is therefore considered a negative cell cycle regulator. However, during early G_1 phase the p21 protein is required for proper assembly of cyclin-CDK complexes. Consequently at this early stage of the cell cycle, p21 has a positive affect on cell cycle progression.

Since MAP kinase is active in the nuclei of cells during G_1, and there are potential MAP kinase sites in Pax-3, this protein kinase could be responsible for increasing the level of Pax-3 phosphorylation at this stage of the ND7 cell cycle. MAP kinase is believed to be involved in the control of c-Myc activity by phosphorylation (Gupta *et al.*, 1993). Like Pax-3, c-Myc is a transcription factor involved in the control of cell proliferation and differentiation (Hopewell *et al.*, 1995). The Myc protein has an N-terminal

transactivation domain. Two sites (Thr-58 and Ser-62) in this domain were phosphorylated *in vivo* resulting in the stimulation of gene expression by c-Myc. Ser-62 could be phosphorylated by MAP kinase *in vitro*. It was later shown that transient expression of MAP kinase increased the amount of c-Myc phosphorylated *in vivo* at Ser-62, as well as the transactivation potential of the c-Myc protein. Thus it was proposed that the c-Myc transactivation domain is regulated, at least in part, by MAP kinase mediated phosphorylation of Ser-62.

In addition to MAP kinase sites, the Pax-3 sequence contains putative CKII sites, and there is evidence to suggest that this protein kinase is also active during G_1 phase of the cell cycle. Carroll *et al.* (1989) showed that CKII activity oscillated during the cell cycle of human lung fibroblast cells. Quiescent cells were stimulated to re-enter the cell cycle by the addition of serum to the growth media. A 6-fold increase in CKII activity was observed within 15 minutes of serum being added to the cells. CKII activity then returned to the level seen in the absence of serum within 2 hours. This initial peak in CKII activity correlated with the progression of the cells from G_0 into G_1 phase. A second peak in CKII activity occurred just before the cells progressed from G_1 phase into S phase. A third peak occurred during S phase. Similar results were obtained when *de novo* protein synthesis in the cells was inhibited. Therefore the changes in CKII activity in this human cell line during the cell cycle appear to have been regulated by post-translational modification of the CKII protein rather than changes in CKII protein synthesis. The results suggested that CKII is active both at the start and end of G_1 phase, and during S phase. It was later shown that CKII could phosphorylate the cdc2 protein *in vitro*. This protein was also phosphorylated by CKII *in vivo*, during G_1 phase of the cell cycle (Russo *et al.* 1992). The cdc2 protein plays a key role in the control the eukaryotic

cell cycle. In yeast it is required for both G_1–S and G_2–M phase transitions. There is evidence linking cdc2 to the control of the G_1–S transition in human cells. For example, antisense oligonucleotides directed against human cdc2 mRNA prevented primary human T cells from entering S phase (Furakawa *et al.* 1990). The activity of cdc2 is regulated by its interaction with cyclins, and by phosphorylation / dephosphorylation of the protein kinase itself. In human lymphoid cells cdc2 was shown to interact with cyclin E during G_1 phase (Koff *et al.* 1991). This interaction was a prerequisite for cdc2 activation. Dephosphorylation of specific Tyr and Thr residues in the cdc2 protein (by the phosphatase cdc25) is required in order to activate cdc2 during M phase. Activation of cdc2 during G_1 phase is also regulated by phosphorylation. As already mentioned, CKII appears to be involved in the regulation of cdc2 activity at this stage of the cell cycle. In addition, CKII mediated phosphorylation of the E7 protein from papillomavirus type 18 was demonstrated by Chien *et al.* (2000). The E7 protein promotes S-phase re-entry in postmitotic, differentiated keratinocytes. This allows viral DNA replication to occur using the cellular DNA replication machinery. E7 binds to and inactivates the underphosphorylated form of pRB, and promotes its degradation by the proteosome pathway. However, it was shown that binding of E7 to pRB was necessary but not sufficient to reactivate DNA replication in differentiated keratinocytes. Progression of these cells into S phase required phosphorylation of E7 by CKII in addition to the binding of E7 to pRB.

Thus CKII is active during G_1, and it has been shown to phosphorylate proteins at this stage of the cell cycle. Moreover, the Pax-3 sequence contains several putative CKII sites. Therefore CKII may have contributed to the increased level of Pax-3 phosphorylation that was observed in late G_1 phase of the ND7 cell cycle.

Although it may not be directly phosphorylated by the CDKs that phosphorylate pRB, Pax-3 does itself interact with the RB family (pRB, p107, p130) of proteins. As already described RB proteins have been identified as negative cell cycle regulators. These proteins are also thought to be involved in the control of normal embryonic development. Mice homozygously deleted for pRB die *in utero* by embryonic day 14 as a result of developmental defects (Lee *et al.*, 1992). However, rather than being widespread throughout the embryo, these defects are restricted to cells of the developing nervous system and erythropoeitic cells. This may be due to pRB failing to interact with specific factors that determine cell fate. Significantly pRB has been shown to interact with a range of proteins, including Pax-3, that contain paired type homeodomains (Wiggan et al., 1998). As with the E2F-RB interaction, these homeodomain-containing proteins only bind to the active unphosphorylated form of pRB. Also the interaction of RB proteins with these factors has been shown to cause repression of activated transcription. For example, Pax-3 activates transcription from the c-met promoter, but this activity is repressed by pRB. The same is true for Pax3-dependent transcription from the myosin light chain (MLC) promoter. Both MyoD and Pax-3 activate transcription from the MLC promoter. However pRB augments MyoD dependent transcription while repressing Pax3-dependent transcription.

It is possible that Pax-3 could be regulated by pRB during the cell cycle in the same way as E2F. The unphosphorylated form of pRB could bind to and thus inactivate Pax-3 during the G_0 and G_1 phases. At the G_1/S phase boundary and during S phase when pRB is phosphorylated, Pax-3 would not interact with pRB and would therefore be active. *Pax-3* expression increases at this stage of the cell cycle. The level of phosphorylated Pax-3 protein may also increase at this time. Therefore increased phosphorylation of

Pax-3 at the G_1/S phase boundary may coincide with Pax-3 activation in terms of its ability to activate the transcription of target genes. Thus phosphorylation may be involved in the regulation of Pax-3 activity *in vivo*.

Chapter 4

The effects of PKA and PKC-mediated phosphorylation on the DNA binding properties of Pax-3

4 The effects of PKA and PKC mediated phosphorylation on the DNA binding properties of Pax-3

4.1 Introduction

Pax-3 is a bipartite DNA binding protein. Both the paired domain and the homeodomain of Pax-3 are capable of sequence specific DNA binding. The Pax-3 paired domain consists of two subdomains, both of which possess a helix-turn-helix motif that can bind to DNA. Similarly the homeodomain contains a helix-turn-helix motif for DNA binding. Due to cooperative interactions between the paired domain and the homeodomain, Pax-3 binds most strongly *in vitro* to DNA sites that contain recognition motifs for both these domains. For example, Pax-3 binds with high affinity *in vitro* to e5, a DNA sequence derived from the promoter of the *Drosophila even-skipped* gene (Chalepakis *et al.*, 1994). The e5 sequence contains a GTTCC motif that the paired domain binds to, located 5 nucleotides downstream from an ATTA motif that the homeodomain binds to. Pax-3 can also bind to DNA *in vitro* exclusively through its homeodomain. Underhill *et al.* (1995) showed that the full length Pax-3 protein could bind to the palindromic homeodomain site P2, in which two ATTA homeodomain recognition motifs (on opposite DNA strands) are separated by two base pairs. However, in order to detect any binding of Pax-3 to the single ATTA homeodomain site called P1, a four-fold higher concentration of Pax-3 protein was required. The preference Pax-3 shows for P2 over P1 is due to the fact that Pax-3 can form cooperative dimers on P2 sites. Both homo-dimers of Pax-3 and hetero-dimers with Pax-7 can be formed on P2.

Using a GST fusion protein containing only the DNA binding domains of Pax-3, Phelan and Loecken (1998) described an alternative Pax-3 binding site that is related to e5, but

has a GTTAT motif in place of the GTTCC motif for paired domain binding. The number of nucleotides separating the GTTAT and ATTA motifs was shown to affect the affinity with which the GST-Pax3 protein could bind to this site. High affinity binding was observed, when the two motifs were separated by either 5 or 8 nucleotides, whereas a single nucleotide or 13 nucleotides between the motifs resulted in low affinity binding. Binding affinity was also reduced when either the paired domain or the homeodomain recognition motif was removed, leaving only one binding site for Pax-3. In cotransfection experiments these lower affinity sites also mediated less transactivation by Pax-3 than sites containing recognition motifs for both Pax-3 DNA binding domains. Interestingly, almost all identified Pax3-responsive genes contain low affinity sites in their promoters. For example, the promoter of the Myelin Basic Protein (MBP) gene, the expression of which is repressed by Pax-3 (Kioussi *et al.*, 1995), contains only paired domain recognition sites. Secondly, expression of the c-met gene is believed to be upregulated by Pax-3, since it is greatly reduced in splotch mice that do not express a functional Pax-3 protein. As with the MBP gene, the human c-MET promoter only contains paired domain binding sites. It was proposed that Pax-3 might directly activate c-MET expression by binding to a recognition site in the c-MET promoter. *In vitro* DNA binding studies showed that the isolated Pax-3 paired domain could bind specifically to a paired domain-binding site in the c-MET promoter. In co-transfection experiments, when the region of the c-MET promoter containing this paired domain-binding site was cloned upstream of a minimal promoter in a luciferase reporter construct, Pax-3 was shown to induce expression of the luciferase reporter gene (Epstein *et al.*, 1996).

Pax-3 also induces the expression of *MyoD*, which codes for a muscle regulatory factor (MyoD) that is required during the early stages of skeletal muscle development (Maroto

et al., 1997). However in contrast to the promoters of the MBP and c-MET genes, the *MyoD* promoter contains both a paired domain and a homeodomain binding site, which are separated by 9 base pairs. Genes that contain such high affinity sites in their promoters may be induced in response to a lower level of Pax-3 protein than that which is required to mediate transactivation from low affinity sites. This could facilitate the sequential activation of Pax-3 responsive genes following the induction of *Pax-3* expression during embryogenesis.

Potentially Pax-3 could utilise different modes of DNA binding *in vivo* to activate the transcription of different target genes. Being able to bind to individual paired domain and homeodomain sites as well as to composite paired domain and homeodomain sites could allow Pax-3 to bind DNA in different conformations. This may lead to the recruitment of different sets of cofactors by Pax-3 to different promoters. In addition it could allow the transactivation domain of Pax-3 to interact in different ways with the transcriptional machinery assembled at each of these promoters.

As described in the previous chapter, a GST fusion protein of the full-length Pax-3 protein could not be expressed in bacteria. The Pax3-DBD protein that was expressed in bacteria and purified contains amino acids 1-284 of Pax-3, and terminates at the C-terminal end of the homeodomain. The aim of the work described in the first part of this chapter was to fully investigate the *in vitro* DNA binding properties of Pax3-DBD so that they could be compared with those of the full-length Pax-3 protein. It was considered important to do this since there is experimental evidence to suggest that, in the absence of the Pax-3 C-terminus, the DNA sequence requirements of the Pax-3 paired domain and homeodomain may alter. Firstly, as described by Phelan and Loeken (1998), when a

GST fusion protein containing only the DNA binding domains of Pax-3 was used to select optimal binding sites from a random pool of oligonucleotides, the paired recognition motif GTTAT was recognised in preference to the GTTCC motif that is present in the e5-binding site. Secondly, the C-terminus of Pax-3 affects the DNA binding properties of the Pax-3 homeodomain. In Alveolar Rhabdomyosarcoma, a soft tissue tumour of skeletal muscle lineage, a chromosomal translocation fuses the transactivation domain of the fork-head protein FKHR to the DNA binding domains of PAX3. In cotransfection experiments PAX3-FKHR but not wild type PAX3 activated transcription from the platelet derived growth factor α receptor (PDGFαR) promoter (Epstein *et al.*, 1998). Transcription was also activated from this promoter when a viral transactivation domain was fused to the DNA binding domains of PAX3 in place of the PAX3 C-terminus (Cao & Wang, 2000). A palindromic homeodomain binding site in the PDGFαR promoter was required to mediate transactivation. This site, called P3, contains two ATTA homeodomain binding sites (on opposite DNA strands) that are separated by 3 base pairs. Underhill and Gross (1997) showed that although wild type Pax-3 binds to the P2 site as a cooperative dimer, it only binds very weakly to the P3 site as a monomer. Therefore the C-terminus of PAX3 appears to affect the type of DNA recognition sites that the PAX3 homeodomain can bind to.

As well as studying the *in vitro* DNA binding properties of Pax3-DBD, the ability of the individual paired domain (PD) and homeodomain (HD) proteins to bind to DNA *in vitro* was also investigated. Having compared the *in vitro* DNA binding properties of all three of these proteins with those of full-length Pax-3, the effects of phosphorylation on the DNA binding activities of Pax3-DBD, PD and HD were investigated. Potential PKA and PKC sites in the Pax-3 sequence are located near to and in some cases overlap with

amino acids thought to contact DNA. Therefore phosphorylation of Pax-3 within its DNA binding domains could affect its DNA binding activity *in vitro* and *in vivo*.

4.2 DNA binding properties of bacterially expressed Pax-3 proteins

The DNA binding activities of the Pax3-DBD, PD and HD proteins were studied. The ability of these proteins to bind *in vitro* to paired domain and homeodomain sites was investigated using an electrophoretic mobility shift assay (EMSA). The principle behind this technique is illustrated in figure 4.1. Synthetic oligonucleotides containing potential binding sites for Pax-3 were radiolabelled using [γ-^{32}P] ATP. In each case, the resulting DNA probe was then incubated with the Pax-3 protein *in vitro*, either alone or in the presence of unlabelled ('cold') specific oligonucleotides containing recognition sites for Pax-3, or non-specific oligonucleotides that did not have any Pax-3 recognition sites. Protein-DNA complexes were resolved on a non-denaturing gel, and visualised by autoradiography. Specific protein-DNA complexes should be competed out by a large molar excess of cold specific DNA but not by an excess of cold non-specific DNA.

4.2.1 Binding of Pax3-DBD *in vitro* to the e5 recognition site

Initially binding of Pax3-DBD to the composite paired domain and homeodomain site e5 was studied. Only the Pax-3 moiety of the GST - Pax3-DBD fusion protein was used to analyse Pax-3 DNA binding by EMSA. As illustrated in figure 4.2, thrombin was used to cleave Pax3-DBD from GST. After centrifugation to sediment the glutathione beads, the supernatant was collected, which contained the Pax3-DBD protein.

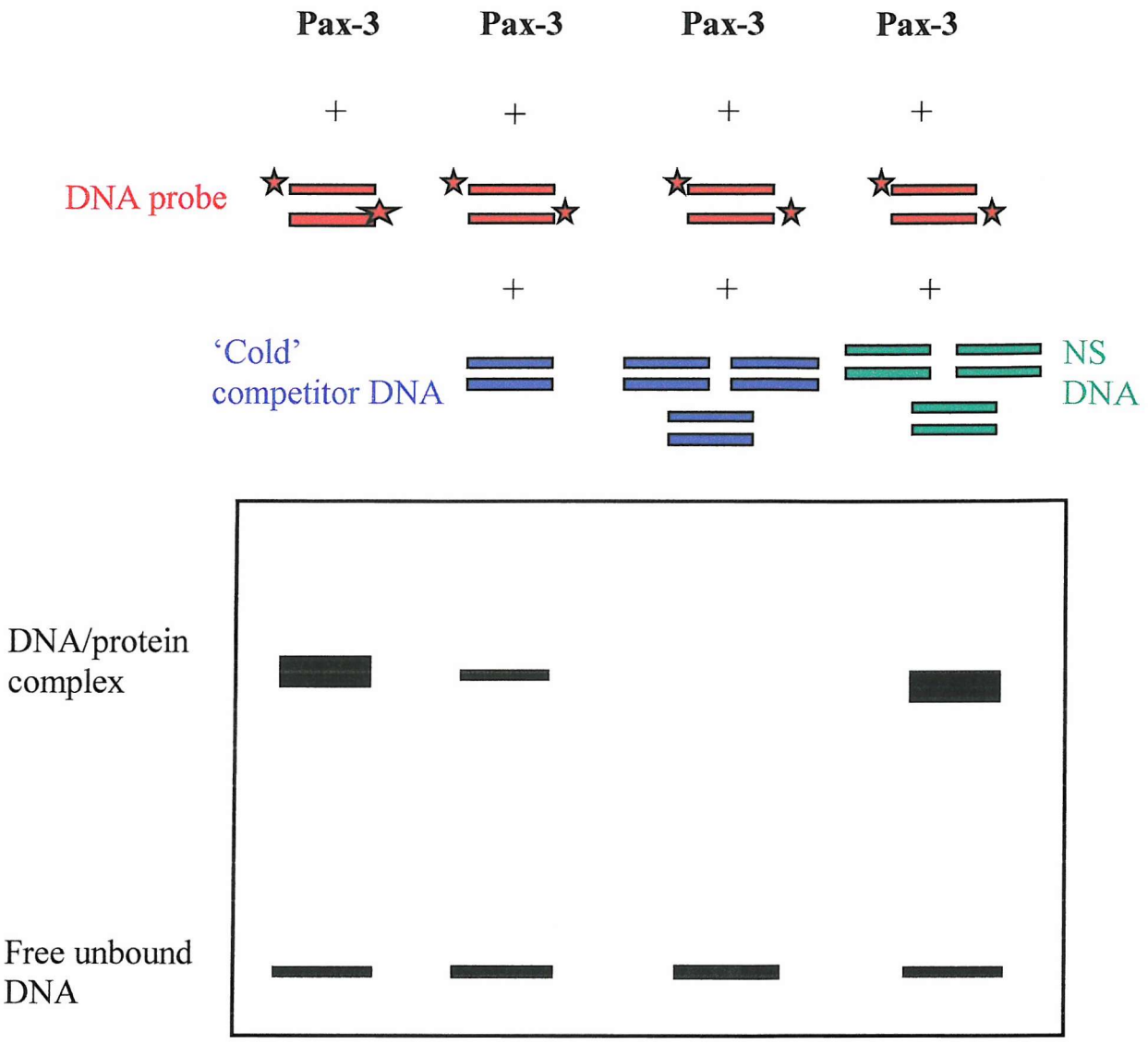

Fig. 4.1 Use of the Electrophoretic Mobility Shift Assay (EMSA) to study protein-DNA interactions

Binding of Pax-3 *in vitro* to radiolabelled oligonucleotides that contain a recognition site for the protein is shown at the top of the diagram. An autoradiograph of the polyacrylamide gel is illustrated at the bottom of the figure, which shows that a Pax3-DNA complex is formed in the absence of any competitor DNA, and in the presence of excess non-specific (NS) DNA. However, this complex is competed out using a large molar excess of unlabelled specific DNA.

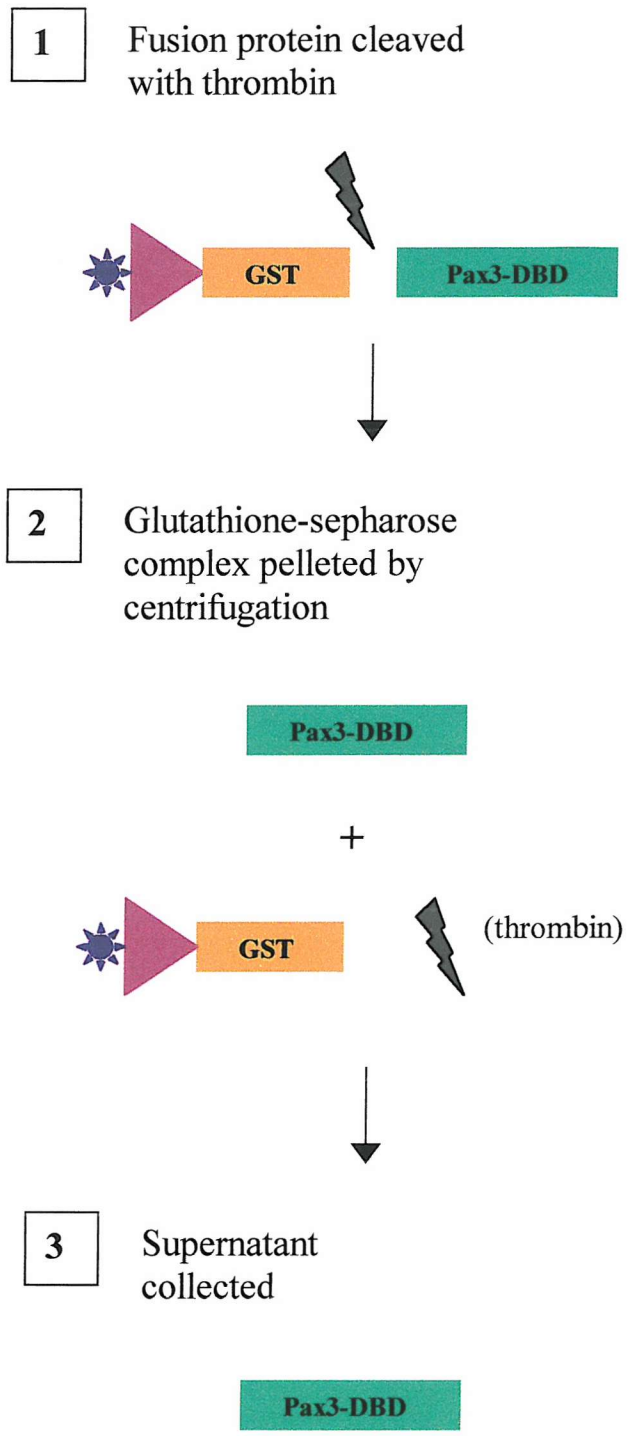

Fig. 4.2 Cleavage of Pax3-DBD from GST using thrombin protease

The Pax3-DBD protein is represented by a green rectangle. The GST protein is represented by an orange rectangle, and the glutathione-sepharose complex is shown as a pink triangle attached to a purple star. Details of the experimental procedure described here are given in Materials and Methods.

GST protein alone, which had also been purified on glutathione-sepharose beads, was incubated in the presence and absence of thrombin under the same conditions as used for GST - Pax3-DBD. Supernatants from the incubations of GST with and without thrombin were analysed by SDS-PAGE, as shown in figure 4.3 (A). For the GST / Pax3-DBD protein, aliquots of glutathione-sepharose beads before and after incubation with thrombin were analysed by SDS-PAGE, in addition to an aliquot of the supernatant collected after incubation of GST / Pax3-DBD with thrombin. This is shown in figure 4.3 (B). For the GST supernatants with and without thrombin, single bands were seen at 26 kDa following staining of the protein gel with Coomassie blue. This corresponds to the size of the GST protein. The presence of GST in the supernatant following incubation with and without thrombin suggests that, after centrifuging to sediment the glutathione-sepharose beads, some of the beads were removed with the supernatant. Presumably more GST was present in the supernatant from the incubation carried out in the presence of thrombin than without thrombin because a greater amount of beads were inadvertently removed with the supernatant. As shown in figure 4.3 (B), following digestion of GST / Pax3-DBD with thrombin, the supernatant produced a band at 32 kDa on the protein gel, which corresponds to the predicted size of the Pax3-DBD protein. A fainter band of 26 kDa, corresponding to GST, was also seen in the supernatant. As for the incubation of GST alone with and without thrombin, it is assumed that the presence of GST in the Pax3-DBD supernatant was due to the transfer of some glutathione-sepharose beads to the supernatant.

Aliquots of the GST and Pax3-DBD supernatants from the incubations carried out in the presence of thrombin were then used in an EMSA with the e5 DNA probe. The results are shown in figure 4.3 (C). No protein-DNA complexes were formed when the DNA

binding activity of the GST protein was analysed (lanes 1-3). This showed that GST is unable to bind to the e5 recognition site. Analysis of the DNA binding activity of the Pax3-DBD protein revealed two bands. The lower mobility band (lane 4) was competed out by a 100x molar excess of cold e5 DNA (lane 5), but not by a 100x molar excess of non-specific DNA (lane 6). These results indicated that Pax3-DBD could bind specifically to the e5 recognition site.

The higher mobility band observed in lanes 4-6 of figure 4.3 (C) was not seen in lanes 1-3. This implied that it did not result from either GST or thrombin binding non-specifically to the e5 DNA probe. In fact this band did not compete out with either a 100x molar excess of cold e5 DNA or a 100x molar excess of cold non-specific DNA. This may suggest that the higher mobility band in lanes 4-6 was due to DNA alone rather than a protein-DNA complex, which may have been caused by dissociation of the Pax3-DBD – e5 complex during electrophoresis. Such dissociation of a protein from the DNA probe is thought possible due to the fact that the length of time that the gel is run for usually far exceeds the half-life of the protein – DNA complex (Carey 1991). If DNA became displaced from the Pax3-DBD – DNA complex during elctrophoresis, the resulting free DNA would not be able to catch up with the DNA that was already free from protein at the start of electrophoresis. This would result in a second free DNA band that had not migrated as far through the gel, as appears to be the case in lanes 4-6 of figure 4.3 (C).

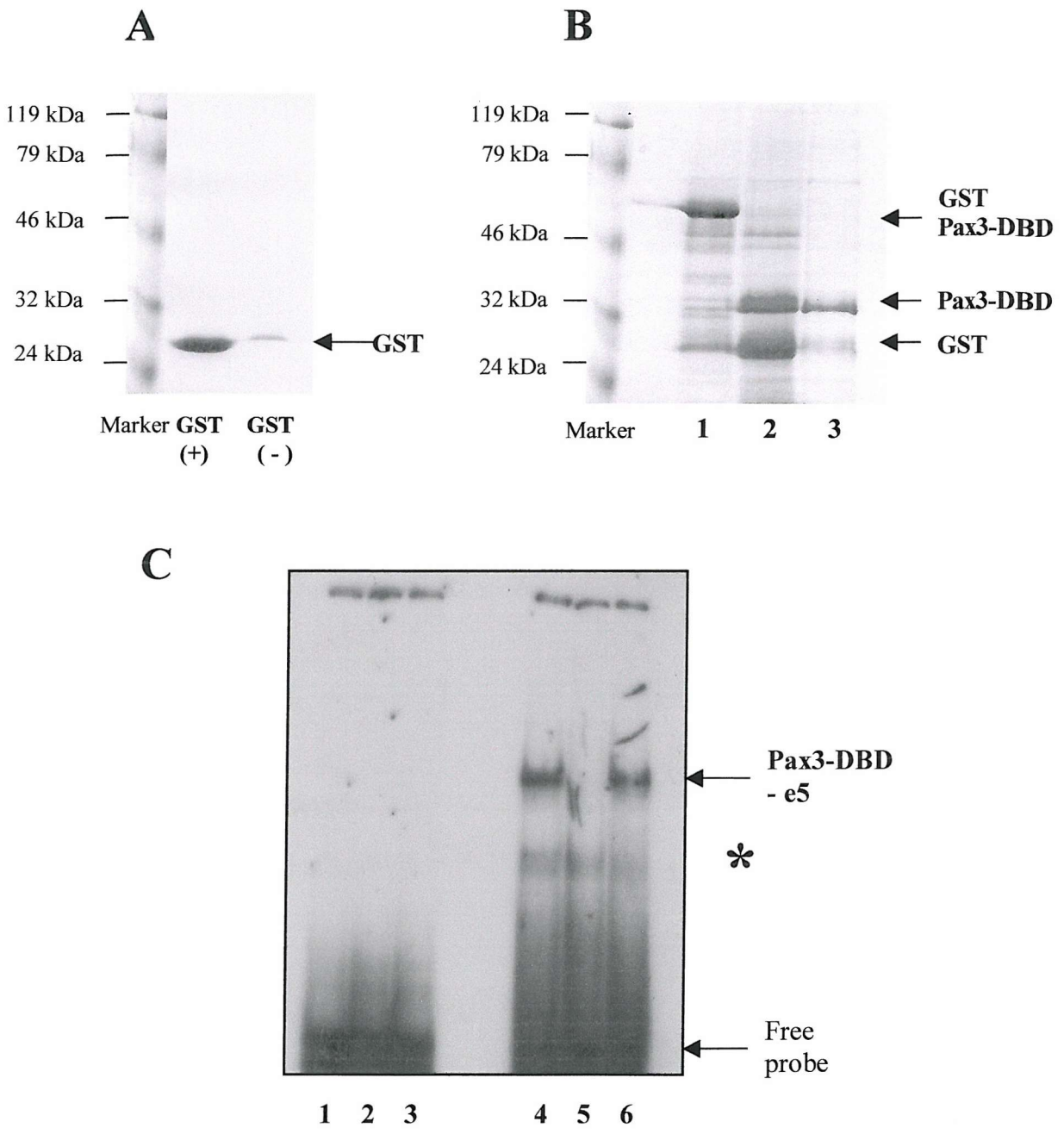

Fig. 4.3 DNA binding analysis of the GST and Pax-3 proteins using the e5 site

(A) GST protein gel: 5 µl of each GST supernatant were resolved by 10% SDS-PAGE. The + and – signs show whether or not thrombin was present. **(B)** GST/Pax3-DBD protein gel: 5 µl of glutathione beads before (lane 1) and after (lane 2) digestion with thrombin, and 5 µl of the Pax3-DBD supernatant (lane 3) after digestion with thrombin were resolved by 10% SDS-PAGE. **(C)** EMSA of GST (lanes 1-3) and Pax3-DBD (lanes 4-6) supernatants with an e5 DNA probe. **1** and **4** are controls, **2** and **5** contain 100x excess cold e5 and **3** and **6** contain 100x excess cold non-specific oligonucleotides. * Faster migrating of the two retarded bands.

Western blot to confirm the identity of the purified Pax3-DBD protein

As described above, following digestion of the GST / Pax3-DBD protein with thrombin, the supernatant produced a distinct band at 32 kDa on a Coomassie blue stained-protein gel when resolved by 10% SDS-PAGE. To confirm that this band represented the Pax3-DBD protein, a Western blot was carried out using an antibody raised against the paired domain of Pax-3. Aliquots of the supernatants obtained after digesting the GST protein alone and the GST / Pax3-DBD protein with thrombin, were used in this Western blot. Figure 4.4 shows an autoradiograph of the Western blot, probed with the Pax-3 antibody. A single distinct band is visible at 32 kDa, the predicted size for the Pax3-DBD protein.

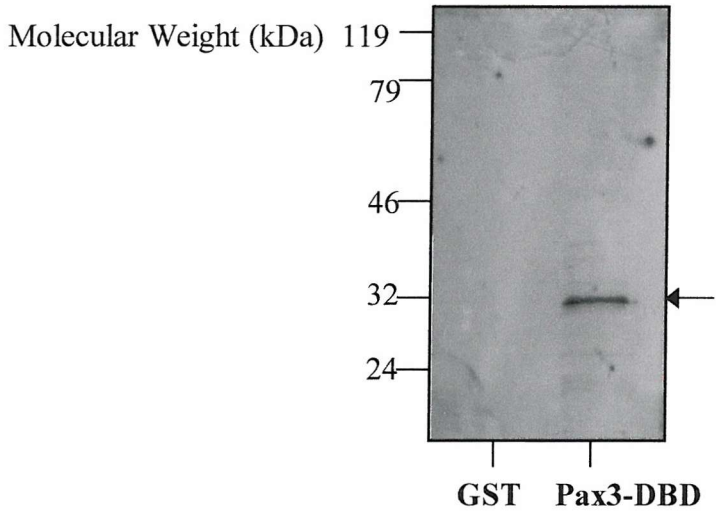

Fig. 4.4 Pax-3 Western blot to identify the Pax3-DBD protein

5 µl of the GST and Pax3-DBD supernatants, obtained after digestion with thrombin, were resolved by 10% SDS-PAGE. The proteins were transferred to a nitrocellulose membrane, and then probed with a Pax-3 specific antibody (1 in 2000). A secondary antibody (1in 5000) conjugated to HRP was used to detect bound Pax-3 antibody with the ECL kit, as described in Materials and Methods. An arrow marks the position of the Pax3-DBD protein on the protein gel.

Size of the protein / e5 DNA complex

To confirm that the lower mobility band in lanes 4 and 6 of figure 4.3 (C) represented Pax3-DBD bound to the e5 DNA probe, the approximate size of this complex was determined. This was achieved by first cross-linking Pax3-DBD to the e5 probe by irradiating the protein-DNA complex with UV light. Such UV irradiation results in the formation of stable covalent bonds between a protein and its DNA binding site (Cooney *et al.*, 1993). These covalent interactions should remain intact, even under the denaturing conditions of SDS-PAGE.

Following UV cross-linking, the protein - DNA complex was first resolved on a non-denaturing polyacrylamide gel, and visualised by autoradiography. The gel fragment containing the Pax3-DBD – e5 complex was then excised, placed in Laemmli buffer and loaded onto a 10% SDS protein gel. After resolving the protein-DNA complex by SDS-PAGE, it was visualised by autoradiography. The size the complex was then estimated by comparison with bands from a molecular weight marker. As shown in figure 4.5, autoradiography detected an intense low molecular weight band in all lanes of the protein gel. This is presumed to represent free e5 DNA that did not become cross-linked to the protein, and as a result was separated from it under the denaturing conditions of SDS-PAGE. When UV cross-linking was carried out, for 45 and 90 minutes, a second band of lower mobility was also observed on the autoradiograph. This band, which was between 30 and 35 kDa in size, corresponds to the predicted size of the Pax3-DBD protein (32 kDa). Thus it can be concluded that the lower mobility band in figure 4.3 (C) does represent Pax3-DBD bound to the e5 DNA probe.

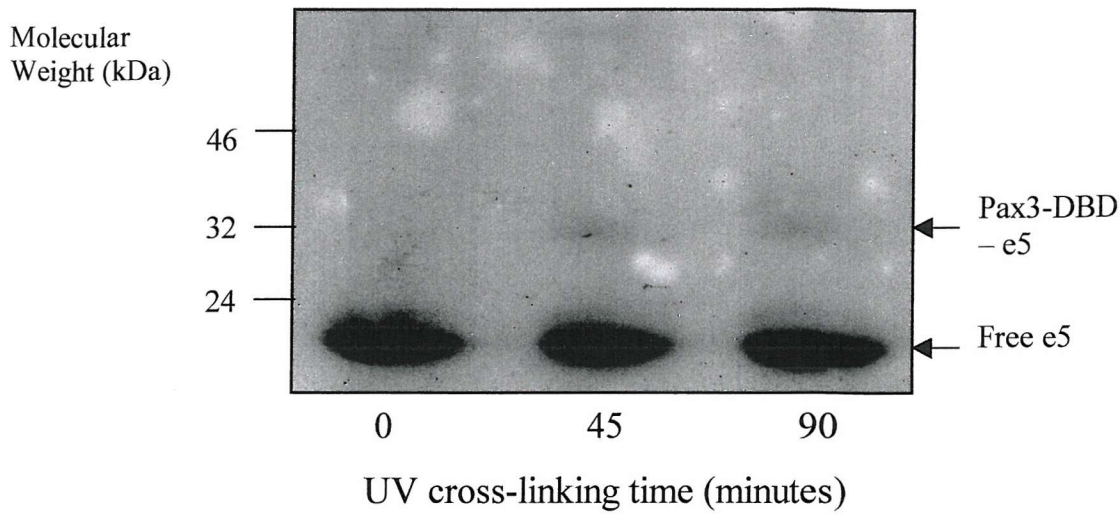

Fig. 4.5 Determination of the size of the protein in the Pax3-DBD – e5 complex
Aliquots of Pax3-DBD supernatant that had either not been exposed to UV light or that had been UV irradiated for 45 or 90 minutes, were resolved on a non-denaturing polyacrylamide gel. Bands representing the specific protein-DNA (e5) complex were then excised and resolved by 10% SDS-PAGE, followed by autoradiography. An autoradiograph of the SDS protein gel is shown. A faint band corresponding to the Pax3-DBD – e5 complex is marked by an arrow, as is the free e5 DNA probe at the bottom of the gel.

4.2.2 Binding of Pax3-DBD *in vitro* to the P2 recognition site

Full-length Pax-3 also binds *in vitro* specifically to the palindromic homeodomain site P2. This binding site contains the homeodomain recognition motif $TAATN_2ATTA$, which the full length Pax-3 protein has been shown to bind to as a co-operative dimer. To study binding of the Pax3-DBD protein to P2, an EMSA was carried out using a ^{32}P-labelled P2 DNA probe. As shown in figure 4.6, three bands were observed in the autoradiograph of this gel. The two slowest migrating bands were both competed out using a 100x molar excess of cold P2 DNA. However, neither of these complexes was competed out when a 100x molar excess of cold non-specific DNA was added. Therefore the Pax3-DBD protein appears to produce two specific complexes with DNA when bound to the P2 site. It may be that Pax3-DBD, like the full length Pax3 protein,

dimerises on this recognition site. However, the faster migrating Pax3-DBD - P2 band may simply represent a breakdown product of Pax3-DBD, with the slower migrating band resulting from the complete Pax3-DBD protein binding as a monomer to P2. Attempts were made to determine the size of the Pax3-DBD – P2 complex using the UV cross-linking method described above. However, no protein-DNA complex could be detected on autoradiographs of the SDS gel, even after very long exposure times. This may have been because the Pax3-DBD protein bound with lower affinity to P2 than it did to e5.

As had been observed in the EMSA using an e5 DNA probe, a band that migrated faster than the bands representing specific protein-DNA complexes was seen in all three lanes of figure 4.6. As described for e5, this band may have been produced by the dissociation of the protein – DNA complexes during electrophoresis.

4.2.3 Binding of Pax3-DBD *in vitro* to the Met and P1 recognition sites

When the *in vitro* DNA binding properties of the full length Pax-3 protein were analysed by EMSA (Underhill *et al.*, 1995), only very weak binding to the single homeodomain site P1 was detected in comparison to e5 and P2 binding, even when four times as much Pax-3 protein was used to study binding to P1. As shown in figure 4.7, although the Pax3-DBD protein formed complexes with e5 and P2 DNA probes, Pax3-DBD failed to produce a complex with a P1 DNA probe. The mobility of the Pax3-DBD – P2 complex suggests that Pax3-DBD binds to P2 as a monomer. Since the oligonucleotides containing the P1 recognition site are approximately the same length as those containing the e5 and P2 recognition sites, a Pax3-DBD – P1 complex, if formed, should have approximately the same mobility as the Pax3-DBD – e5 and Pax3-DBD – P2 complexes.

However, no such complex was observed between the Pax3-DBD protein and the P1 DNA probe.

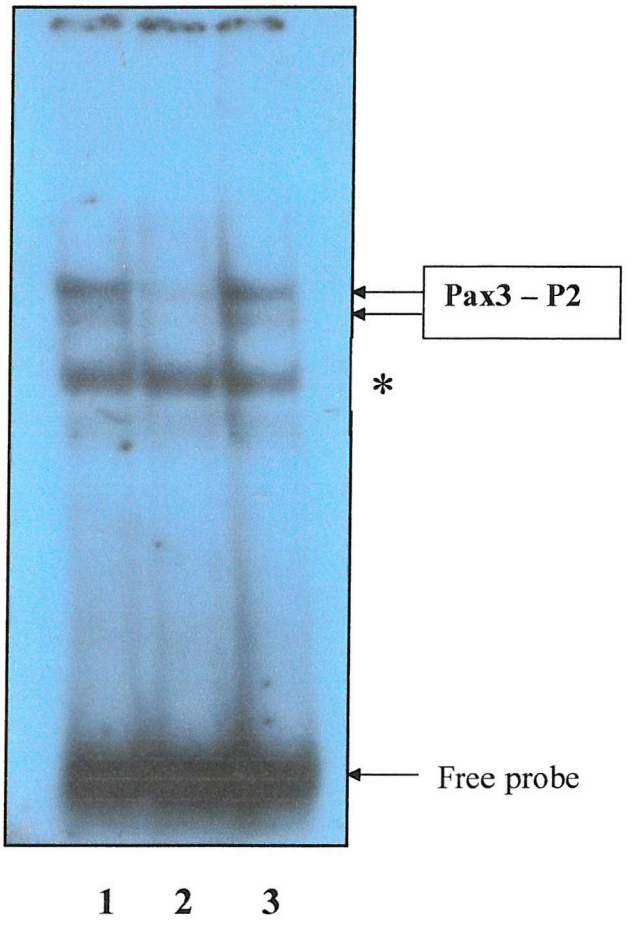

Fig. 4.6 Pax3-DBD Binding *in vitro* to a ^{32}P-labelled P2 Probe

Equal amounts of Pax3-DBD supernatant were incubated with a ^{32}P-labelled P2 DNA probe and then resolved on a non-denaturing polyacrylamide gel as described in Materials and Methods. **(1)** Pax3-DBD + P2 DNA probe **(2)** Pax3-DBD + P2 probe + 100x excess cold P2 **(3)** Pax3-DBD + P2 probe + 100x excess cold non-specific oligonucleotides. Two bands are labelled for the Pax3-DBD - P2 complex, the possible identities of which are described in the text. * Faster migrating band described in the text.

Epstein *et al.* (1996) showed that the isolated Pax-3 paired domain, when expressed as a GST fusion protein, could bind to the paired domain recognition site Met *in vitro* with the same affinity as it bound to e5. To determine whether the Pax3-DBD protein could bind to Met *in vitro*, Pax3-DBD was incubated with a Met DNA probe. Met oligonucleotides are slightly shorter than the e5 and P2 oligonucleotides, which could result in a slight difference in the mobility of a Pax3-DBD – Met complex relative to the mobilities of the complexes formed with e5 and P2. However, as shown in figure 4.7, no complex could be detected between Pax3-DBD and the Met DNA probe. Thus, it appears that pax3-DBD could not bind specifically *in vitro* to either the Met or P1 recognition site.

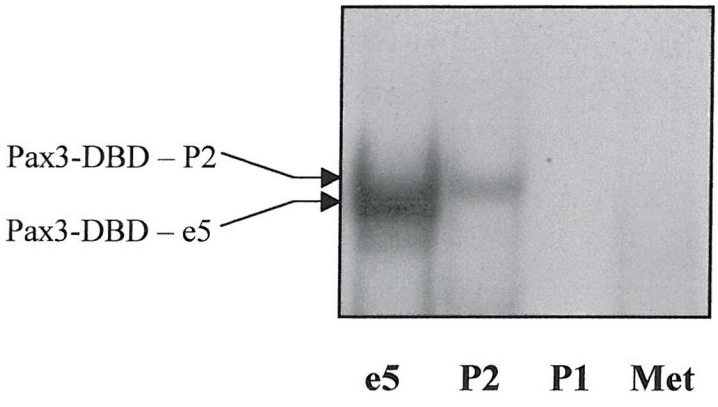

Fig. 4.7 EMSA to examine whether Pax3-DBD can form complexes with DNA probes containing the P1 and Met recognition sites

Pax3-DBD was incubated separately with e5, P2, P1 and Met DNA probes. These reactions were then resolved on the same non-denaturing polyacrylamide gel. The specific complexes, identified previously, that are formed between Pax3-DBD and the e5 and P2 probes are labelled.

4.2.4 Comparison of the DNA binding affinities of Pax3-DBD relative to e5 binding

The affinity of the Pax3-DBD protein for e5 relative to its affinity for other potential binding sites *in vitro* was determined by EMSA. This was achieved by using increasing concentrations of unlabelled oligonucleotides to compete with Pax3-DBD for binding to a ^{32}P-labelled e5 probe. If the unlabelled oligonucleotides contain Pax-3 binding sites, the amount of bound e5 probe should gradually decrease as the amount of unlabelled oligonucleotides increases. The higher the affinity with which Pax3-DBD binds to the recognition site in the unlabelled oligonucleotides, the greater the expected reduction in binding to the DNA probe. Thus Pax3-DBD binding to e5 was analysed using increasing concentrations of Met, P2, P1 and non-specific oligonucleotides as cold competitors. EMSAs carried out using each of these oligonucleotides were analysed on a phospho-imager in order to quantify the amount of bound e5 probe in each lane. In all cases a value of 100% was assigned to bound e5 probe in the absence of any competitor DNA. The results, which represent the mean values from 2 independent experiments for each type of competitor DNA, are shown in figure 4.8.

Using non-specific oligonucleotides to compete with Pax3-DBD binding to the e5 probe, binding was only slightly reduced, even when a 500x molar excess of this cold competitor was added. As expected, using e5 as a cold competitor led to a major reduction in the amount of Pax3-DBD bound to the probe. This confirmed that Pax3-DBD is able to bind specifically *in vitro* to the composite paired domain and homeodomain site e5.

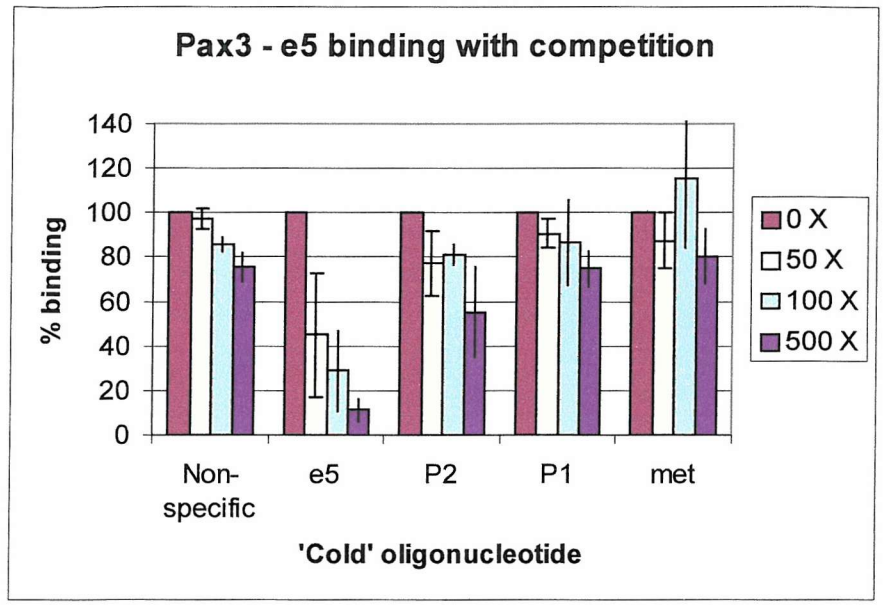

Fig. 4.8 Binding of Pax3-DBD to the e5 probe in the presence of increasing concentrations of cold competitor DNA

A phosphorimager was used to analyse Pax3-DBD binding to a ^{32}P-labelled e5 DNA probe in the presence of a 50X, 100X and 500X molar excess of unlabelled competitor DNA. At each concentration of competitor DNA, the amount of Pax3-DBD protein bound to the e5 probe was expressed as a percentage of that bound to e5 in the absence of cold competitor.

The unlabelled P2 oligonucleotides reduced Pax3-DBD binding to e5 more than the non-specific oligonucleotides, although not as much as the unlabelled e5 oligonucleotides had done. This suggested that Pax3-DBD was binding to P2 *in vitro* with lower affinity than had bound to e5. To quantify this difference in binding affinity, graphs were plotted to show how the level of Pax3-DBD – e5 binding decreased as the concentrations of cold e5 and cold P2 oligonucleotides respectively were increased. For each type of cold competitor, the molar excess of unlabelled oligonucleotides that resulted in a 50% reduction in Pax3-DBD – e5 binding was determined from the graph. The results (figure 4.9 and table 4.1) implied that Pax3-DBD could bind to e5 *in vitro* with approximately 11 times the affinity that it could bind to P2.

A

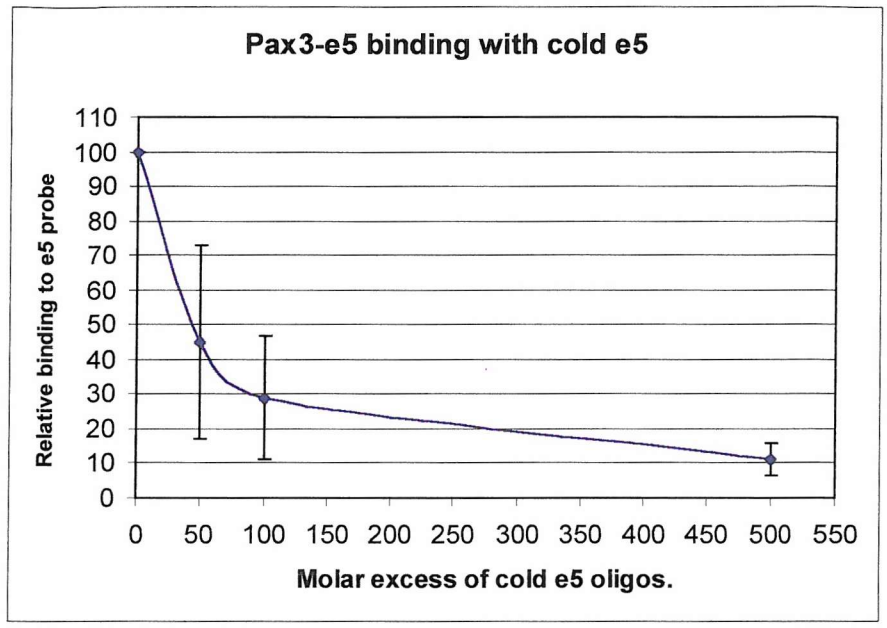

B

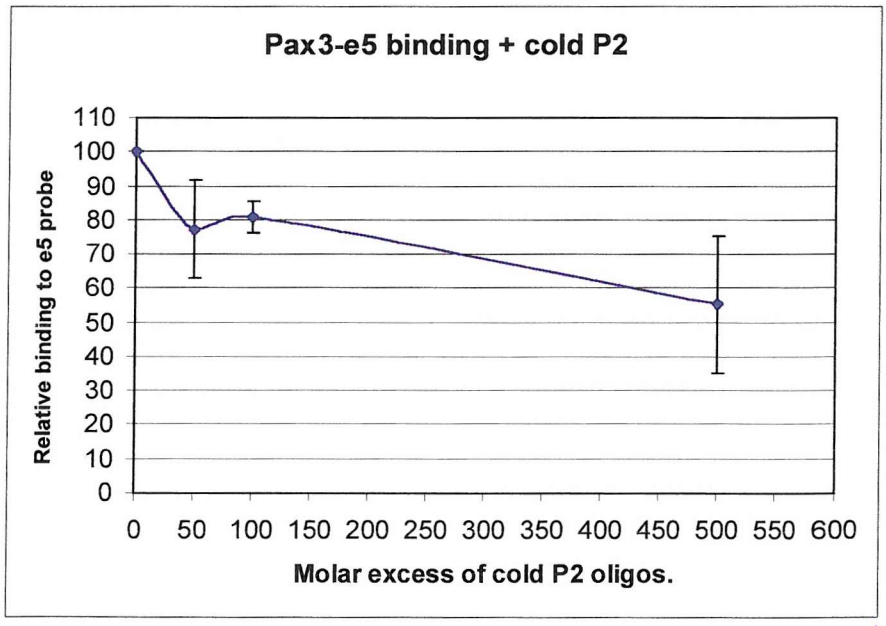

Fig. 4.9 Graphs to compare the affinities of Pax3-DBD for e5 and P2

Graphs were plotted for Pax3-BDB binding to the e5 probe in the presence of increasing concentrations of cold e5 DNA **(A)**, and Pax3-DBD binding to the e5 probe with increasing concentrations of cold P2 DNA **(B)**. In each case the molar excess of unlabelled oligonucleotides required to give a 50% reduction in the amount of Pax3-DBD bound to the e5 probe was determined from the graph.

Table 4.1 – Molar excesses of unlabelled e5 and P2 oligonucleotides required to reduce Pax3-DBD – e5 binding by 50%

50% reduction in Pax3-DBD – e5 binding	
Molar excess cold e5	Molar excess cold P2
50x	550x

Unlabelled oligonucleotides of the single homeodomain site P1 and the paired domain site Met had little effect on Pax3-DBD binding to e5. In fact P1 and Met oligonucleotides were no more effective at reducing the amount of Pax3-DBD bound to the e5 probe than the non-specific oligonucleotides. As was shown by the EMSA in figure 4.7, this indicated that the Pax3-DBD protein was unable to bind specifically to either the P1 or Met recognition site. Therefore the inability of unlabelled P1 oligonucleotides to prevent the Pax3-DBD protein from binding to an e5 probe was not surprising. This also applies to Met since, although the isolated Pax-3 paired domain has been shown to bind to Met *in vitro* (Epstein *et al.*, 1996), our results indicate that a Pax-3 protein containing both the paired domain and the homeodomain is unable to bind to the Met site *in vitro*.

4.2.5 Comparison of the DNA binding affinities of Pax3-DBD relative to P2 binding

EMSA was also used to analyse binding of Pax3-DBD to a P2 DNA probe in the presence of increasing amounts of unlabelled oligonucleotides. The results are shown in figure 4.10, which represent the mean values from 2 independent experiments for each type of cold competitor DNA. As expected the Pax3-DBD - P2 band was competed out progressively using increasing amounts of cold P2 DNA. A greater amount of this

complex appeared to be competed out when e5 oligonucleotides were used as the cold competitor. This again suggested that the Pax3-DBD protein could bind more strongly to the e5 site than the P2 site *in vitro*. As before, the difference in binding affinity was quantified by plotting graphs to show how the level of Pax3-DBD – P2 binding decreased as the concentrations of cold P2 and cold e5 oligonucleotides respectively were increased. The results (figure 4.11 and table 4.2) indicate that Pax3-DBD could bind to e5 *in vitro* with approximately 3 times the affinity that it could bind to P2.

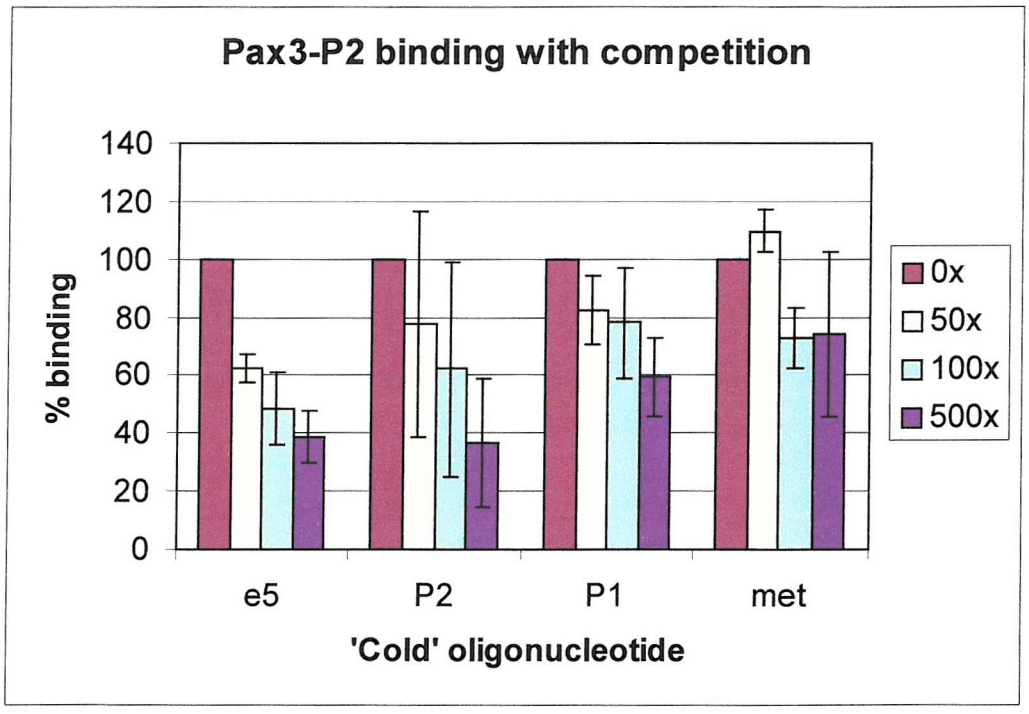

Fig. 4.10 Binding of Pax3-DBD to the P2 probe in the presence of increasing concentrations of cold competitor DNA

A phosphorimager was used to analyse Pax3-DBD binding to a ^{32}P-labelled P2 DNA probe in the presence of a 50X, 100X and 500X molar excess of unlabelled competitor DNA. At each concentration of competitor DNA, the amount of Pax3-DBD protein bound to the P2 probe was expressed as a percentage of that bound to e5 in the absence of cold competitor.

A

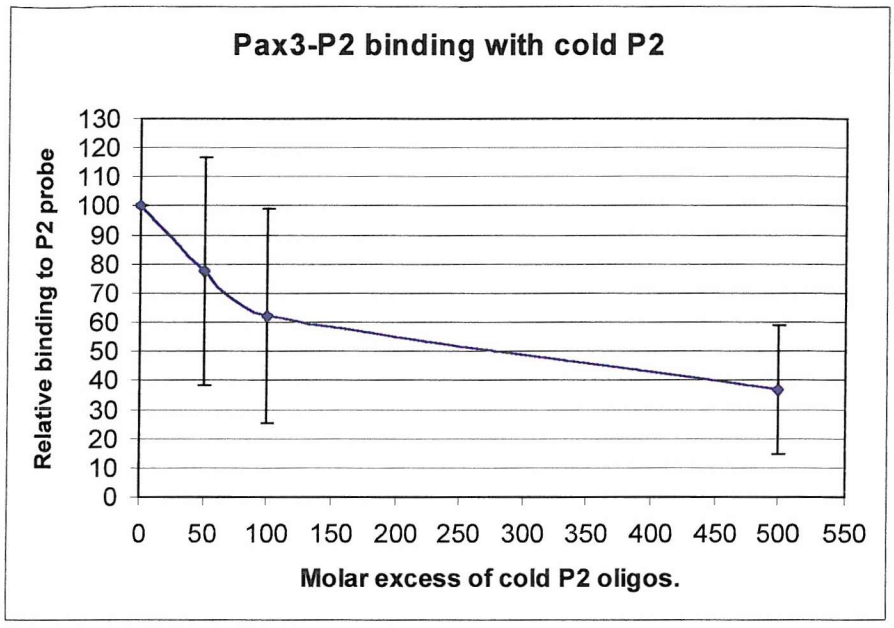

B

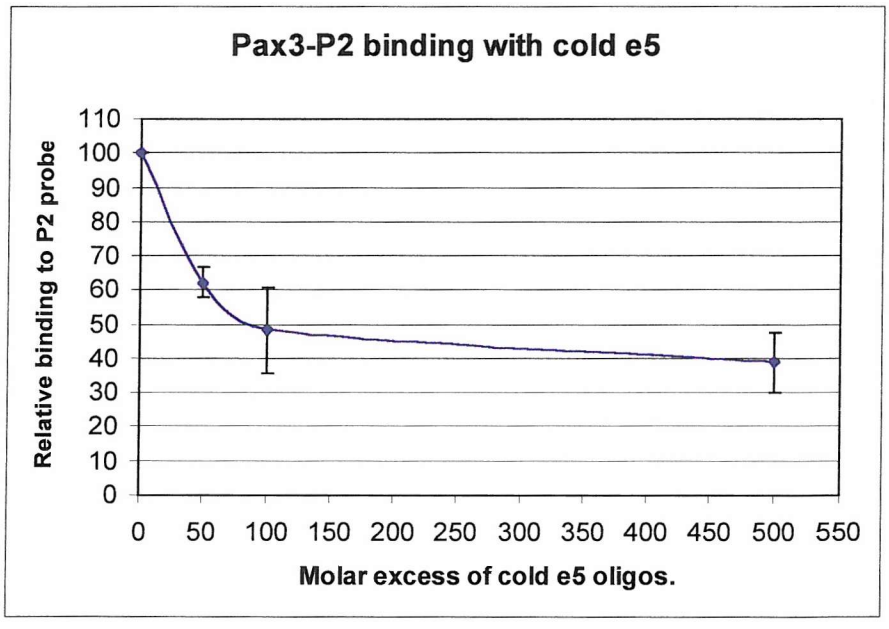

Fig. 4.11 Graphs to compare the affinities of Pax3-DBD for P2 and e5

Graphs were plotted for Pax3-BDB binding to the P2 probe in the presence of increasing concentrations of cold P2 DNA **(A)**, and Pax3-DBD binding to the P2 probe with increasing concentrations of cold e5 DNA **(B)**. In each case the molar excess of unlabelled oligonucleotides required to give a 50% reduction in the amount of Pax3-DBD bound to the P2 probe was determined from the graph.

Table 4.2 – Molar excesses of unlabelled P2 and e5 oligonucleotides required to reduce Pax3-DBD – P2 binding by 50%

50% reduction in Pax3-DBD – P2 binding	
Molar excess cold P2	Molar excess cold e5
275x	85x

Although their effects on binding were not as great as those of the cold e5 and cold P2 competitors, both cold P1 and cold Met did reduce binding to the P2 DNA probe slightly. If, as proposed, the binding affinity of Pax3-DBD for P2 is weaker than its affinity for e5, then 100-500x molar excesses of cold P1 and cold Met competitors may be sufficient to reduce Pax3-DBD - P2 binding. This is because when used in such high molar excesses relative to the P2 DNA probe, very weak binding of Pax3-DBD to the P1 and Met sites might be sufficient to reduce Pax3-DBD – P2 binding. This might explain why the P1 and Met cold competitors, which both failed to form specific complexes with the Pax3-DBD protein, reduced binding to a P2 DNA probe, but had very little effect on binding to an e5 DNA probe.

4.2.6 DNA binding properties of the PD and HD proteins

To determine whether the PD protein, which incorporates the first 189 amino acids of Pax-3, could bind to the paired domain recognition site Met *in vitro*, an EMSA was carried out using the PD protein and a ^{32}P-labelled Met probe. As shown in figure 4.12 (A), the PD protein formed a complex with the Met probe that was competed out by a 100x molar excess of unlabelled Met oligonucleotides. These results show that although a Pax-3 protein containing both the paired domain and the homeodomain is unable to

bind to the Met recognition site *in vitro*, a protein containing only the Pax-3 paired domain can bind to this site.

The Pax3-DBD protein was shown to bind *in vitro* to the homeodomain site P2. As shown in figure 4.12 (B), the HD protein, which incorporates amino acids 190-284 of Pax-3, could also bind to the P2 site *in vitro*. The HD – P2 complex was competed out by a 100x molar excess of unlabelled P2 oligonucleotides, but not by a 100x molar excess of unlabelled non-specific oligonucleotides. This shows that the isolated Pax-3 homeodomain can bind to the homeodomain recognition site P2 *in vitro*.

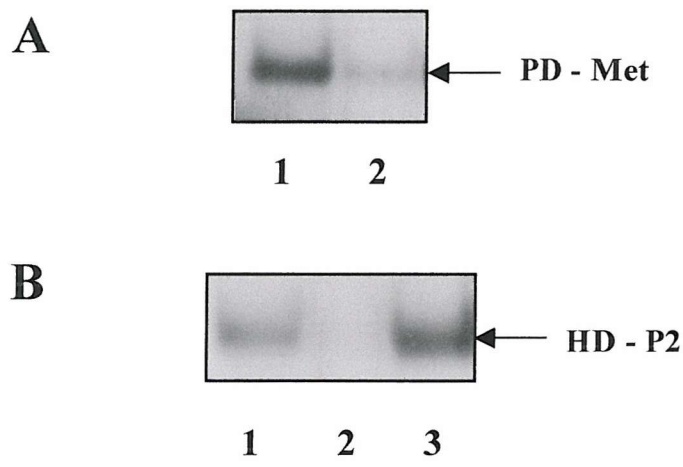

Fig. 4.12 The *in vitro* DNA binding properties of the PD and HD proteins
Equal amounts of PD and HD supernatants were incubated with ^{32}P-labelled DNA probes and then resolved on a non-denaturing gel as described in Materials and Methods. **(A)** The PD protein was incubated with a Met DNA probe in the absence of cold competitor DNA (lane1) or in the presence of a 100x molar excess of unlabelled Met oligonucleotides (lane 2). **(B)** The HD protein was incubated with a P2 DNA probe in the absence of cold competitor DNA (lane 1), in the presence of a 100x molar excess of unlabelled P2 oligonucleotides (lane 2), or in the presence of a 100x molar excess of unlabelled non-specific oligonucleotides (lane 3).

4.2.7 DNA binding activity of Pax-3 in nuclear extracts

As described, the Pax3-DBD protein can bind to the e5 and P2 recognition sites *in vitro*. The complexes formed between Pax3-DBD and these two binding sites have very similar mobilities on a polyacrylamide gel, which suggests that Pax3-DBD binds to P2 as a monomer. However, full-length Pax-3 binds to P2 as a dimer. As shown in figure 4.13, nuclear extracts from ND7 cells produced specific protein-DNA complexes with both the e5 and P2 oligonucleotides. However, the Pax-3 – P2 complex migrated more slowly than the Pax-3 – e5 complex, as would be expected if full-length Pax-3 binds to P2 as a dimer.

Interestingly ND7 nuclear extracts also formed a specific complex with Met oligonucleotides, showing that a full-length Pax-3 protein isolated from cultured cells can bind to the Met recognition site *in vitro*. However, the bacterially expressed Pax3-DBD protein was unable to bind to the Met site *in vitro*. This could be due to the fact that Pax-3 undergoes post-translational modification in cultured eukaryotic cells but not when expressed as a fusion protein in bacteria. This in turn may alter its ability to bind to DNA *in vitro*.

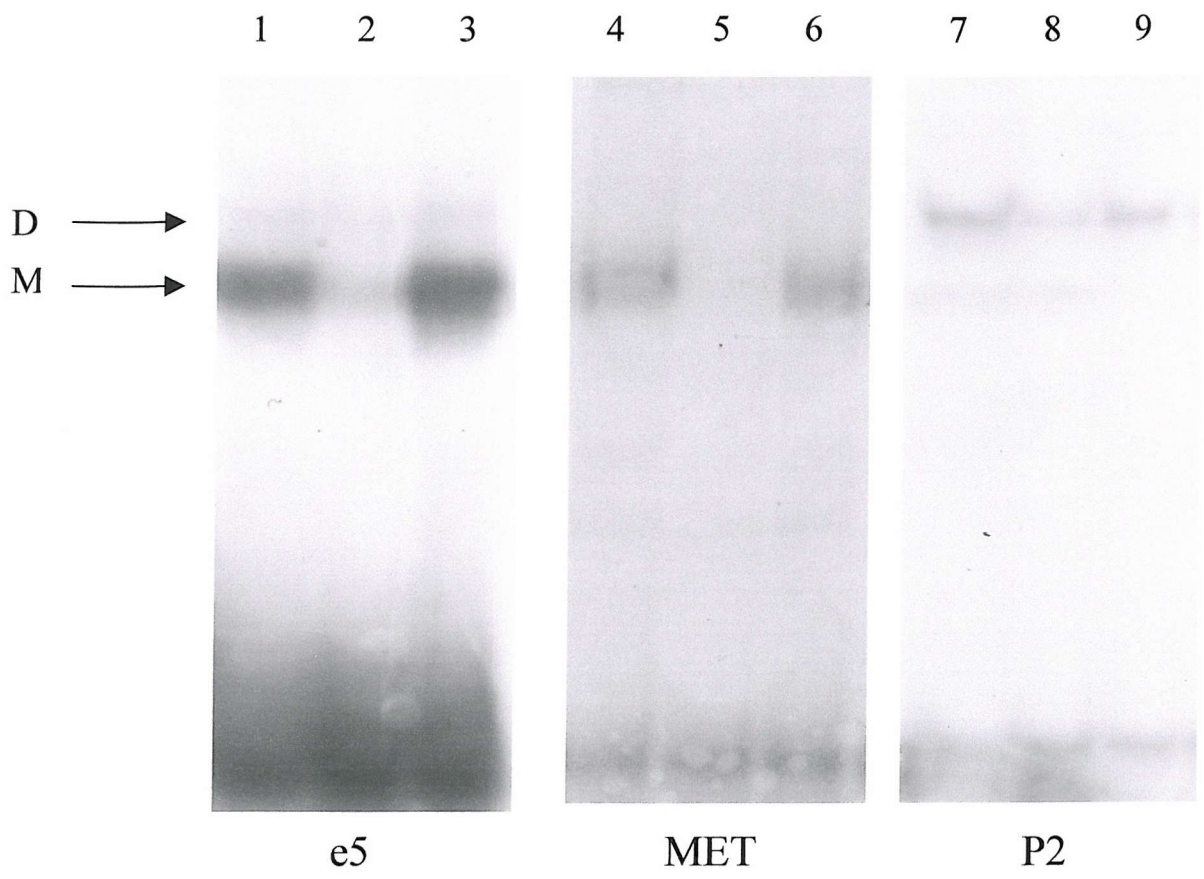

Fig. 4.13 *In vitro* DNA binding activity of Pax-3 in ND7 nuclear extracts

ND7 nuclear extracts were incubated with radiolabelled oligonucleotides, which contained e5, P2 or MET recognition sites, and the protein-DNA complexes were then resolved on a non-denaturing polyacrylamide gel. Lanes 1, 4, 7: nuclear extract + e5/MET/P2 DNA probe, lanes 2, 5, 8: nuclear extract + e5/MET/P2 DNA probe + 100x molar excess of cold e5/MET/P2 oligonucleotides, lanes 3, 6, 9: nuclear extract + e5/MET/P2 DNA probe + 100x molar excess of cold non-specific oligonucleotides. D, dimer of Pax-3 bound to P2 site. M, Pax-3 monomer bound to e5 and MET sites.

4.3 The effect of phosphorylation on Pax-3 DNA binding activity

As described in chapter 1, X-ray crystal structures of the paired domain and homeodomain of the *Drosophila* prd protein bound to DNA, and a crystal structure of the human Pax-6 paired domain bound to DNA, have provided insights into how the Pax-3 protein interacts with its DNA binding sites. In addition, these structures have indicated which amino acids in Pax-3 make sequence specific DNA contacts, as well as indicating which residues make non-specific contacts with the DNA backbone.

The results presented in chapter 3 showed that the Pax3-DBD protein could be phosphorylated *in vitro* by PKA and PKC. The PD protein, containing the entire Pax-3 paired domain but not the homeodomain, was also phosphorylated *in vitro* by PKA and PKC. The HD protein, containing the entire Pax-3 homeodomain but not the paired domain, could be phosporylated *in vitro* by PKA but not by PKC. Figure 4.14 shows the positions of potential PKA and PKC sites in the Pax-3 paired domain that are located in or near to the helix-turn-helix (H-T-H) structures, which facilitate sequence specific DNA binding.

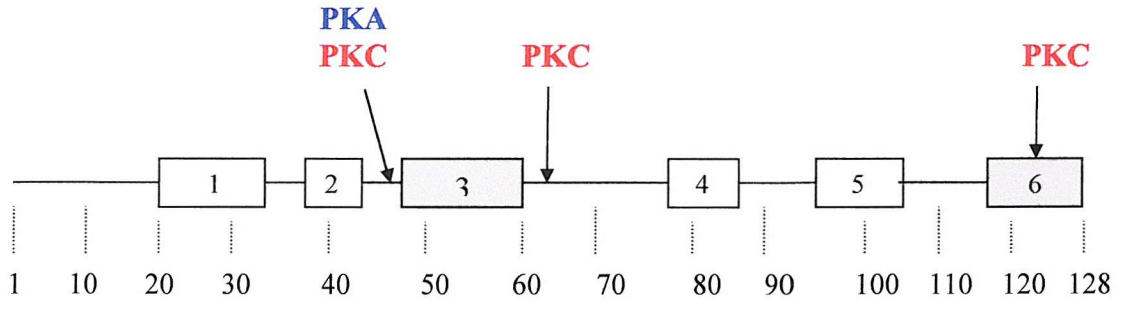

Fig. 4.14 Locations of potential PKA and PKC sites in the Pax-3 paired domain
The three α helices of the N-terminal subdomain (1-3) and the three α helices of the C-terminal subdomain (4-6) are represented by rectangles. The recognition helix of each H-T-H motif is shaded grey. Numbers refer to amino acids in the paired domain.

The potential PKA site (also a PKC site) at Ser 46 in the paired domain is situated in the turn between the 2nd and 3rd α helices of the N-terminal subdomain. This site either overlaps or is near to several amino acids that contact the DNA. Residues 46, 47, 48, and 49 make contacts in the major groove, while residues 41, 45, 46 and 49 contact the DNA backbone. Residues that make DNA contacts are also located close to the potential PKC site at Ser 62 in the paired domain. This site is located just after the recognition helix of the N-terminal subdomain. Amino acid 69 binds in the minor groove while residues 65 and 66 make contacts with the DNA backbone. Thus, phosphorylation within the N-terminal subdomain by PKA and/or PKC could affect the DNA binding properties of the Pax-3 paired domain. In addition, a potential PKC site in the Pax-3 paired domain occurs at Ser 120. This site lies within the recognition helix of the C-terminal subdomain. In Pax-6, residues 118, 121, 122 and 125 make sequence specific contacts in the major groove, while residues 116, 119, 121, 122 and 125 make contacts with the DNA backbone. If similar DNA contacts are made by Pax-3, then phosphorylation within the recognition helix of the C-terminal subdomain by PKC could affect the DNA binding properties of the Pax-3 paired domain.

Figure 4.15 shows the position of a potential PKA site in the Pax-3 homeodomain. This site, located at Ser 4 in the homeodomain, occurs within the N-terminal arm, which makes sequence specific DNA contacts in the minor groove via residues at positions 2 and 5. Therefore, phosphorylation of the Pax-3 homeodomain by PKA could affect the DNA binding activity of this domain.

Phosphorylation within the linker region between the paired domain and homeodomain might also affect the DNA binding properties of Pax-3. In particular binding to

composite paired domain and homeodomain sites, in which the protein conformation must allow both binding domains to contact the DNA, could be altered. There are four potential PKC sites and one PKA site in the linker region between the paired domain and homeodomain.

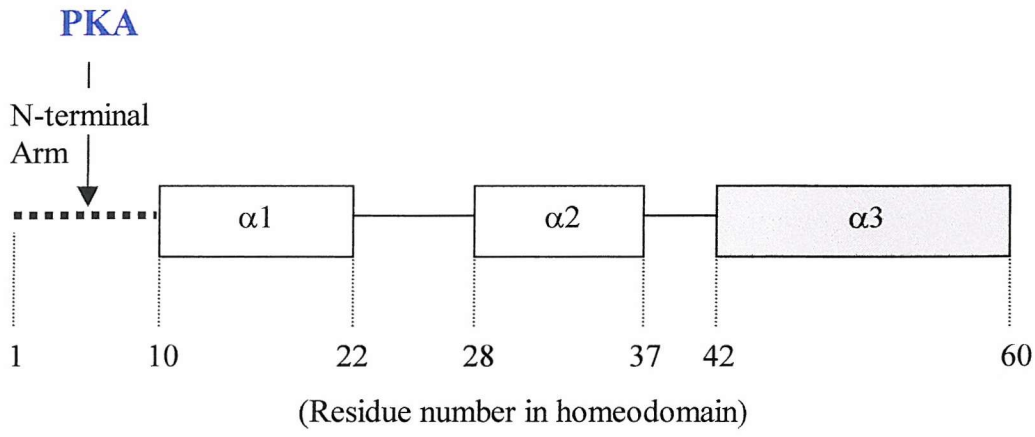

Fig. 4.15 The location of a potential PKA site in the Pax-3 homeodomain
The 3 α helices in the homeodomain are represented by rectangles. The recognition helix of the H-T-H motif is shaded grey. The first 9 residues of the homeodomain constitute the N-terminal arm, which binds to DNA in the minor groove.

Having established that Pax3-DBD could bind to the e5 and P2 recognition sites *in vitro*, the effects of PKA and PKC mediated phosphorylation of Pax3-DBD on its affinity for each of these sites was investigated. In addition, the effect of PKA mediated phosphorylation of the PD protein on its affinity for the paired domain recognition site Met was studied. PKA mediated phosphorylation of the HD protein was also carried out in order to determine whether this affected its affinity for the P2 recognition site.

4.3.1 PKA mediated phosphorylation

The Pax3-DBD protein

First the effect of PKA mediated phosphorylation on Pax3-DBD binding to the e5 site was investigated. *In vitro* kinase assays and subsequent EMSAs were carried out as described in materials and methods. As shown in figure 4.16 (A), adding PKA to the kinase reaction in the absence of ATP had no effect on Pax3-DBD – e5 binding, when compared to a control lane of Pax3-DBD without PKA or ATP. However, adding PKA to the kinase assay in the presence of ATP increased the amount of bound e5 probe relative to the control. This indicates that *in vitro* phosphorylation of Pax3-DBD by PKA increases its binding affinity for the e5 site.

The effect of PKA mediated phosphorylation on the binding affinity of Pax3-DBD for the P2 site was also studied by EMSA. Figure 4.16 (B) shows that adding PKA to the kinase reaction in the absence of ATP had no affect on Pax3-DBD - P2 binding when compared to the control lane. However, in contrast to the result with e5, PKA did not affect the level of bound P2 probe in the presence of ATP either. This suggests that PKA mediated phosphorylation of Pax3-DBD does not affect binding to the P2 site.

The PD protein

The effect of PKA mediated phosphorylation on the DNA binding properties of the individual paired domain protein was investigated. The paired domain protein (PD) was used in an EMSA with a Met probe, which contains a single paired domain recognition site. Figure 4.17 (lanes 1 and 2) indicates that, in contrast to Pax3-DBD, the PD protein was able to bind specifically to the Met site. In the presence of PKA and ATP, the amount of bound Met probe was the same as it was in the presence of PKA alone. This

implied that phosphorylation by PKA does not affect the binding affinity of the isolated Pax-3 paired domain for the Met recognition site.

The HD protein

The effect of PKA mediated phosphorylation on the DNA binding properties of the individual homeodomain protein (HD) was also investigated. Lanes 5-7 of figure 4.17 show that HD could bind specifically to the palindromic homeodomain site P2. The HD – P2 complex migrated faster than the complex formed between PD and Met. Since Pax-3 binds to Met as a monomer, this suggests that the HD – P2 complex was also composed of a monomeric protein. A dimer of the homeodomain protein (11 kDa) bound to P2 would be expected to produce a band that has approximately the same mobility as the paired domain protein (22 kDa) bound to Met as a monomer.

In this case of HD – P2 binding, addition of PKA in the presence of ATP (lane 8) resulted in an increase in the level of HD – P2 complex when compared to the amount of complex formed (lane 9) in the absence of ATP. This indicated that phosphorylation of the homeodomain in the absence of the paired domain increased the binding affinity of the homeodomain for the P2 site.

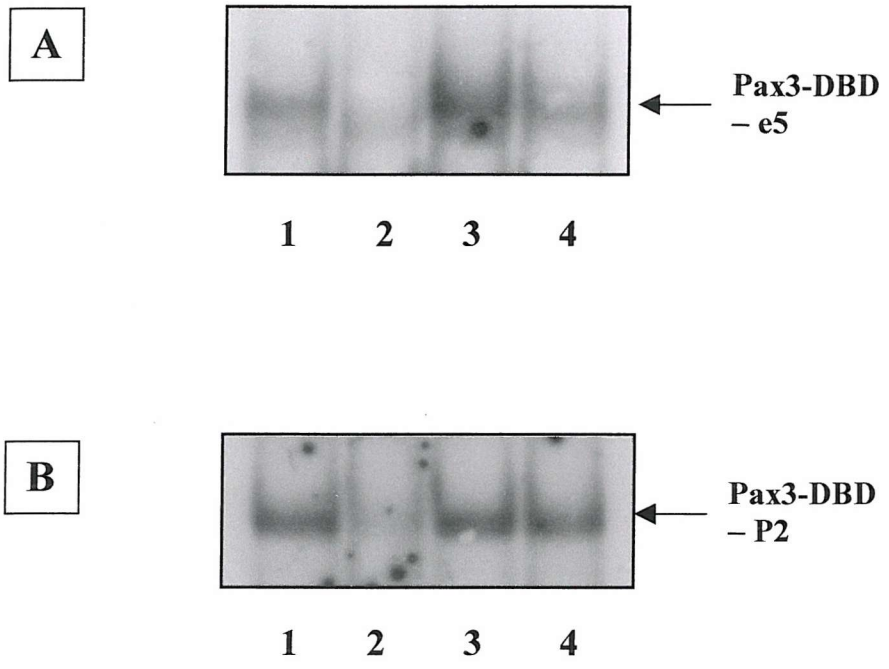

Fig. 4.16 The effect of PKA mediated phosphorylation of Pax3-DBD *in vitro* on binding to the e5 and P2 recognition sites

Bacterially produced Pax3-DBD protein was treated with PKA in the presence (lane 3) or absence (lane 4) of 30μM ATP, and its affinities for the e5 **(A)** and P2 **(B)** sites then analysed by EMSA as described in Materials and Methods. In each case, the first two lanes were controls: Pax-3 + e5/P2 probe (lane 1), Pax-3 + e5/P2 probe + 100x excess cold e5/P2 oligonucleotides (lane 2). The specific complexes formed between Pax3-DBD and the e5/P2 DNA probes are marked on the autoradiographs by arrows.

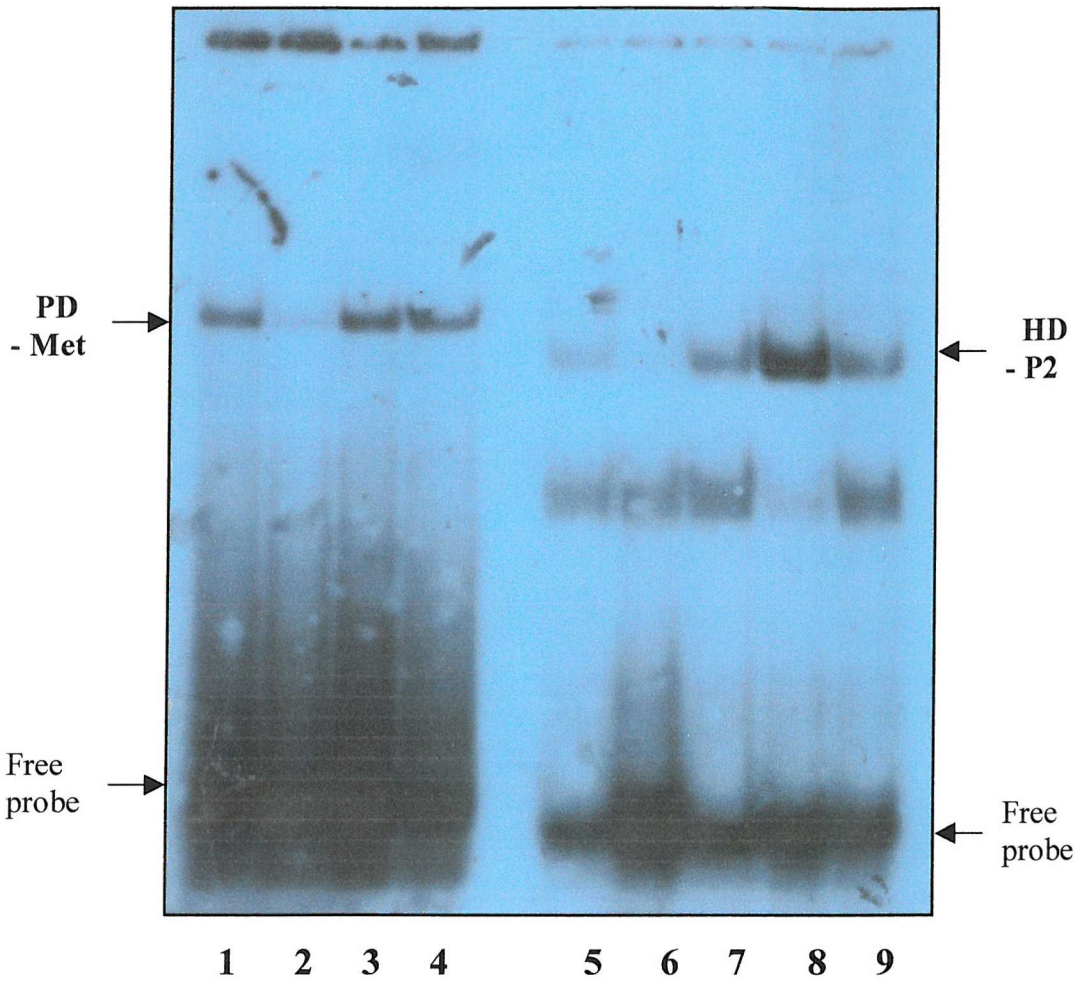

Fig. 4.17 The effect of PKA mediated phosphorylation of the Pax-3 paired domain (PD) and homeodomain (HD) proteins *in vitro* on binding to the Met and P2 sites respectively

The bacterially expressed PD and HD proteins were treated with PKA in the presence **(3 & 8)** and absence **(4 & 9)** of ATP, and their affinities for the Met and P2 sites respectively were then analysed by EMSA as described in Materials and Methods. The first two lanes for the Met experiment and the first 3 lanes for the P2 experiment are controls: **(1)** PD + Met probe **(2)** 100x excess cold Met **(5)** HD + P2 probe **(6)** 100x cold P2 **(7)** 100x cold non-specific oligonucleotide.

4.3.2 PKC mediated phosphorylation

The effect of PKC mediated phosphorylation on Pax3-DBD binding to the e5 and P2 sites was also studied. Figure 4.18 (A) shows the Pax3-DBD protein bound to the e5 probe. In this EMSA, the Pax3-DBD - e5 band was competed out by a 100x molar excess of cold e5 but not by a 100x molar excess of non-specific oligonucleotides. As expected the amount of bound e5 probe also remained unchanged when PKC was added to the kinase assay in the absence of ATP. The same level of binding to e5 was observed when PKC and ATP were added together. This showed that the binding activity of Pax3-DBD *in vitro* to the composite paired domain and homeodomain site e5 remained unchanged when the Pax3-DBD protein was phosphorylated by PKC.

Figure 4.18 (B) shows the effect of PKC mediated phosphorylation on the binding of Pax3-DBD to the P2 site. As already described the purified Pax3-DBD protein binds more weakly to P2 than it does to e5. However, as shown in lanes 1-3 of figure 4.16, specific binding of the Pax-3 protein to P2 was still observed in this EMSA. The low intensity of the Pax3-DBD – P2 bands produced in this experiment probably resulted from inefficient labelling of the P2 probe, since relatively low levels of free P2 DNA (compared to the amount of free e5 DNA) were seen at the bottom of the gel. As expected, the amount of bound P2 probe remained unchanged when PKC was added to the kinase assay in the absence of ATP. However, as for Pax3-DBD - e5 binding no change in the level of Pax3-DBD - P2 binding was observed when PKC and ATP were added together. Therefore it can be concluded that the binding affinity of Pax3-DBD for the homedomain site P2 *in vitro* was unaffected by PKC mediated phosphorylation.

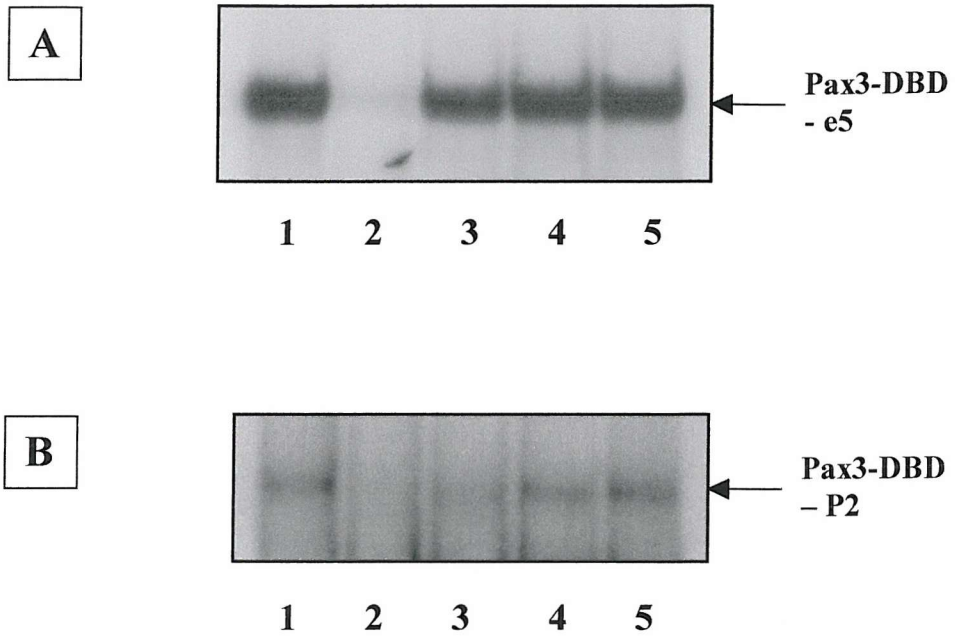

Fig. 4.18 The effect of PKC mediated phosphorylation of Pax3-DBD *in vitro* on binding to the e5 and P2 sites

Bacterially expressed Pax3-DBD protein was treated with PKC in the presence (lane 4) or absence (lane 5) of ATP and its affinity for the e5 **(A)** and P2 **(B)** sites analysed by EMSA as described in Materials and Methods. In each case, the first three lanes on the autoradiograph represent controls: Pax-3 + e5/P2 probe (lane 1), Pax-3 + e5/P2 probe + 100x excess cold e5/P2 oligonucleotides (lane 2), Pax-3 + e5/P2 probe + 100x excess cold non-specific oligonucleotides (lane 3). The specific complexes formed between Pax3-DBD and the e5/P2 DNA probes are marked on the autoradiographs by arrows.

4.4 Discussion

The DNA binding properties of the full length Pax-3 protein have been studied extensively *in vitro*. The aim of the work described in the first part of this chapter was to examine the *in vitro* DNA binding properties of Pax3-DBD, a truncated form of Pax-3 that contains both DNA binding domains but no C-terminal transactivation domain. It was first shown that Pax3-DBD binds specifically to the composite paired domain and homeodomain recognition site e5, to which the full length Pax-3 protein has been shown to bind with high affinity *in vitro*. The Pax3-DBD protein was also shown to bind specifically *in vitro* to the palindromic homeodomain site P2. The results of competition assays, using increasing concentrations of unlabelled oligonucleotides to compete with Pax3-DBD for binding to e5 and P2 DNA probes, indicated that the Pax3-DBD protein could bind with higher affinity to e5 than P2. A 3-fold difference in binding affinity was determined using the P2 DNA probe, whilst a 11-fold difference was demonstrated for Pax3-DBD binding to the e5 DNA probe. However, in both cases the difference between the affinities with which Pax3-DBD bound to the e5 and P2 recognition sites was not statistically significant. Quite considerable variations were seen between experiments for the competition assays carried out. Therefore, more experiments of this type are required if a statistically significant difference between e5 and P2 binding is to be confirmed.

Despite binding to e5 and P2 *in vitro*, Pax3-DBD was unable to bind specifically to the paired domain recognition site Met, or the single homeodomain site P1. Binding of the full-length Pax-3 protein to P1 is extremely weak in comparison to its affinities for the e5 and P2 sites. Therefore, the results presented here show that Pax3-DBD behaves in the same way as the full-length protein with regards to P1 binding *in vitro*. With regards binding to the Met site, Chalepakis *et al.* (1994 B) used EMSAs to show that within the

context of the full-length Pax-3 protein, the paired domain was unable to bind to the GTTCC recognition motif from the e5 binding site when the homeodomain recognition motif from this site was deleted. This could explain why the Pax3-DBD protein failed to bind to Met. This binding site contains a paired domain recognition site only, and was selected in an *in vitro* binding assay as a consensus site for the isolated Pax-3 paired domain (Epstein *et al.* 1996). Moreover, the PD protein, containing the entire Pax-3 paired domain but no homeodomain, could bind to the Met site *in vitro*. Thus, failure of Pax3-DBD to bind Met *in vitro* may be due to the presence of the homeodomain as well as the paired domain in this protein. The situation *in vivo* with regards to Pax-3 binding to paired domain recognition sites may well be different. Indeed, Epstein *et al.* (1996) showed that cotransfection of a full-length Pax-3 expression vector with a reporter plasmid containing a luciferase reporter gene downstream of a minimal promoter and the Met binding site, led to increased induction of luciferase activity. This suggested that full-length Pax-3 was able to bind to Met *in vivo*, and thus activate transcription of a downstream reporter gene. In support of this, we have shown that ND7 nuclear extracts form a specific complex with the Met binding site in an EMSA, demonstrating that full length Pax-3 in cultured cells is capable of binding to Met *in vitro*.

The mobility of the Pax3-DBD – P2 complex on a non-denaturing polyacrylamide gel was the same as that of the Pax3-DBD – e5 complex, which indicated that the Pax3-DBD protein was bound to P2 as a monomer. The same conclusion was made for the Pax-3 homeodomain protein (HD), which could also bind specifically to P2. Schafer *et al.* (1994) showed that full-length Pax-3 binds to P2 both as a homo-dimer and as a hetero-dimer with PAX7. Therefore the Pax3-DBD and HD proteins might also have been expected to dimerise on the P2 recognition site. It would be useful to obtain more

direct evidence from EMSAs to show whether Pax3-DBD binds P2 as a monomer or as a dimer. Full-length Pax-3 and Pax3-DBD proteins could be incubated individually with a P2 DNA probe, or they could be mixed together and then incubated with the P2 probe. To compare the sizes of the protein-DNA complexes produced in each case, they could be resolved on the same non-denaturing polyacrylamide gel, and visualised by autoradiography. Due to its larger size, the full-length Pax-3 protein would produce a slower migrating band than the Pax3-DBD protein. If the Pax3-DBD protein formed dimers on P2, then a band of intermediate mobility would be produced when this protein was mixed with full-length Pax-3. However, if Pax3-DBD was unable to dimerise, only two band would be seen, representing a full-length Pax3 – P2 complex and a Pax3-DBD – P2 complex respectively. The inability of Pax3-DBD to form dimers on the P2 site could explain why binding to P2 appeared to be weaker than binding to e5. The full-length Pax-3 protein forms co-operative dimers on P2. Consequently, as long as the concentration of Pax-3 is high enough, much more of this protein binds to P2 as a dimer than as a monomer. Therefore, if Pax3-DBD can only bind as a monomer to P2, the amount of Pax3-DBD complex formed will be less than that formed with the full-length protein.

The only difference between Pax3-DBD and the full-length Pax-3 protein is that the former protein lacks the region C-terminal to the homeodomain, which includes the transactivation domain of Pax-3. It may be that the C-terminus of Pax-3 is required to allow the Pax-3 homeodomain to dimerise on palindromic recognition sites. Indeed it has already been shown that the transactivation domain of Pax-3 influences the DNA binding properties of the homeodomain (Epstein *et al.*, 1998). In ARMS, a soft tissue tumour of skeletal muscle lineage, a chromosomal translocation produces a PAX3–FKHR fusion

protein. This fusion protein contains the DNA binding domains of PAX3 fused to the transactivation domain of the forkhead protein FKHR. A partially formed FKHR DNA binding domain is also present but this is inactive, as shown by the fact that PAX3-FKHR is unable to bind to FKHR binding sites *in vitro*. However, PAX3-FKHR can bind to PAX3 sites *in vitro*. It also activates transcription from PAX3-responsive sequences *in vivo* more strongly than PAX3 (Bennicelli *et al.* 1996). Therefore one way in which PAX3-FKHR is thought to cause cell transformation in ARMS is by abnormally regulating PAX3 target genes that are involved in muscle cell proliferation, differentiation or migration. However, co-transfection experiments in cell culture showed that PAX3-FKHR, but not PAX3, could also activate transcription from the platelet derived growth factor α receptor (PDGRαR). Only the PAX3 homeodomain, and not the paired domain, was required for PAX3-FKHR to have this effect. A paired type homeodomain binding-site in the PDGFαR promoter was required for transactivation to occur. Therefore in ARMS oncogenicity may also result from PAX3-FKHR being able to activate genes that PAX3 does not regulate. This could be due to PAX3-FKHR binding to paired type homeodomain sites in the promoters of these genes. Both PDGFα and its ligand platelet derived growth factor are expressed in developing muscle. They are both required for the proliferation of muscle cell precursors prior to differentiation. Therefore up regulation of PDGFαR by PAX3-FKHR could contribute to the phenotype of ARMS by causing excessive muscle cell proliferation.

To determine why PAX3-FKHR, but not PAX3 alone activated transcription from the PDGFαR, the homeodomain binding-site from this promoter was placed upstream of the thymidine kinase promoter and CAT gene (Cao and Wang 2000). In co-transfection experiments this reporter construct was induced by PAX3-FKHR but not by PAX3

alone. Replacing the PAX3 transactivation domain with a viral transactivation domain also resulted in transcriptional activation. However replacing the FKHR transactivation domain with that of PAX3 prevented transcriptional activation. This implied that the PAX3 transactivation domain could prevent PAX3 from activating target genes through the interaction of its homeodomain alone with DNA. However when the PAX3 transactivation domain was removed, as in the case of PAX3-FKHR, the protein could bind to promoter sequences using just its homeodomain.

Having shown that the Pax3-DBD protein, as well as the individual paired domain and homeodomain proteins could bind to established Pax-3 sites *in vitro*, the affects of PKA and PKC mediated phosphorylation on binding to these sites was investigated. A crystal structure has been solved of the isolated paired domain from the *Drosophila* prd protein bound to DNA. Only the N-terminal subdomain of this paired domain makes contact with the DNA. In contrast a crystal structure of the human PAX6 paired domain – DNA complex shows that residues in both subdomains of this paired domain make DNA contacts. In addition, a third crystal structure has shown how the isolated homeodomain of prd binds to a palindromic homeodomain site as a dimer. These structures have provided insights into how the paired domain and homeodomain of the Pax-3 protein may interact with Pax-3 DNA binding sites. These studies also indicate which amino acids in Pax-3 may be involved in forming specific as well as non-specific contacts with DNA. Phosphorylation of Pax-3 by PKA and PKC may affect the DNA binding properties of the protein, especially if phosphorylation occurs at sites close to or overlapping with amino acids that make DNA contacts. Therefore the locations of putative PKA and PKC sites in Pax-3 were compared with the positions of amino acids in the protein thought to be involved in contacting DNA. This information was used to

analyse the affects of phosphorylation on DNA binding *in vitro* for the Pax3-DBD, PD and HD proteins.

In the Pax-3 paired domain, a potential PKA site occurs in the turn between the 2nd and 3rd α helices of the N-terminal subdomain. The 3rd α helix is the recognition helix that makes sequence specific contacts in the major groove of DNA. The PKA site in the paired domain is highly conserved amongst the Pax family of proteins. Also, as described in the previous chapter, the GST-PD protein was phosphorylated *in vitro* by PKA. Since the putative PKA site in the paired domain described here is the only one present in the GST-PD protein, it is assumed that Pax-3 was phosphorylated at this site by PKA *in vitro*. However, the isolated paired domain protein was shown to bind with equal affinity to Met, whether it had been phosphorylated by PKA or not. The Met DNA site binds the N-terminal subdomain of the paired domain. Therefore, if phosphorylation of Pax-3 by PKA within the N-terminal subdomain of the paired domain did occur, it did not appear to affect the affinity with which this subdomain binds to DNA. However, in contrast to the result obtained with the isolated paired domain binding to DNA, the affinity of the Pax3-DBD protein for e5 was shown to increase upon phosphorylation by PKA. Like Met, e5 is recognised by the N-terminal subdomain of the paired domain, but it contains a recognition site for the homeodomain as well. Thus Pax proteins bind to e5 using both their DNA binding domains. This requires the Pax protein to be in a conformation that permits both the paired domain and the homeodomain to contact DNA. The linker region joining these two domains is likely to be involved in determining how they are arranged on the DNA. The Pax-3 linker contains a putative PKA site that, as described in the previous chapter, is the most likely of the three sites present in Pax-3 to be phosphorylated by PKA *in vitro*. Thus phosphorylation of a site in

the Pax-3 linker by PKA may alter the way in which the paired domain and homeodomain are arranged on binding sites that recognise both these domains together. This could explain why the Pax3-DBD protein was found to bind more strongly to the e5 site after it had been phosphorylated by PKA.

A third potential PKA site is located within the N-terminal arm of the Pax-3 homeodomain, which is thought to make minor groove DNA contacts. The GST-HD protein, which was phosphorylated *in vitro* by PKA, contains both this site and the PKA site present in the linker region referred to above. As already described, the PKA site in the homeodomain is considered least likely to be phosphorylated by PKA *in vitro* whereas the site in the linker region represents the most likely substrate for PKA. Therefore PKA may not have phosphorylated Pax-3 within the homeodomain itself, but rather in the linker region that joins the two DNA binding domains. This may explain why PKA mediated phosphorylation of the Pax3-DBD protein failed to alter its affinity for the P2 site, which recognises only the homeodomain of Pax proteins. However, in contrast to Pax3-DBD, the isolated Pax-3 homeodomain protein did show increased binding affinity for P2 in response to phosphorylation by PKA. It may be the case that the PKA site in the Pax-3 homeodomain was phosphorylated when the homeodomain was expressed alone, but not when the two DNA binding domains (Pax3-DBD) were expressed together in the same protein. Phosphorylation within the N-terminal arm of the homeodomain may have altered its conformation, thus facilitating higher affinity binding to the P2 site.

Three potential PKC sites in the Pax-3 paired domain are all located in the vicinity of amino acids thought to make DNA contacts. The PKC site in the turn just before the

recognition helix of the N-terminal subdomain (equivalent to the putative PKA site described above) is highly conserved amongst Pax proteins. In addition a PKC site that occurs just after the recognition helix of the N-terminal subdomain, and a site in the recognition helix of the C-terminal subdomian are also conserved in other Pax proteins. The Pax3-DBD protein was phosphorylated *in vitro* by PKC. Moreover, the GST-PD protein, which incorporates all three of the sites described above, was also phosphorylated *in vitro* by PKC. However, the phosphorylated form of Pax3-DBD did not display any differences in binding affinity towards the e5 site when compared to the unphosphorylated form of the protein. The failure of PKA mediated phosphorylation to have any affect on Pax-3 paired domain binding to Met, suggested that phosphorylation of Ser 46 in the turn just before the recognition helix of the N-terminal subdomain does not alter the DNA binding affinity of the paired domain. Therefore phosphorylation at this site by PKC might occur without having any affect on Pax3-DBD binding to e5. Similarly the PKC site at Ser 62 in the Pax-3 paired domain occurs just after the recognition helix of the N-terminal subdomain. The crystal structure of the *Prd* paired domain – DNA complex shows that this region of the protein does not make any DNA contacts when only the N-terminal subdomain is bound to DNA. Since e5 only recognises the N-terminal subdomain (in conjunction with the homeodomain), it might be possible for phosphorylation to occur at Ser 62 in the Pax-3 paired domain without this having any affect on the affinity with which Pax3-DBD binds to the e5 site. Finally the PKC site at Ser 120 of the paired domain occurs within the C-terminal subdomain. Since e5 binds only the N-terminal subdomain, it is possible that phosphorylation within the C-terminal subdomain does not affect binding to this site.

The homeodomain of Pax-3 also contains potential PKC sites. There are two sites in the N-terminal arm of the homeodomain, and one site in the recognition helix. All these sites are conserved in the Pax-7 protein. Despite the presence of putative PKC sites in the homeodomain of Pax-3, the GST-HD protein could not be phosphorylated *in vitro* by PKC. This may be because the conformation of the Pax-3 moiety in the GST-HD protein is such that PKC mediated phosphorylation is prevented. However, these sites may be phosphorylated within the context of the full length Pax-3 protein *in vitro,* and the fact that they are all conserved in Pax-7 suggests that phosphorylation may also occur at these sites *in vivo*. However, since PKC failed to phosphorylate the homeodomain of Pax-3 *in vitro*, it was not surprising that the affinity of the Pax3-DBD protein for the P2 site remained unchanged in the presence of PKC and ATP.

The DNA binding properties of the PD protein, phosphorylated by PKC, have yet to be compared to those of the unphosphorylated protein. The same is true for the HD protein, although in this case PKC mediated phosphorylation was not observed *in vitro*, and so no differences in binding activity would be expected. As well as looking at binding to Met, it would be interesting to compare the affinities of phosphorylated and unphosphorylated PD proteins for a consensus Pax-6 paired domain site (Xu *et al.* 1999). This site contains recognition motifs for both the N and C-terminal subdomains of the paired domain. If the PD protein was phosphorylated at the putative PKC site in the C-terminal subdomain, this might affect the affinity with which it binds to the Pax-6 paired domain recognition site. However, such an effect may be specific to the Q^- isoform of Pax-3, which has been shown to bind to a consensus Pax-6 paired domain binding site twice as strongly as the Pax-3 Q^+ isoform.

Chapter 5

Regulation of Pax-3 promoter activity

5 Regulation of Pax-3 promoter activity

5.1 Introduction

Pax-3 is a developmental control gene, and as such its expression is tightly controlled during embryogenesis. *Pax-3* is expressed in dividing cells during embryogenesis and is downregulated when cells differentiate (Goulding *et al.*, 1991). The restriction of *Pax-3* expression to mitotically active neuronal cells during development is also seen in cultured neuronal cell lines. The neuronal cell line ND7 was created by the fusion of mouse neuroblastoma cells with rat primary sensory neurons (Wood *et al.*, 1990). ND7 cells proliferate indefinitely in tissue culture when grown in medium containing 10% serum. However upon transfer to serum-free medium, ND7s were shown to undergo cell cycle arrest and began to undergo morphological differentiation, extending long dendritic processes and secreting sensory neuropeptides. An increase in the rate of apoptotic cell death was also observed under these conditions, with some ND7 cells undergoing programmed cell death rather than morphological differentiation (Budhram-Mahadeo *et al.*, 1994a). Growth factors present in serum have previously been shown to be required to induce the expression of *Pax-3* mRNA in ND7 cells (Evans and Lillycrop 1996). RT-PCR was used to compare the level of *Pax-3* mRNA in ND7 cells grown in medium containing 10% serum with that of cells grown in the absence of serum. Although *Pax-3* mRNA was expressed in ND7 cells grown in the presence of 10% serum, expression decreased to undetectable levels when serum was removed from the growth medium of these cells. This decrease in *Pax-3* mRNA expression also coincided with a reduction in the rate of cell proliferation, and the morphological differentiation of ND7 cells. The addition of peptide growth factors (EGF, bFGF or aFGF) to serum starved ND7 cells led to an increase both in the level of *Pax-3* mRNA expression and the rate of cell proliferation, whilst the number of cells showing signs of morphological

differentiation was reduced. The increase in *Pax-3* mRNA expression preceded any changes in cell proliferation and differentiation, and was independent of protein synthesis. This suggested that *Pax-3* belongs to a group of genes known as the immediate early genes, where expression is induced by growth factors without the need for *de novo* protein synthesis. These results also suggest that serum growth factors may directly induce the transcription of *Pax-3*.

In eukaryotic cells gene expression is controlled by regulatory proteins, which bind to sequence elements in the gene promoter. These regulatory proteins can enhance the rate of transcription via activation domains, or repress transcription via inhibitory domains as described in chapter 1. Natoli *et al.* (1997) showed that sequence elements located within 1.6kbp 5' to the transcription start site in the Pax-3 promoter were sufficient to mediate the induction of a linked reporter gene in embryonal carcinoma cells that had been transfected with this reporter gene construct. In addition, in transgenic mice, this 1.6kbp region of the Pax-3 promoter was sufficient to activate transcription of the lacZ reporter gene, with expression being detected at embryonic day 8.5 in the dorsal neural tube and early somites. This implied that elements required for the initial expression of *Pax-3* in the dorsal neural tube and somites are located in the region of the Pax-3 promoter 1.6 kbp 5' to the transcription start site.

Previously this 1.6 kbp region of the Pax-3 promoter, as well as the region of the promoter from –1000 to +50 (relative to the transcription start site), were cloned upstream of the CAT reporter gene to produce two separate CAT reporter gene constructs. Subsequently it was shown that the 1050bp region of the promoter exhibited the same basal level of activity as the 1.6kbp promoter region in neuronal cells and like

the 1.6kbp region, was downregulated in the absence of serum. A construct containing only –157 to +53 was not found to be serum responsive indicating that sequences between –1000 and –157 are involved in serum regulation of *Pax-3*. Therefore to study what type of extracellular mediators affect the expression of *Pax-3*, the region of the Pax-3 promoter from –1000 to +50 was cloned into the luciferase vector pGL3-Basic. The ability of sequence elements in this region of the promoter to mediate trans-activation or repression of the luciferase reporter gene was then examined.

5.2 Regulation of Pax-3 promoter activity by extracellular mediators

5.2.1 Pax-3 promoter activity declines upon ND7 cell differentiation

We first investigated the effect on Pax-3 promoter activity of serum starving ND7 cells. Thus ND7s were transfected with 3μg of the P3prom-pGL3 reporter plasmid in the presence of 10% serum, before being cultured for increasing amounts of time in the presence of serum-free medium. Luciferase assays were carried out on the cell lysates. The luciferase readings were normalised on the basis of the total protein levels in the cell lysates, as determined by performing BCA protein assays. Relative luciferase values were calculated such that the normalised luciferase reading for cells grown in the presence of 10% serum was assigned a value of 100. The results, shown in figure 5.1, represent the means from two independent experiments.

A transient increase in Pax-3 promoter activity occurred after 3 hours growth in serum-free medium. After this time, Pax-3 promoter activity steadily decreased. After 48 hours growth in the absence of serum, the level of promoter activity was only 40% of that observed in the presence of 10% serum. This agrees with previous data that the 1050bp region of the promoter is controlled by serum, with serum deprivation of ND7 cells

leading to decreased promoter activity in these cells. However, there is a transient increase in Pax-3 promoter activity that occurs when ND7 cells are first deprived of serum.

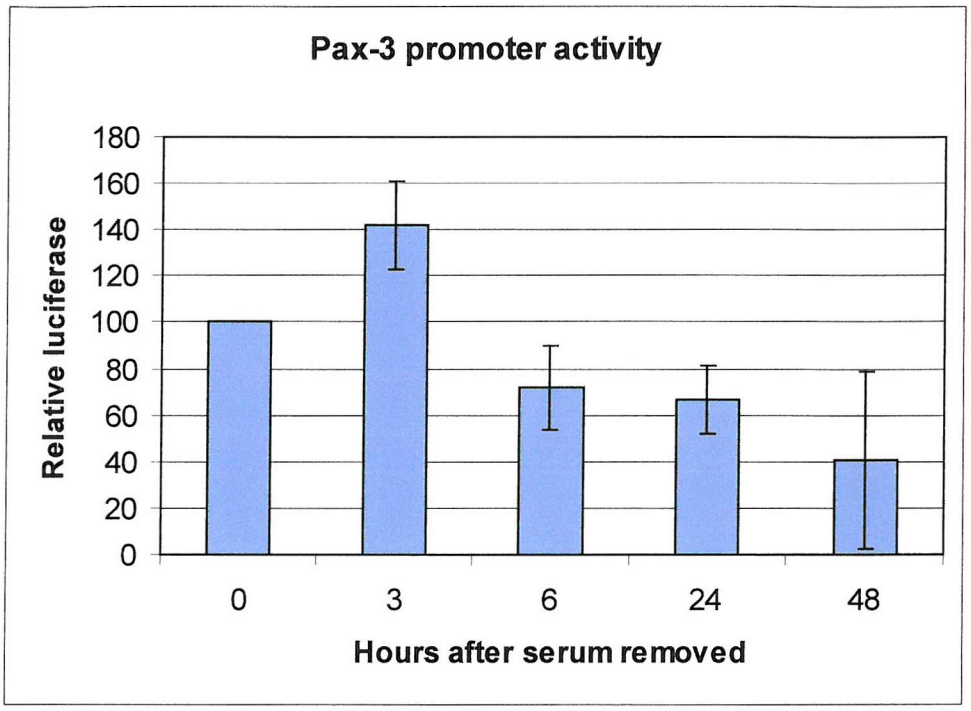

Fig. 5.1 Effect of removing serum from the growth medium of ND7 cells on Pax-3 promoter activity

ND7 cells were transiently transfected with 3μg of P3prom-pGL3 DNA and cultured over-night in medium containing 10% serum. The cells were then grown in serum free medium for the number of hours indicated, before being harvested. Cell lysates were used in luciferase assays to measure Pax-3 promoter activity. The results represent the mean values obtained from two independent experiments +/- s.e.m.

5.2.2 Pax-3 promoter activity is modulated by serum factors

Budhram-Mahadeo *et al.* (1994a) showed that culture of ND7 cells in media containing different concentrations of serum induced distinct cellular effects. In the complete

absence of serum ND7 cells underwent cell cycle arrest, and either underwent morphological differentiation or died by apoptosis. When transferred to media containing either 0.5% or 1% serum however, there was no increase in the rate of apoptotic cell death when compared to cells grown in the presence of 10% serum. In contrast, growth in 0.5% serum resulted in decreased cell proliferation and increased differentiation, the extent of which was equivalent to that seen in the complete absence of serum. In the presence of 1% serum however, ND7 cells continued to proliferate, with the rate of cell proliferation being only slightly lower than that seen in the presence of 10% serum. In addition, for ND7s grown in 1% and 10% serum, there was no difference in the proportion of cells showing signs of morphological differentiation. Therefore it appears that the induction of ND7 cell death by apoptosis that was observed in the absence of serum can be prevented by low concentrations of serum factors. However, higher concentrations of serum factors may be required to maintain ND7 cells in a proliferating state, and prevent the onset of morphological differentiation.

To study the effect of serum factors on Pax-3 promoter activity, ND7 cells were transfected with 3μg of the P3prom-pGL3 reporter plasmid in the presence of 10% serum. Growth arrest of the transfected cells was then induced, by culturing them in serum-free medium for 24 hours. After this time medium containing either 0.5%, 1% or 10% serum was added back to the cells, which were then cultured for a further 24 hours before being harvested. As before, cell lysates were used in luciferase assays to quantify Pax-3 promoter activity. Relative luciferase values were calculated such that the normalised luciferase reading for cells grown in the presence of 10% serum was assigned a value of 100. The results, which represent the mean values of two independent experiments, are shown in figure 5.2. With respect to its activity in the presence of 10%

serum, the level of Pax-3 promoter activity was reduced by 50% in the presence of 1% serum, and by 60% in the presence of 0.5% serum.

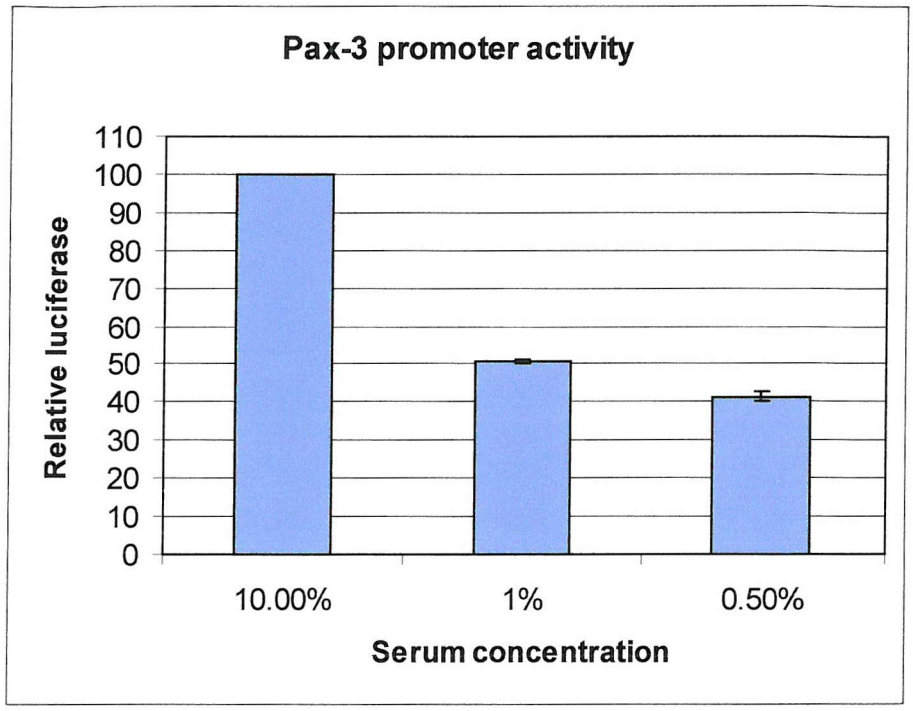

Fig. 5.2 Pax-3 promoter activity in ND7 cells grown in the presence of different concentrations of serum

Growth arrested ND7 cells were cultured for 24 hours in medium that contained 10%, 1% or 0.5% serum. Cell lysates were then used in luciferase assays to measure Pax-3 promoter activity. The results represent the mean values obtained from two independent experiments +/- s.e.m.

The results confirm that Pax-3 promoter activity is dependent upon serum, and declines when the level of serum is reduced. There was little difference between the level of Pax-3 promoter activity in the presence of 0.5% and 1% serum, despite the fact that a decrease in cell proliferation is only observed in 0.5% serum. This suggests that the extent of ND7 cell proliferation may not be directly dependent upon the level of Pax-3 promoter activity.

5.2.3 Pax-3 promoter activity is modulated by serum lipids

Serum contains many mitogens including peptide growth factors and mitogenic lipids. We therefore investigated whether the removal of serum lipids was sufficient to down-regulate Pax-3 promoter activity. Thus serum was delipidated using the method of Cham and Knowles (1976). This process leaves peptide growth factors intact but removes the following lipids from serum: neutral lipid, S-1-P (sphingosine 1-phosphate), LPA (lysophosphatidic acid), fatty acids, sphingomyelin, lysophosphatidylcholine, phosphatidylcholine and phosphatidylethaolamine. This makes it possible to distinguish the effect of serum lipids on Pax-3 promoter activity from that of growth factors. Thus ND7 cells were transfected with 3μg of the P3prom-pGL3 reporter plasmid, and then cultured for 24 hours in the presence of either 10% serum or delipidated serum. Luciferase assays were carried out on cell lysates, and luciferase activity for cells grown in the presence of delipidated serum was expressed relative to that observed in the presence of 10% serum. The mean values from two independent experiments are shown in figure 5.3. The results showed that Pax-3 promoter activity was reduced by 50% in the presence of delipidated serum when compared to promoter activity in cells grown in the presence of 10% serum.

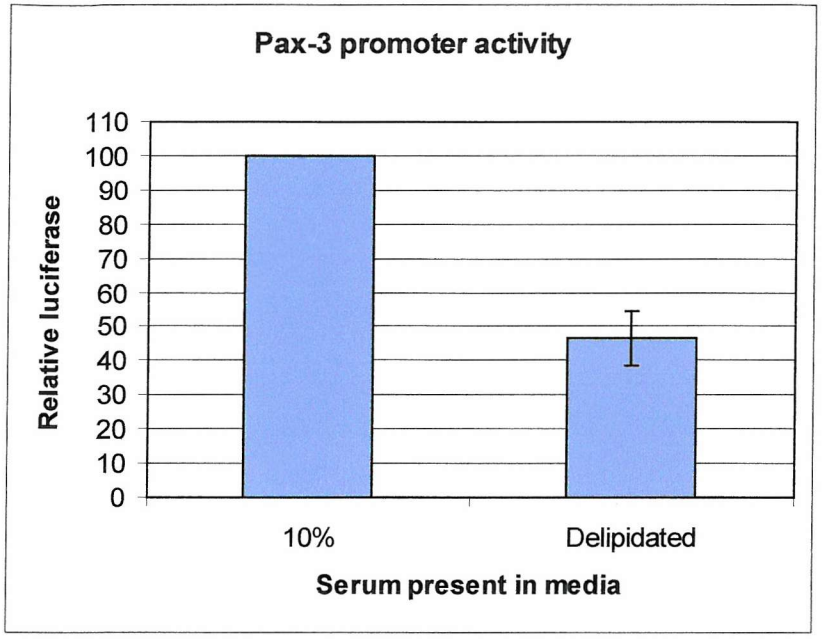

Fig. 5.3 The effect of serum lipids on Pax-3 promoter activity

ND7 cells were transfected with 3μg of P3prom-pGL3 reporter plasmid, and then cultured for 24 hours in medium containing either 10% serum or delipidated serum. Cell lysates were then used in luciferase assays. The relative luciferase values determined from two independent experiments are shown +/- s.e.m.

5.2.4 ND7 cell growth rate is reduced in the presence of delipidated serum

To determine whether serum lipids can affect the rate of ND7 cell growth, ND7 cells were cultured in medium containing either 10% serum or delipidated serum for increasing amounts of time. At each time point the number of viable ND7 cells was counted using the Trypan Blue exclusion assay. As shown in figure 5.4 (A), ND7 cells in delipidated medium grew more slowly than in the presence of 10% serum, with little increase in cell number being observed over 72 hours. No effect on cell survival was observed, as shown in figure 5.4 (B). Therefore Pax-3 promoter activity appears, as seen in previous experiments, to be closely associated with undifferentiated cells and declines upon a decrease in cell proliferation.

A

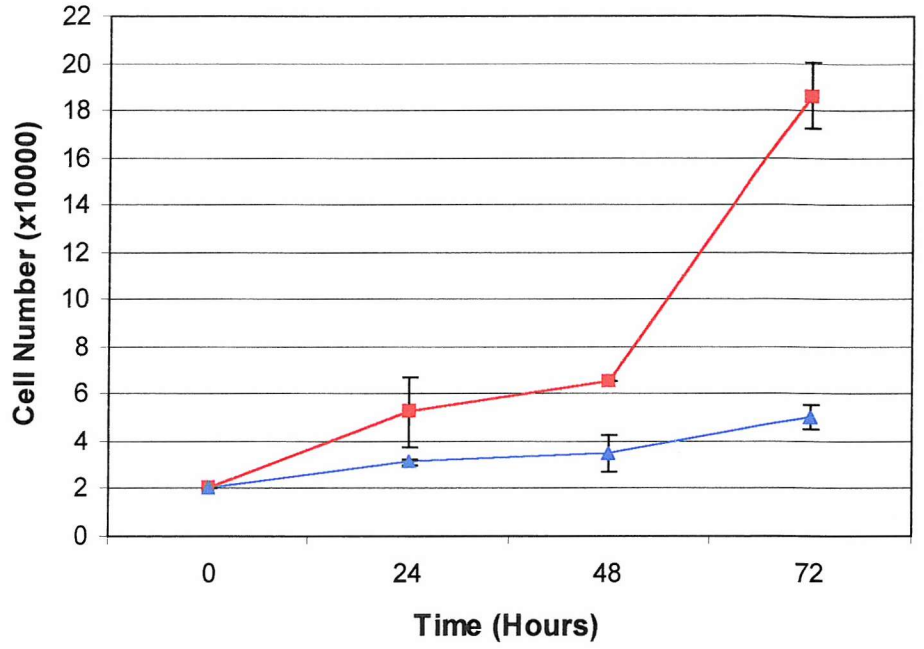

B

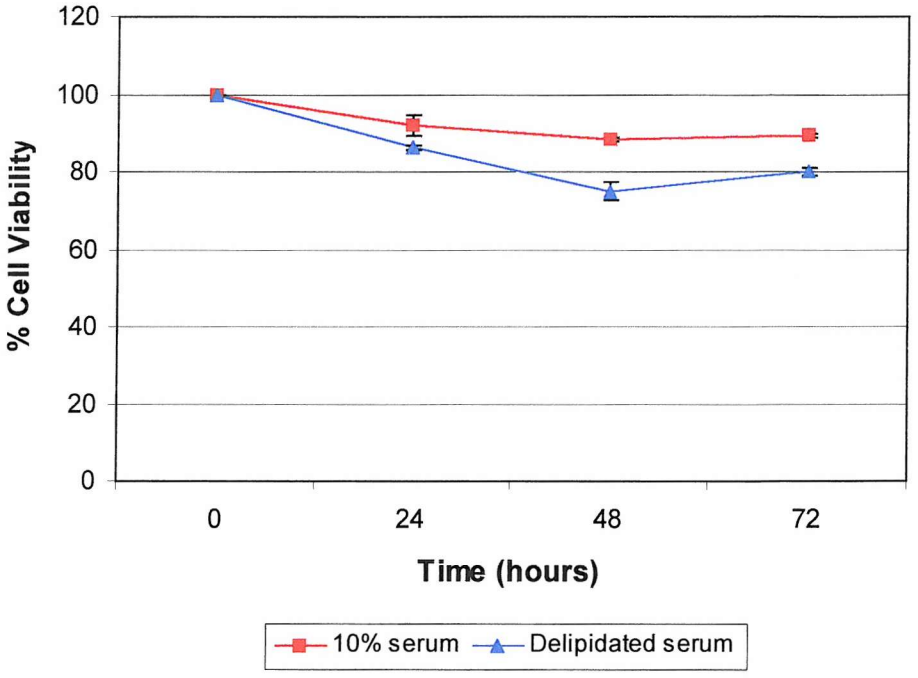

Fig. 5.4 Rates of cell growth and cell death observed in ND7 cells grown in the presence of either 10% or delipidated serum

ND7 cells ($1x10^4$) were grown on 9.6 cm^2 dishes in medium that contained either 10% or delipidated (DL) serum for up to 72 hours. Using the Trypan Blue exclusion assay, the number of viable cells was counted at each time point **(A)**. The number of viable cells at each time point was also expressed as a percentage of the total cell number **(B)**. Values shown represent the means from two independent experiments +/- s.e.m.

The serum lipids LPA (Van Corven *et al.*, 1989) and S-1-P (Wu *et al.*, 1996, Pyne *et al.*, 1996) are both known to have mitogenic effects on cells. Therefore the absence of LPA and S-1-P in delipidated serum may have been responsible for the reduced growth rate of ND7 cells under these conditions. Since *Pax-3* expression is associated with mitotically active cells, the removal of LPA and S-1-P may also have contributed to the repression of Pax-3 promoter activity observed in delipidated serum. It should be noted however, that the lack of other serum lipids apart from LPA and S-1-P may have contributed to the effects on cell growth and on Pax-3 promoter activity that were observed in the presence of delipidated serum.

5.2.5 Pax-3 DNA binding activity in ND7 cells grown in media containing different types of serum

To determine if the decrease in Pax-3 promoter activity coincided with a decrease in Pax-3 DNA binding activity in ND7 cells, an EMSA was carried out with a ^{32}P-labelled oligonucleotide containing the e5 binding-site. As shown in figure 5.5(A), Pax3 – e5 binding was detected in nuclear extracts of ND7 cells that had been cultured for 24 hours in the presence of 10%, 1%, 0.5% or delipidated serum. Pax-3 DNA binding activity was highest for cells grown in the presence of 10% serum. The amount of bound e5 probe in each lane of the EMSA was quantified by phosphor-image analysis of the polyacrylamide gel. The results, shown in figure 5.5(B), are expressed relative to the amount of bound e5 for cells grown in the presence of 10% serum, which was assigned a value of 100. From this graph it can be seen that cells cultured in medium containing either 0.5% or 1% serum resulted in Pax-3 DNA binding activities of 70-80% relative to the level of binding in the presence of 10% serum. A value of just less than 60% was obtained for cells grown in the presence of delipidated serum. Therefore the levels of

both peptide growth factors and mitogenic lipids in serum appear to influence the DNA binding activity of Pax-3 in ND7 cells. As in the case of Pax-3 promoter activity, no significant difference in Pax-3 DNA binding activity was observed between cells grown in 0.5% serum and 1% serum. This suggests that *Pax-3* mRNA expression may be reduced by similar amounts in ND7 cells grown in the presence of 0.5% and 1% serum, thus giving rise to similar levels of Pax-3 protein under each of these growth conditions. Therefore the distinct cellular effects induced by 0.5% and 1% serum may not be directly related to the level of Pax-3 DNA binding in ND7 cells

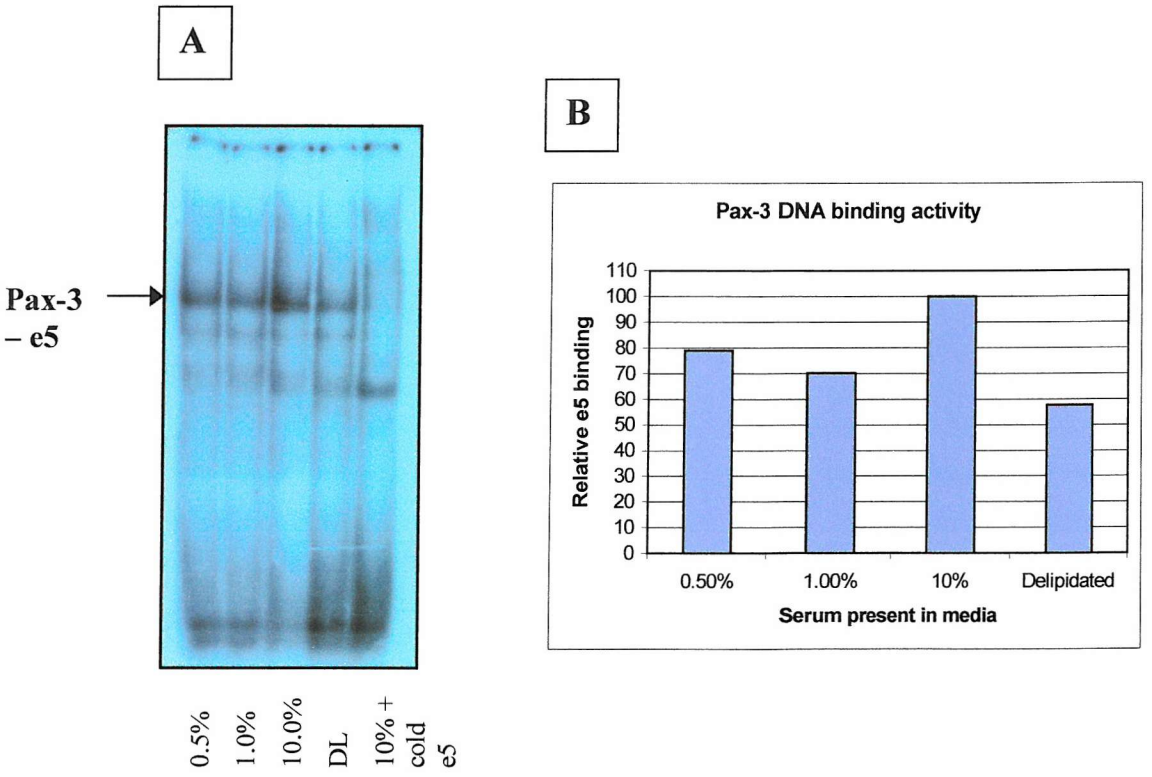

Fig. 5.5 DNA binding activity of Pax-3 in ND7 cells that had been grown in the presence of different types of serum

(A) EMSA in which ND7 nuclear extracts made from cells that had been cultured for 24 hours in the presence of 10%, 1%, 0.5% or delipidated (DL) serum, were incubated with an e5 DNA probe. **(B)** Quantification of the amount of Pax-3 bound to the e5 probe. The polyacrylamide gel was analysed on a phosphor-imager, and the level of Pax3-e5 binding expressed relative to that detected in the presence of 10% serum.

5.3 Identification of potential regulatory factors involved in the control of Pax-3 promoter activity

To identify what factors may bind and activate the Pax-3 promoter in response to serum lipids and growth factors, the Pax-3 promoter sequence was analysed using the MatInspector computer program (Quandt *et al.*, 1995). This revealed several potential serum response elements (SREs), as well as potential Pax-3 paired domain and homeodomain binding sites, and potential binding sites for POU domain proteins including Brn-2 and Oct-1. The locations of all these potential binding sites in the region of the Pax-3 promoter that had been cloned into the pGL3-Basic reporter plasmid are shown in figure 5.6. The SRE is present in the upstream regulatory sequence of immediate early genes such as *c-fos* (Ramirez *et al.*, 1997). It binds the serum response factor (SRF), along with transcription factors from the Ets family that, in response to signals induced by mitogens, activate transcription from the SRE. The ability of individual SREs in the Pax-3 promoter to mediate the activation of Pax-3 promoter activity is currently being investigated.

5.3.1 Auto-regulation of the Pax-3 promoter

In addition to the SREs, computer analysis of the Pax-3 promoter sequence revealed potential binding sites for the Pax-3 protein itself. Therefore the potential for Pax-3 to bind directly to its own promoter and activate transcription of *Pax-3* was investigated. To achieve this ND7 cells were cotransfected with a constant amount of P3prom-pGL3 reporter plasmid, and increasing amounts of Pax-3 expression vector. After 48 hours growth in the presence of 10% serum, cells were harvested and their lysates used in luciferase assays. Figure 5.7 shows the effects of increasing amounts of exogenous Pax-3 protein on Pax-3 promoter activity. Using amounts of Pax-3 expression vector lower

than 1μg, Pax-3 promoter activity was increased when compared to its activity in the absence of exogenous Pax-3 protein. Adding between 1 and 4μg of Pax-3 expression vector however, resulted in a gradual reduction in Pax-3 promoter activity. The repression of the Pax-3 promoter seen with higher levels of Pax-3 could be due to squelching (Chalepakis *et al.*, 1994). High levels of Pax-3 protein may bind out general transcription factors in solution, preventing them from assembling on the Pax-3 promoter. This in turn would inhibit the effects of positively acting transcription factors on the promoter. Therefore, the level of promoter activity will be reduced to levels lower than those seen in the absence of Pax-3. However, Chalepakis *et al.* (1994) also showed that Pax-3 contains a transcription inhibitory domain. Therefore the decrease in Pax-3 promoter activity seen with higher levels of Pax-3 expression vector may have due to Pax-3 binding to sequences in its promoter and specifically repressing transcription via its inhibitory domain.

ATAAATAAAAGGCTAGGCACAATGGTACCTTCTCTAAGGACAGACAGTCTT -950

TACAACACTCCTGGCGTCATATCCTGCTGGGGACACTTCAGCTCCTAGCC -900

AAGACGTTGCTTCTTTTATTTTTCCAGCAGTTTAGTCTGAATGCCATAAT -850

AAATTCCTGAGAACAAACGCTGCACCCGGGCAAAACCTCAACATATAGAT -800

GCAAGTGCATCGGGGATGAATGTGTACGTGGAGATTTAAAGTCCCCGCTT -750

CTCAGAAGGGTTTTTAAACCAAGAAAAGGAGCTGGCTTCCCCATTTCAGC -700

TTGCAACTTGGAGCCCAGGGGAGGCCTAACCTCTTCAGTCTCTGTCATGG -650

CTATGCCACCTGTCTTTTCATTCCCAGCCTAAGAAAGACAAAAGGACCTT -600

CTGGGCACATCTTGGACTCTTCCTGAGAGATGCCTTTCTGGGAGGCTCAC -550

ATAGGGAGCTCAGGCCCAGAGGCAGACCAGAGAAAGGAAAAGGAAACACA -500

TCCGGAATTCCTCTGTGCCCCTTTCCAAATTTGCTCCACCGCCATCTCCG -450

TATTAGTAATCCCGAAGCGAAATCCACAGGTGAAAAGCAGGGGCAGACAG -400

AGGAAATAAGGGGCGGATATAGCAAGGCTTCCAGAGAAAGGCGGAAAGAG -350

ATTAGGACAGAGTAATAGAAAACCAAGATGATCAAGGCTGAATCTCATGT -300

AGAGGGACAGGGACACCGTGAGCCTTTTTCCATCCTCACTGGCTCTTGCC -250

ACCCAAGCTGCCTCTCCTAGTTTCAACCTGTCCACCCTTCTCTTGAGAAA -200

GGGACACAGAGCTAGTCCCCCTCTGGGTCGGCGGAGGCCTGGGGACCGTC -150

AGGGATGGGAAGAGAAGTAGCTTCTGTCGCCCAATCAGCGCGTGTCTTTG -100

CCACCCGGGACGGTCTCCTCCTCGGCCAATCGCAGCTCAGGGCTCCTGAT -50

CAAGCTTTGGGTGAAAGAACTAATAAATGCTCCCTAGTCCGGATCCCTGC +1

ACTCGGTGTCACGACGGGAGGAGACTTGGGACGTGTTCCTGCCTCGTC +50

TAATAAATG - TATA Box C - Possible start of transcription

GTTCC – Potential Pax-3 paired domain binding-sites
GTCAC

ATTAGTAAT – Potential Pax-3 palindromic homeodomain binding site
ATTA – potential Pax-3 homeodomain binding site

GCCATAATAAATTCCT - Potential Brn-2 binding site TCTTTTCATT - Potential Oct-1 binding site

AGGCTCACATAGGGAGCT - Potential SRE

Fig. 5.6 Nucleotide sequence of the 5' flanking region of *Pax-3*

The coding strand of the region of the Pax-3 promoter from –1000 to +50 (relative to the transcription start site) is shown. The TATA box is underlined and the start site of transcription is shown in red. Potential binding sites for the Pax-3 paired domain and homeodomain are highlighted, as well as other binding sites described in the text.

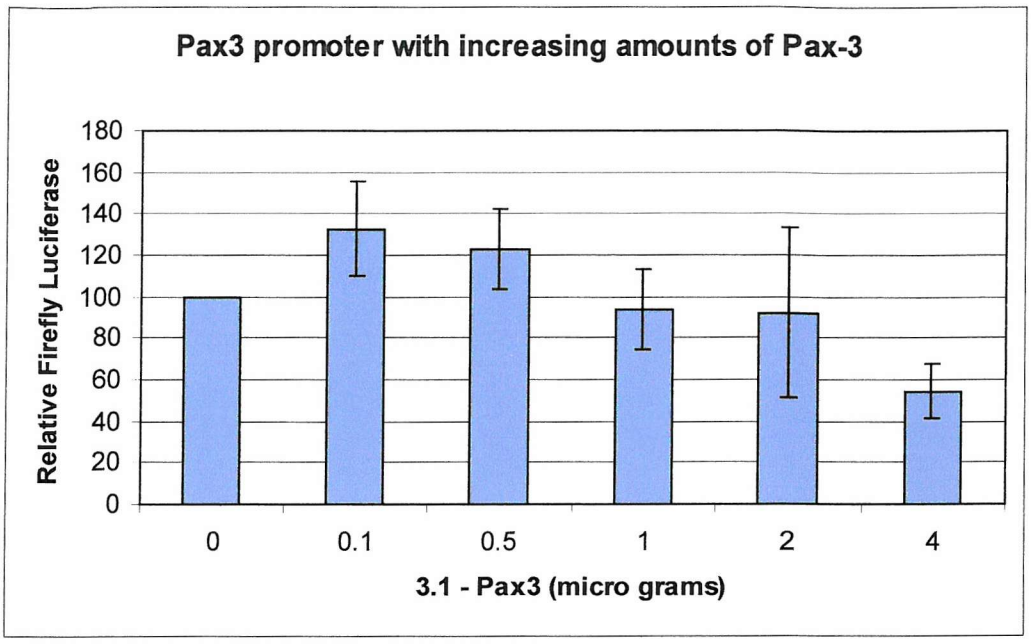

Fig. 5.7 The effect that increasing amounts of Pax-3 protein has on Pax-3 promoter activity

ND7 cells were cotransfected with 2μg of the P3prom-pGL3 reporter construct, and increasing amounts of pcDNA3.1-Pax3 expression vector. In each case the total amount of expression vector DNA was made up to 4μg using pcDNA3.1 DNA. Transient transfections were cultured in medium containing 10% serum for 48 hours. The cells were then harvested, and aliquots of the cell lysates were used in luciferase assays, and BCA protein assays. Luciferase readings were then normalised using the results of the protein assays. The results shown are the means of 2 independent experiments +/- s.e.m.

It was important to show that the differences in reporter gene expression observed in response to increasing amounts of exogenous Pax-3 protein were not due to a non-specific effect mediated by increasing amounts of the expression vector. Therefore the Pax-3 expression vector was cotransfected with the pRL-TK reporter plasmid. In this plasmid the TK minimal promoter that contains no potential binding sites for Pax-3 is cloned upstream of the Renilla luciferase reporter gene. As shown in figure 5.8, Pax-3

only induced basal levels of transcription from the pRL-TK reporter construct, irrespective of the amount of Pax-3 expression vector transfected.

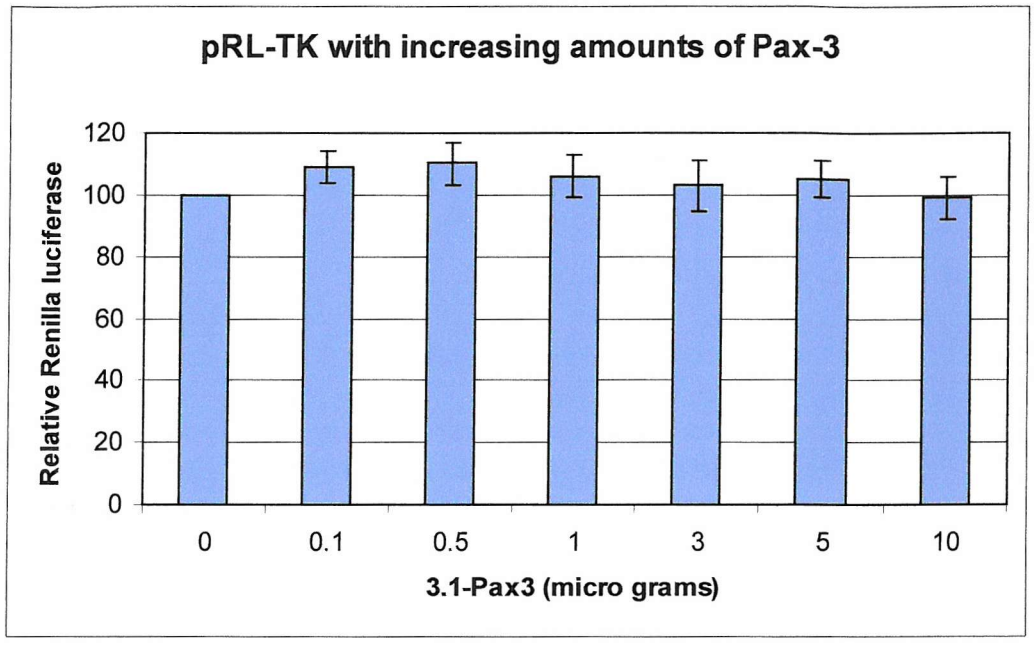

Fig. 5.8 The effect that increasing amounts of Pax-3 has on expression of the luciferase reporter gene from the pRL-TK reporter plasmid

ND7 cells were cotransfected with 2μg of the pRL-TK reporter plasmid, and increasing amounts of pcDNA3.1-Pax3 expression vector. In each case the total amount of expression vector DNA was made up to 4μg using pcDNA3.1 DNA. Transient transfections were cultured in medium containing 10% serum for 48 hours. Cell lysates were used in luciferase assays and BCA protein assays. Luciferase readings were then normalised using the results of the protein assays. The results shown are the means of 2 independent experiments +/- s.e.m.

.

Together these results suggest that sequence elements in the Pax-3 promoter mediated the effects of the Pax-3 protein on Pax-3 promoter activity. Therefore the Pax-3 promoter may be subject to auto-regulation whereby low levels of Pax-3 protein increase promoter activity, but higher levels of Pax-3 inhibit it.

5.3.2 Effects of Pax-3 deletion proteins on Pax-3 promoter activity

In order to study the mechanism by which Pax-3 may activate at low concentration and inhibit Pax-3 expression at higher concentrations, the P3prom-pGL3 reporter was cotransfected with Pax-3 deletion constructs. First, increasing amounts of a pJ7 expression vector containing the coding region for the first 284 amino acids of Pax-3 was cotransfected with P3prom-pGL3. The truncated Pax-3 protein produced by this expression vector lacks the whole of the C-terminus of Pax-3, which contains the transactivation domain (Chalepakis *et al.* 1994). The *Pax-3* cDNA sequence coding for this truncated Pax-3 protein (Pax-3ΔAct), was cloned into the pJ7 vector by Harris (2000). Expression from this vector is under the control of the cytomegalovirus (CMV) promoter. Figure 5.9 shows the effect that increasing amounts of Pax-3ΔAct had on expression from the Pax-3 promoter. In contrast to the effects of wild type Pax-3, low levels of the Pax-3ΔAct protein (less than 1μg of expression vector) did not induce the Pax-3 promoter. This suggests that the C-terminal activation domain of Pax-3 is required to trans-activate the Pax-3 promoter. Higher levels of Pax-3ΔAct protein (between 1 and 4μg of expression vector) repressed transcription from the Pax-3 promoter. The first 90 amino acids at the N-terminus of Pax-3, which are present in both wild type and Pax-3ΔAct proteins, is known to have inhibitory effects on transcription (Chalepakis *et al.*, 1994). Thus, high levels of Pax-3 and Pax-3ΔAct proteins may have inhibited transcription from the Pax-3 promoter specifically, by binding to sequence elements in the promoter and then using the transcription inhibitory domain to disrupt the general transcription machinery. High levels of Pax3ΔAct protein repressed Pax-3 promoter activity to a greater extent than high levels of wild type Pax-3. This may be because the ability of the Pax-3 inhibitory domain to repress transcription is impaired when the Pax-3

activation domain is also present. Therefore when the activation domain is removed, as in Pax-3ΔAct, the inhibitory domain is more effective.

To investigate further the inhibitory effect that higher concentrations of Pax-3 protein have on Pax-3 promoter activity, a second pJ7 expression construct (also cloned by Harris, 2000) containing the coding region for the whole of Pax-3 minus the first 33 amino acids (Pax-3ΔInhib), was cotransfected with the P3prom-pGL3 reporter construct. Although the first 90 amino acids of Pax-3 constitute a transcription inhibitory domain, only the first 33 amino acids up to the start of the paired domain were deleted, since further deletions into the paired domain have been shown to inhibit the DNA binding activity of Pax-3 (Chalepakis *et al.*, 1994). Since two of the potential Pax-3 binding sites in the Pax-3 promoter correspond to paired domain recognition motifs, it was important not to impair the DNA binding potential of the Pax-3 paired domain. Figure 5.10 shows the effect that increasing amounts of Pax-3ΔInhib had on expression from the Pax-3 promoter. Interestingly, the induction of Pax-3 promoter activity produced in response to low levels of wild type Pax-3 was not detected using the Pax-3ΔInhib protein. Since the C-terminus of Pax-3 remains intact in the Pax-3ΔInhib protein, these results suggest that the first 33 N-terminal amino acids of Pax-3 may contribute to its transcription activation properties.

Higher amounts of Pax-3ΔInhib reduced Pax-3 promoter activity promoter activity, as had been observed using the wild type and Pax-3ΔAct proteins. Chalepakis *et al.* (1994) reported that a domain for transcription inhibition is located in the first 90 N-terminal amino acids of Pax-3. However, in the Pax-3ΔInhib protein, only the first 33 amino acids N-terminal to the Pax-3 paired domain, have been removed. Therefore, it is possible that

the first 57 amino acids of the Pax-3 paired domain also contribute towards the inhibition of transcription. If this were true, then the reduction in Pax-3 promoter activity in response to high levels of the Pax3 proteins may have been mediated in a specific manner, at least in part, by the Pax-3 inhibitory domain.

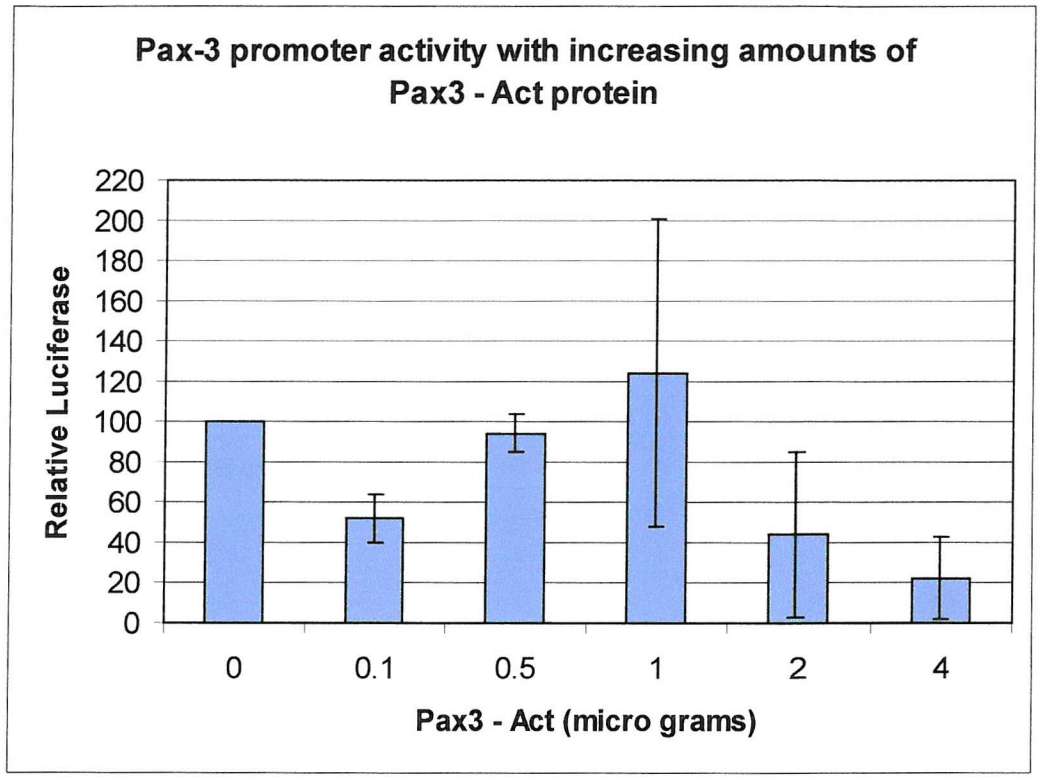

Fig. 5.9 The effect that increasing amounts of Pax-3ΔAct protein has on Pax-3 promoter activity

ND7 cells were cotransfected with 2μg of P3prom-pGL3 reporter construct, and increasing amounts of pJ7-Pax-3ΔAct expression vector. Transient transfections were cultured in medium containing 10% serum for 48 hours. Cell lysates were then used in luciferase assays. The results shown represent the mean values derived from two independent experiments +/- s.e.m.

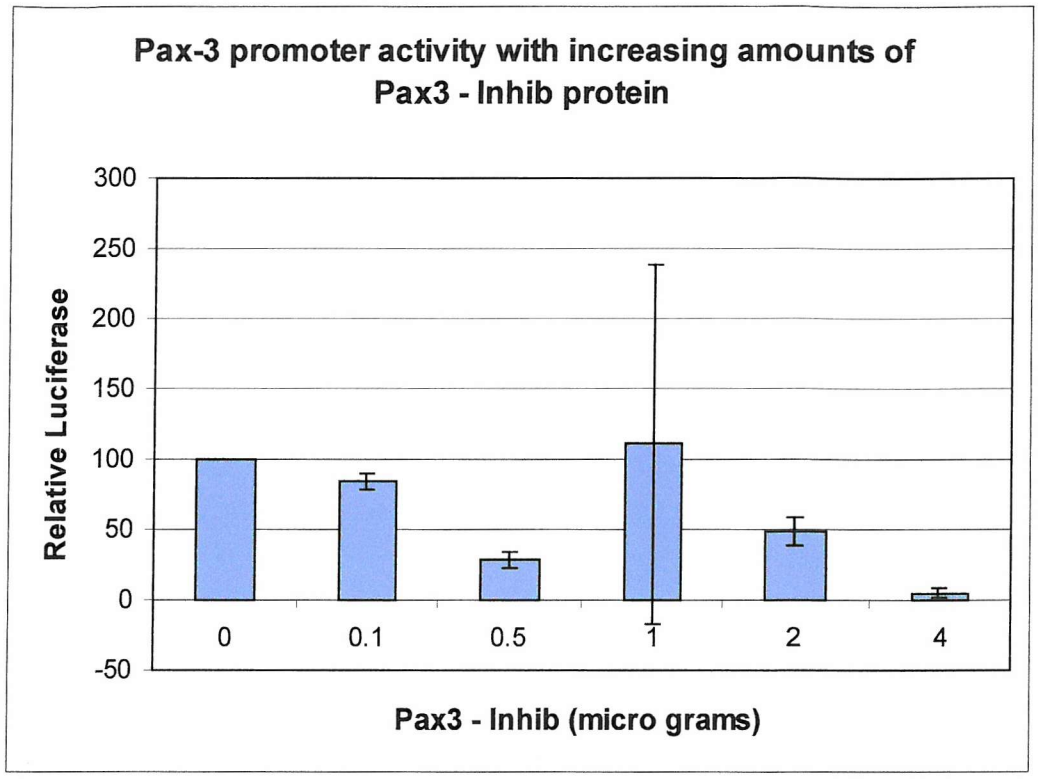

Fig. 5.10 The effect that increasing amounts of Pax-3ΔInhib protein has on Pax-3 promoter activity

ND7 cells were cotransfected with 2μg of P3prom-pGL3 reporter construct, and increasing amounts of pJ7-Pax-3ΔInhib expression vector. Transient transfections were cultured in medium containing 10% serum for 48 hours. Cell lysates were then used in luciferase assays. The results shown represent the mean values derived from two independent experiments +/- s.e.m.

5.3.3 The effects of Brn-3 proteins on Pax-3 promoter activity

Analysis of the Pax-3 promoter showed a number of binding sites for POU domain transcription factors. These proteins are transcription factors that contain a common amino acid sequence of 150-160 residues called the POU domain, so named because it was originally discovered in the mammalian proteins Pit-1, Oct-1 and Oct-2, and the nematode protein Unc-86. The POU domain constitutes the DNA binding domain of

these transcription factors, and is composed of a POU specific domain and a POU-homeodomain, which are joined together by a linker (Latchman, 1999). Many more POU domain proteins have subsequently been discovered in a range of species, which have cell type specific functions. Different classes of POU-domain proteins have been specified, based on amino acid similarities within the POU domain. Thus Pit-1 is considered a class I POU domain protein, Oct-1 and Oct-2 are in class II, the Brn-1, Brn-2 and Testes-1 proteins are in class III, while Brn-3 and Unc-86 are in class IV (He *et al.*, 1989).

The low level of Pax-3 promoter activity seen in ND7 cells cultured in low serum conditions, supports the *Pax-3* mRNA expression data which shows that *Pax-3* is expressed at low levels in differentiated, mitotically inactive cells. Interestingly the Brain-3 (Brn-3) POU domain proteins have been shown to play a key role in the regulation of neuronal cell differentiation. Brn-3 is expressed in the mammalian central and peripheral nervous systems during development (He *et al.*, 1989). Three distinct Brn-3 proteins have been discovered, each coded for by a separate gene, called Brn-3a (Brn-3.0), Brn-3b (Brn-3.2) and Brn-3c (Brn-3.1). Brn-3a knockout mice are severely lacking in sensory and motor neurons and die shortly after birth (McEvilly *et al.*, 1996). Less severe phenotypes are observed in knockout mice that fail to produce either the Brn-3b or Brn-3c protein. These mice are viable, but Brn-3b knockouts have a shortage of retinal neurons, leading to blindness, while Brn-3c knockout mice are lacking in vestibular neurons, which leads to deafness (Erkman *et al.*, 1996). Thus Brn-3 proteins play important roles in the development of the mammalian nervous system.

The spatial and temporal expression patterns of Brn-3a and Brn-3c overlap with the expression of *Pax-3* in the developing peripheral nervous system (PNS). Ninkina *et al.* (1993) showed that in rat nervous tissue Brn-3a is expressed in the central nervous system (CNS) and in most neurons of the dorsal root ganglia, which is a constituent of the PNS. Brn-3c is expressed at much lower levels than Brn-3a in the CNS (only seen in the spinal cord), and is only expressed in a subset of neurons in the dorsal root ganglia. However, both Brn-3a and Brn-3c are expressed in dorsal root ganglia neurons during embryogenesis when these neurons are still dividing. Furthermore, Fedtsova and Turner (1995) showed that at embryonic day 9.5 in the mouse, Brn-3a is expressed in the dividing precursor cells of trigeminal and dorsal root ganglia, which migrate from the neural crest. *Pax-3* is also expressed at this stage of mouse embryogenesis in neural crest cells that give rise to neurons of the peripheral and autonomic nervous systems. Therefore, like Pax-3, both Brn-3a and Brn-3c are involved in establishing and maintaining the neuronal phenotype of sensory neurons in the PNS.

As described, computer analysis of the Pax-3 promoter region cloned into the pGL3-Basic vector showed that the sequence contains several potential binding sites for POU-domain proteins (figure 5.6). Given that the expression of the Brn-3a and Brn-3c genes overlaps with that of *Pax-3* in the developing PNS, the potential for Pax-3 promoter activity to be altered in response to these proteins was investigated. Thus, ND7 cells were cotransfected with 2μg of P3prom-pGL3 reporter plasmid and 4μg of either a Brn-3a expression vector, a Brn-3c expression vector or a pcDNA3.1 empty expression vector. Cells were then cultured in medium containing 10% serum for 48 hours. As before, cell lysates were used in luciferase assays, and the average readings obtained were normalised by performing BCA protein assays. The results, which represent the

mean values from two independent experiments, are shown in figure 5.11. It can clearly be seen that the Brn-3a and Brn-3c proteins had different effects on the Pax-3 promoter. Brn-3a increased expression almost 2-fold, when compared to promoter activity in the presence of the empty expression vector. In contrast, Pax-3 promoter activity was reduced by more than 50% in the presence of Brn-3c, when expressed relative to the activity observed in the presence of the empty expression vector.

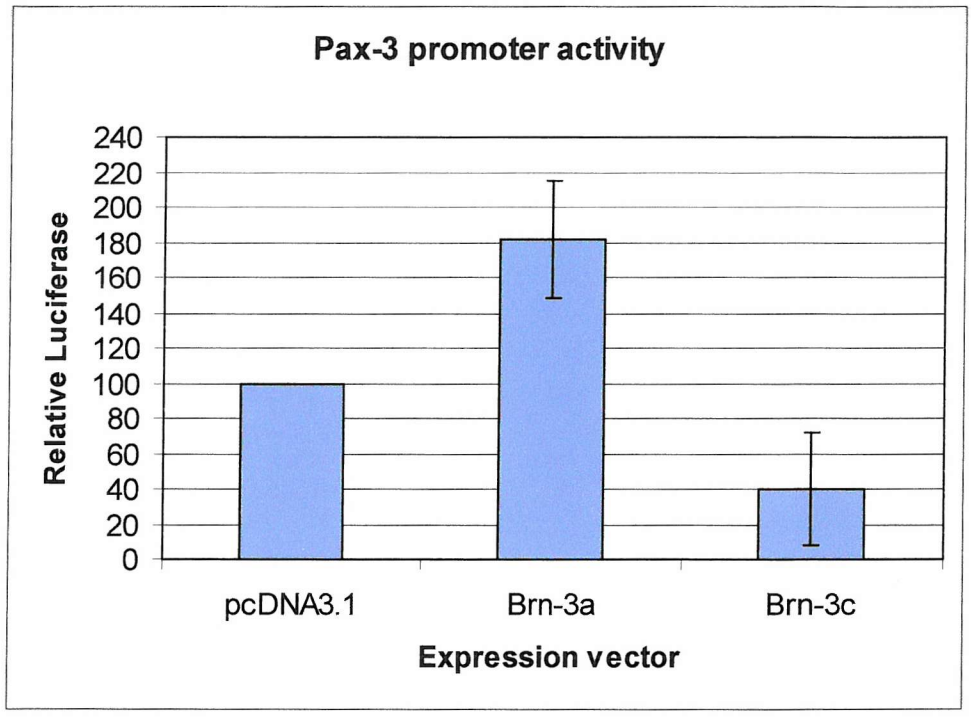

Fig. 5.11 Effects of the Brn-3a and Brn-3c proteins on Pax-3 promoter activity

ND7 cells were cotransfected with 2μg of P3prom-pGL3 reporter plasmid and 4μg of either a Brn-3a expression vector, a Brn-3c expression vector or pcDNA3.1 DNA alone, before being cultured for 48 hours in the presence of 10% serum. Cell lysates were then used in luciferase assays to measure Pax-3 promoter activity. The results shown represent the mean values obtained from two independent experiments +/- s.e.m.

5.4 Discussion

Regulation of the Pax-3 promoter activity by extracellular mediators

In situ hybridisation studies showed that *Pax-3* expression in neuronal cells is restricted to mitotically active cells, and is downregulated when these cells differentiate (Goulding *et al.* 1991). In addition Evans and Lillycrop (1996) showed a close correlation between *Pax-3* mRNA expression and mitotically active immature neuronal cells. In ND7 cells cultured in the absence of serum *Pax-3* mRNA levels rapidly decrease. This is followed by the onset of morphological differentiation, a cessation of cell proliferation and an increase in the rate of apoptotic cell death. Pax-3 DNA binding activity is also reduced to undetectable levels in ND7 cells that are grown under conditions which induce morphological differentiation (Reeves *et al.*, 1998). Therefore to examine this correlation further and to investigate whether changes in Pax-3 expression are mediated through a change in the rate of transcription, we examined Pax-3 promoter activity in conditions of low serum. Budhram-Mahadeo *et al.* (1994a) have shown that when ND7 cells are incubated in 1% serum there is no reduction in the rate of cell proliferation and no increase in morphological differentiation or apoptosis. Culturing ND7 cells in 0.5% serum however, led to a decrease in cell proliferation and an increase in morphological differentiation. Therefore we used these two low serum conditions to study whether Pax-3 promoter activity would be affected.

We observed a 50% reduction in Pax-3 promoter activity when the cells were grown in the presence of 1% serum, and a 60% reduction in Pax-3 promoter activity in the presence of 0.5% serum, when compared to the level of promoter activity observed in cells cultured with 10% serum. The reduction in Pax-3 promoter activity in low serum conditions, suggests that activation of transcription is dependent upon factors within

serum. However, Pax-3 promoter activity was considerably reduced in both 0.5% and 1% serum even though the rate of cell proliferation was only reduced in the presence of 0.5% serum. This suggests that the rate of cell proliferation is not directly dependent upon the level of Pax-3 transcription in ND7 cells.

Evans and Lillycrop (1996) showed that the addition of EGF, aFGF or bFGF alone to serum starved ND7 cells was sufficient to induce *Pax-3* mRNA expression. This implied that growth factor-stimulated signalling pathways could up-regulate *Pax-3* expression in ND7 cells. In addition the results presented in this chapter show that Pax-3 promoter activity was reduced by more than 50% in ND7 cells cultured in the presence of delipidated serum, when compared to cells grown in 10% serum. Since peptide growth factors remain intact when serum undergoes the process of delipidation, this shows that serum lipids are also required to induce Pax-3 promoter activity. In addition delipidated serum reduced the growth rate of ND7 cells when compared to cell growth in the presence of 10% serum. The decreased rate of cell growth was presumably caused by a reduction in the rate of cell proliferation, since no effect was observed on cell viability in the presence of delipidated serum.

Certain lipid components of serum are known to have mitogenic effects on cells. LPA was shown to induce DNA synthesis and cell proliferation in quiescent Swiss 3T3 fibroblasts (Van Corven *et al.*, 1989). S-1-P has also been shown to stimulate proliferation of quiescent fibroblasts (Wu *et al.*, 1996), as well as airway smooth muscle cells (Pyne *et al.*, 1996). The mitogenic effects of LPA and S-1-P are mediated by the induction of mitogen-activated protein kinase (MAP kinase) cascades, as well as by the activation of Rho-dependent kinases (An *et al.*, 1998). The MAP kinase pathway

stimulates the Ternary Complex Factor (composed of Ets proteins), while Rho-dependent kinases stimulate the Serum Response Factor. Binding of these transcriptional activators together to the Serum Response Element found in the promoters of immediate-early genes like *c-fos*, results in the transcriptional activation of these genes, which in turn stimulates DNA synthesis and cell division. LPA and S-1-P exert their cellular effects by binding to G protein coupled receptors on the cell surface, the activation of which results in the initiation of intracellular signalling cascades. Thus, both S-1-P and LPA may activate G protein coupled receptors on the surface of ND7 cells, thus promoting cell proliferation and inhibiting differentiation. The removal of these mitogenic lipids from serum would lead to the down-regulation of such signalling cascades in cells grown in the presence of delipidated serum.

The mitogenic roles of the serum lipids S-1-P and LPA have been well documented. However, since S-1-P and LPA are not the only lipids removed from serum when it is delipidated, the lack of other serum lipids may be responsible for the reduction in Pax-3 promoter activity and the reduced level of ND7 cell growth seen in the presence of delipidated serum. Serum lipids could be added back individually to ND7 cells grown in the presence of delipidated serum in order to determine which lipids are required to induce Pax-3 promoter activity and to maintain ND7 cells in a proliferating state.

Growth of ND7 cells in media containing 0.5%, 1% or delipidated serum reduced the DNA binding activity of Pax-3 in these cells, when compared to the level of Pax-3 DNA binding observed in cells that had been grown in the presence of 10% serum. This may reflect a reduced level of *Pax-3* mRNA expression in cells grown in the presence of low serum concentrations, or in the presence of delipidated serum. Such an effect was

implied by the results of the luciferase assays described above, which showed reduced Pax-3 promoter activity under each of these conditions. As described, the growth rate of ND7 cells was reduced in the presence of 0.5% and delipidated serum, whereas growth in 1% serum occurred at approximately the same rate as in the presence of 10% serum. In addition growth in 0.5% serum but not in 1% serum, induced the onset of morphological differentiation in ND7 cells. The DNA binding data suggest that these distinct cellular effects may not be mediated by differences in Pax-3 DNA binding activity alone, since growth in 0.5%, 1% and delipidated serum resulted in similar levels of Pax-3 DNA binding *in vitro*. This is in agreement with the Pax-3 promoter data, which showed equally low levels of Pax-3 promoter activity in ND7 cells cultured in the presence of 0.5% and 1% serum.

Auto-regulation of the Pax-3 promoter

Analysis of the Pax-3 promoter revealed a number of transcription factor binding sites including the SRE, which has been shown to be responsible for serum regulation of immediate-early gene transcription. There are also two potential Pax-3 paired domain-binding sites and two potential Pax-3 homeodomain binding sites in the Pax-3 promoter sequence, suggesting the possibility of auto-regulation. Using transient transfection assays, it was shown that Pax-3 could indeed regulate its own promoter. At low concentrations, Pax-3 activated its promoter and at higher concentrations repression was observed. Similarly Chalepakis *et al.* (1994) showed that at low concentration Pax-3 enhanced the rate of transcription from a CAT reporter gene construct containing 6 Pax-3 paired domain binding sites upstream of TK-CAT. However, higher concentrations of Pax-3 repressed transcription from this reporter gene construct. When fused to the DNA binding domains of GAL4, it was also demonstrated that the C-terminal 78 amino acids

of Pax-3 alone could activate transcription of a reporter gene construct containing GAL4 binding sites. We showed that deletion of the C-terminal activation domain abolished the ability of Pax-3 to activate its own promoter at low concentrations, and led to a greater inhibition of promoter activity at higher concentrations. This suggests that Pax-3 specifically inhibits transcription at higher concentrations, and that when the activation domain is removed the ability of Pax-3 to repress promoter activity is enhanced.

Chalepakis *et al.* (1994) showed that the first 90 amino acids of Pax-3 function as a transcription inhibitory domain. Like the C-terminal activation domain, this inhibitory domain can function independently of the rest of the Pax-3 protein as it can be transferred onto a heterologous GAL4 DNA-binding domain. We showed that at higher concentrations, a Pax-3 protein lacking the first 33 amino acids (Pax-3ΔInhib) still resulted in repression of the Pax-3 promoter. This suggests that the first 57 amino acids of the Pax-3 paired domain also contribute to its transcription inhibitory domain, in addition to the N-terminal 33 amino acids. As a result the Pax3 protein lacking the first 33 amino acids may still be able to repress the Pax-3 promoter in a specific manner, using a transcription inhibitory domain.

Interestingly we showed that deletion of the first 33 amino acids (Pax-3ΔInhib) abolished the ability of Pax-3 to activate its own promoter at low concentration. This may have been because the Pax-3ΔInhib protein was folded differently or its expression may have been lower than that of wild type Pax-3 in these transfection experiments. Alternatively, the inability of Pax-3ΔInhib to activate Pax-3 promoter activity may be because the first 33 amino acids of Pax-3 contribute to the activation domain of the protein. Chalepakis *et al.* (1994) fused different portions of the Pax-3 protein to the DNA binding domains of

GAL4. The ability of each of these fusion proteins to activate transcription from a reporter construct in which the TK-CAT gene had been linked to two GAL4 DNA-binding sites was then examined. As already described, when the first 90 amino acids of Pax-3 were fused to the GAL4 DNA binding domains, a large reduction in transcription was observed when compared to the basal level of transcription in the presence of the empty expression vector. However, a slight increase in transcription occurred using the first 41 amino acids of Pax-3, while the next 49 amino acids resulted in a slight decrease in transcription. Therefore, although the first 90 amino acids of Pax-3 repress transcription strongly, the region of Pax-3 N-terminal to the Paired domain may have a slight stimulatory effect on transcription.

The effects of Brn-3 proteins on Pax-3 promoter activity

Brn-3 proteins have been shown to play important roles during neurogenesis. Three distinct Brn-3 transcription factors have been identified, which are coded for by three separate genes. In the mammalian PNS, both Brn-3a and Brn-3c are expressed in dividing immature neuronal cells derived from neural crest, which give rise to sensory neurons in the dorsal root ganglia. The timing of Brn-3a and Brn-3c expression in these cells (mouse embryonic day 9.5) during neurogenesis therefore overlaps with the expression of *Pax-3*.

The existence of potential binding sites for POU-domain proteins in the Pax-3 promoter implies that Brn-3a and Brn-3c could bind directly to the promoter and thus alter the level of transcription. The octamer consensus sequence has been shown to mediate activation by Brn-3a (Budhram-Mahadeo *et al.*, 1994b). The octamer sequence is recognised by the Oct-1 and Oct-2 proteins, and potential binding sites for these proteins

in the Pax-3 promoter were identified using the MatInspector program. A different binding site, present in the corticotrophin-releasing hormone promoter, can mediate transactivation by both Brn-2 and Brn-3a (Lai *et al.*, 1992), and the Pax-3 promoter sequence contains potential Brn-2 sites. Since the amino acid sequences of the Brn-3 proteins are highly conserved within the POU domain, sites in the Pax-3 promoter that are recognised by Brn-3a may also be recognised by Brn-3c. Indeed, using the P3prom-pGL3 reporter construct, Brn-3a was shown to induce Pax-3 promoter activity, whereas Brn-3c repressed it.

The Brn-3a protein has been shown to act as a trans-activator in neuronal cells. For example, it activates transcription of the SNAP-25 gene in ND7 cells (Lakin *et al.*, 1995). In contrast, this promoter is repressed by Brn-3b, which also interferes with the activation of other promoters by Brn-3a. Although the N-terminal activation domain is required for Brn-3a to induce certain promoters, the POU domain of Brn-3a is sufficient to trans-activate other promoters, including the SNAP-25 promoter. Brn-3a has a valine residue at position 22 of its POU-homeodomain, whereas both Brn-3b and Brn-3c have an isoleucine in this position. In the Oct-1 POU-domain protein, the residue at position 22 of the homeodomain has been shown to be critical for its interaction with the Herpes Simplex Virus transactivating protein VP16 (Ninkina *et al.*, 1993, Latchman, 1999). Therefore, the valine at position 22 of the Brn-3a homeodomain could allow this protein to interact with a co-activator. In contrast, Brn-3b and Brn-3c may interact with a co-repressor by virtue of the isoleucine residue at position 22 of their homeodomains. This could explain why the Pax-3 promoter was induced by Brn-3a, but repressed by Brn-3c. It would be interesting to determine whether the isolated POU domains of Brn-3a and Brn-3c are sufficient to induce and repress the Pax-3 promoter respectively.

Chapter 6

Pax-3 target genes

6 Pax-3 target genes

6.1 Introduction

Pax-3 is an embryonic transcription factor that has been shown to play a key role in the development of the brain and spinal cord, neural crest cells and their derivatives, and skeletal muscle. In addition PAX3 is aberrantly expressed in a number of human cancers. For example, in ARMS, the PAX3-FKHR fusion protein functions as a more potent transcriptional activator than PAX3 itself. PAX3 is also expressed at elevated levels in the embryonal form of RMS. PAX3 has also been implicated in the development of neuroblastoma, a pediatric cancer of sympathetic neurons that are derived from neural crest cells (Niethammer and Handgretinger, 1995). Thirdly PAX3 is expressed in melanomas (Galibert *et al.*, 1999). The expression pattern of Pax-3 during embryogenesis, together with the fact that PAX3 is expressed in a range of human cancers, suggests that the Pax-3 protein may act as a promoter of cell proliferation and cell survival, and inhibit cellular differentiation. Since it is a transcription factor, Pax-3 is likely to exert these effects by modulating the expression of genes involved in the processes of cell proliferation, differentiation and cell death. However, to date few direct target genes for Pax-3 have been discovered. The identification of such molecular targets will provide greater insight into how Pax-3 affects cell behaviour during development and oncogenesis.

6.1.1 Known molecular targets of Pax-3

A number of Pax-3 target genes have been identified. The *c-met* gene has been identified as a molecular target for Pax-3, initially because its expression was absent from splotch mice. Both *Pax-3* and *c-met* are expressed during embryogenesis in cells of the lateral dermamyotome, as well as in migratory limb muscle precursor cells derived from the

lateral dermamyotome. Moreover the upregulation of *c-met* expression by Pax-3 is required for limb muscles to develop properly. During myogenesis Pax-3 has also been reported to upregulate *myoD* expression, whilst maintaining *myf5* expression. The *myoD* and *myf5* gene products are both myogenic transcription factors that function during the early stages of myogenesis. Although the MyoD promoter contains GTTCC and ATTA motifs, it is not known whether Pax-3 directly activates *myoD* expression or whether it exerts its effects by some indirect mechanism.

N-CAM (neural cell adhesion molecule) shows a similar pattern of expression as *Pax-3* in the developing neural tube and neural crest derivatives, while expression is downregulated in migrating neural crest cells. N-CAM is expressed at lower levels in the neural tubes of splotch mouse embryos than in the neural tubes of wild type embryos, suggesting that Pax-3 regulates the expression of N-CAM during development. Although cotransfection experiments with fibroblasts showed that Pax-3 repressed the N-CAM promoter in cell culture, Pax-3 may activate the expression of N-CAM in embryonic schwann cells. In contrast, expression of the MBP (myelin basic protein) gene in embryonic schwann cells is repressed by Pax-3. Thus Pax-3 may serve to maintain the phenotype of embryonic schwann cells partly by repressing myelin-specific genes such as MBP.

During development Pax-3 may also induce expression of the TRP-1 gene, which codes for a protein that is required for pigment formation in melanocytes. Pigmentation defects are apparent both in heterozygous splotch mice and in humans affected by Waardenburg syndrome. Pax-3 is expressed in melanoblasts and in melanocytes, and has been shown to induce the TRP-1 promoter in living cells (Galibert *et al.*, 1999).

In human RMS cell lines PAX3 promotes cell survival, at least in part, by inducing expression of the Bcl-xl gene, which codes for the anti-apoptotic protein BCL-XL. *In vitro* PAX3 binds to an ATTA homeodomain recognition motif in the 5' regulatory region of the BCL-XL promoter. This binding site is required to mediate the induction of BCL-XL promoter activity by PAX3 in cell culture.

6.1.2 Use of the oestrogen receptor ligand-binding domain to investigate the potential target genes of a transcription factor

One method that has been used to identify the molecular targets of a transcription factor, involves the expression of that transcription factor as a fusion protein with the ligand-binding domain of a steroid hormone receptor. The steroid hormone receptors are a family of DNA binding proteins. They activate the transcription of target genes only when associated with their respective hormones. Steroid receptors have conserved domains for DNA binding and ligand (hormone) binding. The ligand-binding domain of the oestrogen receptor (ER) is located at the C-terminus of the protein. As well as binding oestrogen this domain has transcriptional activation properties, and it also allows the ER protein to form homo-dimers. The DNA binding domain of the ER is located in the N-terminal half of the protein (Kumar *et al.*, 1986).

In the absence of hormone, the ER protein is found predominantly in the cytoplasm. Here it is associated with heat shock protein 90 (Hsp90), which binds to both the ligand-binding domain of ER and the C-terminal portion of the DNA binding domain. As this part of the DNA binding domain contains a nuclear localisation signal (NLS), binding of Hsp90 to the ER is thought to mask this NLS, preventing the ER from entering the nucleus and activating its target genes. However, when hormone binds the receptor it induces a conformational change causing Hsp90 to dissociate, which in turns allows the

hormone-receptor complex to translocate to the nucleus, bind to DNA and activate transcription (Chambraud *et al.*, 1990).

The ligand-binding domain of the ER has been used as a molecular switch to control the activity of a range of intracellular proteins. The protein under investigation is fused to the isolated ligand-binding domain of the ER, which is still capable of forming complexes with polypetides such as Hsp90 in the absence of hormone. It is assumed that the formation of such complexes inhibits the activity of the linked protein, perhaps by preventing it from entering the nucleus and binding to DNA in order to transactivate its target genes. For example, a Myc-ER fusion protein was shown to transform a fibroblast cell line. However, cell transformation was only seen in the presence of oestradiol and it was dependent upon a functional Myc protein. This indicated that oestradiol was able to control the activity of c-Myc in the Myc-ER fusion protein (Eilers *et al.*, 1989). However there are problems associated with using the ER in this way to control the activity of a protein. Firstly the transcription activation domain contained within the ligand-binding domain of ER may contribute to the transcriptional effects seen upon activation of ER fusion proteins with oestradiol. Secondly media commonly used for cell culture contains phenol red (a weak agonist of ER) and serum contains oestrogens. Therefore in order to avoid constitutive activation of the ER fusion protein, media that is free of phenol red must be used. In addition serum has to be stripped with charcoal-dextran, a process that may also remove other components of serum as well as the oestrogens (Littlewood *et al.*, 1995). A mutant form of the murine ER ligand-binding domain has been described (ER™) which contains a glycine-to-arginine substitution at position 525. ER™ does not bind oestradiol and has no intrinsic transactivation activity. However it can still bind and is activated by the synthetic steroid 4-hydroxytamoxifen (OHT). Littlewood *et al.* (1995)

fused ER™ to the c-Myc protein, and demonstrated that the resultant c-MycER™ fusion protein was only active in the presence of OHT, with oestradiol having no effect on protein activity.

Our aim was to render Pax-3 activity dependent upon 4-hydroxytamoxifen by stably expressing a Pax3ER™ protein in ND7 cells. The cellular effects and potential gene targets of Pax-3 could then be studied in the presence and absence of OHT. The advantage of this approach is that it can be used to determine whether the expression of a candidate gene is directly regulated by Pax-3. This could be achieved by examining the expression of a potential Pax-3 target gene in Pax3-ER™ expressing cells in the presence or absence of OHT, and in the presence of cyclohexamide to inhibit protein synthesis. Thus if the activation of Pax3-ER™ resulted in a change in gene expression, even when *de novo* protein synthesis was inhibited, then that gene would represent a direct molecular target for Pax-3.

6.2 Pax3-ER™

Other groups are currently studying the cellular effects of the PAX3-FKHR fusion protein using a OHT-dependent transcriptional repressor to target PAX3-FKHR responsive genes. The aim of this work is to identify genes that are directly controlled by Pax-3 in Alveolar Rhabdomyosarcoma (ARMS) cells, in which the PAX3-FKHR fusion protein is expressed. When the KRAB transcription inhibitory domain was fused to the PAX3 DNA binding domains, the resulting KRAB-PAX3 fusion protein could bind PAX3 target DNA sequences and inhibit transcription from PAX3 dependent reporter plasmids in ARMS cells. In addition stable expression of KRAB-PAX3 in ARMS cell lines prevented cell growth in soft agar and in low serum conditions (Fredericks *et al.*,

2000). Furthermore, the activity of KRAB-PAX3 has been rendered OHT-dependent by fusing ER™ to the C-terminus of this protein (Ayyanathan *et al.*, 2000). As described above, this system allows the direct effects of PAX3 target gene repression to be studied in ARMS cell lines. Our aim was to clone and express a full-length Pax3-ER™ fusion protein in ND7 cells. The activity of this protein could then be controlled using OHT. This would allow us to determine the direct affects that elevated Pax-3 protein levels have on biological properties such as cell growth, as well as on gene expression in ND7 cells.

6.2.1 Cloning of *Pax3er*™

To produce a construct that would express a Pax3-ER™ fusion protein when stably transfected into ND7 cells, *er*™ c-DNA was cloned in frame with and downstream of *Pax-3* in the pcDNA3.1(+) expression vector. The cloning steps used to achieve this are summarised in figure 6.1. The 2000bp *Pax-3* cDNA was cut out of the pBS-*Pax3* construct using BamHI and EcoRI, and subcloned into the BamHI and EcoRI sites of pcDNA3.1(+) to create pcDNA3.1(+) – *Pax3*. To facilitate subsequent cloning steps, the BamHI site in this construct was removed by digesting with BamHI, then filling in the ends and religating the plasmid.

A construct of *c-mycer*™ in the pBabepuro vector was used as the source of *er*™ cDNA. The *mycer*™ cDNA was first excised from pBabepuro using EcoRI, and then subcloned into the EcoRI site of pcDNA3.1(+) – *Pax3*. To check for the presence of the *mycer*™ insert, clones were digested with EcoRI. As shown in figure 6.2A, a single clone (clone 6) from 8 individual clones tested produced an insert of 2.3 kbp, which is the correct size for *mycer*™. Therefore this clone must contain *mycer*™ ligated to *Pax-3*.

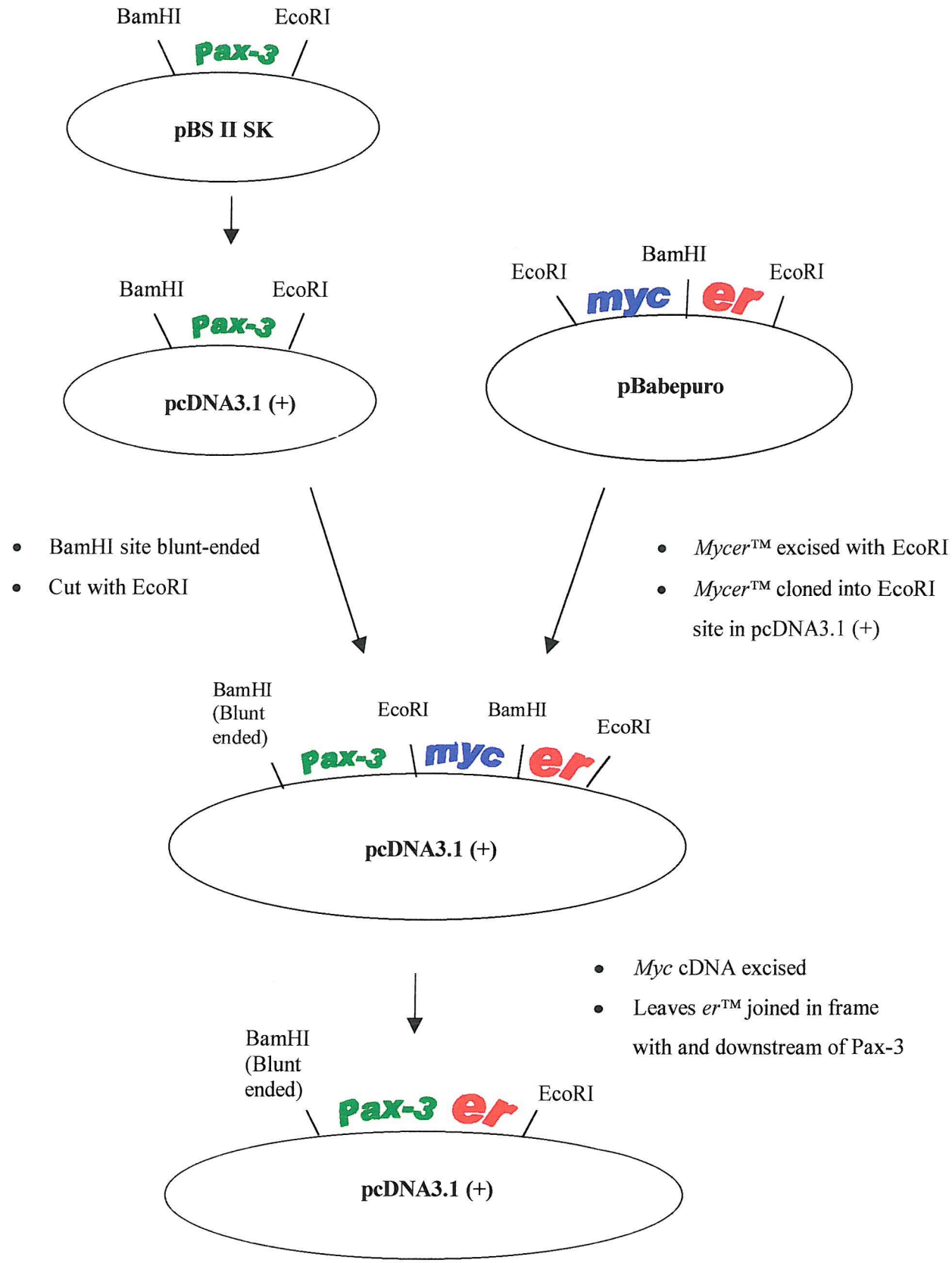

Fig. 6.1 A summary diagram to illustrate how *Pax3er*™ was cloned into the pcDNA3.1 (+) expression vector

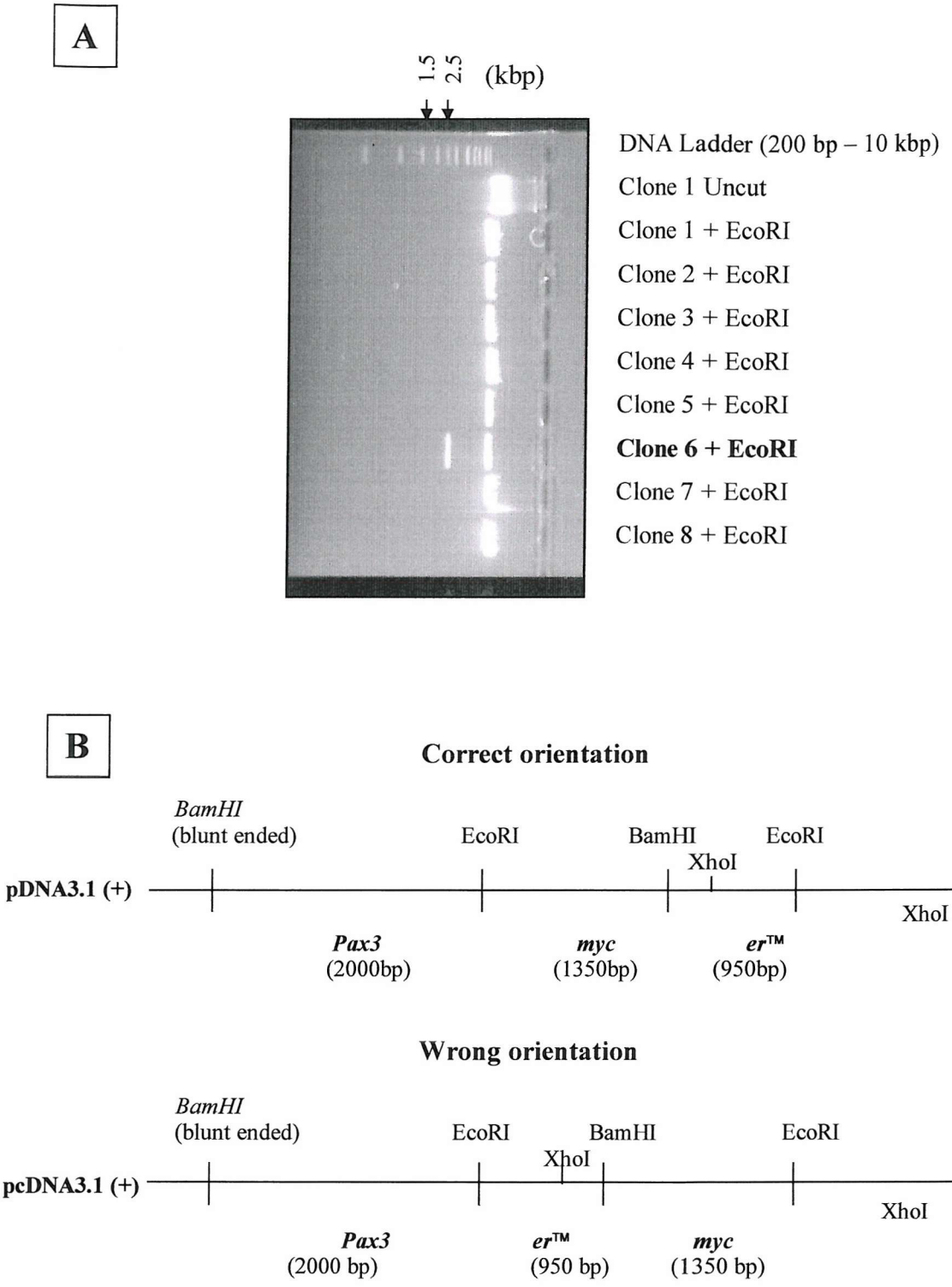

Fig. 6.2 Cloning of *mycer*™ downstream of *Pax-3* in the pcDNA3.1(+) vector

(A) Picture of an agarose gel showing a single clone of pcDNA3.1(+)-*Pax3* that contains the *mycer*™ insert.

(B) Two possible orientations of the *mycer*™ insert in the pcDNA3.1(+)-*Pax3* construct.

As illustrated in figure 6.2B, the *mycer*™ cDNA can insert into the pcDNA3.1(+) vector in either of two orientations. To check whether *mycer*™ had been cloned into pcDNA3.1(+) in the correct orientation in clone 6, the DNA was digested with XhoI. This enzyme has no restriction sites in *Pax-3* or *c-myc*. However, it has one site in the vector that is located at the 3' end of the multiple cloning site. There is also a single XhoI site in the *er*™ sequence, 650 bases from the 3' end. Therefore if *mycer*™ were in the correct orientation, then complete digestion with XhoI would produce a 680 base pair insert band. However, if *mycer*™ were in the wrong orientation an insert band of 1680 base pairs would be produced. As shown in figure 6.3, digestion of clone 6 with XhoI produced a band on the agarose gel between the 500 base pair and 1000 base pair marker bands. This result showed that in clone 6 the *mycer*™ insert was in the correct orientation with respect to *Pax-3* in the pcDNA3.1 (+) vector.

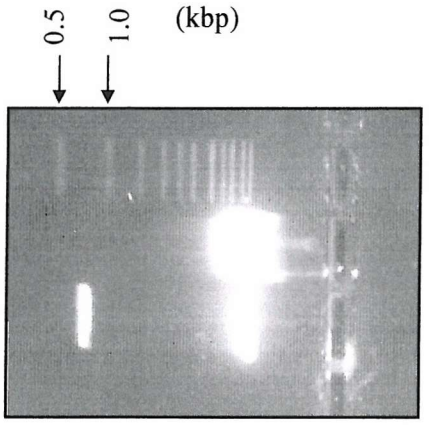

Fig. 6.3 Picture of an agarose gel showing a clone of pcDNA3.1(+)-*Pax3-mycer*™ that contains the *mycer*™ insert in the correct orientation

Having produced a construct in which *mycer*™ was fused to *Pax-3* in the pcDNA3.1(+) vector, the next step was to remove the *c-myc* cDNA so as to leave the *Pax-3* coding region fused directly to the coding region for the ligand binding domain of ER. It was essential that *er*™ be linked to *Pax-3* in frame in order to produce the Pax3ER™ fusion protein. For the same reason the translation stop codon (TAG) at position 1734 of the *Pax-3* cDNA could not be included in the *Pax3er*™ construct. Therefore the *c-myc* cDNA was removed using the restriction enzymes EcoNI and BamHI. The EcoNI site occurs at position 1685 of the *Pax-3* cDNA. This is the closest restriction site to the *Pax-3* translation stop codon. The BamHI site separates the *myc* and *er*™ sequences, as shown in figure 6.4. After being digested with BamHI and EcoNI, the *Pax3-myc-er* DNA was blunt-ended. Religating the plasmid then allowed *er*™ to be joined in frame to *Pax-3*. This *Pax3er*™ construct codes for a Pax3-ER™ protein that contains the entire ligand-binding domain of the ER and all but the last 16 amino acids of Pax-3.

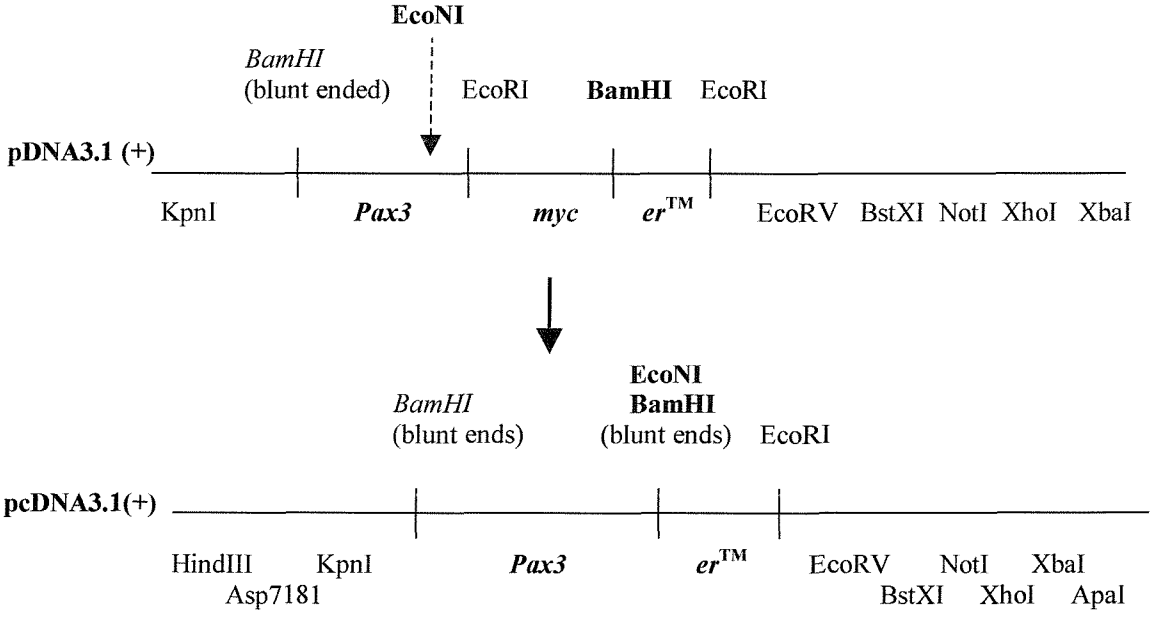

Fig. 6.4 Cloning of *Pax3* – *er*™ in the pcDNA3.1(+) vector

To confirm their identity, two individual *Pax3er*™ clones were digested first with HindIII and then with XhoI. The locations of these restriction sites in the *Pax3er*™ construct as well as the results of the restriction digests are shown in figure 6.5. Following digestion with HindIII and XhoI, both clones produced inserts of 650 base pairs, 770 base pairs and 920 base pairs. The sizes of these inserts are those expected when *Pax3er*™ is digested with HindIII and XhoI, as shown in the diagram at the top of figure 6.5. The two clones also produced an insert of 1.7 kbp when cut with HindIII and XhoI. This is probably due to partially cut DNA from the initial HindIII digest, which has then been completely cut by XhoI. Cutting at the HindIII site in the vector and at the XhoI site in *er*™ would produce a 1.7 kbp DNA fragment. Thus it was concluded that two individual clones of *Pax3 er*™ in pcDNA3.1 (+) had been isolated.

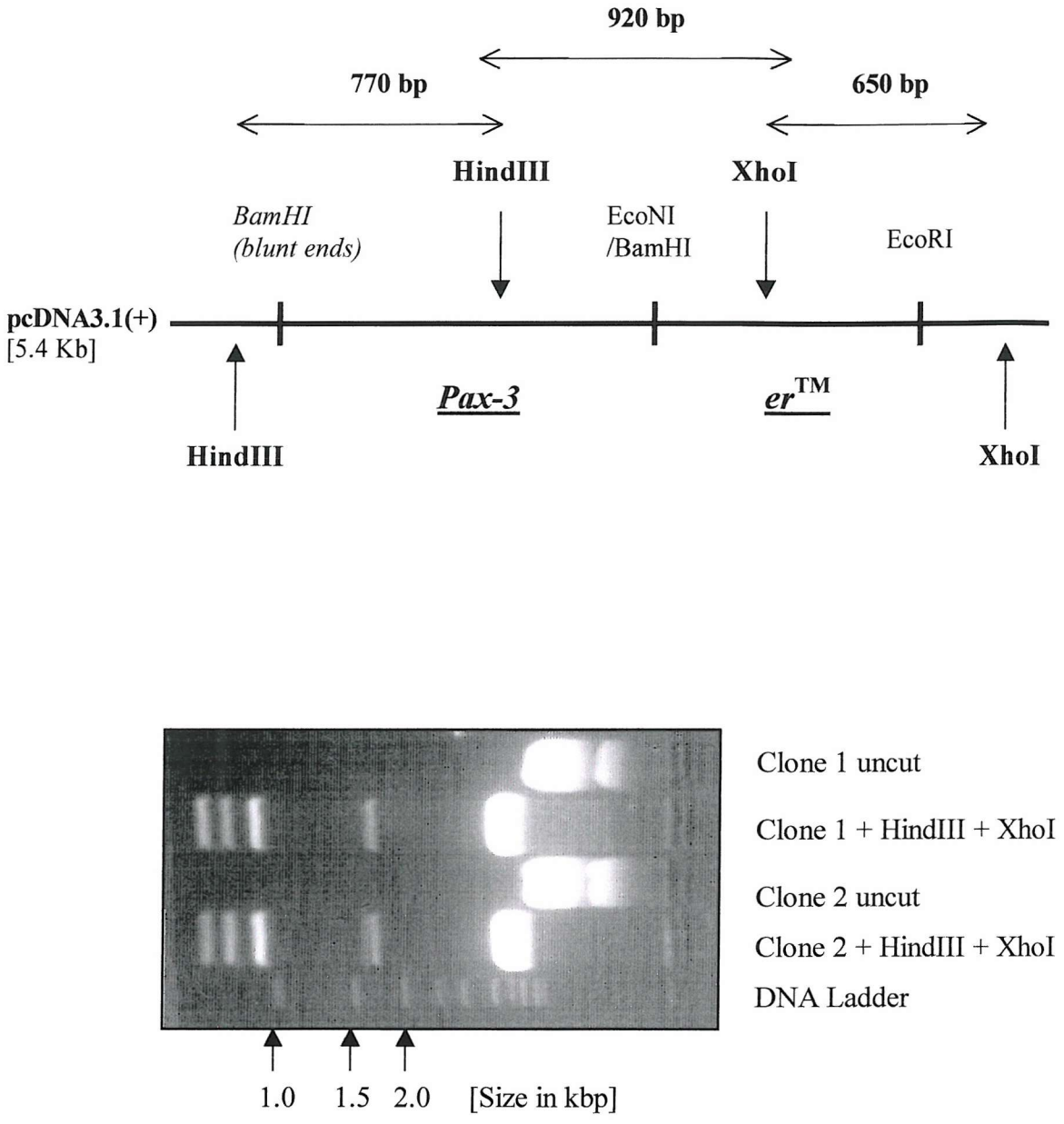

Fig. 6.5 Restriction mapping of *Pax3er*™

The diagram at the top shows the positions of the XhoI and HindIII sites in the *Pax3er*™ construct. The agarose gel picture at the bottom shows the result of digesting two separate clones of *Pax3er*™ with HindIII and XhoI.

6.2.2 Expression of Pax3ER™ in ND7 Cells

ND7 cells were stably transfected with either 5 μg of pcDNA3.1-*Pax3-er* DNA or 5 μg of the pcDNA3.1 empty expression vector. Stable transfectants were selected by supplementing the medium, 48 hours after transfection, with 800μg/ml G418. The neomycin resistance gene in the pcDNA3.1 vector permits only cells that have taken up the plasmid to grow in the presence of G418. Independent clones were selected after 1-2 weeks, when individual foci of cells were evident. These cells were grown up and maintained in medium containing 800μg/ml G418. In this way two Pax3ER™ cell lines (ER1 and ER2) and one vector control cell line (V1) were established.

6.2.3 Western Blot with anti-Pax3 antibody

It was important initially to determine whether the Pax3ER™ fusion protein was expressed in the two established cell lines. Therefore cells from the ER1 and ER2 cell lines as well as V1 cells were incubated in the presence and absence of OHT (0.25 μM) for 8 hours. Cells were then harvested and nuclear extracts made from them. These nuclear extracts were used in a Western blot using an antibody raised against the paired domain of Pax-3. Total protein levels were the same for each sample as determined by BCA protein assay. In addition staining the nitrocellulose membrane after the Western blot showed that approximately equal amounts of protein had been transferred from the protein gel to the membrane. Figure 6.6 shows an autoradiograph of the Western blot, probed with the Pax-3 antibody.

A band at 55-60 kDa was present in all V1 and ER lanes. This represents endogenous Pax-3 that is expressed in dividing ND7 cells. A larger protein of 85-90 kDa was also detected in the ER cells that had been treated with OHT, but not in the untreated ER cells

or in either treated or untreated V1 cells. This 85-90 kDa band is the expected size for the Pax3-ER™ protein. The fact that Pax3ER™ was only detected in nuclear extracts of cells treated with OHT suggested that treatment with 4-hydroxyamoxifen had resulted in the translocation of Pax3ER™ to the nucleus. A more intense Pax3ER™ band was seen in extracts from ER2 cells that had been treated with OHT than in treated ER1 cells, suggesting that expression of Pax3ER™ was higher in the ER2 cell line.

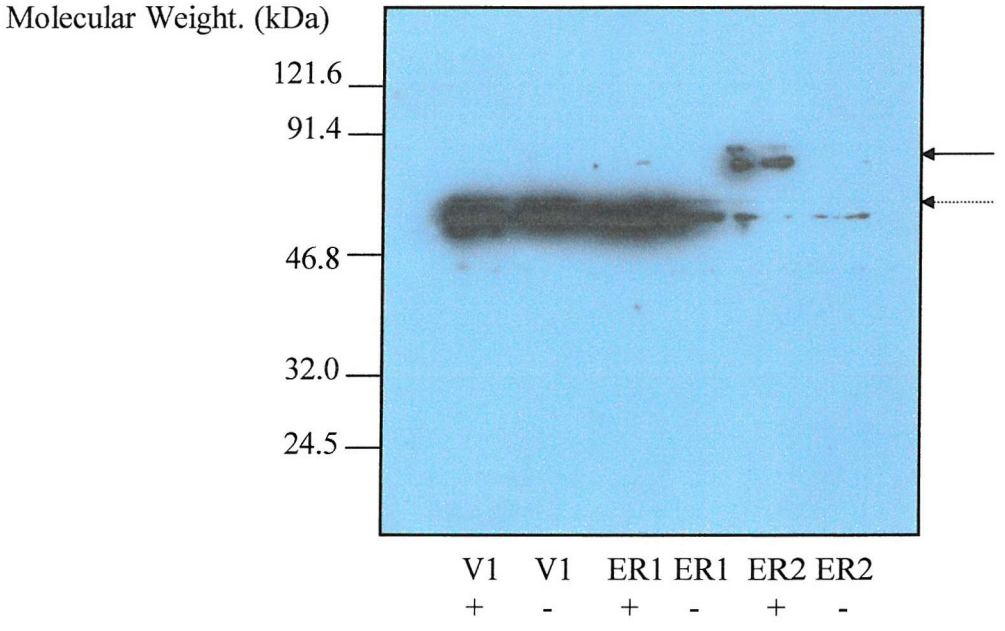

Fig. 6.6 Western blot carried out on nuclear extracts from vector control (V1) and Pax3ER™ (ER1 and ER2) cell lines using an anti-Pax3 antibody

V1, ER1 and ER2 cells were either treated with 4-hydroxyamoxifen for 8 hours or left untreated for the same length of time prior to harvesting. The + and – signs refer to the treatment of cells with 4-hydroxyamoxifen. The location of the Pax3ER™ on the autoradiograph is marked with an arrow. A dashed arrow shows the location of endogenous Pax-3.

6.2.4 Activation of Pax3-ER™ in dividing ND7 cells

To determine what effect the activation of Pax3-ER™ has on ND7 cell growth, the rate of cell growth was compared in the ER2 and V1 cell lines, in the presence and absence of OHT. Cells were grown on 6 well plates for 4 days in complete growth medium containing 10% serum. Cells were harvested every 24 hours and the number of live and dead cells was counted using the Trypan Blue exclusion assay. Each day fresh media was added to the cells and the OHT was replaced. The results are shown in figure 6.7.

Cells expressing both endogenous Pax-3 and Pax3ER™ displayed similar growth rates to those cells that expressed only endogenous Pax-3, as shown by the fact that the number of live cells increased at approximately the same rate for the ER2 and V1 cell lines. Moreover OHT did not significantly affect either the growth of ER2 cells or V1 cells. The rate of cell death also appeared to be very similar for ER2 and V1 cells that were grown in the presence of 10% serum, irrespective of whether OHT was applied to the cells.

In the ER2 cell line, the expressed Pax3-ER™ protein translocated to the nucleus only when the ND7 cells were treated with OHT. The activity of Pax3-ER™ in terms of its ability to activate transcription is also likely to be regulated by OHT. However, in ND7 cells grown in the presence of 10% serum, OHT did not significantly affect the growth rate of Pax3ER™ expressing cells.

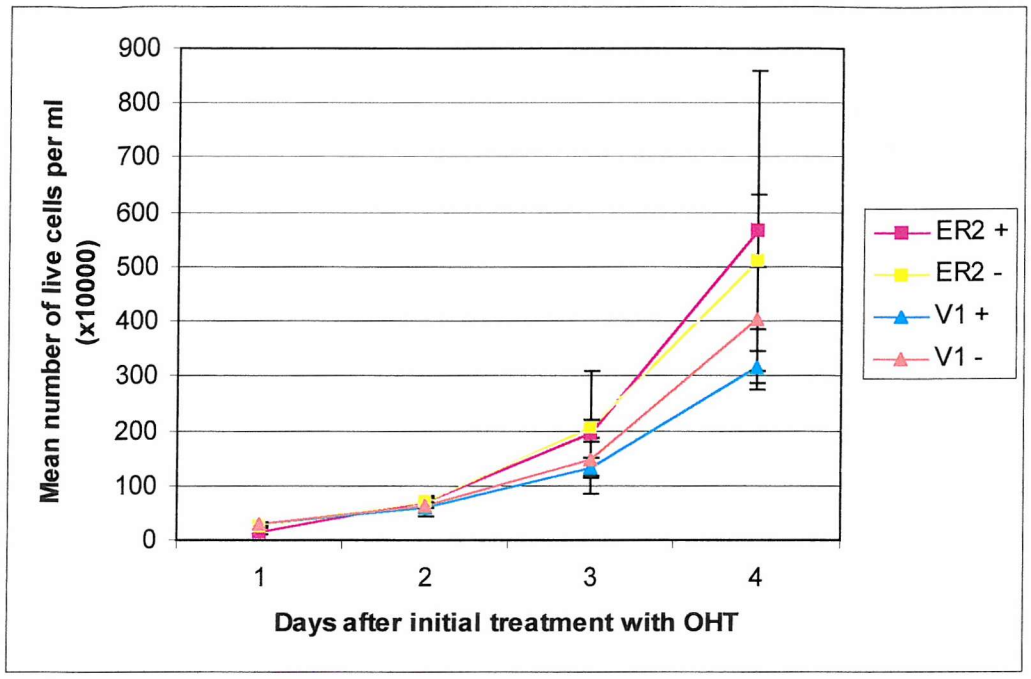

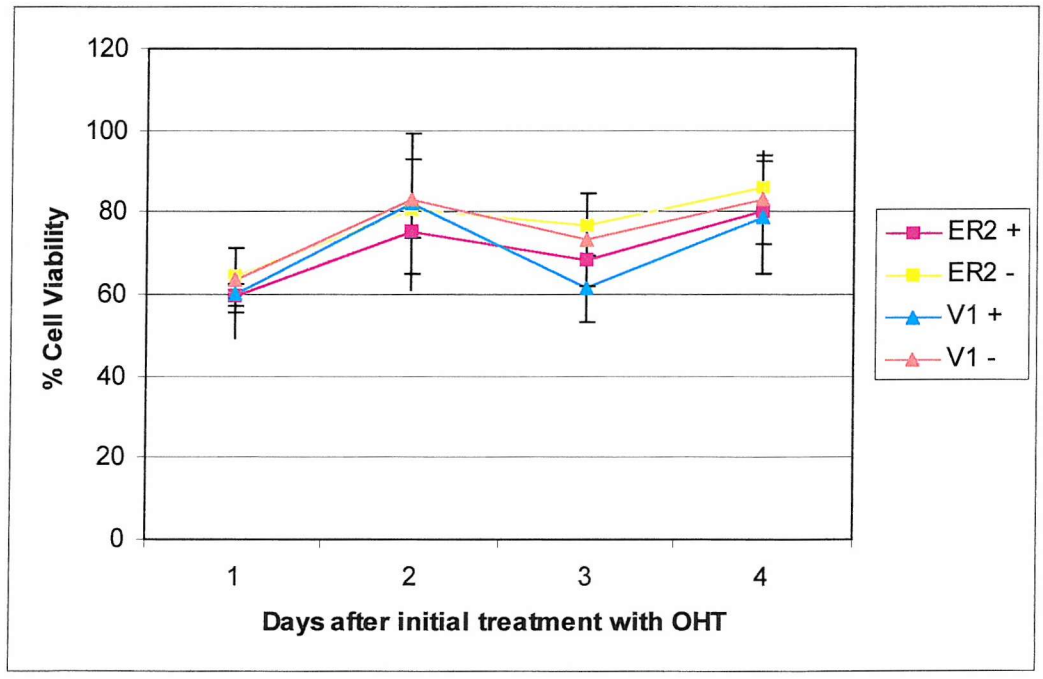

Fig. 6.7 4-day growth experiment with ER2 and V1 cell lines that were grown in the presence of 10% serum with (+) or without (-) OHT

Using the Trypan blue exclusion assay, the mean number of viable (live) cells was counted at each time point. The number of viable cells at each time point was also expressed as a percentage of the total cells number (% cell viability).

6.2.5 Activation of Pax3-ER™ in serum starved ND7 cells

The Myc transcription factor is expressed in dividing cells, and is downregulated upon cell differentiation. Genes activated by Myc have been shown to stimulate cell proliferation (Hopewell *et al.*, 1995). In addition, like Pax-3, Myc has been implicated in tumourigenesis, with high levels of N-Myc being expressed in neuroblastomas (Niethammer *et al.*, 1995). Over-expressing exogenous Myc protein in dividing cells that are already expressing high levels of endogenous Myc, has been shown to have little effect on cell growth. This was suggested to occur because Myc target genes that promote cell proliferation are saturated by endogenous Myc, and so exogenous Myc protein is unable to stimulate any further increase in cell proliferation. However, when proliferating fibroblast cells are deprived of serum they cease to express endogenous Myc and exit the cell cycle. Activation of the Myc-ER™ protein in these quiescent cells is sufficient to drive them back into the cell cycle, but also induces cell death by apoptosis (Littlewood *et al.*, 1995). It had previously been shown by Evan *et al.* (1992) that over-expression of exogenous Myc protein in serum-deprived fibroblasts causes some of these cells to re-enter the cell cycle and divide, whereas other cells in the population immediately undergo apoptosis. In the cells that continue to proliferate, the absence of mitogens in the growth medium eventually leads to cell cycle arrest, followed by Myc-induced apoptosis.

As *Pax-3* is expressed at high levels in dividing ND7 cells, the failure of Pax3-ER™ to exert any effects on cell growth in ER2 cells that were cultured in the presence of 10% serum, may have been because Pax-3 target genes were already saturated by endogenous Pax-3. However, in the absence of serum Pax-3 is rapidly downregulated, and the ND7s undergo cell cycle arrest. Therefore to investigate whether Pax3-ER™ could affect the

growth of ND7 cells that had been serum starved, ER2 and V1 cells were growth arrested by culturing them in serum-free medium for 24 hours. The cells were then maintained in serum-free medium in the presence or absence of OHT, before being harvested and used in Trypan Blue exclusion assays to count the number of live and dead cells. The results are shown in figure 6.8.

In the ER2 cell line, 18 hours after treating the cells with OHT, the growth rate was slightly lower than in untreated ER2 cells. In addition, the viability of ER2 cells cultured in the presence of OHT decreased steadily and by 18 hours was considerably lower than that of untreated ER2 cells. In contrast, both OHT-treated and untreated V1 cells showed very similar growth rates and cell viabilities throughout. The reduced cell viability of serum starved ER2 cells in the presence of OHT suggests that Pax3-ER™ may induce cell death in ND7 cells that have been deprived of mitogens and are no longer able to proliferate. This would also explain why the growth rate of serum starved ER2 cells that had been treated with OHT was slightly lower than that of untreated ER2 cells.

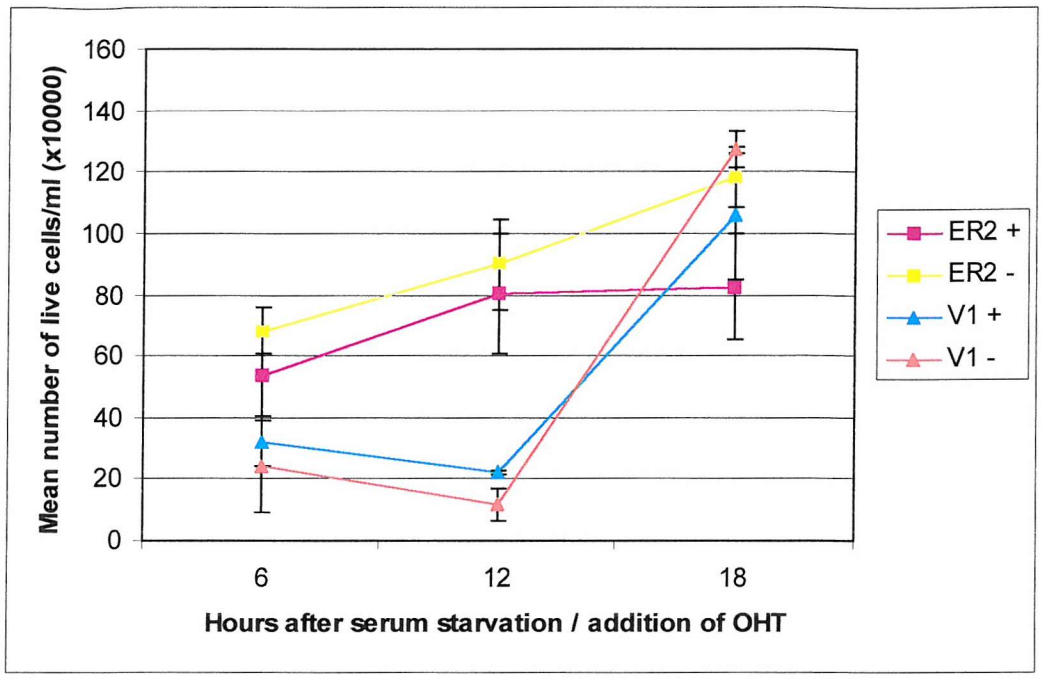

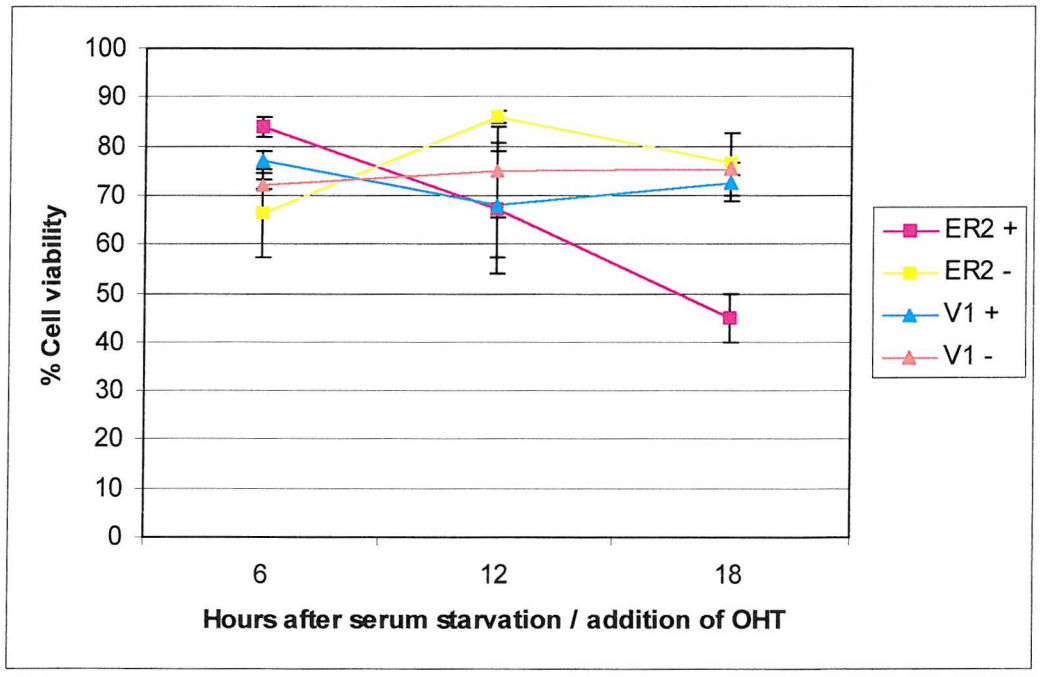

Fig. 6.8 Growth experiment for ER2 and V1 cell lines cultured in serum-free medium for increasing amounts of time in the presence (+) or absence (-) of 4-hydroxytamoxifen

ND7 cells were growth arrested by culturing them in the absence of serum for 24 hours. The cells were then maintained in serum-free medium, with or without OHT, and cell counts were carried out at each of the times points shown, as described in figure 6.7.

6.2.6 Transactivation potential of Pax3ER™

The activation of Pax3-ER™ in serum starved ND7 cells that are devoid of endogenous Pax-3, led to an increased rate of cell death. Therefore in order to determine whether the Pax3ER™ protein is transcriptionally active in these cells, its ability to activate transcription of a reporter gene construct containing an e5-binding site upstream of a minimal promoter was studied. To achieve this ER2 and V1 cells were transiently transfected with either pBL2CAT plasmid DNA alone or e5-CAT DNA. The cells were treated with OHT for 24 hours or left untreated for the same amount of time. Cell lysates made from these cells were then used in CAT assays. A representative CAT assay is shown in figure 6.9. As expected basal levels of transcription were observed in ER2 and V1 cells that had been transfected with the pBL2CAT vector alone. However, the level of CAT activity produced from the e5-CAT transfection was very low, indicating a low level of expression and/or low levels of transfection efficiency. Repeated experiments did not result in increased expression or transfection efficiency. Therefore from these experiments it was very difficult to determine whether Pax3-ER™ is transcriptionally active as no activation of transcription was observed in the presence or absence of OHT.

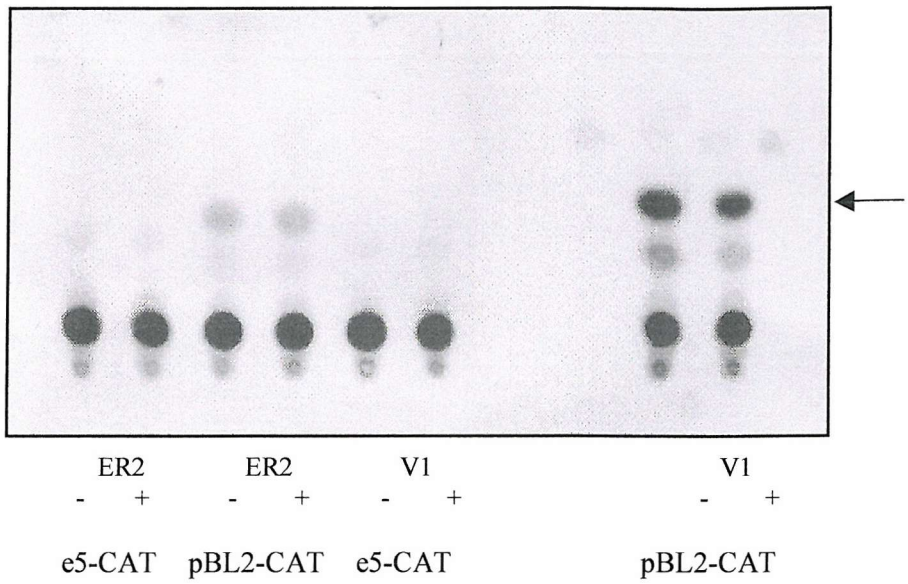

Fig. 6.9 CAT assay of ER2 and V1 cell lines that had been transiently transfected with e5-CAT or pBL2CAT alone

The + and – signs refer to the treatment of cells with OHT. The arrow marks the position of the acetylated chloramphenicol.

6.2.7 Cloning of a second Pax3ER™ construct

As the expressed Pax3-ER™ protein lacked the last 16 amino acids of Pax-3, its transactivation function may be impaired as Chalepakis *et al.* (1994) have shown that the last 78 amino acids at the C-terminus of Pax-3 constitute the transactivation domain of the protein. Therefore a second *Pax3er*™ construct was cloned that coded for the entire Pax-3 protein. This was achieved using PCR to amplify up the coding region for the last 16 amino acids of Pax-3, as illustrated in figure 6.10. The *Pax-3* PCR product was subsequently cloned into pGEMT-Easy. It was then cut out of this vector using EcoNI and BamHI, and ligated in between the *Pax-3* and *er*™ sequences of the first *Pax3er*™ construct, as illustrated in figure 6.11.

The new *Pax3er*™ construct codes for a fusion protein in which the last amino acid of Pax-3 is changed from a Phe to a Leu. However this protein will still contain 15 amino acids at the C-terminus of Pax-3 that were absent in the previous Pax3-ER™ protein. Restriction mapping was used to confirm the identity of the new *Pax3er*™ clone. The construct was digested first with HindIII and then with XhoI. Aliquots of the restriction digests were run out on an agarose gel. The locations of the restriction sites as well as the results of the restriction digests are shown in figure 6.12. As predicted complete digestion of the DNA with HindIII and XhoI produced bands on an agarose gel of 650, 770 and 970 base pairs. This showed that a second *Pax3er*™ construct, which coded for all but the last amino acid of Pax-3, had been isolated.

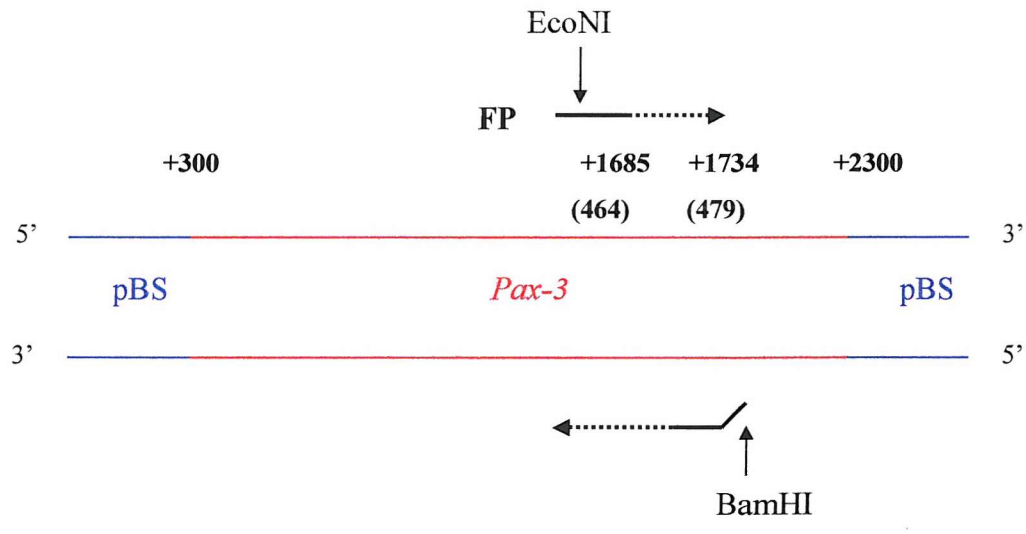

Fig. 6.10 PCR method to amplify the region of *Pax-3* cDNA that codes for the last 16 amino acids of the Pax-3 protein

Pax-3 cDNA from the EcoNI site to the translation stop codon were amplified by PCR, using the pBS-*Pax3* clone as a template There is an EcoNI site in the forward primer, and a BamHI site at the 5' end of the reverse primer. The + and – signs refer to positions in the *Pax-3* cDNA sequence. The corresponding amino acids are shown in brackets.

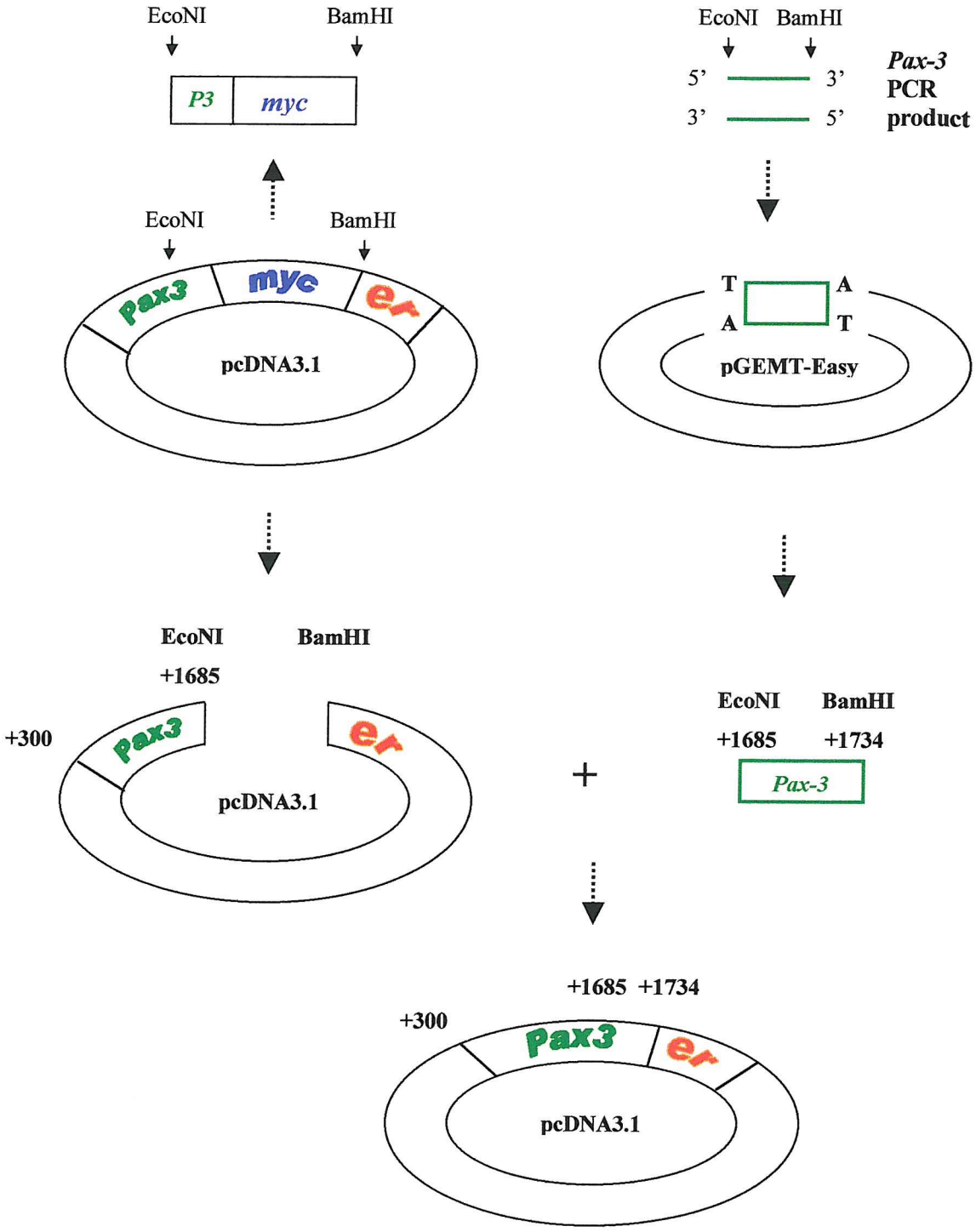

Fig. 6.11 Summary of the steps used to clone a *Pax3er*™ construct that contains the entire coding region of Pax-3

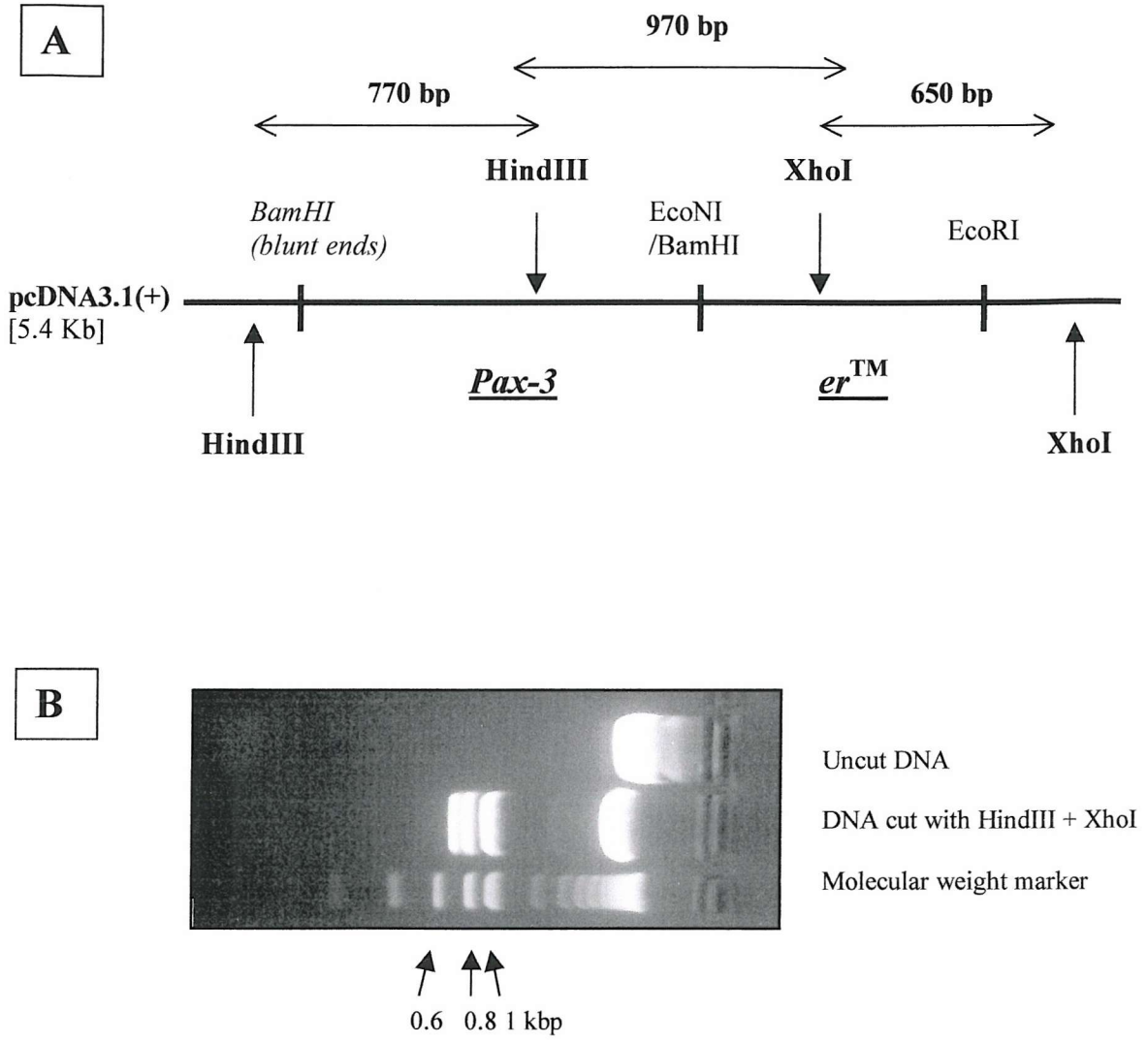

Fig. 6.12 Restriction mapping of the second *Pax3er*™ construct

(A) Locations of the HindIII and XhoI restriction sites in the *Pax3er*™ cDNA sequence.

(B) Agarose gel to show the result of cutting the new *Pax3er*™ construct with HindIII and XhoI.

Time restrictions meant that stable cell lines expressing the second Pax3-ER™ protein could not be established. It will be interesting to compare the effect on cell growth and viability of this second Pax3-ER™ protein, which codes for all but the last amino acid of Pax-3, with that of the first Pax3-ER™ protein, which lacks the last 16 amino acids of Pax-3. The transactivation function of both constructs should also be compared.

6.3 Identification of Pax-3 regulated genes in neuronal cells

6.3.1 Introduction

Another approach that has been used to investigate the function of Pax-3, involves the expression of antisense *Pax-3* RNA in cells that express the Pax-3 protein. To achieve this, *Pax-3* cDNA is inserted into an expression vector in the antisense orientation, which is then transfected into Pax-3 expressing cells. The antisense RNA subsequently expressed in these cells binds to the *Pax-3* mRNA by complementary base pairing, forming an RNA duplex. RNase H, a double strand specific nuclease, degrades this RNA duplex, thus inhibiting translation of the *Pax-3* mRNA. An inducible promoter in the expression vector is used to control the expression of the antisense *Pax-3* RNA, and thus regulate the expression of the Pax-3 protein. Using this technique, the expression of candidate Pax-3 target genes can be studied in response to the specific down-regulation of Pax-3. This method will not show whether the expression of such genes is regulated directly by Pax-3. However, when used in conjunction with the Pax3-ER™ approach, this technique could lead to the identification of direct Pax-3 target genes *in vivo*.

6.3.2 Construction of an antisense *Pax-3* neuronal cell line

An antisense *Pax-3* expression vector was constructed by Emma Phillips, and stably transfected into the neuroblastoma cell line Kelly. To achieve this, the 2347bp *Pax-3* cDNA from the pBS II SK (-) vector was cloned into the pJ4Ω expression vector in the antisense orientation. This expression vector was then cotransfected into Kelly cells with pcDNA3.1, which has the neomycin resistance gene for selection in media containing G418. Treatment of the antisense *Pax-3* Kelly cells with dexamethasome induced expression of antisense RNA from the pJ4Ω expression vector, leading to a reduction in endogenous Pax-3 protein levels. Antisense *Pax-3* Kelly cells (as1) that had been treated

with dexamethasome grew more slowly than untreated as1 cells. They also grew more slowly than both treated and untreated vector control cells, which had been stably transfected with an empty expression vector. The reduced growth rate of the treated as1 cells was due to both a reduction in cell proliferation and an increased rate of cell death. Bernasconi *et al.* (1996) showed that in alveolar rhabdomyosarcoma cells, down-regulation of the PAX3-FKHR fusion protein using antisense oligonucleotides resulted in increased cell death by apoptosis. In addition in embryonal rhabdomyosarcoma cells that express wild type PAX3 protein at elevated levels, down-regulation of PAX3 also resulted in increased cell death by apoptosis. In the as1 Kelly cell line, it is thought that apoptosis may have accounted for the increased cell death that occurred in response to the down-regulation of Pax-3 in these cells.

In an attempt to discover novel molecular targets for Pax-3, the levels of mRNA and protein expressed from potential target genes were compared in the presence and absence of antisense *Pax-3* RNA using the as1 and vector control Kelly cell lines. Candidate target genes were selected on the basis of their overlapping patterns of expression with Pax-3 in neuronal cells.

6.3.3 Expression of *Rb* mRNA in Kelly cells

As previously described, the Retinoblastoma protein (RB) is a negative regulator of the cell cycle, which has been shown to interact with Pax-3 in living cells. Like Pax-3, RB is expressed in dividing neuronal and muscle cells, and RB protein levels have been shown to increase as cells pass from G_1 into S phase, and then on through the cell cycle (Mihira *et al.*, 1989). Therefore the potential for Pax-3 to affect the expression of *Rb* mRNA in Kelly cells was investigated. This was achieved by treating antisense *Pax-3* Kelly cells (as1) as well as vector control cells with 1μM dexamethasome for 24 hours. The cells were then harvested and total RNA prepared from them. 1μg of this RNA was used to prepare cDNA using reverse transcriptase (RT). The cDNA was then amplified using Taq DNA polymerase with specific primers for *Rb* and *Cyclophilin*. The PCR conditions in which the input cDNA was linearly proportional to the PCR product was initially established for the *Cyclophilin* and *Rb* primers by taking aliquots at 25, 30 and 35 cycles. On the basis of these results, one tenth of the cDNA samples from both the as1 and vector control cells was amplified for 30 cycles with the *Cyclophilin* primers, and for 30 cycles with the *Rb* primers. A 30 cycle negative control PCR was also carried out, in which sterile water was used in place of the cDNA.

As shown in figure 6.13, the *Cyclophilin* PCR product resulted in a band of equal intensity in the as1 and vector control lanes of an agarose gel, indicating that total cDNA levels were the same for each cell type. Similarly there was no difference in the intensities of the *Rb* PCR products from the as1 and vector control cells when analysed on the agarose gel. Thus *Rb* mRNA expression in Kelly cells was unaffected by the expression of antisense *Pax-3* RNA in these cells. This suggests that Pax-3 does not affect the expression of *Rb* mRNA in Kelly cells.

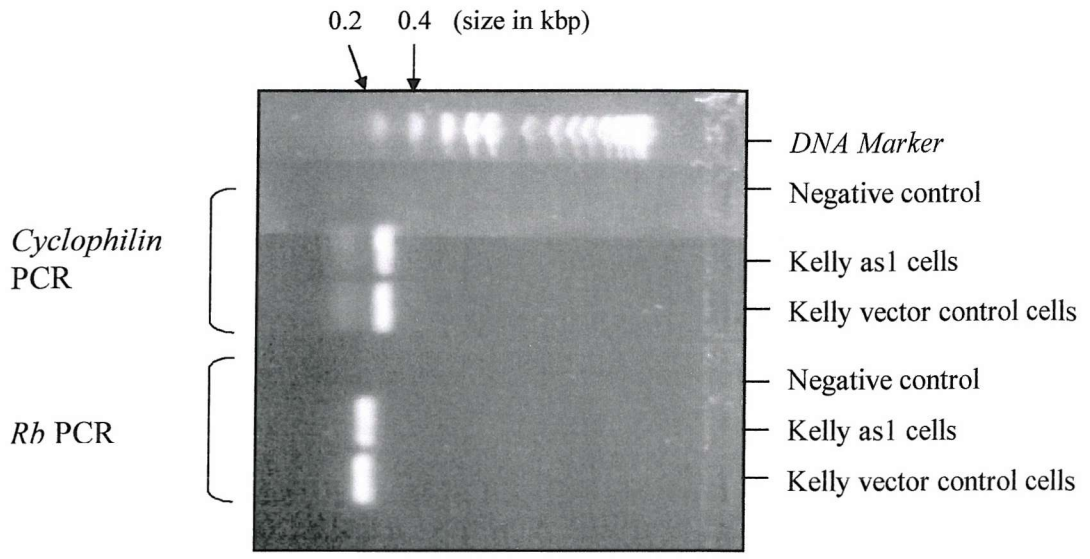

Fig. 6.13 RT-PCR to compare the expression of *Rb* mRNA in the presence and absence of antisense *Pax-3* RNA

Complementary DNA derived from as1 Kelly cells that had been induced to express antisense *Pax-3* RNA, as well as from vector control cells, was used in RT-PCR assays. The *Cyclophilin* and *Rb* PCR products from both as1 and vector control cells were analysed on a 1.2% agarose gel.

6.3.4 Expression of *PPARγ* mRNA in Kelly cells

PPARs (Peroxisome Proliferator-activated Receptors) are members of the nuclear receptor superfamily, which function as ligand activated transcription factors. The γ isoform of PPAR is activated by $15dPGJ_2$ and synthetic ligands in a range of cancer cell lines, resulting in growth arrest and the induction of either cell differentiation or apoptosis (Clay *et al.*, 1999). The level of PPARγ expression varies between different

types of neuroblastoma cells, with high levels of PPARγ expressed in differentiated tumours, and lower levels of PPARγ in tumours that contain dividing neuroblasts (Han *et al.*, 2001). Therefore, because of the association between PPARγ and differentiated neuroblastomas, the level of *PPARγ* mRNA expression was examined in the antisense *Pax-3* Kelly cell line.

RT-PCR was used to study the expression of *PPARγ* mRNA in as1 and vector control Kelly cells that had been cultured in the presence of 1μM dexamethasome for 24 hours. One tenth of the cDNA samples derived from both as1 and vector control cells, was amplified for 30 cycles with the *Cyclophilin* primers. One quarter of the cDNA from both cell types was amplified for 35 cycles with the *PPARγ* primers. The *Cyclophilin* PCR products in the as1 and vector control lanes of the agarose gel were of equal intensity, indicating that total cDNA levels were the same for each cell type (figure 6.14A). Bands of equal intensity were also seen in the as1 and vector control lanes for the *PPARγ* PCR assay (figure 6.14B). This showed that the expression of antisense *Pax-3* RNA in Kelly cells did not alter the expression of *PPARγ* mRNA in this cell line. Therefore it appears that Pax-3 does not affect the expression of *PPARγ* in Kelly cells.

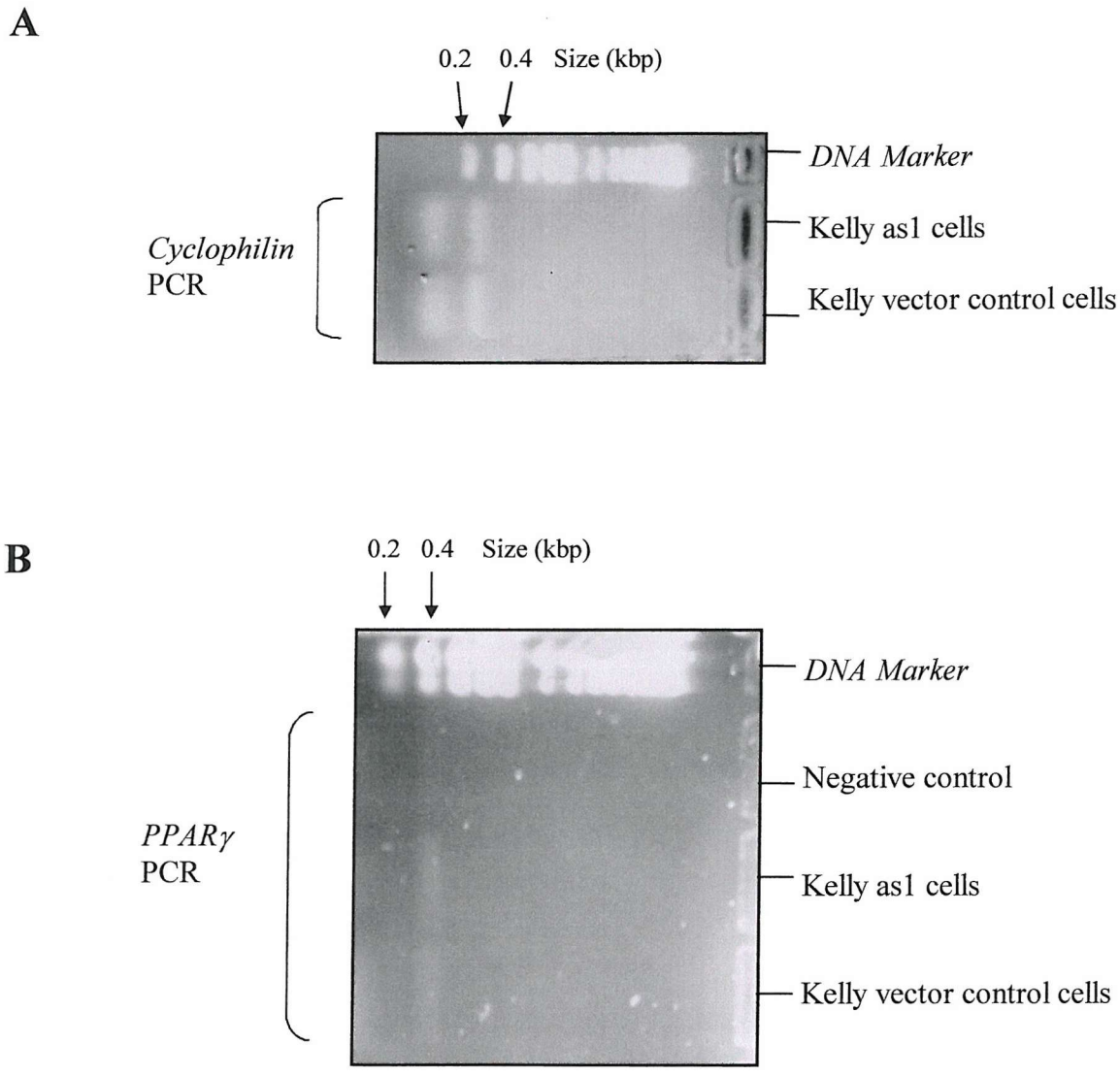

Fig. 6.14 RT-PCR to compare the expression of *PPARγ* mRNA in the presence and absence of antisense *Pax-3* RNA

Complementary DNA derived from as1 Kelly cells that had been induced to express antisense *Pax-3* RNA, as well as from vector control cells, was used in RT-PCR assays. The *Cyclophilin* **(A)** and *PPARγ* **(B)** PCR products from both as1 and vector control cells were analysed on a 1.2% agarose gel.

6.3.5 Expression of the N-Myc protein in Kelly cells

The Myc family of proteins are basic helix-loop-helix / leucine zipper transcription factors. They bind to DNA as dimers, recognising the E box sequence element (CANNTG) in the promoters of their target genes. When overexpressed in fibroblast cells in tissue culture, the c-Myc protein was shown to induce cell transformation, leading to growth of these cells in soft agar (Small *et al.*, 1987). In low serum conditions c-Myc also induces apoptosis in fibroblast cells. In serum-deprived fibroblasts expressing a Myc-ER™ fusion protein, treatment with OHT led to an increased rate of apoptotic cell death. This effect was dependent upon a functional c-Myc protein (Littlewood *et al.*, 1995). Thus the *myc* proto-oncogene has been implicated in apoptosis, as well as cell proliferation and transformation.

N-Myc is expressed in the developing spinal cord, neural crest and muscle, where it functions as an important regulator of cell proliferation and differentiation. In addition N-Myc is expressed at high levels in neuroblastoma cells. As N-Myc expression overlaps with that of Pax-3 during development, to determine whether Pax-3 could affect the amount of N-Myc protein expressed in neuronal cells, N-Myc levels were compared in vector control and as1 Kelly cells. In each case nuclear extracts were made from cells that had been grown in the presence of 1μM dexamethasome for 24 hours, or left untreated for the same amount of time. For each nuclear extract, equal amounts of protein were resolved by 10% SDS-PAGE and transferred to a nitrocellulose membrane, before being probed with an antibody that specifically recognises the N-Myc protein. An autoradiograph of this Western blot is shown in figure 6.15A. A band of 55-60 kDa can be seen in all 4 lanes of figure 6.15A, which represents the N-Myc protein. The N-Myc band is of equal intensity in the treated and untreated vector control lanes, as well as the

untreated as1 lane. However, this band is of higher intensity in the treated as1 lane. As shown in figure 6.15B, staining the nitrocellulose membrane following protein transfer confirmed that the total protein levels in each extract were approximately the same. Therefore it appears that the level of N-Myc protein in the treated as1 Kelly cells was higher than in the untreated as1 cells and vector control cells. This suggests that down-regulation of Pax-3 in Kelly cells in response to the induction of antisense *Pax-3* RNA leads to an increase in the level of nuclear N-Myc protein.

A

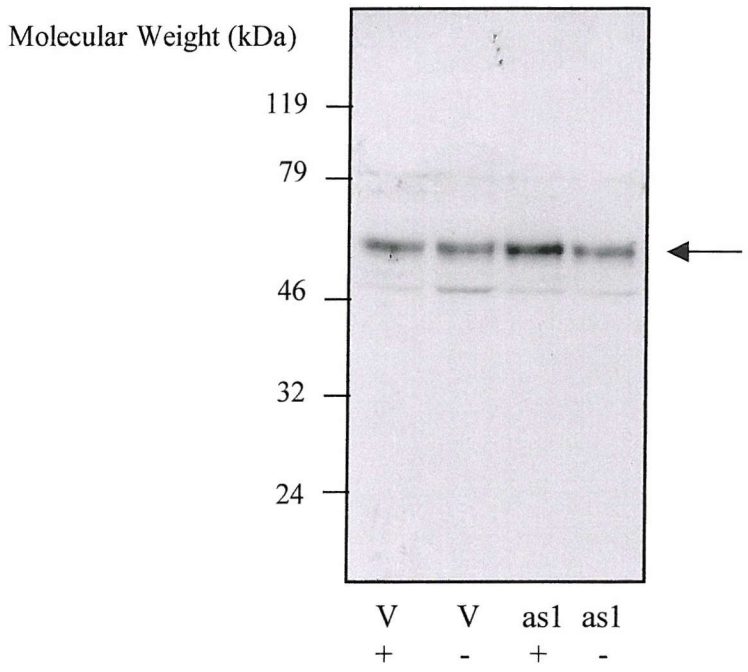

B

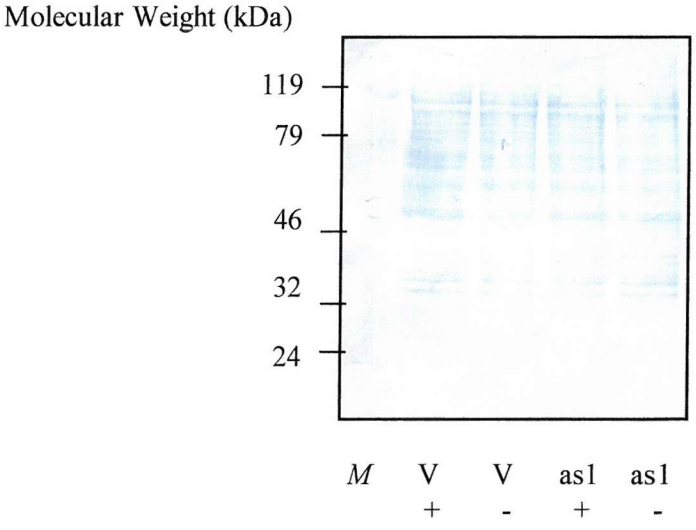

Fig. 6.15 N-Myc Western blot of as1 and vector control Kelly nuclear extracts

(A) Autoradiograph of the Western blot, with the location of the N-Myc band marked by an arrow. V, vector control, + and – signs refer to treatment of cells with dexamethasome.

(B) Picture of stained membrane following protein transfer. *M*, molecular weight marker.

6.4 Discussion

Pax-3 is an embryonic transcription factor that has been shown to act during development to help maintain progenitor cells in a dividing state and prevent the onset of morphological differentiation until the appropriate signals are received. Pax-3 is also capable of promoting cell survival by inhibiting apoptosis. Since few direct target genes for Pax-3 have been discovered to date, we have attempted to uncover novel molecular targets for this transcription factor. Firstly a Pax3-ER™ fusion protein was cloned and expressed in ND7 cells. The nuclear localisation of this protein could be regulated by treatment with 4-hydroxytamoxifen (OHT). It was hoped that by fusing Pax-3 with the ligand-binding domain of the ER, the transactivation function of Pax-3 would also be rendered hormone-dependent. Such an effect has previously been demonstrated for a range of other transcription factors including c-Myc, as well as for a KRAB-PAX3 fusion protein in ARMS cell lines. This approach facilitates the study of hormone-dependent changes in biological properties such as cell growth, as well as changes in gene expression. Moreover, it can be used to identify direct target genes for the transcription factor being studied.

Growth experiments in dividing ND7 cells showed no difference between the growth rates of ER2 and V1 cell lines in the presence or absence of OHT. It has been suggested that Pax-3 can promote cell survival during embryogenesis by inhibiting p53-induced apoptosis in the developing neural tube (Pani *et al.*, 2002). In addition Pax-3 may also promote the survival of cancer cells by protecting them from apoptosis (Bernasconi *et al.*, 1996). However in serum starved ND7 cells, 18 hours after growth arrest, the ER2 cells that had been cultured in the presence of OHT, showed a lower rate of cell growth

than untreated ER2 cells and V1 cells. This coincided with an increased rate of cell death in the OHT-treated ER2 cells.

The Myc-ER™ protein has previously been shown to induce similar effects in serum-deprived fibroblasts (Littlewood *et al.*, 1995). Like Pax-3, Myc is expressed in mitotically active cells and is downregulated upon cell differentiation. Therefore in serum-deprived cells Myc-ER™ is thought to induce cell proliferation but, due to the lack of mitogens in the growth medium, it also promotes cell death by apoptosis. The cells that continue to progress through the cell cycle when Myc-ER™ is activated, are likely to eventually undergo growth arrest, followed by Myc-induced apoptosis. Pax-3 may exert similar effects on serum-deprived ND7 cells. Thus, in the absence of endogenous Pax-3, the Pax3-ER™ protein may regulate the expression of Pax-3 target genes, resulting in an increased rate of cell death. When ND7 cells are grown in the presence of 10% serum, however, Pax-3 target genes may be saturated by endogenous Pax-3, which is expressed at high levels in dividing ND7 cells. This could prevent Pax3-ER™ from exerting any cellular effects on dividing ND7 cells, as proposed for the c-Myc protein in dividing fibroblasts.

To confirm that the expressed Pax3-ER™ protein was transcriptionally active and to demonstrate that the transactivation function of Pax3-ER™ was hormone-dependent, the potential for Pax3-ER™ to activate transcription of a CAT reporter gene construct containing a single Pax-3 (e5) binding site was investigated. This proved inconclusive, however, since no signal was detected in CAT assays using the e5-CAT reporter construct, which may have been the result of poor transfection efficiency. To try and remedy this, a reporter construct could be designed that contains a series of six e5

binding sites upstream of the CAT reporter gene. This might give a stronger signal in response to Pax3-ER™, allowing the level of transcriptional activation to be compared between treated and untreated ER2 cells. It is also possible that the transactivation function of the Pax3-ER™ protein is impaired because it is missing the last 16 amino acids of Pax-3. Chalepakis *et al.* (1994) showed that the last 78 amino acids at the C-terminus of Pax-3 constitute a transcription-activating domain. Therefore a second *Pax3-er*™ construct that codes for all but the last amino acid of Pax-3 was cloned. However, stable cell lines expressing this second Pax3-ER™ protein have yet to be created.

An antisense approach was also used to study genes whose expression might be regulated by Pax-3. In the neuroblastma cell line Kelly, expression of antisense *Pax-3* RNA significantly reduces the level of endogenous Pax-3 protein. This leads to the onset of morphological differentiation, a reduction in the rate of cell proliferation and an increased rate of cell death. The work described in this chapter used antisense *Pax-3* (as1) and vector control Kelly cell lines in RT-PCR assays and Western blots to compare mRNA and protein expression respectively from potential Pax-3 target genes. The aim of such experiments was to help demonstrate the function of Pax-3 in neuronal cells. This is of interest since few target genes have so far been discovered for Pax-3 in neuronal cells. In addition, the antisense approach could potentially be combined with the Pax3-ER™ method to determine whether the expression of a certain gene is regulated directly by Pax-3. Therefore candidate genes were selected whose expression patterns overlap with that of *Pax-3*. It was subsequently demonstrated that the levels of *Rb* mRNA were equivalent in as1 and vector control Kelly cells. Moreover the level of *Rb* mRNA remained unchanged in both as1 and vector control cells upon treatment with dexamethasome to induce expression of antisense *Pax-3* RNA. Similarly the levels of

PPARγ mRNA were the same in both as1 and vector control cells that had been treated with dexamethasome. This suggests that Pax-3 does not regulate the expression of either the *Rb* or *PPARγ* genes in Kelly cells.

The N-Myc protein is expressed at high levels in Kelly cells. The induction of antisense *Pax-3* RNA expression in these cells resulted in an increased level of nuclear N-Myc protein. However, it is not clear whether this effect is a direct one. To study this further, the N-Myc promoter could be analysed to see whether it contains any potential Pax-3 binding sites. If so, then a region of the promoter encompassing these sites could be cloned into a reporter plasmid and cotransfected into cells with a Pax-3 expression vector to see if Pax-3 could modulate N-Myc promoter activity. In addition, the Pax3-ER™ system could be used to complement this, and to show whether N-Myc represents a direct target gene for Pax-3.

N-*myc* has been implicated in the development of neurons that are derived from neural crest cells (Wakamatsu *et al.*, 1997). Comparing N-*myc* knockout mouse embryos with wild type embryos, revealed a significant reduction in the number of dorsal root ganglia and sympathetic ganglia, both of which contain neurons derived from neural crest. Endogenous N-Myc protein is expressed uniformly in migrating neural crest cells, but its expression later becomes restricted to and is transiently upregulated in neural crest cells that are destined to become neurons. *Pax-3* expression is also associated with proliferating migratory neural crest cells before the onset of differentiation. The similar expression patterns of N-Myc and Pax-3 in neural crest cells, suggests that either of these proteins could potentially affect the expression of the other one *in vivo*.

The increased levels of N-Myc protein in Kelly cells, in which Pax-3 has been downregulated, may be due to a post-transcriptional effect rather than a direct effect on N-*Myc* mRNA expression. This would be equivalent to the effect that reduced levels of Pax-3 have on the level p53 protein in the neural tubes of splotch embryos. The tumour-suppressor protein p53 promotes apoptotic cell death, thus inhibiting the growth of transformed cells *in vivo*. In addition p53 has been implicated in the control of apoptosis during embryogenesis. The lack of a functional Pax-3 protein in homozygous splotch mouse embryos results in the neural tube defects spina bifida and exencephaly. These defects are associated with enhanced apoptotic cell death in the dorsal part of the neural tube where *Pax-3* is expressed. It is thought that the lack of a functional Pax-3 protein in splotch may lead to problems with the development of cells in the neural tube, which in turn signals for p53 to induce apoptosis. In support of this, it has been shown that Pax-3 deficiency in splotch leads to increased levels of p53 protein in the mutant embryos (Pani *et al.*, 2002). This could potentially cause increased apoptosis in cells of the dorsal neural tube, preventing the neural tube from closing properly. Thus in normal embryonic development Pax-3 may function to prevent p53 induced-apoptosis of cells in the neural tube. It is not known whether Pax-3 may have a similar role in the development of neural crest derivatives and limb muscle. Therefore it would be interesting to study the levels of p53 protein in the presence and absence of endogenous Pax-3, using the antisense *Pax-3* Kelly cells. Since Kelly cells are derived from the neural crest, this could provide some evidence to suggest whether Pax-3 may also repress p53 induced-apoptosis in neural crest cell development.

Chapter 7

Discussion

7 Discussion

Pax-3 has been shown to play a key role in embryogenesis. Mutations in the *Pax-3* gene have been shown to cause developmental defects in both humans and mice. *Pax-3* expression is restricted during embryogenesis to mitotically active progenitor cells within the developing CNS, PNS and limb muscle. This had led to the suggestion that Pax-3 plays roles in cell proliferation, differentiation, migration and survival. Although few Pax-3 target genes have been discovered to date, Pax-3 has been shown to induce expression of a growth factor receptor (c-met), as well as the anti-apoptotic protein BCL-XL, although Pax-3 downregulates expression of the neural cell adhesion molecule (NCAM) and MBP, which is required for terminal differentiation. This supports the hypothesis that Pax-3 affects the development of progenitor cells in specific ways during embryogenesis. To gain further insight into the function of Pax-3 we studied the expression and regulation of *Pax-3* in the sensory neuron-derived cell line ND7, which is a good model system to use because, in line with its expression pattern during embryogenesis, *Pax-3* is only expressed in undifferentiated ND7 cells. In the presence of 0% serum, which induces cell cycle arrest and the onset of morphological differentiation, *Pax-3* expression rapidly decreases to undetectable levels. Moreover the fall in *Pax-3* expression occurs prior to any detectable change in cell proliferation or morphological differentiation suggesting that the decrease in *Pax-3* expression is not merely a consequence of differentiation but may be a necessary requirement for the onset of cell cycle arrest and morphological differentiation.

To further investigate this association between Pax-3 and mitotically active cells, we have analysed Pax-3 promoter activity during ND7 differentiation. A downregualtion in Pax-3 promoter activity was observed when ND7 cells were incubated with 0% serum,

suggesting that the fall in *Pax-3* mRNA previously reported upon ND7 cell differentiation was mediated by a decrease in the rate of transcription. However a time course experiment did reveal that Pax-3 transcription transiently increased 3 hrs after the removal of serum, Pax-3 promoter activity subsequently decreased until by 48 hrs, Pax-3 promoter activity was 40% of that observed in 10% serum. Interestingly the expression of the N-Myc transcription factor, which has been implicated in the control of cell proliferation and differentiation, has also been shown to increase transiently upon cell differentiation, in neurons derived from the neural crest.

In 0.5% and 1% serum Pax-3 promoter activity also decreased. Interestingly culture of ND7 cells in the presence of 0.5% versus 1% serum results in distinct cellular effects, with only 0.5% serum leading to a reduction in the rate of cell proliferation. In both 0.5% serum and 1% serum, Pax-3 promoter activity was reduced by approximately the same amount as it was in the complete absence of serum when compared to its activity in the presence of 10% serum. This confirms that the Pax-3 promoter activity is dependent upon serum factors. A decrease in Pax-3 DNA binding activity was also observed in 0.5% and 1% serum. Again no significant difference in Pax-3 DNA binding activity was detectable in ND7 cells grown in 0.5% or 1% serum. This suggests that the distinct cellular effects observed under each of these conditions are not directly dependent on the level of Pax-3 DNA binding activity in ND7 cells.

It was also shown that Pax-3 promoter activity decreased in ND7 cells cultured in delipidated serum compared to that in cells cultured in 10% serum. This indicates that serum lipids are required to maintain Pax-3 promoter activity. It would be interesting to determine which lipids were involved in maintaining *Pax-3* expression and the signalling

pathway involved. This could be achieved by assessing the effects on Pax-3 promoter activity of adding individual lipids back to cells that had been cultured in the presence of delipidated serum. Inhibitors of the different signalling pathways could also be added to the cells to determine which signal transduction pathway is required to maintain *Pax-3* expression in neuronal cells.

The region of the promoter used in these studies (-1000bp to +50bp) contained a number of potential binding sites including sites for SRF. This transcription factor binds to the serum response element in the upstream regulatory sequences of immediate early genes such as *c-fos*, and activates transcription of these genes in response to mitogenic signals. The 1050bp region of the Pax-3 promoter that was studied was also found to contain several potential Pax-3 binding sites. Using transient transfection assays it was shown that Pax-3 could induce Pax-3 promoter activity at low levels, but represses promoter activity at higher levels. The activation of the Pax-3 promoter seen at low levels was dependent on the presence of the Pax-3 C-terminus, which has been shown to contain a transcription activation domain. Repression of promoter activity at higher levels was still seen when the first 33 amino acids of Pax-3 were deleted. It has previously been shown that the first 90 amino acids of Pax-3 can strongly repress transcription when fused to a heterologous DNA binding domain. Therefore our results imply that the first 57 amino acids of the Pax-3 paired domain contribute to its inhibitory domain, in addition to the first 33 amino acids. Together the results suggest that the Pax-3 promoter may undergo auto-regulation. In this way, when *Pax-3* is first expressed, positive feedback by low levels of Pax-3 protein could increase the rate of *Pax-3* transcription. However, when a sufficient amount of Pax-3 has been synthesised, Pax-3 promoter activity would be repressed to prevent more protein being synthesised than is needed.

Analysis of the Pax-3 promoter also revealed potential binding sites for POU domain proteins. The Brn-3 transcription factors are POU domain proteins that play important roles in the regulation of neuronal cell differentiation. In addition, the expression patterns of Brn-3a and Brn-3c overlap with that of *Pax-3* in the developing PNS. We showed that Brn-3a could activate Pax-3 promoter activity whilst Brn-3c repressed the Pax-3 promoter. Therefore during neurogenesis Brn-3 proteins may act to regulate the level of *Pax-3* transcription. This could form part of the regulatory mechanism that restricts *Pax-3* expression to mitotically active cells during embryogenesis.

As well as being controlled at the level of transcription, the activity of a transcription factor may be controlled by post-translational modification. In particular phosphorylation has been shown to control the activity of a wide range of transcription factors. Both PKA and PKC have been implicated in the control of cell proliferation and differentiation. Both these enzymes have also been implicated in the control of transcription factor activity. Three potential PKA sites and 10 potential PKC sites are located within the first 284 amino acids of Pax-3 that incorporates the DNA binding domains of the protein. We showed that Pax-3 could be phosphorylated within its DNA binding domains *in vitro* by PKA and PKC. A bacterially expressed protein containing only the DNA binding domains of Pax-3 (Pax3-DBD), as well as individual paired domain (PD) and homeodomain (HD) proteins were phosphorylated *in vitro* by PKA. However, only the Pax3-DBD and PD proteins were phosphorylated *in vitro* by PKC. With regard to the effect of phosphorylation on the DNA binding activity Pax-3, PKA phosphorylation increased the affinity of Pax3-DBD for the composite paired domain and homeodomain site e5, but had no effect on the affinity of PD for the paired domain site Met. Therefore

phosphorylation of Pax-3 within its paired domain may not affect its DNA binding activity. However, PKA mediated phosphorylation within the linker region could alter the way in which the two DNA binding domains of Pax-3 are arranged on composite paired domain and homeodomain binding sites, thus increasing the DNA binding activity of the protein. With regards to the DNA binding activity of the Pax-3 homeodomain, phosphorylation by PKA was shown to increase the affinity of HD for the palindromic homeodomain site P2. However, the affinity of Pax3-DBD for P2 was unaffected by PKA mediated phosphorylation. Therefore it is unclear whether phosphorylation of Pax-3 by PKA can regulate its DNA binding activity with respect to homeodomain recognition sites. In addition, PKC mediated phosphorylation had no effect on Pax3-DBD binding to either the e5 or P2 site, suggesting that it may not alter the affinity of Pax-3 for either homeodomain-specific binding sites or composite paired domain and homeodomain sites.

To investigate whether Pax-3 may also be phosphorylated *in vivo*, the bacterially expressed Pax-3 proteins were incubated with nuclear extracts. It was shown that the Pax3-DBD and HD proteins were strongly phosphorylated by extracts from ND7 cells and IMR-32 cells that express endogenous Pax-3, but not by extracts from Cos-1 cells that do not express Pax-3. The PD protein was weakly phosphorylated by ND7 extracts, but not by IMR-32 or Cos-1 extracts. This suggests that phosphorylation of Pax-3 *in vivo* may be mediated by neuronal specific kinases, or is dependent upon neuronal specific cofactors. In order to establish whether this is the case, Pax-3 would need to be subjected to phosphorylation by nuclear extracts from a range of other neuronal as well as non-neuronal cell types. Two of the potential PKA sites and 7 of the potential PKC sites within the DNA binding domains of Pax-3 are conserved in other Pax proteins,

suggesting that Pax-3 may be phosphorylated by PKA and PKC *in vivo*. Therefore PKA and PKC could have been responsible for the phosphorylation of Pax-3 mediated by nuclear extracts. However, to determine which sites in the Pax-3 sequence can be phosphorylated by these protein kinases, individual PKA and PKC sites could be mutated by replacing the phospho-acceptor serine or threonine residue with a non-phosphorylatable residue such as alanine. Two-dimensional phospho-peptide mapping could then be carried out on the wild type and mutant proteins to show whether a potential PKA or PKC site in Pax-3 can be phosphorylated by this kinase *in vitro* and *in vivo*. As well as PKA and PKC sites, the Pax-3 amino acid sequence contains potential recognition sites for other protein kinases that have also been implicated in the control of cell proliferation and differentiation, such as MAP Kinase and CKII. Therefore phosphoryaltion of Pax-3 by nuclear extracts may be mediated by distinct but functionally related protein kinases.

In line with the potential role of Pax-3 in the promotion of cell proliferation, *Pax-3* expression has been shown to increase and reach its peak during G_1 phase of the cell cycle, just before the onset of DNA synthesis. Interestingly we showed that ND7 nuclear extracts made at different phases of the cell cycle phosphorylated Pax-3 within its DNA binding domains to varying degrees. The highest level of Pax-3 phosphorylation was mediated by nuclear extracts made from cells in late G_1 phase of the cell cycle. Therefore induction of *Pax-3* expression during G_1 may coincide with an increase in the level of Pax-3 phosphorylation, suggesting that phosphorylation may help to control Pax-3 activity *in vivo*. If this is the case, then Pax-3 must be phosphorylated *in vivo* by protein kinases that are active during G_1 phase of the cell cycle. Both MAP Kinase and CKII have been shown to be active at this stage of the cell cycle, and so either of these

enzymes could potentially bring about an increase in the level of phosphorylated Pax-3 protein during G_1. In summary Pax-3 activity is regulated at multiple levels. Both the control of Pax-3 expression, as well as phosphorylation of the Pax-3 protein may well be important in terms of regulating Pax-3 function during early embryogenesis.

Although Pax-3 has been implicated in the promotion of cell proliferation and cell survival, and the inhibition of cell differentiation, few direct Pax-3 target genes have been identified to date. A modified form of the ER ligand-binding domain (ER™) has been shown to render the activity of certain transcription factors such as c-Myc dependent on 4-hydroxytamoxifen (OHT). Therefore to try and identify novel molecular targets for Pax-3 in neuronal cells, a Pax3-ER™ fusion protein was cloned and expressed in ND7 cells. It was hoped that Pax3-ER™ could be shown to activate transcription in an OHT-dependent fashion. Pax3-ER™ expressing cells could then be cultured in the presence of cyclohexamide with or without OHT, to determine whether the expression of a potential Pax-3 target gene is regulated directly by Pax-3.

We expressed a Pax3-ER™ fusion protein containing all but the last 16 amino acids of Pax-3 in ND7 cells, and showed that the nuclear localisation of this protein was dependent on OHT. The last 78 amino acids at the C-terminus of Pax-3 constitute its transcription activation domain, which is rich in Pro, Ser and Thr residues. Although there are 11 serines, 10 threonines and 9 prolines present in this part of the Pax-3 sequence, only a small proportion of these residues (1 Ser, 2 Thr and 1 Pro) occur within the last 16 amino acids of the protein, and so their absence was not expected to affect the transactivation function of Pax-3. Although activation of Pax3-ER™ had no effect on the growth of ND7 cells in the presence of 10% serum, in serum starved ND7s Pax3-ER™

activation resulted in a decreased rate of cell growth, which was caused by an increase in the rate of cell death. During embryogenesis and in certain cancers such as RMS, however, Pax-3 has been shown to promote cell survival. It is therefore possible that Pax3-ER™ only induces cell death in serum-starved ND7 cells because of the lack of mitogens available to them. Myc-ER™ was shown to have similar effects in serum-starved fibroblasts. Activation of Myc-ER™ was shown to drive serum-starved fibroblasts back into the cell cycle, but also caused an increase in the rate of cell death by apoptosis.

Cotransfection experiments failed to show whether the Pax3-ER™ protein was transcriptionally active due to very low transfection efficiency of the e5-CAT reporter construct. Therefore the use of a reporter gene construct containing six e5 binding sites cloned in series upstream of the CAT reporter gene, may prove more successful in determining whether Pax3-ER™ is transcriptionaly active. In case this protein proves to be transcriptionally inactive because it lacks the last 16 amino acids of Pax-3, another construct has been cloned that codes for a Pax3-ER™ protein containing all but the last amino acid of Pax-3. However, this construct has yet to be stably transfected into ND7 cells. Therefore an established antisense *Pax-3* method was employed as another means of identifying potential Pax-3 target genes. Using this antisense approach, downregulation of Pax-3 in the neuroblastoma cell line Kelly has been shown to lead to a reduced rate of cell proliferation and an increase in the rate of cell death. We showed that the levels of N-Myc protein in Kelly cells were increased upon downregulation of Pax-3. If the transactivation function of the Pax3-ER™ protein can be demonstrated, it would be interesting to use the Pax3-ER™ approach to determine whether N-Myc represents a direct Pax-3 target gene.

To identify additional downstream targets of Pax-3, cDNA arrays could be used. In this technique, cDNA fragments from hundreds of genes are immobilised on a membrane. To compare the levels at which these genes are expressed in control and antisense *Pax-3* cells, the mRNA from each of these two cell types would be purified. cDNA probes would then be synthesised from the mRNA in the presence of radiolabelled nucleotides using a primer mix that contains primers for all of the genes represented on the membrane. The cDNA probes would then be hybridised to the membrane, and the strength of signal produced would reflect the level of expression of each gene in the control and antisense *Pax-3* cells. The promoters of genes whose expression levels differed between the control and antisense *Pax-3* cells could then be examined to see if they contain any potential Pax-3 binding sites. The regions of promoters containing such sites would be cloned upstream of a reporter gene. Cotransfection assays with a Pax-3 expression vector would then show whether overexpression of Pax-3 affects the level of transcription activated from this promoter. The Pax3-ER™ technique could be used to complement this approach, and to show whether the gene being studied represents a direct molecular target for Pax-3.

References

References

Adams, B., Dorfler, P., Aguzzi, A., Kozmik, Z., Urbanek, P., Mourer-Fogi, I., and Bushinger, M., (1992). Pax-5 encodes the transcription factor BSAP and is expressed in B lymphocytes, the developing CNS, and adult testis. *Genes & Development* **6,** 1589-1607.

Albanese, C., Johnson, J., Watanabe, G., Eklund, N., Vu, D., Arnold, A., and Pestell, R., (1995). Transforming $p21^{ras}$ mutants and c-Ets-2 activate the cyclin D1 promoter through distinguishable regions. *The Journal of Biological Chemistry* **270,** 23589-23597.

An, S., Bleu, T., Hallmark, O. G., and Goetzl, E. J., (1998). Characterisation of a novel subtype of human G protein-coupled receptor for lysophosphatidic acid. *J. Biol. Chem.* **273,** 7906-7910.

Asamoah, K.A., Atkinson, P.G.P., Carter, W.G., and Sale, G. (1995). Studies on the insulin-stimulated insulin receptor serine kinase activity: separation of the kinase activity from the insulin receptor and its reconstitution back to the insulin receptor. *Biochem. J.* **308,** 915-922.

Ayyanathan, K., Fredericks, J.W., Berking, C., Herlyn, M., Balakrishnan, C., Gunther, E., and Rauscher, J. III (2000). Hormone-dependent tumour regression *in vivo* by an inducible transcriptional repressor directed at the PAX3-FKHR oncogene. *Cancer Research* **60**, 5803-5814.

Bennicelli, J.L., Edwards, R.H., and Barr, F.G., (1996). Mechanism of transcriptional gain of function resulting from chromosomal translocation in alveolar rhabdomyosarcoma. *Proc. Natl. Acad. Sci. USA* **93,** 5455-5459.

Berberich, S.J., and Cole, M.D., (1992). Casein Kinase II inhibits the DNA-binding activity of Max homodimers but not Myc-Max heterodimers. *Genes and Development* **6,** 166-176.

Bernasconi, M., Remppis, A., Fredericks, W., Rauscher III, F., and Schafer, B., (1996). Induction of apoptosis in rhabdomyosarcoma cells through down-regulation of PAX proteins. *Proc. Natl. Acad. Sci. USA* **93,** 13164-13169.

Bertuccioli, C., Fasano, L., Jun, S., Sheng, G., and Desplan, C., (1996). *In vivo* requirement for the paired domain and the homeodomain of the *paired* segmentation gene product. *Development* **122,** 2673-2685.

Bober, E., Franz, T., Arnold, H., Gruss, P., and Tremblay, P., (1994). Pax-3 is required for the development of limb muscles: a possible role for the migration of dermamyotomal muscle progenitor cells. *Development* **120,** 603-612.

Borycki, A-G., and Emerson, C., (1997). Muscle determination: Another key player in myogenesis? *Current Biology* **7,** R620-R623.

Bottazzi, M., Zhu, X., Bohmer, R., and Assoian, R., (1999). Regulation of $p21^{cip1}$ expression by growth factors and the extracellular matrix reveals a role for transient ERK activity in G_1 phase. *The Journal of Cell Biology* **146,** 1255-1264.

Bouwman, P., and Philipsen, S., (2002). Regulation of the activity of Sp1-related transcription factors. *Mol Cell Endocrinol.* **195,** 27-38.

Boyle, W.J., Smeal, T., Defize, L., Angel, P., Woodgett, J., Karin, M., and Hunter, T., (1991). Activation of protein kinase C decreases phosphorylation of c-Jun at sites that negatively regulate its DNA binding activity. *Cell* **64,** 573-584.

Brazil, D.P., and Hemmings, B.A., (2001). Ten years of protein kinase B signalling: a hard Akt to follow. *TRENDS in Biochemical Sciences* **26,** 657-664.

Brunet, A., Roux, D., Lenormand, P., Doud, S., Keyse, S., and Pouyssegur, J., (1999). Nuclear translocation of p42/p44 mitogen-activates protein kinase is required for growth factor-induced gene expression and cell cycle entry. *The EMBO Journal* **18,** 664-674.

Budhram-Mahadeo, V.S., Lillycrop, K.A., and Latchman, D.S., (1994a). Cell cycle arrest and morphological differentiation can occur in the absence of apoptosis in a neuronal cell line. *Neuroscience Letters* **165,** 18-22.

Budhram-Mahadeo, V.S., Theil, T., Morris, P.J., Lilycrop, K.A., Moroy, T., and Latchman, D.S., (1994b). The DNA target site for the Brn-3 POU family transcription factors can confer responsiveness to cyclic AMP and removal of serum in neuronal cells. *Nucleic Acids Research* **22,** 3092-3098.

Caelles, C., Hennemann, H., Karin, M., (1995). M-phase-specific phosphorylation of the POU transcription factor GHF-1 by a cell cycle-regulated protein kinase inhibits DNA binding. *Molecular and Cellular Biology* **15,** 6694-6701.

Cao, Y., and Wang, C., (2000). The COOH-terminal transactivation domain plays a key role in regulating the *in vitro* and *in vivo* function of Pax3 homeodomain. *The Journal of Biological Chemistry* **275,** 9854-9862.

Carey, J., (1991). Gel Retardation. *Methods in Enzymology* **208,** 103-117.

Carpenter, E.M., (2002). Hox genes and spinal cord development. *Dev. Neurosci* **24,** 24-34.

Carroll, D., and Marshak, D., (1989). Serum-stimulated cell growth causes oscillations in casein kinase II activity. *The Journal of Biological Chemistry* **264,** 7345-7348.

Chalepakis, G., Fritsch, R., Fickenscher, H., Deutsch, U., Goulding, M., and Gruss, P., (1991). The molecular basis of the undulated / *Pax-1* mutation. *Cell* **66,** 873-884.

Chalepakis, G., Tremblay, P., Gruss, P., (1992). *Pax* genes, mutants and molecular function. *Journal of Cell Science* **Supplement 16,** 61-67.

Chalepakis, G., Jones, F., Edelman, G., Gruss, P., (1994). Pax-3 contains domains for transcription activation and inhibition. *Proc. Natl. Acad. Sci. USA* **91,** 12745-12749.

Cham, B., and Knowles, B., (1976). A solvent system for delipidation of plasma or serum without protein precipitaton. *Journal of Lipid Research* **41,** 142-147.

Chambraud, B., Berry, M., Redeuilh, G., Chambon, P., Baulieu, E., (1990). Several regions of the human estrogen receptor are involved in the formation of receptor-heat shock protein 90 complexes. *The Journal of Biological Chemistry* **265,** 20686-20691.

Chellappan, S., Hiebert, S., Mudryl, M., Horowitz, J., and Nevins, J., (1991). The E2F transcription factor is a cellular target for the RB protein. *Cell* **65,** 1053-1061.

Chen, T., Hinton, D., Zidovetzki, R., and Hofman, F., (1998). Up-regulation of the cAMP/PKA pathway inhibits proliferation, induces differentiation, and leads to apoptosis in malignant gliomas. *Laboratory Investigation* **78,** 165-174.

Chien, W-M., Parker, J., Schmidt-Grimminger, D-C., Broker, T., and Chow, L., (2000). Casein kinase II phosphorylation of the human papillomavirus-18 E7 protein is critical for promoting S-phase entry. *Cell Growth & Differentiation* **11,** 425-435.

Chinenov, Y., and Kerppola, T.K., (2001). Close encounters of many kinds: Fos-Jun interactions that mediate transcription regulatory specificity. *Oncogene* **20,** 2438-2452.

Cho-Chung, Y., (1990). Role of cyclic AMP receptor proteins in growth, differentiation, and suppression of malignancy: new approaches to therapy. *Cancer Research* **50,** 7093-7100.

Clay. C., Namen, A., Atsumi, G., Willingham, K., High, T., Trimboli, A., Dawson, P., and Chilton, F., (1999). Influence of J series prostaglandins on apoptosis and tumourigenesis of breast cancer cells. *Carcinogenesis* **20,** 1905-1911.

Clemens, M.J., Trayner, I., and Menaya, J., (1992). The role of protein kinase C isoenzymes in the regulation of cell proliferation and differentiation. *Journal of Cell Science* **103,** 881-887.

Cooney, J.A., Tsai, S.Y., and Tsai, M-J., (1993). *Transcription Factors – A Practical Approach, Oxford University Press.* Chapter 3 – Biochemical characterisation of transcription factors.

Dahl, E., Koseki, H., and Balling, R., (1997). *Pax* genes and organogenesis. *BioEssays* **19,** 755-765.

Daston, G., Lamar, E., Olivier, M., and Goulding, M., (1996). *Pax-3* is necessary for migration but not differentiation of limb muscle precursors in the mouse. *Development* **122,** 1017-1027.

Davis, R.J., (1993). The Mitogen-activated Protein Kinase Signal Transduction Pathway. *The Journal of Biological Chemistry* **268,** 14553-14556.

De Boja, P.F., Collins, N.K., Du, P., Zizkhan-Clifford, J.A., and Mudryj, M., (2001). Cyclin A-CDK2 phosphorylates SP1 and enhances SP1 mediated transcription. *The EMBO Journal* **20,** 5737-47.

Diehl, J., Cheng, M., Roussel, M., and Sherr, C., (1988). Glycogen synthase kinase-3β regulates cyclin D1 proteolysis and subcellular localisation. *Genes & Development* **12,** 3499-3511.

Edmondson, D., and Olson, E., (1993). Helix-loop-helix proteins as regulators of muscle-specific transcription. *The Journal of Biological Chemistry* **268,** 755-758.

Eilers, M., Picard, D., Yamamoto, K., and Bishop, M., (1989). Chimaeras of Myc oncoprotein and steroid receptors cause hormone-dependent transformation of cells. *Nature* **340,** 66-68.

Ekholm, S.V., and Reed, S.J., (2000). Regulation of G_1 cyclin dependent kinases in the mammalian cell cycle. *Current opinion in cell biology* **12,** 676-684.

Endicott, J.A., Noble, M.E.M., and Tucker, J.A., (1999). Cyclin-dependent kinases: inhibition and substrate recognition. *Current opinion in structural biology* **9,** 738-744.

Epstein, D., Velemans, M., and Gros, P., (1991). Splotch (Sp^{2H}), a mutation affecting development of the mouse neural tube, shows a deletion within the paired homeodomain of *Pax-3*. *Cell* **67,** 767-774.

Epstein, D., Vogan, K., Trasler, D., and Gros, P., (1993). A mutation within intron 3 of the *Pax-3* gene produces aberrantly spliced mRNA transcripts in the splotch (*sp*) mouse mutant. *Proc. Natl. Acad. Sci. USA* **90,** 532-536.

Epstein, J.A., Glaser, T., Cai, J., Jepeal, L., Walton, D., and Maas, R., (1994). Two independent and interactive DNA-binding subdomians of the Pax6 paired domain are regulated by alternative splicing. *Genes & Development* **8,** 2022-2034.

Epstein, J., Lam, P., Jepeal, L., Maas, R., and Shapiro, D., (1995). Pax3 inhibits myogenic differentiation of cultured myoblast cells. *The Journal of Biological Chemistry* **270,** 11719-11722.

Epstein, J., Shapiro, D., Cheng, J., Lam, P., and Maas, R., (1996). Pax3 modulates expression of the c-met receptor during limb muscle development. *Proc. Natl. Acad. Sci. USA* **93,** 4213-4218.

Epstein, J., Song, B., Lakkis, M., Wang, C., (1998). Tumor-specific PAX3-FKHR transcription factor, but not PAX3, activates the platelet-derived growth factor alpha receptor. *Molecular and Cellular Biology* **18,** 4118-4130.

Erkman, L., McEvilly, J., Luo, L., Ryan, AK., Hooshmand, F., O'Connel, S., Keithley, E., Rapaport, D., Ryan, AF., and Rosenfeld, M., (1996). Role of transcription factors Brn-3.1 and Brn-3.2 in auditory and visual system development. *Nature* **381,** 603-606.

Evan, G., Wylie, A., Gilbert, C., Littlewood, T., Waters, C., Penn, L., and Hancock, D., (1992). Induction of apoptosis in fibroblasts by c-myc protein. *Cell* **69,** 119-128.

Evans, J., and Lillycrop, K. A., (1996). Serum growth factor regulation of the paired-box transcription factor Pax-3 in neuronal cells. *Neuroscience Letters* **220,** 125-128.

Favier, B., and Dolle, P., (1997). Developmental functions of mammalian Hox genes. *Mol Hum Reprod.* **3,** 115-131.

Favor, J., Sandulache, R., Neuhauser-Klaus, A., Pretsh, W., Chatterjee, B., Senft, E., Wurst, W., Blanquet, V., Grimey, P., Sporle, R., and Schughort, K., (1996). The mouse Pax-2 ^{1Neu} is identical to a human PAX2 mutation in a family with renal-coloboma syndrome and results in developmental defects of the brain, eye, ear and kidney. *PNAS USA* **93,** 13870-13875.

Fedtsova, N., and Turner, E., (1995). Brn-3.0 expression identifies early post-mitotic CNS neurons and sensory neural precursors. *Mechanisms of Development* **53,** 291-304.

Feramisco, J.R., Glass, D.B., and Krebs, E.G., (1980). Optimal spatial requirements for the location of basic residues in peptide substrates for the cyclic AMP-dependent protein kinase. *The Journal of Biological Chemistry* **255,** 4240-4245.

Fortin, A., Underhill, D., and Gros, P., (1998). Helix 2 of the paired domain plays a key role in the regulation of DNA-binding by the Pax-3 homeodomain. *Nucleic Acids Research* **26,** 4574-4581.

Fredericks, W., Ayyanathan, K., Herlyn, M., Friedman, J., and Rauscher III, F., (2000). An engineered PAX3-KRAB transcriptional repressor inhibits the malignant phenotype of alveolar rhabdomyosarcoma cells harbouring the endogenous PAX3-FKHR oncogene. *Molecular and Cellular Biology* **20,** 5019-5031.

Furakawa, Y., Piwnica-Worms, H., Ernst, T., Kanakura, Y., and Griffin, J., (1990). cdc2 gene expression at the G_1 to S transition in human T lymphocytes. *Science* **250,** 805-808.

Galibert, M-D., Yavuzer, U., Dexter, T., and Goding, C., (1999). Pax-3 and regulation of the melanocyte-specific tyrosinase-related protein-1 promoter. *The Journal of Biological Chemistry* **274,** 26894-26900.

Ghosh, S., and Baltimore, D., (1990). Activation *in vitro* of NF-κB by phosphorylation of its inhibitor IκB. *Nature* **344,** 678-682.

Gjersten, B.T., and Doskeland, A., (1995). Protein phosphorylation in apoptosis. *Biochim. Biophys. Acta* **1269,** 187.

Gonzalez, G., and Montminy, M., (1989). Cyclic AMP stimulates somatostatin gene transcription by phosphorylation of CREB at serine 133. *Cell* **59,** 675-680.

Gorman, C., (1985). Chapter 6 – High efficiency gene transfer into mammalian cells. *DNA Cloning Volume II - a practical approach. Cambridge Univ. Press.*

Goulding, M., Chalepakis, G., Deutsch, U., Erselius, J., and Gruss, P., (1991). Pax-3, a novel DNA binding protein expressed during early neurogenesis. *The EMBO Journal* **10,** 1135-1147.

Graba, Y., Aragnol, D., and Pradel, J., (1997). *Drosophila* Hox complex downstream targets and the function of homeotic genes. *Bioessays* **19,** 379-88.

Gruss, P., and Walther, C., (1992). Pax in development. *Cell* **69,** 719-722.

Gstaiger, M., Georgiev, O., Van Leeuwen, H., van der Vliet, P.C., Schaffner, W., (1996). The B cell coactivator Bob1 shows DNA sequence-dependent complex formation with Oct-1/Oct-2 factors, leading to differential promoter activation. *EMBO J* **15,** 2781-2790.

Guerra, B., Boldyreff, B., Sarno, S., Cesaro, L., Issinger, O.G., and Pinna, L.A., (1999). CKII: A Protein Kinase in Need of Control. *Pharmacol. Ther.* **82,** 303-313.

Gupta, S., Seth, A., and Davis, R., (1993). Transactivation of gene expression by Myc is inhibited by mutation at the phosphorylation sites Thr-58 and Ser-62. *Proc. Natl. Acad. Sci. USA* **90,** 3216-3220.

Han, S., Greene, M., Pitts, M.,Wada, J., and Sidell, N., (2001). Novel expression and function of peroxisome proliferator-activated receptor gamma (PPARγ) in human neuroblastoma cells. *Clinical cancer research* **7,** 98-104.

Harris, R.G., (2000). The regulation of the embryonic transcription factor Pax-3. *PhD Thesis,* 100-101.

He, X., Treacy, M., Simmons, D., Ingraham, H., Swanson, L., and Rosenfeld, M., (1989). Expression of a large family of POU-domain regulatory genes in mammalian brain development. *Nature* **340,** 35-42.

Herr, W., and Cleary, M., (1995). The POU domain: versatility in transcriptional regulation by a flexible two-in-one DNA-binding domain. *Genes & Development* **9,** 1679-1693.

Hill, R., Favor, J., Hogan, B., Ton, C., Saunders, G., Hanson, I., Prosser, J., Jorban, T., Hastie, N., and Heyningen, V., (1991). Mouse small eye results from mutations in a paired-like homeobox containing gene. *Nature* **354,** 522-525.

Hopewell, R., Linheng, L., Macgregor, D., Nerlov, C., and Ziff, E., (1995). Regulation of cell proliferation and differentiation by Myc. *Journal of Cell Science* **Supplement 19,** 85-89.

House, C., Wettenhall, R., and Kemp, B., (1987). The influence of basic residues on the substrate specificity of protein kinase C. *The Journal of Biological Chemistry* **262,** 772-777.

Hubbard, M. J., and Chen, P., (1993). On target with a new mechanism for the regulation of protein phosphorylation. *Trends Biochem. Sci* **18,** 172.

Hunter, T., and Karin, M., (1992). The regulation of transcription by phosphorylation. *Cell* **70,** 375-387.

Jostes, B., Walther, C., and Gruss, P., (1990). The murine paired-box gene, *Pax-7*, is expressed specifically during the development of the nervous and muscular system. *Mech. Dev.* **33,** 27-37.

Jun, S., and Desplan, C., (1996). Cooperative interactions between paired domain and homeodomain. *Development* **122,** 2639-2650.

Kapiloff, M., Farkash, Y., Wegner, M., Rosenfeld, M., (1991). Variable effects of phosphorylation of Pit-1 dictated by the DNA response elements. *Science* **253,** 786-789.

Kemp, B., Graves, D., Benjamini, E., and Krebs, E., (1977). Role of multiple basic residues in determining the substrate specificity of cyclic-AMP dependent protein kinase. *The Journal of Biological Chemistry* **252,** 4888-4894.

Kemp, B., and Pearson, R., (1990). Protein kinase recognition sequence motifs. *TIBS* **15,** 342-346.

Kennelly, P. J., and Krebs, E. G., (1991). Consensus sequences as substrate specificity determinants for protein kinases and protein phosphatases. *Journal of Biological Chemistry* **266,** 15555-15558.

Kioussi, C., Gross, M., and Gruss, P., (1995). *Pax3*: A paired domain gene as a regulator in PNS myelination. *Neuron* **15,** 553-562.

Klemm, J.D, Rould, M.A., Aurora, R., Herr, W., Pabo, C.O., (1994). Crystal structure of the Oct-1 POU domain bound to an octamer site: DNA recognition with tethered DNA-binding modules. *Cell* **77,** 21-32.

Koff, A., Cross, F., Fisher, A., Schumacher, J., Leguellec, K., Phillippe, M., and Roberts, J., (1991). Human cyclin E, a new cyclin that interacts with two members of the CDC2 family. *Cell* **66,** 1217-1228.

Kumar, V., Green, S., Staub, A., and Chambon, P., (1986). Localisation of the oestradiol binding and putative DNA-binding domains of the human oestrogen receptor. *The EMBO Journal* **5,** 2231-2236.

Lai, J-S., Cleary, M.A., and Herr, W., (1992). A single amino acid exchange transfers VP-16 induced positive control from the Oct-1 to the Oct-2 POU homeodomain. *Genes and Development* **6,** 2058-2065.

Lakin, N., Morris, P., Theil, T., Sato, T., Moroy, T., Wilson, M., and Latchman, D., (1995). Regulation of neurite outgrowth and SNAP-25 gene expression by the Brn-3a transcription factor. *The Journal of Biological Chemistry* **270,** 15858-15863.

Latchman, D., (1999). POU family transcription factors in the nervous system. *Journal of cellular physiology* **179,** 126-133.

Lee, E., Chang, C., Hu, N., Wang, Y., Lai, C., Herrup, K., Lee, W., and Bradley, A., (1992). Mice deficient for Rb are nonviable and show defects in neurogenesis and haematopoiesis. *Nature* **359,** 288-294.

Lefebvre, T., Planque, N., Leleu, D., Bailly, M., caillet-Boudin, M.L., Saule, S., and Michalski, J.C., (2002). O-glycosylation of the nuclear forms of Pax-6 products in quail neuroretina cells. *J Cell Biochem.* **85,** 208-218.

Levine, M., and Manley, J.L., (1989). Transcriptional repression of eukaryotic promoters. *Cell* **59,** 405-408.

Licht, J.D., Hanna-Rose, W., Reddy, J.C., English, M.A., Ro, M., Grossel, M., Shaknoivh, R., and Hansen, U., (1994). Mapping and mutagenesis of the amino-terminal transcriptional repression domain of the Drosophila Kruppel protein. *Mol Cell Biol.* **14,** 4057-4066.

Lillycrop, K., Budrahan, V., Lakin, N., Terrenghi, G., Wood, J., Polak, J., and Latchman, D., (1992). A novel POU family transcription factor is closely related to Brn-3 but has a distinct expression pattern in neuronal cells. *Nucleic Acids Research* **20,** 5093-5096.

Lin, A., Frost, J., Deng, T., Smeal, T., Al-Alawi, N., Kikkawa, U., Hunter, T., Brenner, D., and Karin, M. (1992). Casein Kinase II Is a Negative Regulator of c-Jun DNA Binding and AP-1 Activity. *Cell* **70,** 777-789.

Littlewood, T., Hancock, D., Danielian, P., Parker, M., and Evan, G., (1995). A modified oestrogen receptor ligand-binding domain as an improved switch for the regulation of heterologous proteins. *Nucleic Acids Research* **23,** 1686-1690.

Livneh, E., and Fishman, D., (1997). Linking protein kinase C to cell cycle control. *Eur. J. Biochem.* **248,** 1-9.

Lobe, C., (1992). Transcription factors and mammalian development. *Current Topics in Developmental Biology* **27,** 351-383.

Ludolph, D., and Konieczny, S., (1995). Transcription factor families: muscling in on the myogenic program. *The FASEB Journal* **9,** 1595-1604.

Luscher, B., and Larsson, L.G., (1999). The basic region/helix-loop-helix/leucine zipper domain of Myc proto-oncoproteins: function and regulation. *Oncogene* **18,** 2955-2966.

Manak, J., and Prywes, R., (1991). Mutation of serum response factor phosphorylation sites and the mechanism by which its DNA-binding activity is increased by casein kinase II. *Molecular and Cellular Biology* **11,** 3652-3659.

Manley, J.L., Um, M., Li, C., and Ashali, H., (1996). Mechanisms of transcriptional activation and repression can both involve TFIID. *Philos Trans R Soc Lond B Biol Sci* **351,** 517-526.

Mansouri, A., Stoykova, A., and Gruss, P., (1994). *Pax* genes in development. *Journal of Cell Science* **supplement 18,** 35-42.

Marais, R., Nguyen, O., Woodgett, J., and Parker, P., (1990). Studies on the primary sequence requirements for PKC-α, -β_1 and -γ peptide substrates. *FEBS LETTERS* **277,** 151-155.

Margue, C., Bernasconi, M., Barr, F., and Schafer, B., (2000). Transcriptional modulation of the anti-apoptotic protein BCL-XL by the paired box transcription factors PAX3 and PAX3/FKHR. *Oncogene* **19,** 2921-2929.

Maroto, M., Rashef, R., Munsterberg, E., Koester, S., Goulding, M., and Lassar, A., (1997). Ectopic *Pax-3* activates *MyoD* and *Myf-5* expression in embryonic mesoderm and neural tube. *Cell* **89,** 139-148.

Martelli, A.M., Sang, N., Borgatti, P., Capitani, S., and Neri, L.M. (1999). Multiple Biological Responses Activated by Nuclear Protein Kinase C. *Journal of Cellular Biochemistry* **74,** 499-521.

Matten, W., Daar, I., and Woude, G., (1994). Protein kinase A acts at multiple points to inhibit Xenopus oocyte maturation. *Molecular and Cellular Biology* **14,** 4419-4426.

Maulbecker, C., and Gruss, P., (1993). The oncogenic potential of Pax genes. *The EMBO Journal* **12,** 2361-2367.

Mayr, B., and Montminy, M., (2001), Transcriptional regulation by the phosphorylation-dependent factor CREB. *Nat Rev Mol Cell Biol.* **2,** 599-609.

McEvilly, RJ., Erkman, L., Luo, L., Sawchenko, PE., Ryan, AF., and Rosenfeld, MG., (1996). Requirement for Brn-3.0 in differentiation and survival of sensory and motor neurons. *Nature* **384,** 574-577.

Mihira, K., Cao, X., Yen, A., Chandler, S., Driscoll, B., Murphree, A., T'Ang, A., and Fung, Y., (1989). Cell cycle-dependent regulation of phosphorylation of the human retinoblastoma gene product. *Science* **246,** 1300-1303.

Moase, C., and Trasler, D., (1991). N-CAM alterations in splotch neural tube defect mouse embryos. *Development* **113,** 1049-1058.

Molkentin, J.D., and Olsen, E.N., (1996). Combinatorial control of muscle development by basic helix-loop-helix and MADS-box transcription factors. *Proc Natl Acad Sci USA* **93,** 9366-9373.

Morgenstern, J.P. and Land, H. (1990). Advanced mammalian gene transfer: high titre retroviral vectors with multiple drug selection markers and a complementary helper-free packaging cell line. *Nucleic Acids Research* **18,** 3587-3596.

Morrisey, E., Ip, H., Tang, Z., Lu, M., and Parmacek, M., (1997). GATA-5: a transcriptional activator expressed in a novel temporally and spatially-restricted pattern during embryonic development. *Developmental Biology* **183,** 21-36.

Natoli, T., Ellsworth, M., Wu, C., Gross, K., and Pruitt, S., (1997). Positive and negative DNA sequence elements are required to establish the pattern of *Pax3* expression. *Development* **124,** 617-626.

Neubuser, A., Koseki, H., and Balling, R., (1995). Characterisation and developmental expression of *Pax-9*, a paired-box containing gene related to *Pax-1*. *Developmental Biology* **170,** 701-716.

Niethammer, D. and Handgretinger, R., (1995). Clinical strategies for the treatment of neuroblastoma. *European Journal of Cancer* **31A,** 568-571.

Ninkina, N., Stevens, G., Wood, J., and Richardson, W., (1993). A novel Brn3-like POU transcription factor expressed in subsets of rat sensory and spinal cord neurons. *Nucleic Acids Research* **21,** 3175-3182.

Ohno, S. and Suzuki, K. (1995). *The protein kinase facts book, protein-serine kinases, section II the protein kinases, PKC*, 80-88.

Pani, L., Horal, M., and Loeken, M., (2002). Rescue of neural tube defects in Pax-3-deficient embryos by p53 loss of function: implications for Pax-3-dependent development and tumorigenesis. *Genes & Development* **16,** 676-680.

Phelan, S. A., and Loeken, M. R., (1998). Identification of a new binding motif for the paired domain of Pax-3 and unusual characteristics of spacing of bipartite recognition elements on binding and transcriptional activation. *The Journal of Biological Chemistry* **273,** 19153-19159.

Plachov, D., Chowdhung, K., Walther, C., Simon, D., Guenet, J., and Gruss, P., (1990). *Pax-8*, a murine paired-box gene expressed in the developing excretory system and thyroid gland. *Development* **110,** 643-651.

Poleev, A., Okladnova, O., Musti, A., Schneider, S., Royer-Pokora, B., Plachov, D., (1997). Determination of functional domains of the human transcription factor PAX8 responsible for its nuclear localisation and transactivating potential. *Eur. J. Biochem* **247,** 860-869.

Pollock, R. and Treisman, R., (1990). A sensitive method for the determination of protein-DNA binding specificities. *Nucleic Acids Research* **18,** 6197-6204.

Pratt, W.B., and Toft, D.O., (1997). Steroid receptor interaction with heat shock protein and immunophilin chaperones. *Endocrine Rev.* **18,** 306-360.

Pyne, S., Chapman, J., Steele, L., and Pyne, N.J., (1996). Sphingomyelin-derived lipids differentially regulate the extracellular signal-regulated kinase 2 (ERK2) and c-Jun N terminal kinase signal cascades in airway smooth muscle. *Eur. J. Biochem.* **237,** 819-826.

Qu, S., Li, L., and Wisdom, R., (1997). Alx-4: cDNA cloning and characterisation of a novel paired-type homeodomain protein. *Gene* **203,** 217-223.

Quandt, K., Frech, K., Haras, H., Wingender, E., and Werner, T., (1995). MatInd and MatInspector: new fast and versatile tools for detection of consensus matches in nucleotide sequence data. *Nucleic Acids Research* **23,** 4878-4884.

Ramirez, S., Slimane, A., Robin, P., Trouch, D., Harel-Bellan, A., (1997). The CREB-binding protein (CBP) cooperates with the serum response factor for transactivation of the *c-fos* serum response element. *The Journal of Biological Chemistry* **272,** 31061-31021.

Reeves, F. C., Fredericks, W. J., Rauscher III, F. J., and Lillycrop, K. A., (1998). The DNA binding activity of the paired box transcription factor Pax-3 is rapidly downregulated during neuronal cell differentiation. *FEBS Letters* **422,** 118-122.

Reeves, F.C., Burdge, G.C., Fredericks, W.J., Rauscher III, F.J., and Lillycrop, K.A., (1999). Induction of antisense *Pax-3* expression leads to the rapid morphological differentiation of neuronal cells and an altered response to the mitogenic growth factor bFGF. *Journal of Cell Science* **112,** 253-261.

Reichert, H., and Simeone, A., (1999). Conserved usage of gap and homeotic genes in patterning the CNS. *Current Opinion in Neurobiology* **9,** 589-595.

Rojo, F., (2001). Mechanisms of transcriptional repression. *Curr Opin Microbiol.* **4,** 145-151.

Rothwarf, D.M., and Karin, M., (1999). The NF-kappa B activation pathway: a paradigm in information transfer from membrane to nucleus. *Sci STKE* **1999,** RE1.

Russo, G., Vandenberg, M., Yu, I., Young-Seuk, B., Franza, B., and Marshak, D., (1992). Casein kinase II phosphorylates $p34^{cdc2}$ kinase in G_1 phase of the HeLa cell division cycle. *The Journal of Biological Chemistry* **267,** 20317-20325.

Ruvkun, G., and Finney, M., (1991). Regulation of transcription and cell identity by POU domain proteins. *Cell* **64,** 475-478.

Sachs, A.B., (1993). Messenger RNA degradation in eukaryotes. *Cell* **74,** 413-421.

Sambrook, J., Fritsch, G. and Maniatis, T. (1989). Molecular cloning, a laboratory manual, *Cold Spring Harbor Press,* New York.

Sauer, F., and Tjian, R., (1997). Mechanisms of transcriptional activation: differences and similarities between yeast, Drosophila, and man. *Curr Opin Genet Dev.* **7,** 176-181.

Schafer, B.W., Czerny, T., Bernasconi, M., Genini, M. and Busslinger, M., (1994). Molecular cloning and characterisation of a human PAX-7 cDNA expressed in normal and neoplastic myocytes. *Nucleic Acids Research* **22,** 4574-4582.

Schwabe J.W.R., Chapman, L., Finch, J.T., (1993). The crystal structure of the estrogen receptor DNA-binding domain bound to DNA: How receptors discriminate between their response elements. *Cell* **75,** 567-578.

Segil, N., Roberts, S., Heintz, N. (1991). Mitotic phosphorylation of the Oct-1 homeodomain and regulation of Oct-1 DNA binding activity. *Science* **254,** 1814-1816.

Serbedzija, G., and McMahon, A., (1997). Analysis of neural crest cell migration in splotch mice using a neural crest-specific LacZ reporter. *Developmental Biology* **185,** 139-147.

Sheng, G., Harris, E., Bertuccioli, C. and Desplan, C., (1997). Modular organisation of Pax/homeodomain proteins in transcriptional regulation. *Biol. Chem.* **378,** 863-872.

Small, M., Hay, N., Schwab, M., and Bishop, J., (1987). Neoplastic transformation by the human gene N-*myc*. *Molecular and Cellular Biochemistry* **7,** 1638-1645.

Smith, S., Ee, H., Conners, J., and German, M., (1999). Paired-homeodomain transcription factor PAX4 acts as a transcriptional regulator in early pancreatic development. *Mol. Cell. Biol.* **19,** 8272-8280.

Stargell, L.A., and Struhl, K., (1996). Mechanisms of transcriptional activation in vivo: two steps forward. *Trends Genet.* **12,** 311-315.

Tajbakhsh, S., Rocancourt, D., Cossu, G., and Buckingham, M., (1997). Redifining the genetic hierarchies controlling skeletal myogenesis: *pax-3* and *myf-5* act upstream of *myoD. Cell* **89,** 127-138.

Tanaka, M. and Herr, W. (1990). Differential transcriptional activation by Oct-1 and Oct-2: Interdependent activation domains induce Oct-2 phosphorylation. *Cell* **60,** 375-386.

Tasken, K., Solberg, R., Foss, K.B., Shalhegg, B.S., Hansson, V. and Jahnsen, T., (1995), in *The Protein Kinase Facts Book, protein-serine kinases, section II the protein kinases, PKA,* 58-63.

Tassabehji, M., Read, A., Newton, V., Harris, R., Balling, R., Gruss, P. and Strachan, T., (1992). Waardenburg's syndrome patients have mutations in the human homologue of the *Pax-3* paired box gene. *Nature* **355,** 635-636.

Tremblay, P., Dietrich, S., Mericskay, M., Schubert, F., Li, Z. and Paulin, D., (1998). A crucial role for *Pax-3* in the development of the hypaxial musculature and the long-range migration of muscle precursors. *Developmental Biology* **203,** 49-61.

Underhill, D.A., Vogan, K. and Gros, P., (1995). Analysis of the mouse splotch-delayed mutation indicates that the Pax-3 paired domain can influence homeodomain DNA-binding activity. *Proc. Natl. Acad. Sci. USA* **92,** 3692-3696.

Underhill, D.A. and Gros, P., (1997). The paired-domain regulates DNA binding by the homeodomain within the intact Pax-3 protein. *The Journal of Biological Chemistry* **272,** 14175-14182.

Van Corven, E. J., Groenink, A., Jalink, K., Eichholtz, T., and Moolenaar, W., (1989). Lysophosphatidate-induced cell proliferation: identification and dissection of signalling pathways mediated by G proteins. *Cell* **59,** 45-54.

Vogan, K., Underhill, A.D. and Gros, P. (1996). An alternative splicing event in the Pax-3 paired domain identifies the linker region as a key determinant of paired domain DNA-binding activity. *Molecular and Cellular Biology* **16,** 6677-6686.

Vogan, K. and Gros, P., (1997). The C-terminal subdomain makes an important contribution to the DNA binding activity of the Pax-3 paired domain. *The Journal of Biological Chemistry* **272,** 28289-28295.

Wakamatsu, Y., Watanabe, Y., Nakamura, H., and Kondoh, H., (1997). Regulation of the neural crest cell fate by N-myc: promotion of ventral migration and neuronal differentiation. *Development* **124,** 1953-1962.

Walsh, D. A., and Van Patten, S, M., (1994). Multiple pathway signal transduction by the cAMP-dependent protein kinase. *The FASEB Journal* **8,** 1227-1236.

Wehr, R. and Gruss, P. (1996). *Pax* and vertebrate development. *Int. J. Dev. Biol.* **40,** 369-377.

Wiggan, O., Taniguchi-Sidle, A. and Hamel, P., (1998). Interaction of the pRB-family proteins with factors containing paired-like homeodomains. *Oncogene* **16,** 227-236.

Wilkinson, M.G., and Millar, J.B.A., (2000). Control of the eukaryotic cell cycle by MAP kinase signalling pathways. *The FASEB Journal* **14,** 2147-2157.

Wilson, D. Sheng, G., Lecuit, T., Dostatni, N. and Desplan, C., (1993). Cooperative dimerisation of paired class homeodomains on DNA. *Genes and development* **7,** 2120-2134.

Wilson, D., Guenther, B., Desplan, C. and Kuriyan, J., (1995). High resolution crystal structure of a paired (Pax) class cooperative homeodomain dimer on DNA. *Cell* **82,** 709-719.

Wolpert, L., (1998). Chapter 8 in: *Principles of Development, Oxford Univ. Press,* pages 258-260.

Wood, J.N., Bevan, S.J., Coote, P.R., Dunn, P.M., Harmar, A., Hogan, P., Latchman, D.S., Morrison, C., Ruogon, G., Theveniau, M. and Wheatley, S. (1990). Novel cell lines display properties of nocioceptive sensory neurons. *Proc. R. Soc. Lond. B,* **241,** 187-194.

Woodgett, J.R., Gould, K.L. and Hunter, T., (1986). Substrate specificity of protein kinase C – use of synthetic peptides corresponding to physiological sites as probes for substrate recognition requirements. *European Journal of Biochemistry* **161,** 177-187.

Wu, S.J., Spiegel, S., and Sturgill, T. W., (1996). Sphingosine-1-phosphate rapidly activates the mitogen activated protein kinase pathway by a G protein dependent mechanism. *J. Biol. Chem.* **270,** 11484-11488.

Xu, W., Rould, M., Jun, S., Desplan, C. and Pabo, C. Crystal structure of a paired domain-DNA complex at 2.5 A resolution reveals structural basis for Pax developmental mutations. *Cell* **80,** 639-650.

Xu, H., Rould, M., Xu, W., Epstein, J., Maas, R. and Pabo, C., (1999). Crystal structure of the human Pax6 paired domain-DNA complex reveals specific roles for the linker region and carboxy-terminal subdomain in DNA binding. *Genes and development* **13,** 1263-1275.

Yang, X., Su, K., Roos, M.D., Chang, Q., Paterson, A.J., and Kudlow, J.E., (2001). O-linkage of N-acetylglucosamine to Sp1 activation domain inhibits its transcriptional capability. *Proc Natl Acad Sci USA* **98,** 6611-6616.

Zannini, M., Francis-Lang, H., Plachov, D., and Di Lauro, R., (1992). Pax-8, a paired domain-containing protein, binds to a sequence overlapping the recognition site of a homeodomain and activates transcription from two thyroid-specific promoters. *Molecular and Cellular Biology* **12,** 4230-4241.